Susana Patrícia da Silva Pereira

PROGRAMMING OF FETAL CARDIO-RENAL MITOCHONDRIA BY MATERNAL NUTRITION

Doctoral thesis in Biosciences, branch of specialization in Toxicology, under the supervision of Paulo J. Oliveira, PhD and Professor António J. Moreno, PhD presented to the Department of Life Sciences, Faculty of Sciences and Technology of the University of Coimbra

September 2015

· U C ·

UNIVERSIDADE DE COIMBRA

PROGRAMMING OF FETAL CARDIO-RENAL MITOCHONDRIA BY MATERNAL NUTRITION

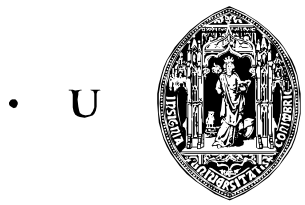

UNIVERSIDADE DE COIMBRA

Susana P. Pereira, BSc, MSc

Tese de Doutoramento em Biociências, orientada pelo Doutor Paulo J. Oliveira e pelo Professor Doutor António J. Moreno e apresentada ao Departamento de Ciências da Vida da Faculdade de Ciências e Tecnologia da Universidade de Coimbra com vista à obtenção do grau de Doutor em Biociências com especialização em Toxicologia.

Doctoral thesis in Biosciences under the supervision of Paulo J. Oliveira, PhD and Professor António J. Moreno, submitted to the Department of Life Sciences, Faculty of Sciences and Technology of the University of Coimbra as requirement for candidature for degree of PhD in Biosciences specialization in Toxicology.

Coimbra, September 2015

pereirasusan@gmail.com

This dissertation contains information obtained from authentic and highly regarded sources. Reprinted material is quoted with permission, and sources are indicated. A wide variety of references are listed. Reasonable efforts have been made to publish reliable data and information, but the author cannot assume responsibility for the validity of all materials or for the consequences of their use.

This dissertation was written in Microsoft Word version 14.5.4 and additional packages were used for data analysis, graphical displaying and illustration. By decision of the author the sections in this dissertation written in Portuguese do not follow the Second Amending Protocol for the Portuguese Language Orthographic Agreement, approved by Parliament's resolution No. 35/2008 and ratified by the President Decree No. 52/2008 by July 29, 2008.

The bibliography style adopted follows the guideline of Nature with few modifications.

Cover Illustration idealization: Susana P. Pereira
Cover Illustration design: Ludgero C. Tavares, ludgeroctavares@gmail.com
Graphical Printing: DualPrint
Published in Coimbra, Portugal on September 2015

This work was conducted under the supervision of

Paulo J. Oliveira, PhD, Center for Neuroscience and Cell Biology, University of Coimbra, Portugal;

Professor António J. Moreno, PhD, Institute for Marine Research, Department of Life Sciences, University of Coimbra, Coimbra, Portugal;

Mark J. Nijland, PhD, University of Texas Health Science Center, Center for Pregnancy and Newborn Research, Department of Obstetrics and Gynecology, San Antonio, Texas, United States of America (USA)

Peter W. Nathanielsz, MD, PhD, ScD, FRCOG, University of Texas Health Science Center, Center for Pregnancy and Newborn Research, Department of Obstetrics and Gynecology, San Antonio, Texas, USA.

This work also resulted from a collaboration with Laura A. Cox, PhD in the Department of Genetics, Texas Biomedical Research Institute, San Antonio, Texas, USA and Alina Maloyan, PhD and Leslie Myatt, PhD FRCOG from the University of Texas Health Science Center, Center for Pregnancy and Newborn Research, Department of Obstetrics and Gynecology, San Antonio, Texas, USA.

The work presented in this dissertation was funded by FEDER funds through the Operational Programme Competitiveness Factors - COMPETE and national funds by FCT - Foundation for Science and Technology under a PhD fellowship addressed to the author (SFRH/BD/64694/2009) and the strategic project UID/NEU/04539/2013, as also funded through the Program Project Grant (P01) from the National Institutes of Health (NIH, PO1 HD021350 to PWN and MJN). This investigation also used resources and facilities which were supported by the Southwest National Primate Research Center grant P51 RR013986 from the National Center for Research Resources, NIH and which are currently supported by the Office of Research Infrastructure Programs through P51 OD011133 and C06 RR013556.

The funding agencies had no role in study design, data collection and analysis, decision to publish, or preparation of this dissertation.

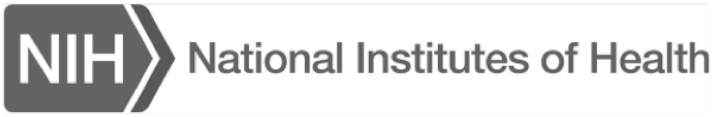

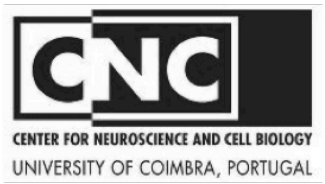

Statement of originality

This dissertation includes material from two original papers, that described work completed during my registration as a graduate student at the University of Coimbra, and have been previously published in a peer reviewed journals.

1. Susana P. Pereira, Gonçalo C. Pereira, António J. Moreno, Paulo J. Oliveira (2009). **Can drug safety be predicted and animal experiments reduced by using isolated mitochondrial fractions?** Alternatives to Laboratory Animals (ATLA) 37, 355-365.

2. Susana P. Pereira, Paulo J. Oliveira, Ludgero Tavares, António J. Moreno, Laura A, Cox, Peter W. Nathanielsz, Mark J. Nijland (2015). **Effects of Moderate Global Maternal Nutrient Reduction on Fetal Baboon Renal Mitochondrial Gene Expression at 0.9 Gestation**. American Journal of Physiology - Renal Physiology.

Part of this dissertation work has been presented in several national and international scientific meetings in the form of oral and poster communication.

Oral communications

1. *Susana P. Pereira*, Paulo J. Oliveira, Laura A. Cox, Peter W. Nathanielsz, Mark J. Nijland. **Effects of Maternal Nutrition Excess (MNE) on Fetal Cardiac Mitochondrial Transcripts and Protein at 0.9 G in Non-Human Primates (NHP).** Center for Pregnancy and Newborn Research Symposium - Influence of Obesity, Maternal Nutrition and Fetal Gender on Placental Function and Pregnancy Outcome, San Antonio, Texas, USA, March 2012.

2. *Susana P. Pereira,* Paulo J. Oliveira, Laura A. Cox, Peter W. Nathanielsz, Mark J. Nijland. **Effects of Maternal Nutrition Excess (MNE) on Fetal Cardiac Mitochondrial Transcripts and Protein at 0.9 G in Non-Human Primates (NHP).** Experimental Biology 2012, San Diego, California, USA, April 2012.

3. *Susana P. Pereira,* Paulo J. Oliveira, Peter W. Nathanielsz, Mark J. Nijland. **Maternal Nutrient Restriction (MNR) Affects fetal Cardiac Mitochondrial Transcripts at 0.9G in Non-Human Primates (NHP).** 47th Annual Scientific Meeting of the European Society for clinical investigation. Albufeira, Portugal, April 2013. Abstract published in the European Journal of Clinical Investigation, 43 (1): 41.

4. *Susana P. Pereira,* Paulo J. Oliveira, Laura A. Cox, Peter W. Nathanielsz, Mark J. Nijland. **The Impact of Maternal Nutrition Excess (MNE) on Fetal Cardiac Mitochondrial Transcripts and Protein at 0.9G in Non-Human Primates (NHP).** 47th Annual Scientific Meeting of the European Society for clinical investigation. Albufeira, Portugal, April 2013. Abstract published in the European Journal of Clinical Investigation, 43 (1): 68.

5. *Susana P. Pereira,* Paulo J. Oliveira, Laura A. Cox, Peter W. Nathanielsz, Mark J. Nijland. **Effects of maternal nutrition excess on fetal baboon cardiac mitochondrial transcripts and protein at 0.9G**. In X Annual Meeting of the Doutoral Program in Experimental Biology and Biomedicine, Cantanhede, Portugal. December 2013

Poster presentations

1. *Susana P. Pereira,* Paulo J. Oliveira, Peter W. Nathanielsz, Mark J. Nijland. **Sex Differences in Fetal Non-Human Primate (NHP) Heart Mitochondrial Transcripts at 0.9 Gestation (G).** 2012 SGI 59th Annual Scientific Meeting, San Diego, California, USA, March 2012.

2. *Susana P. Pereira*, Paulo J. Oliveira, Peter W. Nathanielsz, Mark J. Nijland. **Effects of Maternal Nutrition Restriction (MNR) on Fetal Cardiac Mitochondrial Transcripts at 0.9 G in Non-Human Primates**. 2012 SGI 59th Annual Scientific Meeting, San Diego, California, USA, March 2012.

3. *Susana P. Pereira*, Paulo J. Oliveira, Peter W. Nathanielsz, Mark J. Nijland. **Maternal Nutrition Restriction (MNR) in Non-human Primates (NHP) Down-Regulates Mitochondrial Oxidative Phosphorylation Transcripts at 0.5G**. 2012 SGI 59th Annual Scientific Meeting, San Diego, California, USA, March 2012.

4. *Susana P. Pereira*, Paulo J. Oliveira, Laura A. Cox, Peter W. Nathanielsz, Mark J. Nijland. **Maternal Nutrient Restriction Down Regulates Cardiac Mitochondrial Proliferation in Male Non-Human Primates (NHP) at 0.5 Gestation**. 2012 SGI 59th Annual Scientific Meeting, San Diego, California, USA, March 2012.

5. *Susana P. Pereira*, Paulo J. Oliveira, Laura A. Cox, Peter W. Nathanielsz, Mark J. Nijland. **Gender-Specific Effects of 30% Global Maternal Nutrient Restriction (MNR) on Non-Human Primate Renal Mitochondrial Transcripts at 0.9 Gestation (G).** 2012 SGI 59th Annual Scientific Meeting, San Diego, California, USA, March,2012.

6. *Susana P. Pereira*, Paulo J. Oliveira, Laura A. Cox, Peter W. Nathanielsz, Mark J. Nijland. **Maternal nutrition excess affects fetal cardiac mitochondrial transcripts and protein at 0.9 G in non-human primates**. 46th Annual Scientific Meeting of the European Society for Clinical Investigation, Budapest, Hungary, March 2012.

7. *Susana P. Pereira*, Paulo J. Oliveira, Laura A. Cox, Peter W. Nathanielsz, Mark J. Nijland. **Early Renal Mitochondrial Adjustments to 30% Global Maternal Nutrient Restriction (MNR) at 0.9G in a Non-Human Primates (NHP) model**. 47th Annual Scientific Meeting of the European Society for clinical investigation. Albufeira, Portugal, April 2013. Abstract published in the European Journal of Clinical Investigation, 43 (1): 47.

8. *Susana P. Pereira*, Paulo J. Oliveira, Peter W. Nathanielsz, Mark J. Nijland. **Effect of 30% Maternal Nutrient Restriction (MNR) on Cardiac Gene Expression Relevant to Mitochondrial Oxidative Phosphorylation in the Fetal Baboon**. 47th Annual Scientific Meeting of the European Society for clinical investigation. Albufeira, Portugal, April 2013. Abstract published in the European Journal of Clinical Investigation, 43 (1): 95-96.

9. *Susana P. Pereira*, Paulo J. Oliveira, Peter W. Nathanielsz, Mark J. Nijland. Maternal **Nutrient Restriction and the Kidney: Implications in Mitochondrial Gene Expression.** MiP Summer 2013 – the Mitochondrial Physiology Summer School, Mitochondrial Physiology: Theory and Praxis. Copenhagen, Denmark, August 2013.

10. *Susana P. Pereira*, Paulo J. Oliveira, Ludgero C. Tavares, Ana I. Duarte , Maria S Santos, Inês Baldeiras, António J Moreno, Laura A Cox, Peter W Nathanielsz, Mark J Nijland. **Influence of Maternal Nutrient Reduction on Fetal Nonhuman Primate Cardiac Mitochondria at 0.6 Gestation (G).** XVIII Meeting of the Portuguese Biochemical Society, Coimbra, Portugal. December 2014.

I declare that the general tenor of this dissertation is the consequence of my personal and intellectual work, such as, key ideas, primary contributions, experimental designs, data analysis and interpretation. Nonetheless, all assistance received during the work presented in this dissertation or its preparation has been acknowledged.

I pronounce that, to the best of my knowledge, my thesis does not infringe upon anyone's copyright nor violate any proprietary rights and that any ideas, techniques, quotations, or any other material from the work of other people included in my thesis, published or otherwise, are fully acknowledged in accordance with the standard referencing practices.

I certify that this is a true copy of my thesis, including any final revisions, as approved by my supervisors, and that this thesis has not been submitted for a higher degree to any other University or Institution.

September 2015

A vós a dedico…

… por vós persisto!

Abstract

Early-life malnutrition results in structural alterations to fetal kidney and heart, predisposing offspring to later life cardio-renal dysfunction. Epidemiologic studies link low birth weight to predisposition to cardiovascular disease (CVD) later in life with both sex and diet impacting the incidence of CVD. Kidneys of adults who suffered from growth restriction at birth have substantial variation in nephron endowment. Animal models suggest cardio-renal structural and functional consequences in the offspring exposed to sub-optimal intrauterine nutrition. Mitochondrial bioenergetics plays a key role in cardiac and renal energy metabolism, growth and function. In this relevant work, we hypothesized that moderate maternal nutrient reduction (MNR) would adversely impact fetal cardio-renal mitochondrial metabolism in a well-established non-human primate model which produces intra-uterine growth reduction at term.

Female pregnant baboons were fed normal chow diet or 70% of control diet (maternal nutrient reduction, MNR). Cesarean sections were performed at 0.9 gestation (165 days gestation) under anesthesia. Maternal fasting blood was drawn from the femoral vein in the morning before cesarean section and before the fetus was exteriorized from the uterine cavity. Umbilical vein blood was also sampled. The mother, the placenta and the fetus were analyzed for morphometric measurements and tissue sampling. Fetal kidneys and heart were rapidly harvested and appropriately processed, flash frozen or fixed, for posterior analyses. Biochemical and amino acid analyses were performed in the maternal and fetal blood samples. Analysis of mitochondrial DNA was performed by quantitative real-time PCR, and Human Mitochondrial Energy Metabolism and Human Mitochondria Pathway PCR Arrays were used to analyze mitochondrial relevant mRNA. *In situ* protein content was detected by immunohistochemistry and semi-quantification was performed by Western blot. Enzymatic activity of mitochondrial proteins was determined by alterations in the absorbance of specific substrates or products. Adenine nucleotide levels and energy charge were determined by HPLC, as well determination of vitamin E and reduced and oxidized glutathione contents. Other indicators of oxidative state, as malondialdehyde content (MDA), glutathione peroxidase and glutathione reductase activities were determined spectrophotometrically. Ultimately, transmission electron microscopy was used to assess mitochondrial morphology.

MNR until 0.9 gestation decreased maternal weight gain and placental weight, being the effects more severe in MNR mothers carrying a male fetuses. Despite the smaller overall fetal size, fetal kidney weight-to-body weight or the heart weight-to-body weight ratios were not affected. MNR caused adjustments in the protein metabolism reflected in altered maternal amino acids concentrations and impaired glucose metabolism, with MNR mothers displaying higher levels of cortisol and glucose in blood circulation.

Regarding the fetal kidney, we demonstrated fetal gender-specific differential mRNA expression encoding mitochondrial metabolite transport and dynamics proteins. MNR-related differential gene expression was more evident in female fetuses, with 16 transcripts significantly altered, including 14 downregulated and 2 upregulated. MNR impacted 10 transcripts in male fetuses, with 7 downregulated and 3 upregulated. Alteration in mRNA levels was accompanied by a decrease in mitochondrial protein cytochrome c oxidase subunit VIc. In conclusion, transcripts encoding fetal renal mitochondrial energy metabolism proteins are nutrition sensitive in a gender-dependent manner.

For the fetal cardiac left ventricle, we found that MNR increased mtDNA content and the transcription of key mitochondrial genes involved in mitochondrial dynamics and oxidative phosphorylation (OXPHOS), resulting in increased content of several mitochondrial proteins, namely components of the mitochondrial respiratory chain (NDUFB8, UQCRC1 and cytochrome c) and ATP synthase. However, the activity of OXPHOS enzymes was significantly decreased in MNR fetuses, possibly contributing to a decreased ATP content and an increased oxidative stress in the cardiac left ventricle tissues, as seen by increased lipid peroxidation marker, MDA. Microscopy of the fetal cardiac left ventricles reflected the disturbance induced by MNR, revealing mitochondria with sparse and disarranged cristae. These checkpoints suggest that MNR orchestrated a serial of events that ultimately resulted in an impaired capacity of fetal cardiac left ventricle tissue to produce energy through the OXPHOS system.

The present study provides for the first time evidence of an association between MNR and mitochondrial remodeling in the fetus. Although the MNR fetal manifestation were tissue and gender specific, the overall scenario point to and impairment in mitochondrial function in the fetal tissues analyzed. We speculate that

these differences lead to decreased mitochondrial fitness that contributes to cardio-renal dysfunction in later life. Our work has a translational application in human health, showing that control of maternal health during pregnancy may reduce long term disease risk in the offspring with greatest benefit for the individual and for national health care systems.

Keywords: fetal programming; fetal under-nutrition; metabolic disease; baboon; mitochondria; heart; kidney

Resumo

A ocorrência de subnutrição durante o período gestacional tem como consequência alterações estruturais ao nível dos rins e coração fetais, predispondo a descendência a disfunções cardiorenais. Estudos epidemiológicos associam o baixo peso ao nascer com a predisposição para ocorrerem mais tarde doenças cardiovasculares (DCV) nesses indivíduos, estando o género e a dieta directamente relacionados com a sua incidência. Os rins de adultos que sofreram de subnutrição à nascença apresentam uma variação substancial do número de nefrónios. Modelos animais sugerem existir consequências estruturais e funcionais ao nível cardiorenal associadas à exposição a uma nutrição intra-uterina insuficiente. A bioenergética mitocondrial desempenha um papel-chave no metabolismo energético, no crescimento e funcionamento cardíaco e renal. Neste trabalho com relevância médica, estabelecemos como hipótese que a redução maternal de nutrientes (RMN) teria um impacto negativo no metabolismo mitocondrial cardiorenal do feto num modelo estabelecido de primata não-humano que exibe uma redução do crescimento fetal intra-uterino numa gravidez de termo.

Fêmeas de babuínos grávidas foram alimentadas com uma dieta normal (*ad libitum,* 100%) ou com 70% da dieta normal (redução maternal de nutrientes, RMN). Foram realizadas cesarianas ao tempo gestacional 0,9 (165 dias de gestação), sob anestesia. Foi recolhido sangue maternal em jejum, a partir da veia femoral, na manhã do dia da cesariana e antes da extração do feto da cavidade uterina. O sangue da veia umbilical também foi recolhido. A mãe, a placenta e o feto foram submetidos a medições morfométricas e à recolha de tecidos. Rins e coração fetais foram rapidamente recolhidos e processados de forma adequada, por rápida congelação ou por fixação, de forma a serem posteriormente analisados. Efectuaram-se análises bioquímicas clínicas e do conteúdo em aminoácidos às amostras de sangue maternal e fetal. A análise do *ADN* mitocondrial foi realizada por PCR quantitativo em tempo real, e foram usados *PCR arrays* de Metabolismo Energético Mitocondrial Humano e de Vias Mitocondriais Humanas para avaliar *ARNm* relevantes relacionados com a mitocôndria. O conteúdo proteico foi detectado *in situ* por imunohistoquímica e semi-quantificado por *Western blot*. A actividade enzimática de proteínas mitocondriais foi determinada pela avaliação de alterações na absorvância de

substratos ou de produtos específicos formados. Os níveis de nucleótidos de adenina e a carga energética foram determinados por *HPLC*, bem como a determinação de vitamina E e do conteúdo de glutationa reduzida e oxidada. Outros indicadores de estado oxidativo, como o conteúdo de malondialdeído (MDA), de glutationa peroxidase e de glutationa redutase, foram determinados espectrofotometricamente. Por último, utilizou-se microscopia electrónica de transmissão para avaliar a morfologia mitocondrial.

RMN até ao tempo gestacional 0,9 implica a diminuição do ganho de peso maternal e placentário, sendo os efeitos mais graves em mães RMN em gestação de fetos do sexo masculino. Apesar do menor tamanho fetal global, as proporções peso renal-peso corporal e peso cardíaco-peso corporal não foram afectadas. A RMN causou ajustes no metabolismo de proteínas, reflectido na alteração das concentrações de aminoácidos maternais e no comprometimento do metabolismo da glicose, de forma que as mães RMN apresentavam níveis elevados de cortisol e glicose na circulação sanguínea.

Relativamente ao rim fetal, demonstrámos que a expressão de *ARNm* codificante de proteínas mitocondriais de transporte e dinâmica de metabolitos era diferenciada entre géneros. A expressão génica diferencial relacionada com a RMN foi mais evidente nos fetos do sexo feminino, apresentando estes indivíduos 16 transcritos significativamente alterados, incluindo 14 que diminuíram e 2 que aumentaram. A RMN alterou 10 transcritos em fetos do sexo masculino, e destes, 7 apresentaram-se diminuídos e 3 aumentaram. A alteração dos níveis de *ARNm* foi acompanhada por uma diminuição da proteína mitocondrial subunidade VIc da citocromo c oxidase. Em conclusão, os transcritos que codificam proteínas do metabolismo energético mitocondrial do rim fetal são sensíveis aos níveis nutricionais, de uma forma dependente do género.

Para o ventrículo esquerdo do coração fetal, descobrimos que a RMN aumenta os níveis de *ADNmt* e a transcrição de genes de proteínas mitocondriais-chave envolvidas na dinâmica mitocondrial e na fosforilação oxidativa (FOX), resultando no aumento do teor de várias proteínas mitocondriais, nomeadamente componentes da cadeia respiratória mitocondrial (NDUFB8 , UQCRC1 e citocromo c) e da ATP sintase. No entanto, a actividade de enzimas associadas à FOX revelou-se significativamente mais baixa em fetos RMN, podendo estar associada à diminuição

da quantidade de ATP, e ao aumento do stress oxidativo nos tecidos do ventrículo esquerdo cardíaco revelado pelo aumento do marcador de peroxidação lipídica MDA. A microscopia dos ventrículos esquerdos cardíacos fetais reflectiu a perturbação induzida pela RMN, revelando mitocôndrias com cristas em menor número e mais desordenadas. Estes pontos de controlo sugerem que a RMN orquestrou uma série de eventos que resultaram, em última instância, na diminuição da capacidade do tecido do ventrículo esquerdo cardíaco fetal de produzir energia através do sistema FOX.

O presente estudo fornece, pela primeira vez, a evidência de uma associação entre RMN e a remodelação mitocondrial no feto. Embora a manifestação fetal RMN seja específica de tecidos e género, o cenário global aponta para comprometimento da função mitocondrial em ambos os tecidos fetais analisados. Nós especulamos que essas diferenças levam a uma diminuição da performance mitocondrial, contribuindo para a disfunção cardiorenal a longo termo. O nosso trabalho tem uma aplicação translacional em saúde humana, mostrando que o controlo da saúde materna durante a gravidez pode reduzir o risco de doença a longo termo na descendência, com grandes benefícios para o indivíduo mas de igual modo para os sistemas nacionais de cuidado de saúde.

Palavras-Chave: Programação fetal; subnutrição fetal; doença metabólica; babuíno; mitocôndria; coração; rim.

Acknowledgements

Este trabalho científico não teria sido possível sem o apoio e suporte de várias instituições, entidades e individualidades. Por isso, expresso aqui o meu agradecimento público a tudo e todos que tornaram este trabalho executável.

Expresso o meu agradecimento à Fundação para a Ciência e Tecnologia pela bolsa de doutoramento que me foi atribuída (SFRH/BD/64694/2009) e pelo suporte financeiro para a realização de várias formações que indubitavelmente contribuíram para que me tornasse uma investigadora mais segura e capaz. Agradeço de igual modo os fundos atribuídos para a investigação nacional, nomeadamente sob a forma de projectos financiados ao Doutor Paulo J. Oliveira e ao Professor Doutor António J. Moreno, os quais lhes permitiram manter laboratórios funcionais onde pude realizar diversas experiências.

Agradeço à Universidade de Coimbra, nomeadamente ao Departamento de Ciências da Vida, ao CNC - Centro de Neurociências e Biologia Celular da Universidade de Coimbra e ao UC Biotech por me acolherem e proporcionarem as instalações e as condições físicas para a realização deste trabalho.

Agradeço ao Doutor João Ramalho, coordenador do Doutoramento em Biociências da Universidade de Coimbra, a sua constante disponibilidade, cuidado e auxílio. Em especial gostaria de lhe agradecer o facto de sermos mais do que "um número de aluno", por genuinamente se interessar pelo nosso percurso e por nos estimular a ser melhores investigadores.

Expresso o meu profundo agradecimento ao Doutor Paulo J. Oliveira, por me permitir fazer aquilo de que eu tanto gosto de modo financiado, por suportar a minha candidatura à bolsa de doutoramento e por ao longo destes anos me ter auxiliado a definir o tipo de investigadora que almejo ser. Agradeço-lhe a confiança, a autonomia para testar e errar, as discussões e as imensuráveis correcções. Estou-lhe particularmente grata pela oportunidade de crescer com a sua orientação, por manter um diálogo aberto e por proporcionar as condições para a realização deste trabalho. No outro lado do prisma, mas na mesma pessoa, não posso deixar de enaltecer o seu cuidado e compreensão para com assuntos não científicos, agradecendo genuinamente toda a preocupação e auxílio.

Agradeço ao Professor Doutor António J. Moreno por me proporcionado esta oportunidade singular de continuar sob a orientação de um dos cientistas que mais admiro. Tem sido um privilégio conviver e aprender consigo desfrutando da sua genialidade consolidada com tamanha humanidade.

I am grateful to Doctor Mark J. Nijland for having accepted to be my mentor. I will always have in mind the day you received me at San Antonio's airport, because you didn't need to be there but you were. Thank you for introducing me to San Antonio and for all the treats. You conceded me the privilege of performing my PhD studies in an amazing model! I thank you the transmitted knowledge in animal anatomy and dissection procedures. I am grateful for the long scientific discussions and for always listening to my opinion regardless how right it was. I thank all your help and for always make things possible for me.

I am grateful to Doctor Peter Nathanielsz who kindly welcomed me in his laboratory and provided unreserved support during my PhD, giving me the possibility to enter in the astounding developmental programming research world. I am thankful for his constructive criticism and extensive discussions on my work. However, I am truly thankful for the inspiring environment to perform my research and for making me feel like my opinion count.

I am grateful to Doctor Thomas McDonald, he was more than a senior scientist, he was a fellow that shared the love for science and life and always made my days better! It was amazing to get to know someone like you!

I would like to express my gratitude to Doctor Leslie Myatt and his group for adopting me at laboratory, for treating me as a group member and for allowing me to use various equipments, without forget to mention the moments of good humor and valuable scientific discussion.

I am thankful to Doctor Laura A. Cox and her group for all the guidance and all support during my stay at Texas Biomedical Research Institute for learning qRT-PCR. She has given me some lessons for life.

I gratify Karen Moore for being my Texas mummy! Your house became my home during my stays abroad. Thank you so much for all the hugs that made me feel less family seek, thank you for all the good times. Thank you for showing me your culture and San Antonio city. Thank you for the movies nights, for all the rides, for

all delicious recipes and intense conversations. A very special thank you for sharing baby C, Lorraine, D and Kiely with me and showing me that family are not only the ones we share blood with! Thank you for being always there for me, even miles and miles away.

I would also like to thank to the personnel of Obstetrics and Gynecology Department at the UTHSC, namely the group of Doctor Theresa Powell and Doctor Thomas Jansson, and also to Sue, Michelle, Paulina, Jaehyek, Jesse, Michiyo, Greg, Dr Li, Alina Maloyan, Nagarjun Kasaraneni, Chunming Guo, Balasubashini Muralimanoharan and James Mele by general laboratory help, to my meals friends Vijay, Ganga, Samaya and Susan and to Joyce by her friendship and funny rides in hers "Rolls Royce".

Reconheço o meu apreço à Dr.ª Sancha, a nossa "mãezinha do laboratório", por "*agora não posso, estou ocupada*" não constar do seu vocabulário. Pela sua constante disponibilidade para auxiliar, por zelar cuidadosamente por nós, por incentivar e apoiar as novas ideias tornando-as realizáveis! Por ser um exemplo "vivo" e dinâmico do que deve ser um investigador… e um ser humano! Para mim é o verdadeiro exemplo a seguir! É por pessoas assim que Coimbra terá sempre lugar em mim! Muito agradecida por cuidar de nós!

Retribuo à Dr.ª Maria Augusta Fernandes as graciosas conversas e esse "modo peculiar de pensar" que proporciona momentos únicos. É uma dávida tê-la nas nossas vidas.

Agradeço aos meus colegas e amigos do grupo MitoXT - Mitochondrial Toxicology and Experimental Therapeutics, do grupo da Doutora Paula Moreira, do grupo do Doutor João Ramanho, do grupo da Doutora Amália Jurado e do grupo do Doutor Lino Ferreira pelo seu caloroso acolhimento, pela sua constante disponibilidade, pelos inúmeros pedidos de auxílio sempre atendidos, pela cooperação, pelo constante sorriso, apoio e incentivo. E em especial, pelos amigos que aí descobri. Sem dúvida é mais gratificante trabalhar quando estamos rodeados de pessoas cativantes como as que aqui encontrei.

Todavia, para a realização deste trabalho em particular, tenho de enaltecer o precioso contributo e auxílio do Ludgero. Agradeço-lhe por ser extremamente paciente, por escutar e discutir os meus dilemas estatísticos e científicos, por se disponibilizar a

ajudar, por ratificar o tratamento estatístico e pela melhoria da qualidade de imagens. Agradeço-lhe ainda por personificar os bons jovens investigadores que há em Portugal, ao realizar um trabalho consciente e cuidado. Obrigada por estares na cadeira ao lado.

Agradeço à Cláudia Deus pela sua disponibilidade e ajuda laboratorial. Agradeço-lhe ainda por usar o seu tempo pessoal para introduzir informações em plataformas pouco funcionais por mim.

Agradeço à Tatiana P Pinto, pela sua amizade, a qual me permitiu ter a sua preciosa ajuda na formatação desta tese.

Aos funcionários do Departamento de Ciências da Vida, nomeadamente à "Dona Paula", à "Dona Júlia", à "Dona Clara" e à "Dona Isabel" pela agradável companhia nas longas horas de trabalho laboratorial, pelos incomensuráveis momentos de lazer proporcionados. Pela vossa paciência e constante disponibilidade em auxiliar, a vossa companhia e trabalho tornou os dias muito mais agradáveis e fáceis. Agradeço ainda ao secretariado desta instituição pelos pedidos sempre atendidos e boa disposição.

Aos funcionários do CNC por tornarem todas as burocracias mais fáceis, quando corre tudo bem nem nos apercebemos do enorme trabalho que está por detrás. Tem sido um prazer ter uma equipa tão prestativa e eficiente a auxiliar-nos sempre que solicitado.

Gratifico os funcionários do UC Biotech, nomeadamente a "Dona Alda", a "Dona Adelaide", a Filipa e a Leonor, por com o seu trabalho facilitar imensamente o meu. Obrigada pela gentileza com que atendem os meus pedidos.

Gostaria de agradecer ainda a todos os meus "amigos de sempre", nomeadamente à Sara, à "Lene", à "Chica", à Susana Maria e à "Ni" pela sua constante compreensão com a "amiga ocupada/ausente" e por se manterem a minha ligação umbilical à terra.

Reconheço a "Irmandade do 25", por ser um raio de luz luminoso e caloroso. É indescritível saber que estão aí, seja para proporcionar fraldas para rebentos ou para fazer noitadas para findar tarefas. É óptimo ter-vos e passar a ter 3^5 motivos para sorrir e celebrar!

Congratulo a ti An(J)a Maria, por personificares a bondade e como verdadeiro anjo seres omnipresente. Ter-te nas nossas vidas significa tanto! Obrigada por restaurares

a minha esperança na humanidade.

Agracio todos os meus novos amores, José, Francisco, Clarinha, Joaninha, Inês, Miguel, Santiago e Pedrinho. Obrigada por me expandirem o coração e encherem a vida de emoção, é um orgulho enorme ser vossa "titia".

Agradeço ao Sandro, à Gi e ao Pedrinho, por fazerem parte da família que escolhemos e tornarem casa o local aonde estamos juntos.

A vós minha estrutura nuclear, *"Lulinha", "Liz", "Nel"* e *"Pestinha"*, a vós dedico, a vós agradeço… cada passo dado, cada desafio superado… a vós minha amada família, minha pedra angular, meu conjunto invisível omnipresente… a vós atribuo tudo o que sou!! Não tentarei agradecer a imensurável compreensão, o infindável apoio, os inúmeros sacrifícios… comprometo-me apenas a AMAR-vos cada vez mais!

A ti Carlos, o meu genuíno "Amor Philia". Obrigada por materializares que amar é cumplicidade, companheirismo, respeito, suporte... Querer estar junto, mesmo quando é difícil! É ser capaz de nos manter a flutuar, mesmo quando pesamos mais de uma tonelada e estamos com um humor insuportável! Obrigada por fazeres do nosso amor a história das nossas vidas e multiplicá-lo em mais um coração!

A ti minha Maria, que encerras em ti o milagre da vida, de me fazer redescobrir o mundo pelos teus olhos, de afastar as nuvens cinzentas e encher os meus dias de cor e canções de ninar. Obrigada por me fazeres experienciar o amor no seu estado mais puro, verdadeiro e abnegado. Obrigada por me demonstrares em plenitude o sentido da "vida" e incentivares a ser cada dia uma versão melhorada de mim, só para ser mais de mim para ti!

A todos os supra citados… e a muitos mais… o meu mais sincero e sentido **MUITO OBRIGADA**!

"*A map does not just chart, it unlocks and formulates meaning; it forms bridges between here and there, between disparate ideas that we did not know were previously connected*"

by Reif Larsen

Contents

List of figures

List of tables

List of abbreviations

AAALAC	Association for Assessment and Accreditation of Laboratory Animal Care
Acetyl CoA	Acetyl Coenzyme A
ACTB	Beta-actin
ad lib	*ad libitum*
ADP	Adenosine diphosphate
AEC	Adenylate energy charge
ALP	Alkaline phosphatase
ALT	Alanine aminotransferase
AMP	Adenosine monophosphate
ANT	Adenine nucleotide translocase
ARG	Arginine
ASN	Asparagine
AST	Aspartate aminotransferase
ATP	Adenosine triphosphate
AU	Arbitrary units
BCA	Bicinchoninic acid assay
BMI	Body mass index
BSA	Bovine serum albumin
BUN	Blood urea nitrogen
Bw	body weight
C	Control
C-F	Control female fetuses
C-M	Control male fetuses
ATPase	Adenylpyrophosphatase
CAPS	3-(cyclohexylamino)-1-propanesulfonic acid
CAT	Catalase
CD	Collecting ducts
cDNA	Complementary deoxyribonucleic acid
CI	Complex I (NADH dehydrogenase or NADH:ubiquinone oxidoreductase)
CII	Complex II (succinate dehydrogenase or succinate:ubiquinone oxidoreductase)
CIII	Complex III (ubiquinol cytochrome c oxidoreductase or cytochrome bc1 complex

CIV	Complex IV (cytochrome c oxidase or cytochrome-c:oxygen oxidoreductase)
CoA	Coenzyme A
CoQ	Ubiquinone
CoQ1	Coenzyme Q1
CoQ10	Ubiquinone, Coenzyme Q10 (CoQ, Q)
$CoQH_2$	Ubiquinol
COX	Cytochrome c oxidase
COX6C	Cytochrome C oxidase subunit VIC
CPK	Creatine phosphokinase
CS	Citrate synthase
Ct	Threshold cycle
CV	Complex V (ATP synthase or FoF1-ATPase)
CVD	Cardiovascular disease
CX	Cortex
CypD	Cyclophilin D
CYC1	Cytochrome C-1, UQCR4
Cyt Cox	Oxidized cytochrome c
Cyt Cred	Redudced cytochrome c
DCPIP	Dichlorophenolindophenol
ddH_2O	Double distilled water
DEPC	Diethylpyrocarbonate
DNA	Deoxyribonucleic acid
DOC	Sodium deoxycholate
DT	Distal tubuli
E	Embryonic day
e^-	Electron
ECF	Enhanced chemifluorescence
EDTA	Ethylenediamine coefficient
ETC	Electron transport chain
FAD	Flavin adenine dinucleotide
$FADH_2$	Flavin adenine dinucleotide, hydroquinone form
FIS 1	Mitochondrial fission 1 protein
FMN	Flavin mononucleotide
GDC	Genomic DNA controls
gDNA	Genomic deoxyribonucleic acid
GGT	Gamma-glutamyl transferase

Gl-Px (GPx)	Glutathione peroxidase
Gl-Red (Gred)	Glutathione reductase
GSH	Reduced glutathione
GSSG	Glutathione disulfide
GTP	Guanosine triphosphate
H_2O2	Hydrogen peroxide
HGDC	Human genomic DNA controls
HIS	Histidine
HL	Limbs of Henle's Loop
HPLC	High-performance liquid chromatography
HPRT1	Hypoxanthine phosphoribosyltransferase 1
IMM	Inner mitochondrial membrane
IUGR	Intrauterine growth restriction
Kw	Kidneys weight
LBW	Low birth weight
LDH	Lactate dehydrogenase
LYS	Lysine
Ma	Matrix
MD	Medulla
MDA	Malondaildehyde
MFN1	Mitofusin 1
MFN2	Mitofusin 2
MNR	Maternal nutrient reduction
MNR-F	Maternal nutrient reduction female fetuses
MNR-M	Maternal nutrient reduction male fetuses
MPT	Mitochondrial permeability transition
MPTP	Mitochondrial permeability transition pore
MRC	mitochondrial respiratory chain
mRNA	Messenger ribonucleic acid
mtDNA	Mitochondrial deoxyribonucleic acid
***m*TOR**	Mammalian target of rapamycin
NADH	Nicotinamide adenine nucleotide reduced form
NAD^+	Nicotinamide adenine nucleotide
NADPH	Nicotinamide adenine dinucleotide phosphate, reduced form
nDNA	Nuclear deoxyribonucleic acid
NHP	Nonhuman primates

$^{\cdot}$OH	Hydroxyl radical
OMM	Outer mitochondrial membrane
$ONOO^{-}$	Peroxynitrite anion
OXPHOS	Oxidative phosphorilation system
PBS	Phosphate-buffered saline
PBS-T	Phosphate-buffered saline plus Tween-20
PDH	Pyruvate dehydrogenase
PDHK	Pyruvate dehydrogenase kinase
PEO	Ophthalmoplegia
Pi	Inorganic phosphate
PPC	Positive PCR controls
PT	Proximal tubuli
PVDF	Polyvinylidene difluoride
RefSeq	Reference sequence
RIPA buffer	Radioimmunoprecipitation assay buffer
RNA	Ribonucleic acid
rRNA	Ribosomal ribonucleic acid
ROS	Reactive oxygen species
RPL13A	Ribosomal protein L13a
RT-PCR	Real time polymerase chain reaction
RTC	Reverse transcription controls
SDH	Succinate dehydrogenase
SDS	Sodium dodecyl sulfate
SDS-PAGE	Sodium dodecyl sulfate polyacrylamifde gel electrophoresis
SEM	Standard error of the mean
SER	Serine
SIRT3	Sirtuin 3
Smac/DIABLO	second mitochondria-derived activator of caspases
SOD1	Copper/Zinc-dependent superoxide dismutase
SOD2	Manganese-dependent superoxide dismutase
SOD3	Copper/Zinc-dependent superoxide dismutase (extracellular)
TAN	Total adenine nucleotide pool
TCA	Tricarboxylic acid cycle
TIM	Translocase of the inner membrane
TIMM9A	Mitochondrial import inner membrane translocase subunit TIM9
TOM	Translocase of the outer membrane

TYR	Tyrosine
UCPs	Mitochondrial uncoupling proteins
VAL	Valine
VDAC	Voltage dependent anion channel
$\Delta\Delta\varepsilon Ct$	Difference in threshold cycles for the target and control samples
ε	Molar extinction coefficient

Chapter 1

General Introduction

1.1 Fetal development

Embryonic development is an extraordinary event that involves tightly regulated cell proliferation, the establishment of unique cell lineages that adopt distinct cell roles, and ultimately the regulated collaboration amongst cell types to generate different tissues [1,2]. In placental mammals, these processes take place within the uterus of the mother after implantation of the conceptus. Beyond regulating its own development, it is also required the conceptus ability to orchestrates additional events associated to adjusting maternal physiological functions, development of the uterus and establishment of a supply of oxygen and nutrients through the establishment of the placenta. These processes are among the initial actions of embryogenesis, being critical steps of the fetal development that must be achieved for the embryo to survive [1,2].

Following fertilization, the zygote experiences symmetrical cell divisions originating the morula. Primary differentiation episodes occur in the first days of development by formation of the blastocyst from the morula. External morula cells differentiate to become trophectoderm, leaving undifferentiaded cells of the inner cell mass surrounded by trophectoderm. In humans, the blastocyst implants into the uterus 7-8 days after conception and soon after implantation the trophectoderm gives rise to distinct differentiated cell types, while placental development is initiated [1,2]. Abnormalities in placental formation can compromise the growth of the fetus leading to intrauterine growth restriction (IUGR), or if too severe, causing fetal death. After the formation of the placenta, the heart is the first critical organ to develop in the fetus. The heart develops from two distinct cell lineages, with the majority of the heart being developed from anterior mesodermal cells. The layers of the heart wall (endocardium, myocardium and epicardium), and the valves all progress from the mesodermal progenitors. The "cardiogenic region" begins contracting as early as day 21 in human embryos or day 8 for murine [1,2]. Cardiac defects are common in newborns and estimated to be present in one of every 100 liveborn babies. Importantly, many tissues and organs such as the brain, lung, gut and kidneys are not so essential for intrauterine life. By contrast, fetal survival is highly dependent on function of the placenta, fetal liver and the cardiovascular system [1,2].

1.2 Role of the mitochondria in fetal development

1.2.1 Mitochondrial Biology

During several decades mitochondria were mostly considered as the cell furnaces, producing energy by chemiosmosis [3]. It has been estimated that almost 90% of oxygen consumption by mammals occurs in mitochondria with the ultimate objective of synthesizing adenosine triphosphate, ATP [4,5]. Further advances established that this organelle not only provide cell energy but is also involved in calcium homeostasis [6], in intermediate metabolism, in the generation of reactive oxygen species (ROS) and most importantly, in the progression or initiation of cell death [7,8]. Mitochondria are also implicated in the majority of human diseases including cancer [9], diabetes [10], cardiovascular and neurodegenerative diseases [10], triggering the scientific attention in mitochondrial bioenergetics in cells.

1.2.1.1 Mitochondrial DNA

Mitochondrial DNA (mtDNA, Figure 1.1) accounts for less than one percent of total cellular DNA. Nevertheless, mitochondrial gene products are essential for normal cellular function [11]. The human mtDNA is maternally inherited, being a closed circular, double-stranded DNA molecule of 16,569 base pair located within the mitochondrial matrix. The entire mitochondrial genome encodes 37 genes which encodes for two rRNAs, 22 tRNAs and 13 polypeptides that are essential components of the multi-subunit complexes of the oxidative phosphorylation system (OXPHOS, Figure 1.2). Most of these genes are encoded in the heavy strand, with only eight mitochondrial tRNAs and a single polypeptide encoded by the light strand. The mtDNA also contains a short non-coding region with control elements, including three hypervariable regions and a displacement loop (*D-loop*). The *D-loop* region harbors regulatory elements required for replication and transcription. All the other proteins required for mtDNA maintenance and expression are encoded by the nuclear genome translated in the cytosol and are targeted and imported into the mitochondrial matrix [12].

It is important to remember that there are some unique characteristics of mtDNA and mitochondrial genetics which are dissimilar from the features of nuclear genes and the principles of nuclear inheritance. A very special feature is that only the mother contributes to the mtDNA offspring patrimony [13]. mtDNA does not contain

introns, making mtDNA mutations or deletions more prone to result in an affected phenotype. The occurring of mtDNA mutations is more than 10 times higher in comparison with the nuclear DNA mutation rate [14], which can result from the absence of protective histones, the nonexistence of effective DNA repair systems within mitochondria and additionally by being exposed to remarkable fluxes of oxygen, making mtDNA a presumable target for reactive oxygen species produced as by-products of OXPHOS. Another special feature is heteroplasmy, meaning that an individual may carry several allelic forms of mtDNA, present in singular proportions in special tissues [15,16]. In the context of the present thesis we will focus in some of the major mitochondrial biological functions, including, mitochondria dynamics, energy production, reactive oxygen species generation and antioxidant capacity, calcium buffering ability and apoptosis regulation, which had been associated with the pathogenesis of disease.

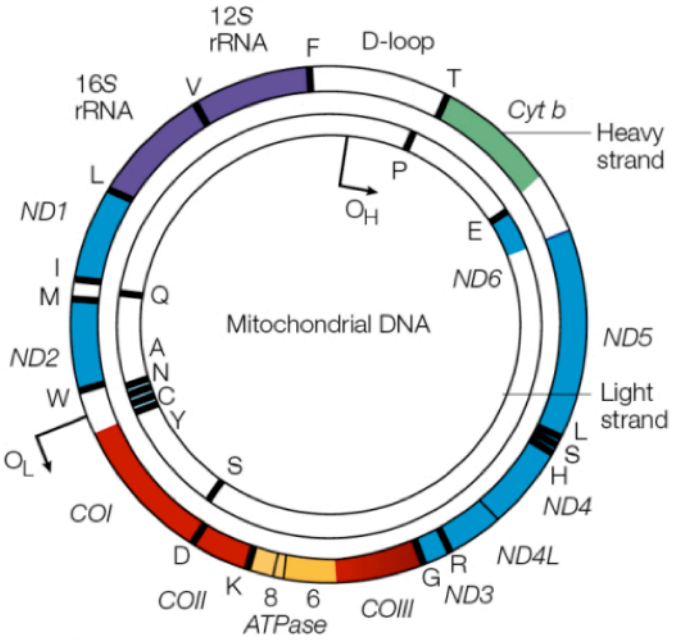

Figure 1.1 Human mitochondrial DNA map.
mtDNA showing location of selected genes. Human mtDNA is a 16569 base pair circular molecule that encodes seven (ND1, ND2, ND3, ND4, ND4L, ND5 and ND6) of the 43 subunits of complex I, shown in blue; one (cytochrome b) of the 11 subunits of complex III, shown in green; three (COI, COII and COIII) of the13 subunits of complex IV, shown in red; and two (ATPase 6 and 8) of the 16 subunits of complex V, shown in yellow. mtDNA also codes for two ribosomal RNAs (rRNAs; 12S and 16S), shown in purple; and 22 tRNAs, indicated by black lines and denoted by their single letter code, which are required for mitochondrial protein synthesis. The displacement loop (*D-loop*), or non-coding control region, contains sequences that are vital for the initiation of both mtDNA replication and transcription, including the proposed origin of heavy-strand replication (shown as OH). The origin of light-strand replication is shown as OL. Image adapted from Taylor et al 2005 [17] with permission (see appendix A1).

1.2.1.2 Mitochondrial morphology

The number of mitochondria varies widely by organism and tissue type. One mitochondrion can range from 2-10 μm length in different species [18]. Mitochondria also vary considerably in shape and size during different phases of the cell cycle [19]. Nevertheless, all mitochondria have a common basic structure (Figure 1.2) composed by compartments that carry out specialized functions. These compartments include the outer mitochondrial membrane (OMM), the intermembrane space, the inner mitochondrial membrane (IMM), the cristae, and the matrix (Figure 1.2). The outer membrane has rather identical amount of phospholipids and proteins, containing numerous integral channels called porins, which are permeable to all molecules up to 5,000 Da, including ATP, ADP, nutrient molecules and ions. One example is the voltage dependent anion channel (VDAC, Figure 1.2, element 13) that acts as a general diffusion pore for small hydrophilic molecules [20]. The inner mitochondrial membrane has numerous invaginations that form the "cristae" and supports the electron transport chain (ETC) components (Figure 1.2 panel C). IMM contains also the adenine nucleotide translocase (ANT), responsible for the exchange of adenine nucleotide (ADP) across the IMM [21]. The matrix is delimited by the IMM and contains mtDNA and several metabolic enzymes, including those from the Krebs cycle, where pyruvate is converted to acetyl coenzyme A and completely oxidized and degraded to generate energy in the form of ATP and reducing agents such as NADH or succinate-derived $FADH_2$ co-factor, carbon dioxide and water [5].

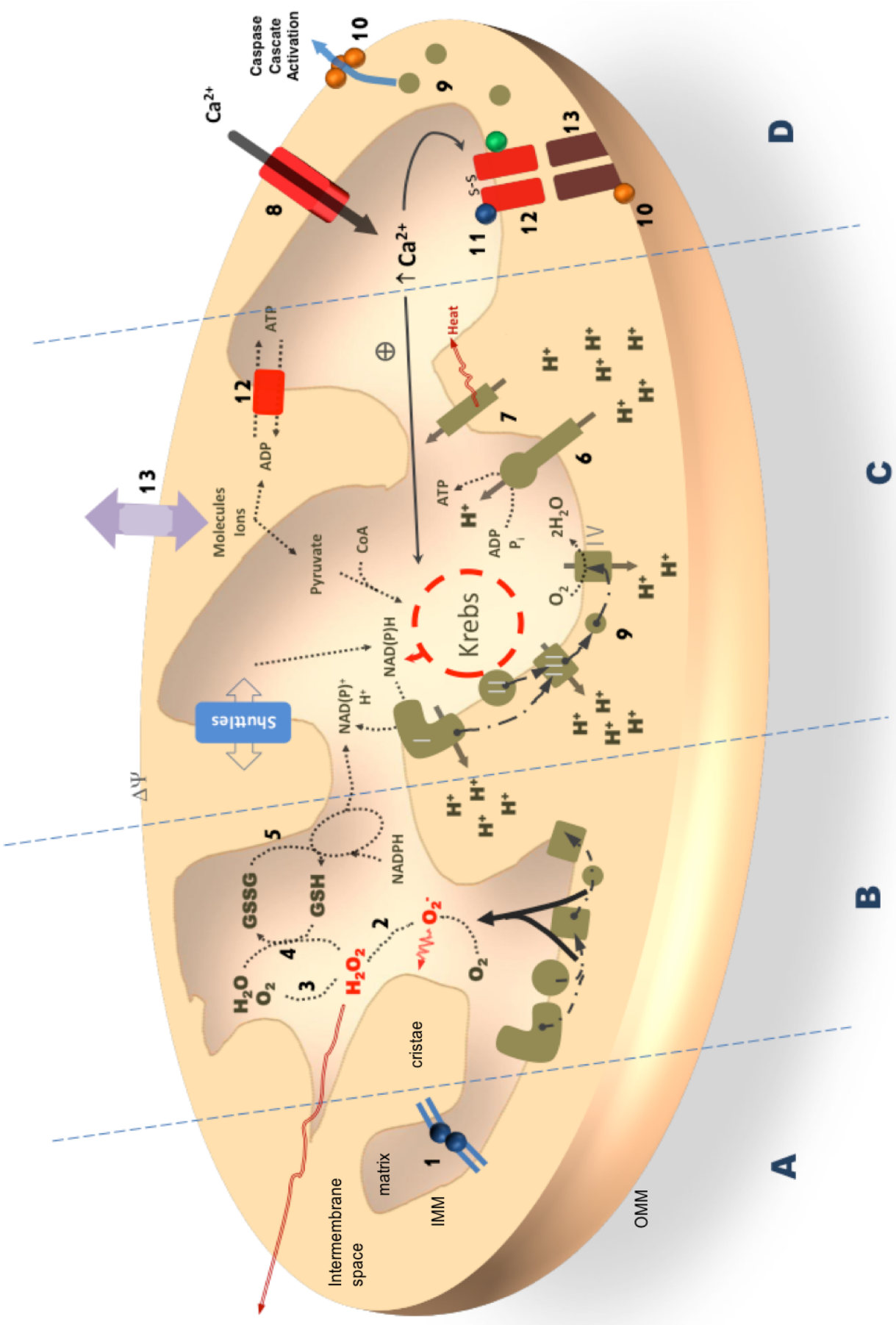
A
B
C
D
OMM
IMM
matrix
cristae
Intermembrane space
Krebs
Pyruvate
CoA
NAD(P)H
NAD(P)+
Shuttles
Molecules Ions
ATP
ADP
Heat
GSH
GSSG
NADPH
Caspase Cascate Activation
Ca2+
ΔΨ

Figure 1.2 Representation of mitochondrial functions.
Mitochondria are dynamic organelles which can undergo fission and fusion, remodeling of the cristae, and alteration of the mitochondrial network (Panel A). These events are regulated by specific proteins, e.g. mitofusin (1), and several phenomena can interfere with their normal physiology. Although mitochondria are effective 'machines' in the conversion of O_2 to water, 1-4% of the O_2 used in respiration is converted to superoxide anion by electrons from the mitochondrial respiratory chain (MRC; lower Panel B). The superoxide anion radical can damage lipid membranes and proteins, or can be dismutated by the superoxide dismutase enzyme (SOD2) to hydrogen peroxide, which is capable of diffusing to remote areas of the cytoplasm. As a detoxification mechanism, mitochondria convert H_2O_2 to water by means of catalase (3) or glutathione peroxidase (4). The latter enzyme oxidizes glutathione (GSH), which is recycled by glutathione reductase (5) through oxidation of NADPH. Panel C shows oxidative phosphorylation. Pyruvate is the bridge between glycolysis and the tricarboxylic acid (TCA) cycle, which produce substrates for the MRC. The electron flux from Complex I to Complex IV creates a proton motive force which can be used to phosphorylate ADP by the ATP synthase (6), or can be dissipated by the uncoupling proteins (UCPs; 7). Mitochondria can also participate in calcium homeostasis (Panel D). After uptake by the mitochondrial calcium uniporter (8), matrix calcium accumulation can have two distinct effects: at lower physiological concentrations, calcium can stimulate dehydrogenases in the TCA cycle, while, at higher concentrations, it can be harmful and induce the opening of the mitochondrial permeability transition pore (MPTP). The consequence of this last is outer membrane rupture and consequent release of cytochrome c (9) into the cytoplasm and cell death. However, cytochrome c can also be released without the loss of membrane integrity, through the formation of Bax oligomers (10) in the outer membrane. 11, cyclophilin D; 12, adenine nucleotide translocase (ANT); 13, voltage-dependent anion channel (VDAC); outer mitochondrial membrane (OMM) and inner mitochondrial membrane (IMM). Novel data has shown that the MPTP appears to be composed mostly from ATP synthase dimers [22]. Image from Pereira et al. 2009 [23] with permission (see appendix A2).

1.2.1.3 Mitochondrial dynamics

Mitochondrial dynamics has implications in many aspects of mitochondrial function and appears to be particularly important in mitochondria quality control [24]. Mitochondria form dynamic tubular networks that continually adjustment their shape and move through the cell (Figure 1.3). New proteins and pathways that control mitochondrial dynamics continue to be identified, demonstrating that the pathways orchestrating mitochondria behavior are more sophisticated than previously thought. Still, the most studied pathways are fusion and fission, which act by GTPases and their binding partners to regulate organelle connectivity, copy number, the redistribution of lipids and proteins along the cell [25–34]. Fission is a necessary event for the correct redistribution of mtDNA during cell division and also for the transport of mitochondria to daughter cells during mitosis and meiosis (Figure 1.3) [35]. On the other hand, fusion is a mechanism by which neighboring mitochondrial membranes fuse (Figure 1.3). It is accepted that this event occurs as a mean of recovering the activities of damaged/depolarized membranes, which ensures the

proper mixing of metabolites and mtDNA [30]. Another perspective may be that fission allows for genetic complementation between two mitochondria, which promotes ATP synthesis in oxygen-deprived regions of a cell through electrical transmission of mitochondrial transmembrane electrical potential across the mitochondrial network. Actually, the energy from GTP hydrolysis is crucial to facilitate the transmission of calcium signals and transmembrane electrical potential across distances in the cell [36]. Loss of fission results in a large network of fused mitochondria, whereas fusion disruption results in smaller mitochondria. Fusion is regulated by the proteins Mfn1, Mfn2, and Opa1 [35,37], while fission is regulated by the proteins Drp1 and Fis1 [38]. These proteins and others were found in both cardiac and non-cardiomyocyte cells and are regulated by post-translational modifications, mediated by ubiquitin and small ubiquitin-like modifier (SUMO) ligases [39]. Importantly, the mitochondrial dynamic behavior is not identical in all cell types and is strongly conditioned by the intracellular motility and the cytoskeleton dynamics [40]. Along these lines, the striated contractile cells of the adult heart and skeletal muscle have a very rigid cytoskeleton and their mitochondria are mostly stationary [41]. Nevertheless, the expression of *Mfn 1* and *Mfn 2* is significant in these cells with immotile mitochondria, indicating that mitofusins are biologically important in different contexts. Parra and collaborators described that ceramide-induced mitochondrial fragmentation in primary neonatal cardiomyocytes was co-occurring with elevated levels and co-localization of Drp1 and Fis1 and increased cell death [42]. By other side, Brady and collaborators were the first to show extensive fragmentation of mitochondria in HL-1 cells (a murine atrial derived cardiac cell line) as a response to simulated ischemia-reperfusion [43]. Importantly, cardiomyocyte-specific genetic interruption of either mitochondrial fusion or fission is incompatible with mammalian life [44–46]. Nevertheless, the actual interplay between mitochondrial dynamics, ROS production and mitochondrial respiration impact requires further investigation.

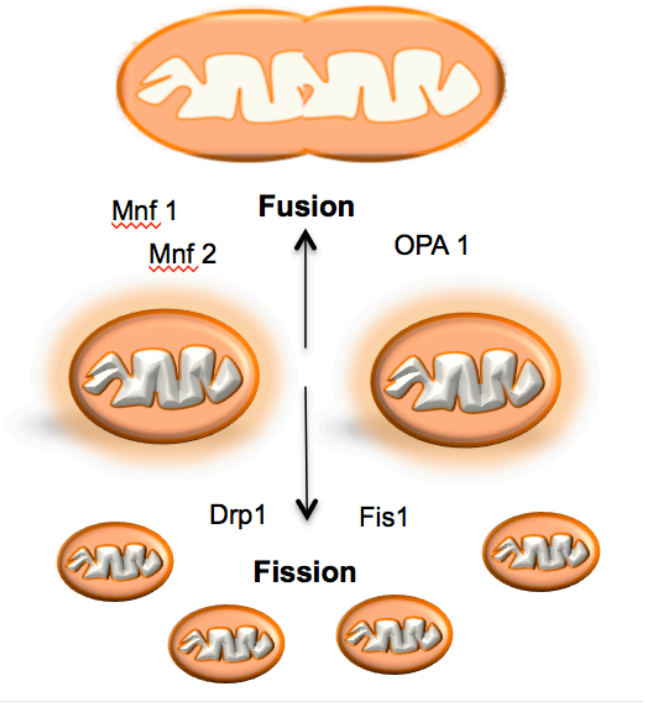

Figure 1.3 Mitochondrial dynamics.
Diagram of mitochondrial fusion–fission. Mitochondria are dynamic organelles that constantly undergo fusion and fission processes to maintain an interconnected network in healthy cells. Mitochondrial fusion is mediated by Mfn1, Mfn2, and OPA1, whereas fission mainly involves Drp1 and Fis1.

1.2.1.4 Mitochondrial oxidative phosphorylation and ATP production

Mitochondria produces about 90-95% energy to cells by electron transfer in the respiratory chain through a process called OXPHOS (Figure 1.4) [3,47]. Aerobic tissues rely on OXPHOS for ATP production and the overall process is greatly controlled and involves integration and balance of the oxidation of fatty acids, pyruvate, ketoacids and a range of other intermediary metabolites and regulatory ions such as calcium. Throughout glycolysis, glucose is converted to pyruvate in the cytosol, reducing cytosolic NAD^+ to NADH. Pyruvate is channeled to mitochondria via pyruvate dehydrogenase (PDH) yielding acetyl coenzyme A (acetyl CoA), NADH + H^+, and CO_2. Acetyl CoA enters the tricarboxylic acid cycle or Krebs cycle, generating NADH + H^+ [48]. Another energy pathway involved is the mitochondrial fatty acids oxidation via β-oxidation to generate Acetyl-CoA, NADH + H^+ and reduced FAD co-factor. Electrons originating from nutrients are carried to the electron transport chain by NADH and succinate and then transferred along a series of carrier molecules in the inner mitochondrial membrane (complexes I to IV). In

detail, two electrons are then transferred from NADH to the OXPHOS complex I (NADH dehydrogenase or NADH:ubiquinone oxidoreductase) or from fatty acids/succinate oxidation to the electron transfer flavoprotein dehydrogenase or complex II (succinate dehydrogenase, SDH; or succinate:ubiquinone oxidoreductase) respectively, to reduce ubiquinone (coenzyme Q10, CoQ) to ubiquinol ($CoQH_2$). Electrons are then transferred to complex III (ubiquinol cytochrome c oxidoreductase or cytochrome *bc1* complex), followed by electron passage through cytochrome c to complex IV (cytochrome c oxidase, COX; or cytochrome c: oxygen oxidoreductase), and ultimately to oxygen, generating H_2O.

The energy that is then released as electrons flow down the redox potential through the ETC is used to pump protons across the mitochondrial inter membrane space by complexes I, III and IV creating a proton electrochemical gradient, which is acidic and positive in the intermembrane space and negative and alkaline in the matrix side. The potential energy stored in the proton gradient is used to import proteins and calcium to the mitochondrial matrix, to generate heat and to synthesize ATP. The energy to convert ADP+Pi to ATP derives from the flow of protons through complex V (ATP synthase) back into the matrix. The matrix ATP can also be exchanged by cytosolic ADP through the ANT located in the IMM (Figure1.2). The production of ATP is conditioned by the effectiveness by which the protons are ejected out of the matrix by ETC complexes and by the proficiency by which proton flux through complex V can yield ATP. This means that the electron transfer is coupled to ATP synthesis via proton gradient, but OXPHOS machinery is actually prone to proton leakage, leading to variations in the coupling efficiency of the respiratory chain [3,5]. During OXPHOS, ATP production yield is up to 38 molecules of ATP, while during glycolysis, only 2 molecules of ATP are formed [5,49].

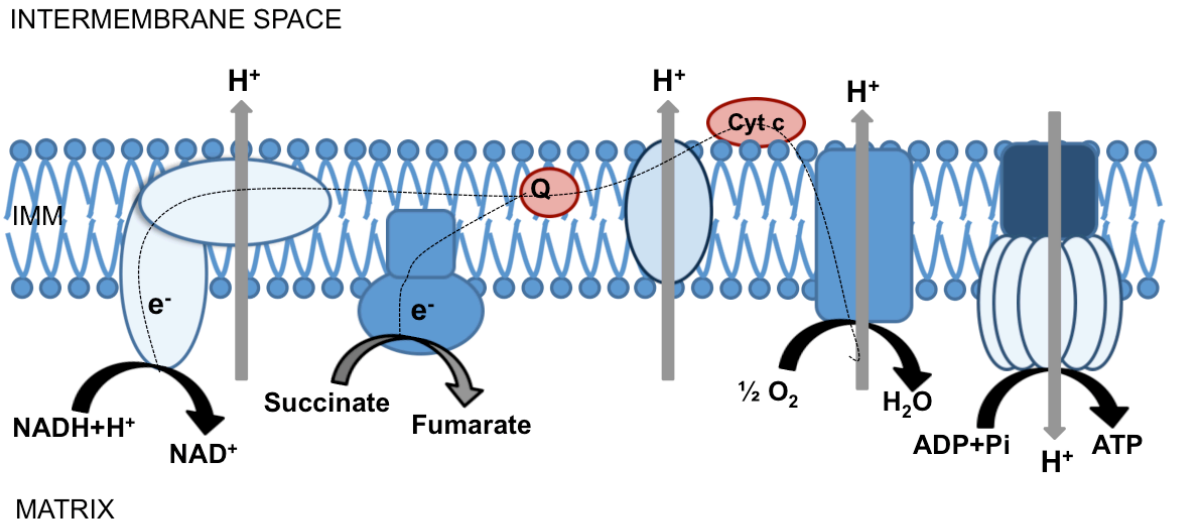

Complex I	Complex II	Complex III	Complex IV	Complex V
NADH dehydrogenase	**Succinate dehydrogenase**	**Ubiquinol cytochrome c oxidoreductase**	**Cytochrome c oxidase**	**ATP synthase**
47 Subunits 7 mtDNA/40 nDNA	4 Subunits 0 mtDNA/4 nDNA	11 Subunits 1 mtDNA/10 nDNA	13 Subunits 3 mtDNA/10 nDNA	17 Subunits 2 mtDNA/15 nDNA

Figure 1.4 Mitochondrial oxidative phosphorylation system.
OXPHOS is composed by the mitochondrial respiratory chain, formed by four enzyme complexes (complexes I - IV) and two intermediary substrates (coenzyme Q, Q; and cytochrome c, Cyt c), plus the complex V. The $NADH^+$, H^+ and succinate produced by the intermediate metabolism are oxidized further by the mitochondrial respiratory chain to establish an electrochemical gradient of protons, which is finally used by the ATP synthase (complex V) to produce ATP, the only form of energy used by the cell. Legend: DNA, deoxyribonucleic acid; mt, mitochondrial; n, nuclear; IMM, inner mitochondrial membrane; H^+, proton; NAD^+, nicotinamide adenine dinucleotide; NADH, nicotinamide adenine dinucleotide (reduced form); e-, electron; Cyt c, cytochrome c; ADP, adenosine diphosphate; ATP, adenosine triphosphate; Q, ubiquinone. Adapted from Bellance et al. 2009 [49].

1.2.1.5 Mitochondrial role in oxidative stress

Mitochondrial reactions are one intracellular source of superoxide anion ($\cdot O_2^-$) and other reactive oxygen species that may result from subsequent reactions of superoxide anion. During the transfer of electrons along the respiratory chain, single electrons occasionally leak out (Figure 1.5) and react with molecular oxygen to form the superoxide anion. Even though superoxide anion is not a strong oxidant, it is a precursor of other more reactive ROS, and it also becomes involved in the propagation of oxidative chain reactions. ROS are highly reactive and uncontrolled increase in the steady-state concentrations of these oxidants lead to free radical-

mediated chain reactions, which indiscriminately target proteins, lipids, polysaccharides and DNA (for review see Turrens 2003 [50]). Mitochondrial reactions are a major source of superoxide anion and other ROS that may result from subsequent reactions of superoxide anion [51]. The latter is converted into hydrogen peroxide (H_2O_2) by the mitochondrial enzyme superoxide dismutase (MnSOD or SOD2). Hydrogen peroxide is further metabolised by glutathione peroxide (Gl-Px) into H_2O. Hydrogen peroxide may lead to the generation of the highly-reactive hydroxyl radical ($^{\cdot}OH$) in the presence of ferrous iron, via the Fenton reaction. Superoxide anion can also react with nitric oxide to form the highly-reactive peroxynitrite anion ($ONOO^-$). Once mitochondrial enzymatic and non-enzymatic antioxidant systems are overwhelmed by ROS, oxidative damage and cell death can occur. Mitochondrial superoxide anion production can be significantly enhanced by functional impairment of the redox chain, especially of Complexes I and III [52,53]. Besides the detrimental side of ROS, we should also mention it beneficial side, which is acting as critical intermediates of cellular signaling pathways. A review from Hamanaka and Chandel [54] underlines a new insight into modulation of local oxidative stress and its advantages to the cell, low levels of ROS are required for cellular processes such as proliferation and differentiation, pointing a new direction for the modulation of ROS production as a means to achieve a beneficial therapeutic outcome.

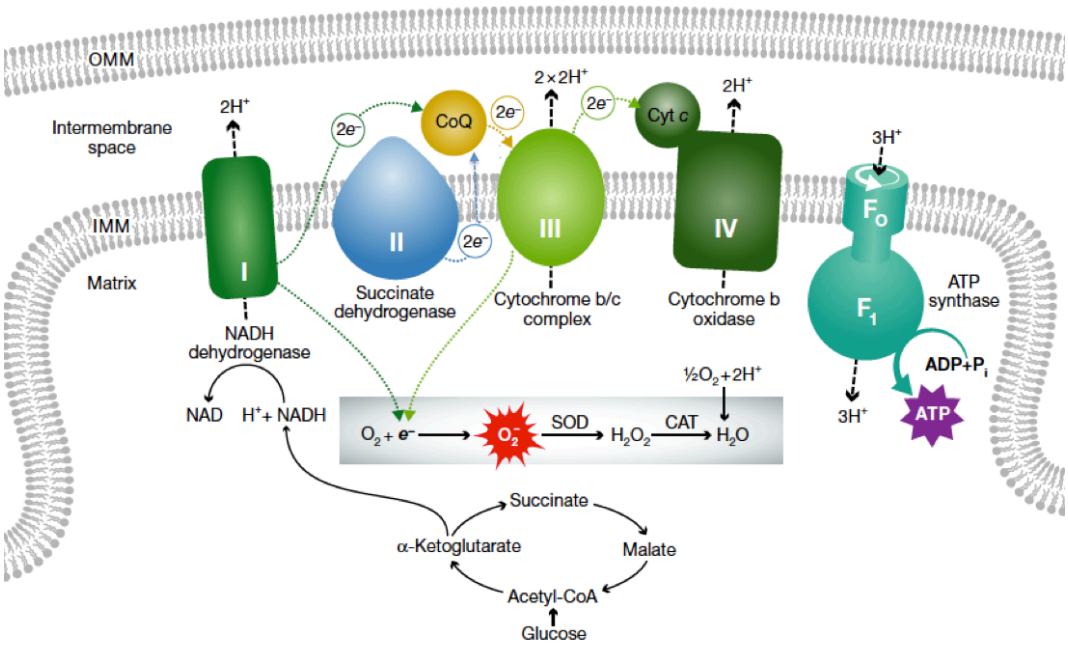

Figure 1.5 The mitochondrial electron transport chain and its relationship to ROS production.

Each of the inner mitochondrial membrane (IMM) ETC enzymatic complexes is colored and indicated by their respective roman numerals (I-V). Electrons are transferred between complexes (dotted arrows), promoting proton (H^+) transport (dashed arrows) from the matrix to the intermembrane space. Proton flow through ATP synthase (complex V) converts ADP to ATP. Normally, O_2 is the terminal electron (e^-) acceptor from complex IV. Electron leak from complexes I or III of damaged mitochondria can produce toxic reactive $\cdot O_2^-$ and H_2O_2. mtDNA mutations can affect complexes I, III, IV, and V, but not complex II that is comprised entirely of nuclear-encoded proteins. Image from Dom 2015 [34] under the terms of the Creative Commons Attribution License (see appendix A3).

1.2.1.6 Mitochondrial antioxidant capacity

Cellular antioxidant defenses have evolved to an efficient network system for prevention, interception and repair of oxidative damage. Antioxidant defenses consist of nonenzymatic scavengers and quenchers, known as antioxidants, as well as enzymatic systems including superoxide dismutases and hydroxyperoxidases, such as glutathione peroxidase, catalase and other hemoprotein peroxidases [55].

Superoxide dismutase (SOD) exists as three different isoforms: SOD1 is a Cu/Zn SOD located in the cytoplasm and in the intermembrane space [56], SOD2 is a manganese superoxide dismutase that is exclusively located in the mitochondrial matrix (MnSOD) [57,58] and SOD3 is a Cu/Zn SOD that has an extracellular localization [59]. Mice lacking mitochondrial MnSOD (SOD2) cannot survive more than a few days after birth suggesting that control of a tight level of mitochondrial superoxide anion is critical for cell survival [60].

Among the arsenal of antioxidants and detoxifying enzymes present in mitochondria, mitochondrial glutathione (GSH) emerges as the main line of defense for the maintenance of the appropriate mitochondrial redox environment to avoid or repair oxidative modifications leading to mitochondrial dysfunction and cell death. GSH acts by reducing cysteine disulfide bonds formed within cytoplasmic proteins by serving as an electron donor [61,62]. GSH importance is based not only on its abundance, since the concentration of the two glutathione forms (GSSG/GSH) is so much higher than that of any other system [63] with mitochondrial matrix glutathione representing 10-15% of the total glutathione in the liver as well as in renal proximal tubules [64,65], but also on its versatility to counteract hydrogen peroxide, lipid hydroperoxides, or xenobiotics, mainly as a cofactor of enzymes such as glutathione peroxidase (Gl-Px) or glutathione-S-transferase [65]. Glutathione peroxidase exists in two forms in mitochondria: Gl-Px1 and phospholipid-hydroperoxide Gl-Px (PHGPx) [66]. The phospholipid hydroperoxide glutathione peroxidase is inducible

under various stress conditions. This enzyme catalyzes the regeneration of phospholipid hydroperoxides using the reducing power of GSH, being present in the cytosol and in the inner mitochondrial membrane of animal cells, while GPX1 occurs mainly in the mitochondrial matrix. Both enzymes use reduced glutathione (GSH) in order to reduce hydrogen peroxide into water, generating glutathione disulfide (GSSG) in the process, which can form protein-mixed disulfides and thus inhibit protein function [67]. The enzyme glutathione reductase can regenerate GSSG to GSH by using NADPH as a co-factor [62]. GSSG is accumulated inside the cells, and the ratio of GSH to GSSG is a good indicator of oxidative stress [68]. The GSH/GSSG redox couple can readily interact with most of the physiologically relevant redox couples, undergoing reversible oxidation or reduction reactions, thereby maintaining the appropriate redox balance in the cell [62,65].

In physiological conditions, the primary defense against superoxide anion and hydrogen peroxide in mitochondria not containing catalase is performed by the concerted action of the above mentioned superoxide dismutase and Gl-Px. However, despite the activity of these enzymes, significant amounts of hydrogen peroxide can diffuse out from mitochondria to cytosol, where detoxification occurs through cytosol Gl-Px or by peroxisome catalase, with catalase representing a key antioxidant defense mechanism for myocardial tissue [69]. Catalase enzyme activity may control the amount of hydrogen peroxide available to produce hydroxyl radical, with these species likewise causing peroxidation of the phospholipid bilayer, with consequent severe damage to membrane integrity. Also, excessive ROS production can trigger the MPTP with release of cytochrome c and activation of cell death [70]. Also, it is known that electron chain complexes and Krebs cycle enzymes in heart mitochondria can be inactivated by hydrogen peroxide. Target enzymes include succinate dehydrogenase, alpha-ketoglutarate dehydrogenase and aconitase [70]. Catalase represents the most economical way of removing hydrogen peroxide is through, since no reducing equivalents are consumed in the process [70].

We would like to highlight that despite glutathione and other systems to keep redox balance, mtDNA is highly susceptible to ROS-generated damage due to proximity to oxidant generation and limited DNA repair [71].

1.2.1.7 Mitochondrial role in calcium homeostasis

Regulation of cytosolic Ca^{2+}concentration provide signals to central events such as muscle contraction, neurotransmitter release, alterations in gene transcription and even cell death [72]. Mitochondria play a major role in shaping cellular calcium signaling. Mitochondria not only take up Ca^{2+} at physiological cytosolic Ca^{2+} concentrations but it has also been shown that mitochondrial Ca^{2+} accumulation rigorously controls the energetic metabolism of the cells. Mitochondria participate in Ca^{2+} signaling as a result of their close apposition to Ca^{2+} release (endoplasmic reticulum, ER [73] and Ca^{2+} entry sites (plasma membrane), where microdomains with high local Ca^{2+} concentrations are formed. Mitochondrial Ca^{2+} accumulation contributes to influential cytosolic Ca^{2+} fluctuation, in turn modulating cellular functions regulated by Ca^{2+} variations [74]. The capacity of mitochondria to accumulate calcium in the matrix depends on the proton gradient, and involves the mitochondrial calcium uniporter (MCU) for uptake, and the antiporters (Na^{+}/Ca^{2+} or H^{+}/Ca^{2}) which export Ca^{2+} from mitochondria. Upon accumulation, mitochondria slowly release calcium back to the cytosol via the antiporters [75,76]. Mitochondria acts as localized cytosolic calcium buffering organelles, modulating several events of Ca^{2+} feedback inhibition or activation [77]. Calcium regulation directly modulate the activity of enzymes located in the matrix such as several dehydrogenases (liver and heart), metalloproteinases (e.g. in cancer cells) and ATP synthase (in heart and skeletal muscle) [78]. On the other hand, in contrast to the beneficial effects of Ca^{2+}, its excess can trigger the MPTP, representing the pathological effects of Ca^{2+}on mitochondria, by triggering cell death and necrosis [74,79–81].

1.2.1.8 Mitochondrial role in cell death

Mitochondria are pivot organelles of convergence and integration of both survival and death signaling pathways. Mitochondria can diffuse death signals between each other and to other organelles such as the sarco-/ER and the nucleus. The mitochondrial power to cause cell death can be tracked by three main factors: increased ROS production, impaired Ca^{2+} homeostasis and mitochondrial permeability transition pore (MPTP) activity.

When a stress stimulus reaches the death/survival threshold, several changes in mitochondrial physiology and ultrastructure, can occur, leading to lethal alterations in the cell. Cell calcium overload, in addition to several stressors, including oxidants,

can cause a sudden increase in the permeability of the IMM, a phenomenon called mitochondrial permeability transition (MPT) that is caused by the opening of the MPTPs. The MPT was initially proposed by Haworth and Hunter in 1979, to be one result of the interaction between excessive calcium accumulation and the alteration of mitochondrial physiology [82]. Up to that time, the MPT was considered to be an *in vitro* artifact with little pathophysiological relevance. Today, however, it has received considerable attention as a potential mechanism for the induction of cell death in different pathologies including neurodegeneration and cardiac disease [5,83,84]. The MPT is normally associated with a deregulation of Ca^{2+} homeostasis. This phenomenon increases the IMM permeability to molecules of less than 1450 Da [5,84–86], and leads to a loss of ionic homeostasis, then to matrix swelling, OMM rupture and cell death. MPTP forms at contact sites between the IMM and OMM [5,84,85]. Based upon initial biochemical and pharmacological studies, it was proposed that the MPTP contains a restricted set of proteins, including the unselective voltage-dependent anion channel (VDAC) in the OMM, the adenine nucleotide translocase (ANT) in the IMM, and cyclophilin D (CypD) in the matrix [86]. Knockout studies, however, indicate that CypD is the only mandatory component of the MPTPs [5,83]. A role for the phosphate transporter in the MPTP complex was later proposed [22,86]. Lately, novel data has shown that the MPTP is actually composed mostly from ATP synthase dimers. The opening of MPTPs requires matrix Ca^{2+} and Pi, and is regulated by the H^+ electrochemical gradient, in the sense that depolarization favors MPTP opening, while extra-mitochondrial acidification inhibits the phenomenon [87]. Oxidative stress is also a known inducer of the MPT, decreasing the calcium threshold for MPTP opening [83]. Irrespective of the initiating mechanism, MPT can cause in some circumstances mitochondrial swelling with matrix expansion and unfolding of the cristae, although this is rarely seen *in vivo*. When matrix expansion exceeds the viscoelastic resistance of the OMM, the latter will burst, and the release of pro-apoptotic intermembrane space proteins, most notably cytochrome c and Smac/DIABLO) will occur. Apoptosis or necrosis may follow, depending on the local ATP levels [86].

As we described, upon different apoptotic stimuli, mitochondria release different proteins such as cytochrome c, Smac/DIABLO and the AIF (apoptotic-inducing factor), which contribute to the apoptotic phenotype [88]. Protein release from mitochondria is complex and includes the oligomerization on the outer

mitochondrial membrane of the pro-apoptotic proteins Bax and Bak, which form a channel permeable to cytochrome c. Nevertheless, despite the initial assumption that the MPT is only involved in necrosis, it appears that MPTP opening is a strong candidate to mediate Ca^{2+}-dependent induction of apoptosis [89,90]. These changes were prevented by Bcl-2 expression as well as by experimental conditions that prevented the rise in cytosolic Ca^{2+} [91]. The alteration of the Ca^{2+} signal reaching mitochondria and/or the combined action of apoptotic agents or pathophysiological conditions (i.e. oxidative stress) can induce a profound alteration of the organelle structure and function [92,93]. Zamzami and collaborators found that mitochondrial fragmentation during apoptosis was closely related with the collapse of the mitochondrial membrane potential. The collapse of mitochondrial membrane potential was considered a point of no return in the death cascade [94], with the integrity and function of outer mitochondrial membrane regulated by proteins of the Bcl-2 family [95,96]. Bcl-2 family members regulate mitochondrial outer membrane permeabilization resulting in the release of cytochrome c, Smac/DIABLO and Omi/HtrA2 and subsequent caspase activation. The Bcl-2 family includes pro- and anti- apoptotic proteins [97] with anti-apoptotic proteins, including Bcl-2 or Bcl-XL, inhibiting the function of pro-apoptotic proteins, such as Bax or Bak. An important subgroup of pro- apoptotic Bcl-2 members is the 'BH3-only' proteins (Bik, Bid, Bim, Bad, Puma), which have a pro-apoptotic role by either activating pro-apoptotic proteins (Bax and Bak) or inhibiting anti-apoptotic members (Bcl-2, Bcl-XL). However, the mechanisms by which the pro-apoptotic Bcl-2 family members regulate the permeabilization of the outer mitochondrial membrane remains controversial [98].

Another form of programmed cell death, autophagic cell death, which is morphologically characterized by the occurrence of numerous autophagic vacuoles has been described [99]. Autophagy is a fundamental route by which macromolecules and organelles can be dispensed to lysosomal degradation. It is assumed that uncontrolled or excessive autophagy can cause cell death via the broad degradation of cytoplasmic constituents [99]. However, it is possible to act though pharmacological or molecular means to inhibit this phenomena preventing cell death [99]. One of the critical homeostasis events requiring autophagy is the removal of damaged or excessive mitochondria (mitophagy). Mitophagy refers to the specific elimination of mitochondria by autophagy [100]. Mitophagy prevents the release of pro-apoptotic proteins from permeable-damaged mitochondria in mammalian cells, with loss of

mitochondrial membrane potential appearing to be a common feature of mitophagy [100–103]. Mitophagy is observed in starved hepatocytes treated with glucagon [104] and in serum-starved neurons treated with caspase inhibitor [105]. Emerging studies suggest mitochondrial morphology to be essential in the selection of damaged depolarized mitochondria for removal by mitophagy [30]. It is now accepted that mitochondrial fusion enables the transfer of soluble and membranous components (including mtDNA) between neighboring mitochondria, thereby providing a mechanism for renewing function in damaged mitochondria [106]. Specifically, selective mitochondrial fusion between two polarized mitochondria occurs along with mitochondrial fission (division) that results in one polarized daughter mitochondria and one depolarized mitochondria to be degraded [30]. This mechanism further supports the theory that the frequency and selectivity of fusion is required to maintain healthy mitochondrial function and allow mitophagy to take place [107].

The seminal work from Huang and collaborators highlight the importance of autophagy and mitophagy in cardiac function, with mitophagy playing a critical role in protecting the heart during ischemia/reperfusion injury [108,109] These results suggested that mitophagy is part of the final common pathway for various cardioprotective interventions, and indeed, may be the ultimate effector [109]. Mitophagy and mitochondrial biogenesis are opposing forces that govern the rate of mitochondrial turnover. This dynamic tension allows for a readily adjustable population of mitochondria to match cellular demands.

1.2.1.9 Mitochondria: from heroes to villains

In addition to the functions previously described we could cite other specific roles of mitochondria related to the cell type in which they are found. Although mitochondria are present in every nucleated cell, they are found in high concentrations in cells with higher energy requirements, such as skeletal muscle cells or in cells with fat storage functions, such as brown fat cells [110]. For instance, mitochondria participate in the production of hormones such as estrogen and testosterone [111]. They are required for cholesterol metabolism, neurotransmitter metabolism, and detoxification of ammonia in the urea cycle [112–114]. Therefore, if mitochondria become dysfunctional, the cell-energy production becomes unbalanced as well as the production of cell-specific components needed for a normal cell functioning (Figure 1.6). Imbalance between energy production and energy demand,

and a disturbance in energy transfer networks, play an important role in various pathologies. Mitochondria regulate the cellular redox state and play very important roles in ionic regulations, namely in Ca^{2+} homeostasis, and in apoptosis [88,115] and can be contemplated as an fundamental part of multiple cellular signaling and a intermediary of cell communication and survival [116,117]. Moreover, mitochondria are mediators in pathophysiological mechanisms of ischemia-reperfusion injury, oxidative stress, preconditioning, inherited diseases, toxicological injury, and side-effects of pharmacological treatments [5,118]. Damaged mitochondria cause organ injury also by several mechanisms, including the diminished cellular energy status (energy stress), production of reactive oxygen species (oxidative stress), disturbance of ionic balance, cytochrome c release and induction of apoptosis (Figure 1.6).

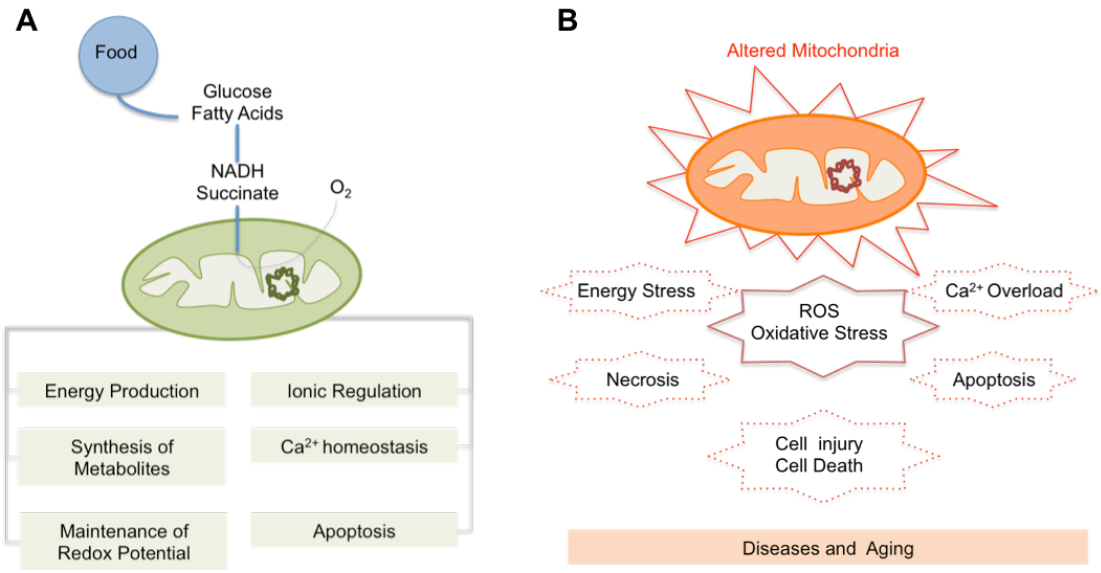

Figure 1.6 Key roles of mitochondria.
(A) In normal cell function. (B) In injury.

1.2.2 Role of mitochondria in cardiac development

1.2.2.1 Cardiac development

The development of the heart is a complex process of interaction between molecular and cellular mechanisms as well as haemodynamic forces. Its complexity is reflected in the fact that cardiac defects represent more than a third of all congenital malformations in humans [119]. During fetal developmental stages, the heart actually takes on several distinct appearances. These heart structures are similar to what occurs in other animal hearts. When the human heart first begins to form, it looks

much like a fish heart, with the structure of a simple tube. Then, fast growth origins the tube to bend and twist backward, starting the establishment of the familiar shape. The second phase of heart development creates two chambers, resembling a frog heart. The third phase initiates when the two atria become completely separate and the ventricles are just beginning to separate, with the fetal heart resembling that of a turtle or a snake heart. Finally, the ventricles gain their individuality completely originating the four-chambered heart structure that distinguishes the human heart from other living creatures [119].

Myocytes are capable of contraction from their first appearance in the heart. As gestation proceeds, myocytes elongate, develop sarcoplasmic reticulum and t-tubules, and their myofilaments become orientated to increase contractile force. Throughout gestation myocytes divide, so that the heart increases in size through hyperplasia. Interestingly, just before or after birth (depending in the species) myocytes cease to divide, and any further growth throughout life must occur by hypertrophy. It is admirable that the same cardiomyocytes that produce heartbeats in our early life must continue to do so throughout our lives! However, a seminal work from Mollova and collaborators in 2013, revealed that cardiomyocytes proliferation contributes to heart growth in young humans, occurring between the age 1-20 years of life, in where the number of cardiomyocytes in the left ventricle increased 3.4 fold, showing that cardiomyocytes proliferation contributes to development heart growth in young humans. This also is a clue that children and adolescents may be able to regenerate myocardium [120].

Hom and collaborators [121] reported that cardiomyocytes differentiation in the embryonic heart is coordinated by mitochondrial maturation. The authors described that at embryonic day (E) 9.5 the mouse heart contains scarce and immature mitochondria, which exhibited rare and disorganized cristae. At E13.5, hearts presented matured mitochondria exhibiting abundant laminar cristae and an increased mitochondrial mass. We could look at these outcomes as a consequence, rather than a cause of cardiomyocytes differentiation and assume that might be regarded to increased contractile and therefore metabolic demands of the developing heart. However, the authors validate that mitochondrial maturation induces cardiomyocytes differentiation. Cardiomyocytes from E9.5 hearts display increased levels of ROS and a reduced mitochondrial membrane potential in comparison to E13.5 cardiomyocytes. These characteristics have been associated with the inducting

of the MPTP within the inner mitochondrial membrane and propose that in early embryonic cardiomyocytes, the MPTP is open but closes during developmental progression. Indeed, Hom and collaborators were able to block the MPTP by pharmacological or genetic manipulation in E9.5 cardiomyocytes, resulting in morphological maturation and functional mitochondria. This effect was determined by intracellular ROS levels, which are elevated in E9.5 cardiomyocytes but drop upon physiological levels as well as induced closure of the MPTP. In this relevant work, the authors demonstrated that reducing ROS levels pharmacologically in early cardiomyocytes mimics the effect of MPTP closure and promotes cardiac differentiation. However, we should take in consideration that the effect of ROS on embryonic heart might be dependent on the stage and dose, evidencing that the balance between ROS and antioxidant enzymes can modulate embryogenesis [121,122].

Kasahara and collaborators [45] presented another mitochondrial mechanism involved in cardiomyocytes differentiation. Mitochondrial fusion was required for proper cardiomyocytes development in the embryonic mouse heart. When the authors performed the ablation of mitochondrial fusion proteins (Mfn1 and Mfn2), this resulted in arrested mouse heart development by interrupting cardiomyocytes proliferation and blocking fetal cardiac development. The findings by Cheng and collaborators also support the idea of a crucial role for Mfn1 and Mfn2, since combined Mfn1/Mfn2 ablation was lethal after E9.5 and conditional combined Mfn1/Mfn2 ablation in adult hearts induced mitochondrial fragmentation, cardiomyocytes respiratory dysfunction, and a rapidly progressive and lethal dilated cardiomyopathy [123]. For a better understanding of this theme consult the excellent review by Dorn et al 2013 [124].

1.2.2.2 Mitochondria and the cardiac metabolism

The heart has the largest metabolic demands per gram of any organ in the body. Adequate amounts of chemical fuel, namely ATP, must be generated to support the heart's contractile demands and maintain viability. Fatty acids, carbohydrates and ketone bodies are the principal substrates of the heart metabolized to generate ATP (Figure 1.7). In cardiomyocytes, ATP is mostly used by myofibrillar actin-myosin ATPase to fuel contraction and relaxation processes. ATP is also consumed by Ca^{2+} ATPase in the sarcoplasmatic reticulum to support Ca^{2+} reuptake and by sarcolemmal Na^{+}/K^{+} ATPase to maintain membrane potential, as well as by anabolic

reactions and by signaling systems [125,126].

Although the concentrations of high-energy phosphates are higher in muscle than in many organs, the levels are still small when compared to the rates of cardiac ATP consumption. For a better notion, if ATP synthesis stopped and utilization rates are kept unchanged, the myocardial ATP stores would be depleted in less than 15 seconds [127]. So, for myocardial life, ATP production and utilization must be narrowly adjusted. There are primarily two pathways for ATP synthesis, oxidative phosphorylation and substrate phosphorylation, with OXPHOS providing more than 95% of the ATP synthesized in the heart [128]. The principal types of carbon substrates used for myocardial ATP synthesis are fatty acids, carbohydrates, and ketone bodies [129–131]. Fatty acids are the predominant substrate used in the heart and generate largest amount of ATP. Succeeding uptake of free fatty acids from plasma with specific sarcolemmal fatty acid transport proteins, they are activated by fatty acyl coenzyme A (acyl-CoA) synthetase and esterified with coenzyme A to form fatty acyl-CoA, which is soluble. After entry into mitochondria, fatty acyl-CoA condenses with carnitine to form acylcarnitine and regenerates fatty acyl-CoA, which undergoes a process of beta-oxidation that takes place in the mitochondrial matrix, producing acetyl-CoA that can enter the Krebs cycle, and NADH and succinate-derived $FADH_2$ co-factor that can enter the electron transport chain [132]. Other source of energy are ketone bodies, they are formed in the liver at times of low blood glucose or during caloric restriction or fasting. They are not metabolized in the liver but other tissues, including muscles, can use them. Two ketone bodies used by the heart are acetoacetate and 3-hydroxybutyrate. In the heart, both molecules are converted into acetyl-CoA, which enters the TCA [125,133]. Myocardial glucose transport depends on the blood glucose concentration and activity of transport proteins, GLUT 1 and GLUT 4 [134], being primarily regulated by insulin [134,135]. The first step of intracellular glucose metabolism is phosphorylation, after which glucose can either enter glycolysis or be stored as glycogen. Glycolysis account for about 4% of myocardial ATP [136]. The pyruvate dehydrogenase reaction is a central step feeding the products of glycolysis or lactate directly into acetyl-CoA for entry into the TCA cycle. Modulation of PDH by fatty acids, for example, limits glucose entry into the TCA and is a critical step regulating myocardial substrate choice and utilization [137]. Lactate oxidation is another important source of pyruvate for PDH, meaning that lactate produced by other organs and skeletal muscle can be obtained from the blood and

rapidly oxidized by lactate dehydrogenase into pyruvate. Pyruvate enters mitochondria with H^+ by means of a special channel located in IMM, in co-transport with H^+. PDH activity depends on the activation state of the enzyme, which is inactivated by PDHK and activated by dephosphorylation by PDH phosphatase [137,138].

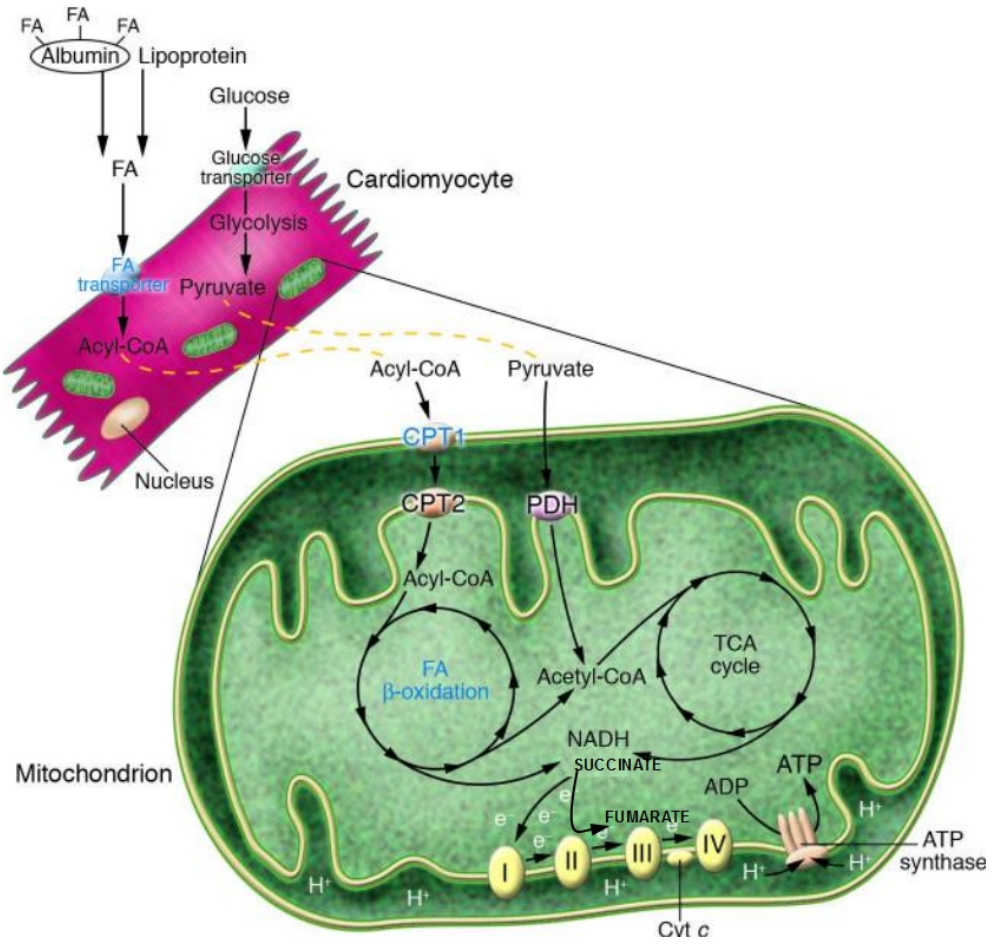

Figure 1.7 Pathways involved in cardiac energy metabolism.
Fatty acid (FA) and glucose oxidation are the main ATP-generating pathways in the adult mammalian heart. Acetyl-CoA derived from FA and glucose oxidation is further oxidized in the TCA cycle to generate NADH and succinate-derived $FADH_2$ co-factor, which enter the OXPHOS pathway and drive ATP synthesis. CPT1 and CPT2, carnitine palmityl transferase 1 and 2; PDH, pyruvate dehydrogenase; Cyt c, cytochrome c. Image adapted from Huss et al. 2005 [126] under the terms of the Creative Commons Attribution License (see appendix A4).

1.2.2.3 Mitochondria, the heart of the matter

Remodeling a fetal into an adult heart is a complex process and relies on important transitions that are triggered shortly after birth. During this early postnatal stage the heart undergoes a switch in substrate utilization to catabolize fatty acids, and carbohydrates become a secondary source of energy [139]. Furthermore, mitochondrial density doubles in cardiac myocytes during early post-natal development, and the small, round and tubular mitochondria that are found in fetal hearts are reformed into large ovoid and rectangular mitochondria [140]. This histological evidence supports that mitochondrial remodeling is important for the passage of the heart from a fetal to an adult state. The proposal that mitochondria are essential to many different aspects of normal heart functioning seems unquestionable. Mitochondria are the source of ATP that drives excitation/contraction coupling. These organelle sense smooth endoplasmic reticulum calcium release to adjust metabolism and anticipate actual physical need [124]. They are a major source of ROS that can act as either physiological signals or damaging elements [141]. Mitochondria can also control the fate of the cell and regulate cardiomyocytes cell death [142]. Finally, mitochondria regulate cardiomyocytes differentiation and embryonic cardiac development [45,143]. Given the multifaceted impact of mitochondria on cardiac development, minute by minute heart functioning, and cardiomyocytes suicide, one might adversely impacting mitochondrial function would be a common cause of cardiac disease [144]. So an understanding of mitochondrial cardiac metabolism is critical for appreciating the causes and consequences of deranged cardiac metabolism in pathologic states.

1.2.3 Role of mitochondria in renal development and disease

However, scarce information exists on kidney energy and metabolism during fetal life. High glycolytic-enzyme activity has been reported as well as oxidation of long-chain fatty acids towards the end of fetal life. Since long-chain fatty acids are the main energy source in the adult renal cortex, this suggests some mitochondrial oxidative capacity [145]. After birth, acute kidney injury is a common clinical entity that is associated with high mortality and morbidity. Acute kidney injury is actually a risk factor for the development and progression of chronic kidney disease. Currently, no successful treatment for acute kidney disease is available, and novel therapeutic approaches are desperately needed. Accumulating evidence highlights mitochondrial dysfunction as an important factor in this pathogenesis [146]. Mitochondrial disease affecting the kidney usually involves the proximal tubules. Ninety percent of oxygen consumption by the kidney is used to generate ATP for Na^+/K^+ ATPase in the proximal tubules and ascending Henle's loop. Dysfunction results in renal Fanconi syndrome with urinary losses of electrolytes, glucose, bicarbonate, amino acids, calcium and phosphate, and water [147]. This occurs more often in children than adults. Loss of phosphate can result in rickets, which consists in softening and poor mineralization of the bones leading to skeletal deformities, and loss of water can produce a dehydrated state. The loss of bicarbonate and subsequent metabolic acidosis can be associated with tissue failure. Less common presentations include more isolated renal tubular acidosis, Bartter syndrome (people affected by Bartter syndrome loose too much sodium through the urine) [148], nephrotic syndrome associated with glomerulosclerosis [149] and tubulo-interstitial nephropathy.

Taking in consideration that mitochondrial OXPHOS provides the ATP that kidneys require for tubular reabsorption, and that the enzymes primarily involved in the metabolism of free ammonium ions are the cytosolic enzyme glutamine synthetase and the mitochondrial enzymes glutaminase [150] and glutamate dehydrogenase [151], it becomes clear that mitochondrial homeostasis is critical for kidneys function [152]. The main pathological phenotype of acute kidney injury is tubular damage, including apoptosis [153] and what has also been largely labeled as a state of tubular ATP depletion [154]. Thus, the present consensus view is that mitochondria play an important role in the pathogenesis of acute kidney injury. In fact, mitochondrial dysfunction is an established component of the pathogenesis of acute kidney injury,

especially as a cause of renal tubular dysfunction and cell death [155]. Under the stress conditions that induce acute kidney injury, mitochondrial fragmentation and the MPT make a significant contribution to tubular cell death. For review about the mitochondrial participation in kidney diseases please consider the review by Ishimoto and Inagi [146].

1.3 The renal-cardiac axis in human disease

As nephrons are the functional units of the kidney a reduction in its number is considered unfavorable to kidney physiology. Nephron deficit is implicated in hypertension and renal disease in adult kidney [156]. The causal link between nephron number and cardiovascular/renal function was first proposed by Brenner and collaborators [157]. The Brenner's hypothesis was that a decline in renal filtration surface area, mainly resulting to either reduced nephron number or diminished filtration surface area per glomerulus, would limited sodium excretion, inducing secondary hypervolaemia, which is characterized by an increased volume of circulating blood, which promotes an increase in glomerular capillary pressure. Over time this excessive workflow and pressure causes glomerular sclerosis [157], trigging a vicious cycle with more reduction in filtration surface area and increasing in systemic blood pressure. Keller and collaborators [158] reported an inverse association between nephron endowment and hypertension in humans. However, it was unclear whether the lower numbers of nephrons in subjects with a history of hypertension were responsible for hypertension or a consequence of hypertension. Strong evidence supports the hypothesis that there is an association between nephron number and blood pressure. Unfortunately, due to the fact that present methods for estimating human nephron endowment can only be conducted post mortem, it is not possible to determine cause and effect.

1.4 The maternal testament

1.4.1 Implications of the nutrition during pregnancy

Deficient maternal nutrition in pregnancy impairs fetal development [159]. In the first half of gestation, placental size and growth are superior than fetal, and the placenta

itself has substantial nutritional requirements for proper formation and function. However, in a situation of reduced food intake by the mother, a higher proportion of glucose and amino acids leaving the uterine circulation crosses to the fetuses instead of being utilized by the placenta. These phenomena can account, at least in part, for the vast diversity of outcomes in fetal growth for the same condition, the reduced nutrition of the pregnant woman. However, several epidemiologic studies reported that the consequences of reduced nutrition in pregnancy could be extensive, even if the effect appears to be subtle during fetal and neonatal life. It is now well accept that the intrauterine environment, including nutrition, determine the risk for several diseases including coronary heart disease, hypertension, stroke and type 2 diabetes [160].

Large human epidemiological studies have indicated that the risk of renal and cardiac diseases in adult life is correlated with low birth weight (LBW) for the age, however, it is unlikely that the condition is so simple, as birth weight is determined by a multifaceted interaction of factors. We should also take into account that body proportions at birth, growth rate and diet during childhood play important roles. Nevertheless, these elegant studies raised the notice of a "womb environment" and the crucial role of the maternal nutrition during fetal development, generating a drastic revision of the concept that risk of cardiovascular disease is uniquely an arrangement of genetics predisposition and lifestyle in adulthood [160–164].

The emergence of the developmental origins of health and disease (DOHaD) hypothesis, also known as fetal programming or the Barker hypothesis, was derived from observed long-term effects for adult health in persons of low birth weight [163]. The first studies pointing at relationships between early life experience and adult health were presented by Forsdahl [165] and Wadsworth [166], however, it was with Barker's works that the scientific community got awareness of the contribution of the gestational environment to the long-term health of the offspring.

These studies revealed a strong relationship between fetal growth restriction and adult sequelae, demonstrating that adults who had been small at birth as a result of growth failure, but not for premature, were at increased risk for heart disease [167]. A similar relationship between birth weight and non-fatal coronary heart disease has also been revealed in the USA population [168]. The developmental origins hypothesis was also corroborated by an epidemiological cohort of approximately 6000 subjects in Finland associating hypertension to health status at birth [169]. During the Dutch

famine, 1944–1945, the caloric intake for the adults in Amsterdam was abruptly reduced to less than 1000 kcal (~1400–1800 kcal in late 1943), reaching a minimum between 400 and 800 kcal during the peak of the famine, from December 1944 to April 1945, whereas after liberation in early May, rations improved rapidly to over 2000 kcal in June 1945. Several pregnant women were subjected to these conditions, becoming an exceptional opportunity to evaluate the DOHaD hypothesis in humans, namely representing the impact of the effects of nutrient restriction at specific periods of pregnancy on fetal development. Since the nutrient restriction occurred in a known and specific time (5 and 6 months), investigators could determine the impact of under nutrition in early, mid or late gestation on birth weight. A major discovery was that babies exposed to enduring famine during early gestation only (i.e., famine was released throughout the rest of gestation) presented a normal birth weight, however these subjects presented an augmented incidence of coronary heart disease in later life compared with persons not exposed to famine during gestation. These results unequivocally determined that poor maternal nutrition account for poor fetal development in humans, even if LBW does not reveal these impacts, these fetuses will have their future mapped in route for an increased incidence of cardiac and renal diseases [169,170]. Another interesting finding was the existence of a conditional adaptive response by the fetus, in a way that the adaptive response of the fetus confers a survival advantage when the postnatal diet remains suboptimal, but becomes harmful when postnatal nutrition is adequate or in excess [171,172].

1.5 Compromised womb: how does it happen?

Pregnancy and the period leading up to conception are critical periods during which adequate nutrition is essential to facilitate the maternal adaptations required to sustain pregnancy and to support proper fetal growth and development [159,163,170,173,174]. Besides poverty or economic instability, maternal dietary insufficiently can result from different causes. Aside from dietary deficiencies, several conditions can contribute to impaired nutritional status during pregnancy. In humans, hyperemesis gravidarum, a clinical condition characterized by persistent and severe vomiting leading to weight loss and dehydration, bulimia, anorexia nervosa and fear of disproportionate weight gain during pregnancy can account to an inadequate diet during gestation [175]. Women with short interpregnancy pauses and young women

(within 2 years of menarche, who may themselves still be growing) may also be at risk and require controlled nutrition [176]. Additionally, factors such as smoking, alcohol, drug may also contribute to poor maternofetal nutrition during gestation [177]. Given that the developmental origins of health and disease area of research is markedly related to data collected from disadvantaged working class populations in Britain and the victims of the Dutch hunger winter during the Second World War, we could just look towards poor populations in developing countries as benefactors of this line of research. Nevertheless, the probability of women in the developed world to consume inadequate diets during pregnancy is well recognized. Hickey and collaborators reported cases of underprivileged women that experienced low prenatal weight gain in southern Alabama [177]. Surprisingly, a cohort with middle class Caucasian women indicated that the majority of the study participants did not consume adequate amounts of micronutrients, such as iron and folate, during pregnancy [178]. It can also occur that due to the negative attitudes to weight gain, young women will scarify an adequate caloric intake and, consequently, weight gain during pregnancy [179,180]. Complementarily, studies reported that women with eating disorders are at greater risk of delivering small-for-gestational age babies [180], that 40% of primigravid women in the UK fear weight gain in pregnancy, and 72% fear an inability to return to prepregnancy weight [181]. Studies in Australia indicate that women that report disordered eating during pregnancy are at a heightened risk of delivering a low birth weight baby [182]. If these observations are viewed in concert with the DOHaD hypotheses, it becomes clear that the consequences of suboptimal nutrition during pregnancy are not confined to women in developing countries. Although the socioeconomic and nutritional realities faced by pregnant mothers in both developed and developing nations in the present day are quite diverse, the importance of maintaining an adequate diet during pregnancy remains the same.

Worldwide, low birth weight is found in 16% of infants (7% in industrialized countries), while 27% of children under 5 years of age are moderately to severely underweight. In addition to inadequate maternal nutrition, fetal malnutrition can also be caused by placental insufficiency [183]. We should also take in consideration that some disorders can conditioned the nutritional availability for the fetus, for example hypertensive disorders that affect placental blood flow and occur independently of nutritional status are the most common medical complications of pregnancy, and comprise a significant proportion of maternal and perinatal morbidity and mortality

worldwide [184]. Maternal disease states, such as gestational hypertension, essential hypertension, pre-eclampsia, as well as complications of pregnancy, such as cord occlusion, all reduce uterine blood flow and compromise fetal development [174,184]. The reduced uterine blood flow to the fetus that is common to hypertensive disorders of pregnancy is strongly related, in animal studies, to compromised fetal and placental development and hypertension in offspring [185]. Moreover, recent studies have demonstrated that maternal nutrient restriction during pregnancy induces pathological vascular dysfunction in the maternal vasculature, further compromising the pregnancy [186]. Thus, the two seemingly independent pathways to fetal nutrient restriction may in fact be strongly linked.

1.6 Animal models to investigate diet-induced *in utero* programming of human disease

When mechanisms of human function are investigated, the preferred modality is evaluation of humans or human tissues. Nevertheless, this approach is not always possible or even practicable in many instances (e.g., many aspects of fetal physiology), and efforts to elucidate mechanisms underlying the DOHaD hypothesis have led to the expansion and characterization of several animal models. Choice of an appropriate experimental model is clearly not an error-free matter, as all animal models have strengths and weaknesses. Rat and mouse models are clearly the preferred nonhuman models, as reflected by the contemporary literature [187], and both have many advantageous traits, including small size, and thus reduced cost of husbandry, as well as short gestation length, which allows for rapid generation of study subjects. Extensive work studying DOHaD has been completed in rodents, primarily in the rat. The long-term effects of modifications in motherly diet in the rat include deviations in postnatal growth, organ size and changed metabolism in the offspring. Feeding pregnant rats a diet low in protein results in lifelong elevations in blood pressure in the progeny [188]. Though small size may be advantageous, it becomes a problem in many physiological studies, as it places limitations on sample collection and instrumentation. Rodent fetal development also occurs at a different rate to that followed by larger animals and humans, with substantial development of organs, including the kidney, occurring *ex utero*. In addition, these animals are typically polytocous and have a different intrauterine environment to that in

monotocous species [189–191]. It still to prove that the same phenomenon observed in the rat holds true in long-gestation, precocial species, such as the sheep or baboon. Previous studies in the sheep and in humans have demonstrated that an extended period of maternal nutrient deprivation during the first half of pregnancy results in relatively normal birth weights, but leads to increases in the length and thinness of the offspring.

To overcome these uncertainties, sheep have become a valuable model in the study of DOHaD, and there are several reasons for considering the sheep a desirable model for fetal research. Perhaps foremost is the fact that the sheep has attained a robust historical position in fetal physiological investigation [187]. In addition, there are strong temporal similarities between sheep and human fetal renal and cardiac development and maturation during gestation, and sheep have a relatively long gestation term (145–150 days), which facilitates study of the specific windows of susceptibility during fetal development. Furthermore, the widespread use of the sheep as a model for pregnancy and fetal research has established well-defined baseline values for many physiological processes. As a result, the literature is replete with studies that have used the sheep as a model for pregnancy and fetal research. Nevertheless, there are several differences between the pregnant ewe as a model organism and the human as the target organism for experimental extrapolation. These differences include, but are not limited to, different placentation, differences in the gastrointestinal tract, digestion, absorption and metabolism, and uncertainty of each animal's genetic background. Of these, perhaps the most important is that the placenta in pregnant ewes is a cotyledonary epitheliochorial placenta, containing three maternal and fetal layers, with discrete placental attachment sites throughout the uterus. The pregnant human has a discoid hemochorial placenta that has no maternal cell layers, with three fetal layers and a single point of interaction between the fetus and the uterus. These differences may alter comparison across species of the dynamics of nutrient supply and waste product removal [187]. Recent efforts have been made to develop a nonhuman primate model for the study of nutrient restriction during pregnancy [187]. Although the nonhuman primate model of pregnancy research is both costly and time consuming, the increased degree of similarity with human gestation offers the opportunity for greater insight into the effects of a suboptimal intrauterine environment on the primate fetus and offspring.

Chapter 2

Hypothesis and aim

The hypothesis to be tested in this study is that maternal nutrition reduction by 30% during gestation affects renal and cardiac mitochondria heritage and function of the progeny.

A secondary question is if these effects are dependent on the fetus's gender.

Chapter 3

Material and Methods

3.1 Reagents

All reagents used were of the highest grade of purity commercially available (analytical grade or better). All aqueous solutions were prepared in ultrapure (type I) water (Milli-Q Biocel A10 with pre-treatment via Elix 5, Millipore, Billerica, Massachusetts, USA). For nonaqueous solutions, ethanol (99.5 %, Sigma-Aldrich, Barcelona, Spain) or dimethyl sulfoxide (DMSO, Sigma-Aldrich) were used as solvents.

3.2 Animal care and maintenance

3.2.1 Ethical approval

All animal procedures, including pain relief, were approved by the Animal Care and Use Committees of the Texas Biomedical Research Institute and the University of Texas Health Science Center at San Antonio (no. 1134PC), and were conducted in Association for Assessment and Accreditation of Laboratory Animal Care-approved facilities.

3.2.2 Housing and weighing conditions

Before pregnancy, maternal morphometric determinations were made to guarantee consistency of weight and general morphometrics in animals used in the present study. Non-pregnant outbred female baboons (*Papio* spp.) of similar morphometric phenotype were selected for the study. Animals were housed at the Southwest National Primate Research Center at the Texas Biomedical Research Institute (TBRI) in Association for Assessment and Accrediton of Laboratory Animal Care (AAALAC)-approved facilities. Groups up to 16 female baboons were initially housed with a vasectomized male to establish a stable social group in outdoor gang cages, thereby providing full social and physical activity.

Each outdoor concrete gang cage (see Figure 3.1 and Figure 3.2) was covered with a roof and had open sides that allowed exposure to normal lighting. Each cage hold 10-16 females and had a floor area of 21 x 37 m, being about 3.5 m high. The enrichment within the cages included nylon bones (Nylabone, Neptune, New Jersey,

USA), rubber Kong toys (Kong Company, Golden, Colorado, USA), and plastic Jolly Balls (Horseman's Pride, Inc., Ravenna, Ohio, USA). A 0.6 m-wide platform, built from expanded metal grating was placed at a height of 1.7 m and ran the full length of the cage. A similar perch was built at the front of the cage, also running the length of the entire cage. Tube perches were present at the back in the corner of each cage. Each cage had an exit into a chute 0.6 m wide by 1 m high positioned along the side of each set of cages. A fine mesh was placed on the side of the chute adjacent to the other group cages between groups of animals as they passed along the chute to the individual feeding cages. The two chutes merged and passed over a scale and into individual feeding cages, which were 0.6 by 0.9 m in floor area and 0.69 m high. All metal components were made of galvanized steel. Prior to pregnancy, animals were trained to be fed in individual cages. Briefly, at feeding time, all baboons passed along a chute into individual feeding cages. Once in the individual cages, they were fed with the designated amount of normal primate chow (Purina Monkey Diet 5038, Purina, St. Louis, Missouri, USA).

Each baboon's weight was obtained while crossing an electronic scale (GSE 665; GSE Scale Systems, Milwaukee, Wisconsin, USA). A commercial software application designed to capture weight data was modified to permit the recording of 50 individual measurements over 3 seconds. If the standard deviation of the weight measurement was great than 0.01 of the mean weight, the weight was automatically discarded and the weighing procedure was re-initiated again.

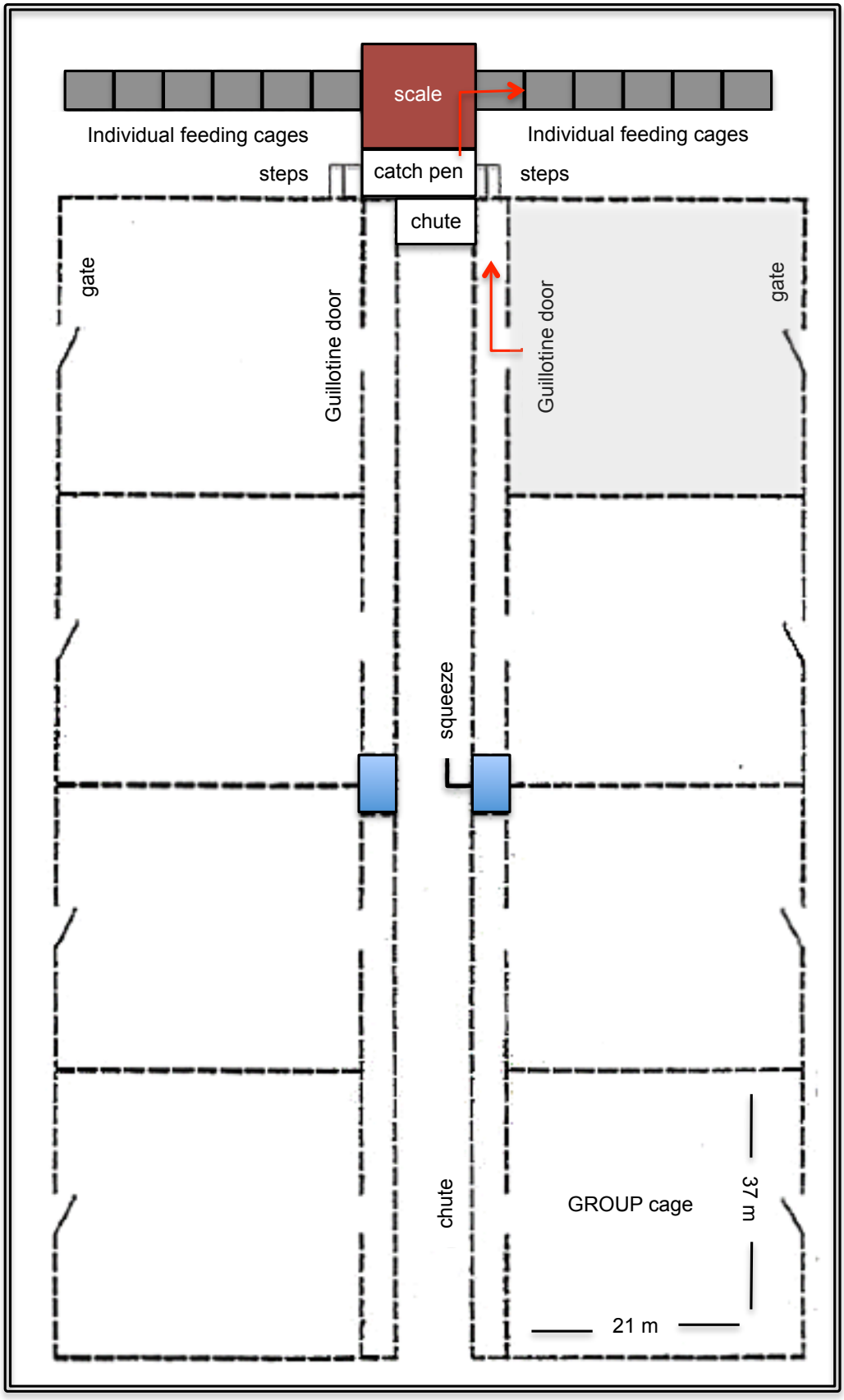

Figure 3.1 Cages plan.
Floor plan of the holding cages, chutes, group cage, scale, and individual feeding cages. Adapted from Schlabritz-Loutsevitch et al 2004 [192].

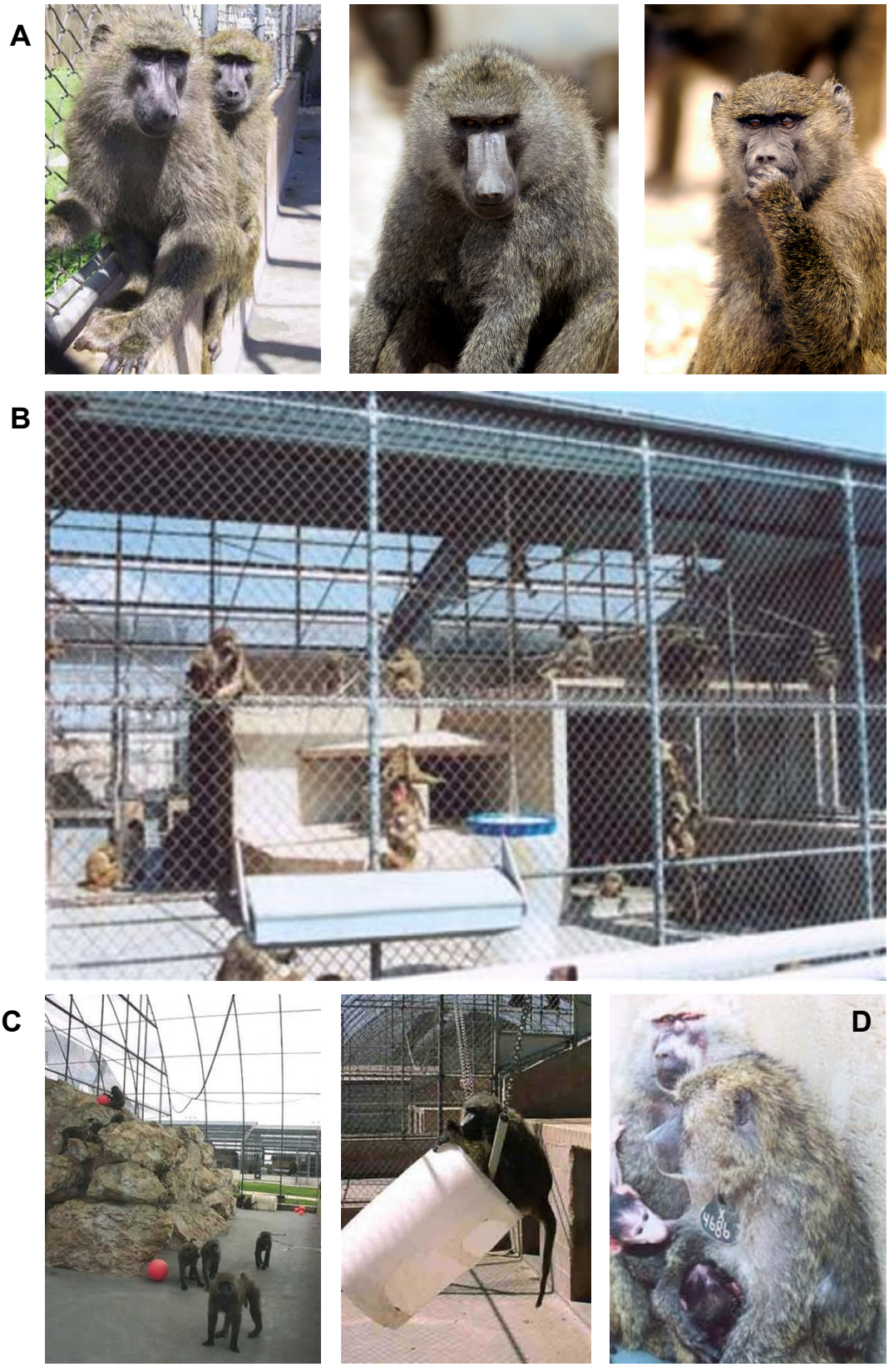

Figure 3.2 Model characterization.
A: physical features of baboons from *Papio* spp. These baboons are highly sexually dimorphic in size and pelage characters. Adult males normally weigh almost the double of females. Male pelage is basically grayish-brown in color, with the ventrum colored like the back or darker. Hairs on the cheeks are lighter. Females are a plain olive-brown color. The skin may be very colorful in some animals. In both males and females, the skin surrounding

the ischial callosities is pink or bright red. Males have skin of a similar color on their muzzle and face, whereas females possess a muted, grayish-brown face. The tail is long, and curved, with a graceful arch at the base. The natal pelage is black (D), although this is lost by approximately six months of age, when it is replaced by an olive-brown coat like that of the adult female [193]. B: image of a group cage. C: environmental enrichment within the cages. D: all animals were assigned a unique identification tag, which was used consistently throughout the study. This tag (80 x 87 mm) was placed around the baboon neck and was easily readable from 5 m. Images available in the Southwest National Primate Research Center.

3.2.3 Groups formation for the study

All female baboons were observed twice a day for well-being and three times a week for turgescence (sex skin swelling) and signs of vaginal bleeding for assessing their reproductive cycle and to enable timing of pregnancy. After a 30-day period of adaptation to the feeding system, a fertile male was introduced into each breeding cage. Pregnancy was dated initially by following the changes in the swelling of the sex skin and confirmed at 30 days of gestation by ultrasonography. On day 30 of pregnancy (term ~ 183 days gestation), twenty-four female baboons were randomly assigned to eat normal primate chow *ad libitum* (control diet) or to receive 70% of the average daily amount of feed eaten by the control female baboons (MNR group) on a body weight-adjusted basis at same gestational age (12 baboons/dietary group, 6 control male fetuses – C-M, 6 control female fetuses – C-F, 6 MNR male fetuses – MNR-M, and 6 MNR female fetuses – MNR-F). Animals remained in these groups until cesarean section at 165 days gestation (0.9 gestation, see Figure 3.3 for study timeline). Each fetus from a singleton pregnant female baboon is considered an experimental unit; in some cases the pregnant female baboon as also assumed as the experimental unit when maternal data is presented.

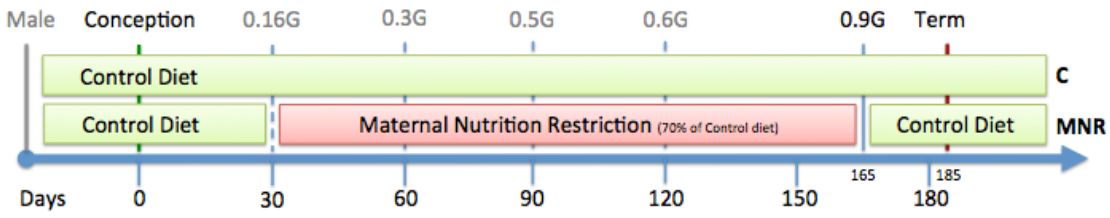

Figure 3.3 Timeline of maternal nutrition during baboon fetal development.

3.2.4 Food consumption

Food was provided once a day as Purina Monkey Diet 5038, standard biscuits. The biscuit is described as a "complete life-cycle diet for all Old World Primates" and contains stabilized vitamin C as well as all other required vitamins. The basic composition includes crude protein (≥ 15%), crude fat (≥ 5%), crude fiber (≤ 6%), ash (≤ 5%) and added minerals (≤ 3%). The full composition of Monkey Diet 5038 can be found at producer's web site (site 1) [192].

At the beginning of the feeding period, between 7-9 h or 11-13 h, each baboon received 60 biscuits in the feeding tray at the individual feeding cage. At the end of the 2 h feeding period, after the baboon had returned to the group cage, the remaining biscuits in the tray and on the floor of the cage were counted and weighted. Following confirmation of pregnancy, food intake was recorded in 8 female baboons fed *ad libitum*, and was calculated as 50.61 ± 3.61 kcal/kg of body weight per day. Before the start of the controlled diet, baboons were fed with the same diet without biscuit limit.

Water was continuously available in the feeding cages via individual waterers (Lixit, Napa, California, USA) and at several locations in the group housing. Food consumption of animals, their weights, and health status were daily recorded.

This feeding system allowed us to manipulate and monitor food intake in a controlled fashion while still maintaining female baboons in group housing in distinction to isolation in individual cages, thereby permitting normal social and physical activity.

More details of housing and environmental enrichment have been previously published [192].

3.2.5 Cesarean section, fetal and maternal morphometry, and blood sampling

Cesarean sections were performed at 165 days of gestation (0.9 gestation) under premedication with ketamine hydrochloride (10 mg/kg) followed by isoflurane anesthesia (2%, 2 l/min) to collect fetal samples and the placenta.

Before the fetus was exteriorized from the uterine cavity, umbilical vein blood

sampling was performed as previously described [192]. Maternal fasting blood samples were drawn from the femoral vein on the morning before cesarean section directly into a 4 ml Vacutainer clot tubes (Becton Dickinson, Franklin Lakes, New Jersey, USA).

The fetus was euthanized by exsanguination while still under general anesthesia. The placenta and fetus were analyzed for morphometric measurements, complete pathological evaluation, and tissue sampling. Fetal kidneys were rapidly removed and longitudinally cut in half. One half was immediately snap-frozen in liquid nitrogen and then stored at -80ºC until used for RNA extractions. The other kidney half was fixed in 10% buffered formalin and embedded in paraffin for histological analyses. Cardiac samples were taken from the free wall of the cardiac left ventricle that was cut transversely in at least four pieces, some pieces were flash frozen and stored at -80ºC until analyses and one piece was fixed for histological analyses.

Maternal analgesia was provided with Buprenorphine hydrochloride 0.015 mg/kg/d during 3 postoperative days (Buprenex Injectable, Reckitt Benckiser Healthcare (UK) Ltd, Hull, England). After recovery from cesarean section in individual cages, mothers were returned to their group. Techniques used and postoperative maintenance of the mother have been previously described in detail [195]. Cesarean sections were evenly spread throughout the year and took place in the morning period, usually between 8 - 12 h. Surgical procedures were performed by a fully certified doctor of medicine or a doctor of veterinary medicine, and postsurgical care was prescribed and monitored by a veterinarian.

3.3 Biochemical analyses

Within 1 h of collection, clotted blood was centrifuged at 10,000 g for 10 min and the serum was removed within 1 hour of collection. Biochemical determinations of glucose, blood urea nitrogen (BUN), creatinine, total protein, albumin and globulin were made in serum using a Beckman Synchron CX5CE Analyzer (Beckman Coulter, Irving, Texas, USA) by a certificated laboratory.

3.4 Amino acid analyses

Heparinized plasma samples (0.1 ml) were deproteinized with 0.1ml of 1.5 M $HClO_4$ and neutralized with 0.05 ml of 2 M K_2CO_3. The solution was centrifuged at 12,000 g at 4°C for 1 min and the supernatant used for analyses. Amino acids were determined by HPLC involving pre-column derivatisation with o-phthaldialdehyde, as previously described in detail [196]. All amino acids were quantified through the use of appropriate standards (Sigma-Aldrich, St. Louis, Missouri, USA) using Millenium-32 Software (Waters, Milford, Massachusetts, USA).

3.5 Analysis of mtDNA copy number by quantitative real-time PCR

Total DNA was extracted from ~20 mg of cardiac left ventricle tissue using the QIAamp DNA mini-kit (#50951304 Qiagen, Düsseldorf, Germany), following the manufacturer's instructions. Briefly, the tissue was cut into small pieces and lysed with proteinase K in buffer ATL (tissue lysis buffer for use in purification of nucleic acids) provided by the kit. When the tissue was completely lysed, buffer AL (tissue lysis buffer containing guanidine salts and detergent) and ethanol 96% were added. The mixture was applied to the QIAamp column and centrifuged at 6,000 g for 1 min in Eppendorf 5415R benchtop centrifuge equipped with a FA-45-24-11 rotor (Eppendorf, Hamburg, Germany). After centrifugation, the column was placed in a new collection tube and the DNA was washed sequentially with buffers AW1 (washing buffer 1) and AW2 (washing buffer 2). Ethanol was completely removed by centrifugation at full speed for 1 min. DNA was eluted with 200 µl Buffer AE and quantified using a Nanodrop 2000 (ThermoFischer Scientific, Waltham, Massachusetts, USA).

RT-PCR was performed using the SsoFast Eva Green Supermix (Bio-Rad, Hercules, California, USA), in a CFX96 real time-PCR system (Bio-Rad), with the primers defined in Table 3.1, at 500 nM each. Amplification of 25 ng DNA was performed with an initial cycle of 2 min at 98ºC, followed by 40 cycles of 5 sec at 98ºC plus 5 sec at 60ºC. At the end of each cycle, Eva Green fluorescence was recorded to enable determination of Ct. For quality control, melting temperature of the PCR products was determined after amplification by performing melting curves, and no

template controls were run.

For absolute quantification and assessment of amplification efficiency, standards at known copy numbers were produced by purification of PCR products. After optimization of the annealing temperature, products were amplified for each primer pair (Table 3.1), using the HotstarTaq Master Mix Kit (#203445 Qiagen). Briefly, 1 μl of a DNA sample was added to a PCR tube containing the HotStar Taq Master Mix and the specific primers, and placed in a CFX96 real time-PCR system. The amplification protocol started with an initial activation step of 15 min at 95ºC degrees, followed by 35 cycles of 1 min at 94ºC (denaturation) plus 1 min at 60ºC (annealing), plus 1 min at 72ºC (extension), and a final extension step of 10 min at 72ºC. After amplification, the products were purified using the MiniElute PCR purification kit (#280006 Qiagen) following the manufacturer's instructions. Eluted DNA was quantified in a Nanodrop 2000, the copy numbers were adjusted to 5×10^9 copies/μl, and tenfold serial dilutions were prepared.

mtDNA copy number was determined by the ratio between the absolute amounts of mitochondrial genes *ND1* or *ND6* versus the absolute amount of the *B2M* nuclear gene in each sample, using the CFX96 Manager software (v. 3.0; Bio-Rad).

Table 3.1 List of primers sets used in quantitative real-time PCR.

	Accession code [a]	Sequence Length (bp)	Sequence [b]	Position	Length (bp)	Tm [c]	Ta Opt [d] (ºC)	Product Length (bp)	Product Tm Predicted (ºC)	Product Tm Observed (ºC)
CYTB	NC_001992.1	1141	ACTTCATCCTACCATTCGGCATC	545	23	68.7	62.0	178	80.5	81.5
	(14172-15312)		GTTATTAGGGCAAGGAGAAGGGGA	722	24	69.9				
D-loop	NC_001992.1	1076	TCCAAAGTCCATGTACTACCCCA	227	23	69.2	58.1	122	74.8	76.5
	(15446-16521)		CCGTGGTGTTTTGAATTTCCTGG	348	23	68.9				
ND1	NC_001992.1	955	CCTATGAATCCGAGCAGCGT	810	20	68.6	61.6	130	79.9	81.5
	(2735-3689)		GCTGGAGATTGCGATGGGTA	939	20	68.7				
ND6	NC_001992.1	525	CACTCCGAACTAACCCCGAC	114	20	68.7	61.2	130	79.3	80.0
	(13573-14097)		GGGCTGATGATGGAAGTGGG	243	20	69.3				
B2M	NC_018158.1	5122	CAGGGCCCAGGACAGTTAAG	4456	20	68.9	59.7	141	77.3	78.5
			GGGATGGGACTCATTCAGGG	4596	20	68.5				
HBB	NM_001168847.1	444	CCCTTGGACCCAGAGGTTCT	108	20	69.9	61.6	91	79.6	81.0
			CTTGCCATGAGCCTTCACCT	198	20	69.2				
RNA16S	NC_001992.2	1570	CGAAACCAGACGAGCTACCC	237	20	69.0	62.0	182	80.6	82.0
	(2334-2527)		AGAGGGATTGGGATTGGGTTATTC	418	24	68.4				

[a] available at the www.ncbi.nlm.nih.gov/nucleotide and http://www.ncbi.nlm.nih.gov/nuccore/NC_001992
[b] the first sequence is the sense sequence and the second is the antisense sequence
[c] Tm is the melting temperature
[d] represents the optimal annealing temperature

3.6 Gene expression analysis by PCR array

3.6.1 RNA extraction

RNA extraction was performed in accordance with the protocol previously described by Cox et al. [197]. Briefly, approximately 20 mg section of frozen tissue was cut (from one pole of a longitudinally sliced kidney half and transversely for heart). The tissue was homogenized in 1 ml Trizol Reagent using a Power General Homogenizer (Omni International, Wilmington, Delaware, USA). Genomic DNA in the sample was sheared by passing the homogenate three times through a 22-gauge needle attached to a 1 ml syringe. The homogenized samples were incubated for 5 min at 25°C. Two hundred microlitres of chloroform was added to each sample, and the samples were shaken vigorously by hand for 15 s and incubated at 25ºC for 3 min. Samples were then centrifuged at 12,000 x g for 15 min at 4ºC. The aqueous phase containing RNA was transferred to a fresh tube and RNA precipitated by addition of 0.5 ml of isopropyl alcohol. Samples were incubated for 10 min at 25ºC and then centrifuged at 12,000 x g for 10 min at 4ºC. The RNA precipitate was washed with 1 ml of 75% ethanol and centrifuged at 7,500 x g for 5 min at 4ºC. After air-drying, the RNA pellet was dissolved in diethylpyrocarbonate (DEPC)-treated ddH_2O. The RNA was quantified spectrophotometrically using Thermo Scientific NanoDrop 2000 spectrophotometer (ThermoFischer Scientific) and stored at −80ºC. The RNA purity and quality were checked by Ultraviolet spectrophotometry by the ratios of A_{260}/A_{280} and A_{260}/A_{230} and electrophoretically by visualization of the ribosomal band integrity for both the 18S and 28S ribosomal RNA. Only RNA samples that demonstrated consistent quality were used.

3.6.2 cDNA Preparation

After RNA preparation, the samples were treated with DNase to ensure elimination of genomic DNA, while extracted RNA was converted to cDNA using the RT^2 First Strand Kit from SuperArray Bioscience Corporation (SA Biosciences, Qiagen, Valencia, California, USA) according to the manufacturer's instructions. Briefly, 1 μg RNA was combined with 2 μL gDNA elimination buffer and brought up to a final volume of 10 μL using RNAse-free H_20. This mixture was incubated at 42ºC for 5 min, and then chilled in ice. Ten μL of RT Cocktail was then added to this mixture

and incubated at 42ºC for exactly 15 min followed by 5 min at 95ºC for stop the reaction. Ninety-one µL ddH20 was added to each 20 µL cDNA synthesis reaction and well mixed. The cDNA mixture was stored at -20ºC until used for gene expression profiling.

3.6.3 Quantitative gene expression profiling

The RT^2 Profiler polymerase chain reaction (PCR) Array System (SuperArray Bioscience, SA Biosciences, Qiagen), was used to evaluate the different renal mitochondrial transcripts between control and MNR fetuses. We used the Human Mitochondrial Energy Metabolism (Table 3.2 and Figure 3.4) and the Human Mitochondria (Table 3.3 and Figure 3.5) PCR Pathway Arrays. Real-time PCR detection was carried out per the manufacturer's instructions. The experimental cocktail was prepared by adding 1350 µL of the SuperArray RT^2 qPCR master mix and 1248 µL ddH_20 to 102 µL of the diluted cDNA mixture. For real-time PCR detection, 25 µL of this cocktail was added to each well in the 96-well PCR array. The array was then processed on a real-time thermal cycler (Applied Biosystems StepOnePlus, ThermoFischer Scientific, Applied Biosystems) by using the following program: 1 cycle of 10 min at 95ºC followed by 40 cycles of 15 seconds at 95ºC and 1 min at 60ºC. A melting curve program for quality control was immediately performed after the cycling program. SYBR Green fluorescence was detected from each well during the annealing step of each cycle, and values were exported to an Excel template file for analysis. Each PCR array contained 84 transcripts of the corresponding signaling pathway, a set of five housekeeping genes as internal controls and additional controls for efficiency of reverse transcription, PCR and the absence of contaminating genomic DNA. Data were normalized with three endogenous controls that did not differ between groups [hypoxanthine phosphoribosyltransferase 1 (*HPRT1*), ribosomal protein L13a (*RPL13A*) and Beta-actin (*ACTB*) and analyzed with the ΔΔCt method (where Ct is threshold cycle) using the PCR Array Data Analysis Web Portal (SA Biosciences).

Table 3.2 Panel of gene expression analyzed using The Human Mitochondrial Energy Metabolism RT² Profiler PCR Array.
This array profiled the expression of 84 key genes involved in mitochondrial energy metabolism, including genes encoding components of the electron transport chain and oxidative phosphorylation complexes. Position indicates the location in the 96-well plate where the gene was assessed, Symbol denotes the gene identification, RefSeq denotes the Reference Sequence from the National Center for Biotechnology Information collection, Description gives summary information about the gene identification and/or function.

Position	Symbol	Refseq	Description
A01	***ATP12A***	NM_001676	ATPase, H+/K+ transporting, nongastric, alpha polypeptide
A02	***ATP4A***	NM_000704	ATPase, H+/K+ exchanging, alpha polypeptide
A03	***ATP4B***	NM_000705	ATPase, H+/K+ exchanging, beta polypeptide
A04	***ATP5A1***	NM_004046	ATP synthase, H+ transporting, mitochondrial F1 complex, alpha subunit 1
A05	***ATP5B***	NM_001686	ATP synthase, H+ transporting, mitochondrial F1 complex, beta polypeptide
A06	***ATP5C1***	NM_005174	ATP synthase, H+ transporting, mitochondrial F1 complex, gamma polypeptide 1
A07	***ATP5F1***	NM_001688	ATP synthase, H+ transporting, mitochondrial Fo complex, subunit B1
A08	***ATP5G1***	NM_005175	ATP synthase, H+ transporting, mitochondrial Fo complex, subunit C1
A09	***ATP5G2***	NM_001002031	ATP synthase, H+ transporting, mitochondrial Fo complex, subunit C2
A10	***ATP5G3***	NM_001689	ATP synthase, H+ transporting, mitochondrial Fo complex, subunit C3
A11	***ATP5H***	NM_006356	ATP synthase, H+ transporting, mitochondrial Fo complex, subunit d
A12	***ATP5I***	NM_007100	ATP synthase, H+ transporting, mitochondrial Fo complex, subunit E
B01	***ATP5J***	NM_001685	ATP synthase, H+ transporting, mitochondrial Fo complex, subunit F6
B02	***ATP5J2***	NM_004889	ATP synthase, H+ transporting, mitochondrial Fo complex, subunit F2
B03	***ATP5L***	NM_006476	ATP synthase, H+ transporting, mitochondrial Fo complex, subunit G
B04	***ATP5O***	NM_001697	ATP synthase, H+ transporting, mitochondrial F1 complex, O subunit
B05	***ATP6V0A2***	NM_012463	ATPase, H+ transporting, lysosomal V0 subunit a2
B06	***ATP6V0D2***	NM_152565	ATPase, H+ transporting, lysosomal 38kDa, V0 subunit d2
B07	***ATP6V1C2***	NM_144583	ATPase, H+ transporting, lysosomal 42kDa, V1 subunit C2
B08	***ATP6V1E2***	NM_080653	ATPase, H+ transporting, lysosomal 31kDa, V1 subunit E2
B09	***ATP6V1G3***	NM_133262	ATPase, H+ transporting, lysosomal 13kDa, V1 subunit G3
B10	***BCS1L***	NM_004328	BCS1-like (S. cerevisiae)
B11	***COX4I1***	NM_001861	Cytochrome c oxidase subunit IV isoform 1
B12	***COX4I2***	NM_032609	Cytochrome c oxidase subunit IV isoform 2
C01	***COX5A***	NM_004255	Cytochrome c oxidase subunit Va
C02	***COX5B***	NM_001862	Cytochrome c oxidase subunit Vb
C03	***COX6A1***	NM_004373	Cytochrome c oxidase subunit VIa polypeptide 1
C04	***COX6A2***	NM_005205	Cytochrome c oxidase subunit VIa polypeptide 2
C05	***COX6B1***	NM_001863	Cytochrome c oxidase subunit Vib polypeptide 1
C06	***COX6B2***	NM_144613	Cytochrome c oxidase subunit VIb polypeptide 2
C07	***COX6C***	NM_004374	Cytochrome c oxidase subunit VIc
C08	***COX7A2***	NM_001865	Cytochrome c oxidase subunit VIIa polypeptide 2
C09	***COX7A2L***	NM_004718	Cytochrome c oxidase subunit VIIa polypeptide 2 like
C10	***COX7B***	NM_001866	Cytochrome c oxidase subunit VIIb
C11	***COX8A***	NM_004074	Cytochrome c oxidase subunit VIIIA
C12	***COX8C***	NM_182971	Cytochrome c oxidase subunit VIIIC
D01	***CYC1***	NM_001916	Cytochrome c-1
D02	***LHPP***	NM_022126	Phospholysine phosphohistidine inorganic pyrophosphate phosphatase
D03	***NDUFA1***	NM_004541	NADH dehydrogenase (ubiquinone) 1 alpha subcomplex, 1
D04	***NDUFA10***	NM_004544	NADH dehydrogenase (ubiquinone) 1 alpha subcomplex, 10
D05	***NDUFA11***	NM_175614	NADH dehydrogenase (ubiquinone) 1 alpha subcomplex, 11
D06	***NDUFA2***	NM_002488	NADH dehydrogenase (ubiquinone) 1 alpha subcomplex, 2
D07	***NDUFA3***	NM_004542	NADH dehydrogenase (ubiquinone) 1 alpha subcomplex, 3
D08	***NDUFA4***	NM_002489	NADH dehydrogenase (ubiquinone) 1 alpha subcomplex, 4

D09	***NDUFA5***	NM_005000	NADH dehydrogenase (ubiquinone) 1 alpha subcomplex, 5
D10	***NDUFA6***	NM_002490	NADH dehydrogenase (ubiquinone) 1 alpha subcomplex, 6
D11	***NDUFA7***	NM_005001	NADH dehydrogenase (ubiquinone) 1 alpha subcomplex, 7
D12	***NDUFA8***	NM_014222	NADH dehydrogenase (ubiquinone) 1 alpha subcomplex, 8
E01	***NDUFAB1***	NM_005003	NADH dehydrogenase (ubiquinone) 1, alpha/beta subcomplex, 1
E02	***NDUFB10***	NM_004548	NADH dehydrogenase (ubiquinone) 1 beta subcomplex, 10
E03	***NDUFB2***	NM_004546	NADH dehydrogenase (ubiquinone) 1 beta subcomplex, 2
E04	***NDUFB3***	NM_002491	NADH dehydrogenase (ubiquinone) 1 beta subcomplex, 3
E05	***NDUFB4***	NM_004547	NADH dehydrogenase (ubiquinone) 1 beta subcomplex, 4
E06	***NDUFB5***	NM_002492	NADH dehydrogenase (ubiquinone) 1 beta subcomplex, 5
E07	***NDUFB6***	NM_182739	NADH dehydrogenase (ubiquinone) 1 beta subcomplex, 6
E08	***NDUFB7***	NM_004146	NADH dehydrogenase (ubiquinone) 1 beta subcomplex, 7
E09	***NDUFB8***	NM_005004	NADH dehydrogenase (ubiquinone) 1 beta subcomplex, 8
E10	***NDUFB9***	NM_005005	NADH dehydrogenase (ubiquinone) 1 beta subcomplex, 9
E11	***NDUFC1***	NM_002494	NADH dehydrogenase (ubiquinone) 1, subcomplex unknown, 1
E12	***NDUFC2***	NM_004549	NADH dehydrogenase (ubiquinone) 1, subcomplex unknown, 2
F01	***NDUFS1***	NM_005006	NADH dehydrogenase (ubiquinone) Fe-S protein 1
F02	***NDUFS2***	NM_004550	NADH dehydrogenase (ubiquinone) Fe-S protein 2
F03	***NDUFS3***	NM_004551	NADH dehydrogenase (ubiquinone) Fe-S protein 3
F04	***NDUFS4***	NM_002495	NADH dehydrogenase (ubiquinone) Fe-S protein 4
F05	***NDUFS5***	NM_004552	NADH dehydrogenase (ubiquinone) Fe-S protein 5
F06	***NDUFS6***	NM_004553	NADH dehydrogenase (ubiquinone) Fe-S protein 6
F07	***NDUFS7***	NM_024407	NADH dehydrogenase (ubiquinone) Fe-S protein 7
F08	***NDUFS8***	NM_002496	NADH dehydrogenase (ubiquinone) Fe-S protein 8
F09	***NDUFV1***	NM_007103	NADH dehydrogenase (ubiquinone) flavoprotein 1
F10	***NDUFV2***	NM_021074	NADH dehydrogenase (ubiquinone) flavoprotein 2
F11	***NDUFV3***	NM_021075	NADH dehydrogenase (ubiquinone) flavoprotein 3
F12	***OXA1L***	NM_005015	Oxidase (cytochrome c) assembly 1-like
G01	***PPA1***	NM_021129	Pyrophosphatase (inorganic) 1
G02	***PPA2***	NM_176869	Pyrophosphatase (inorganic) 2
G03	***SDHA***	NM_004168	Succinate dehydrogenase complex, subunit A, flavoprotein (Fp)
G04	***SDHB***	NM_003000	Succinate dehydrogenase complex, subunit B, iron sulfur (Ip)
G05	***SDHC***	NM_003001	Succinate dehydrogenase complex, subunit C, integral membrane protein
G06	***SDHD***	NM_003002	Succinate dehydrogenase complex, subunit D, integral membrane protein
G07	***UQCR11***	NM_006830	Ubiquinol-cytochrome c reductase, complex III subunit XI
G08	***UQCRC1***	NM_003365	Ubiquinol-cytochrome c reductase core protein I
G09	***UQCRC2***	NM_003366	Ubiquinol-cytochrome c reductase core protein II
G10	***UQCRFS1***	NM_006003	Ubiquinol-cytochrome c reductase, Rieske iron-sulfur polypeptide 1
G11	***UQCRH***	NM_006004	Ubiquinol-cytochrome c reductase hinge protein
G12	***UQCRQ***	NM_014402	Ubiquinol-cytochrome c reductase, complex III subunit VII, 9.5kDa
H01	***B2M***	NM_004048	Beta-2-microglobulin
H02	***HPRT1***	NM_000194	Hypoxanthine phosphoribosyltransferase 1
H03	***RPL13A***	NM_012423	Ribosomal protein L13a
H04	***GAPDH***	NM_002046	Glyceraldehyde-3-phosphate dehydrogenase
H05	***ACTB***	NM_001101	Actin, beta
H06	***HGDC***	SA_00105	Human Genomic DNA Contamination
H07	***RTC***	SA_00104	Reverse Transcription Control
H08	***RTC***	SA_00104	Reverse Transcription Control
H09	***RTC***	SA_00104	Reverse Transcription Control
H10	***PPC***	SA_00103	Positive PCR Control
H11	***PPC***	SA_00103	Positive PCR Control
H12	***PPC***	SA_00103	Positive PCR Control

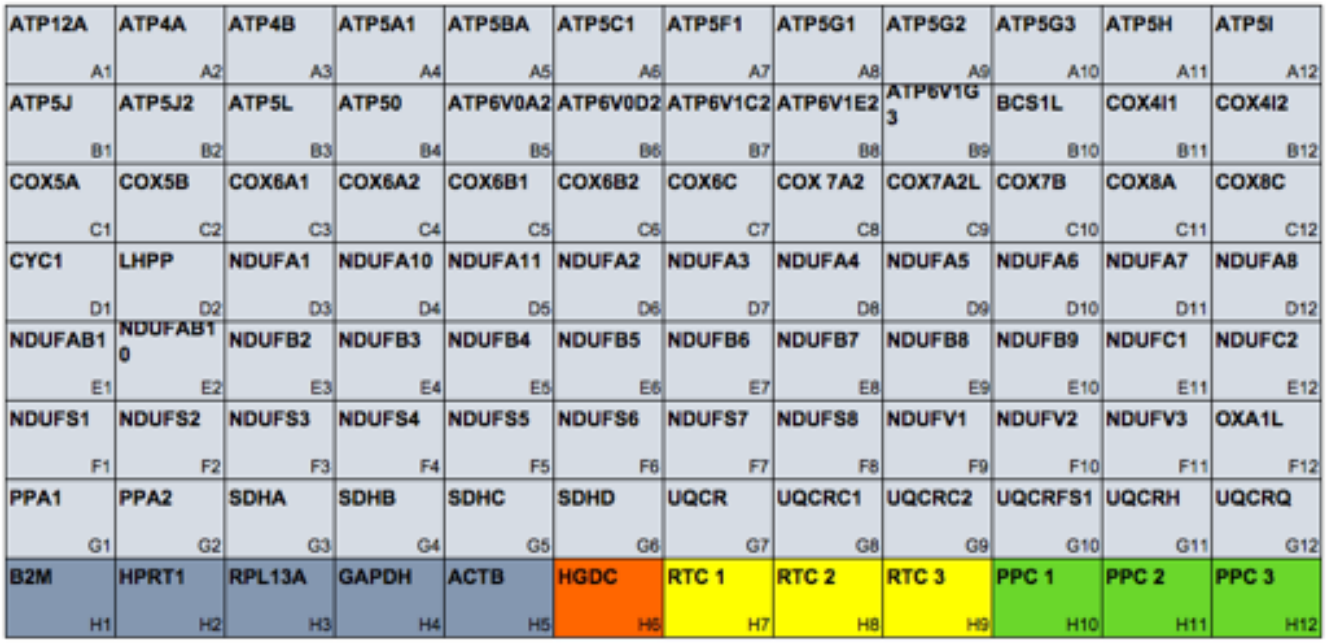

ATP12A A1	ATP4A A2	ATP4B A3	ATP5A1 A4	ATP5BA A5	ATP5C1 A6	ATP5F1 A7	ATP5G1 A8	ATP5G2 A9	ATP5G3 A10	ATP5H A11	ATP5I A12
ATP5J B1	ATP5J2 B2	ATP5L B3	ATP50 B4	ATP6V0A2 B5	ATP6V0D2 B6	ATP6V1C2 B7	ATP6V1E2 B8	ATP6V1G3 B9	BCS1L B10	COX4I1 B11	COX4I2 B12
COX5A C1	COX5B C2	COX6A1 C3	COX6A2 C4	COX6B1 C5	COX6B2 C6	COX6C C7	COX 7A2 C8	COX7A2L C9	COX7B C10	COX8A C11	COX8C C12
CYC1 D1	LHPP D2	NDUFA1 D3	NDUFA10 D4	NDUFA11 D5	NDUFA2 D6	NDUFA3 D7	NDUFA4 D8	NDUFA5 D9	NDUFA6 D10	NDUFA7 D11	NDUFA8 D12
NDUFAB1 E1	NDUFAB10 E2	NDUFB2 E3	NDUFB3 E4	NDUFB4 E5	NDUFB5 E6	NDUFB6 E7	NDUFB7 E8	NDUFB8 E9	NDUFB9 E10	NDUFC1 E11	NDUFC2 E12
NDUFS1 F1	NDUFS2 F2	NDUFS3 F3	NDUFS4 F4	NDUFS5 F5	NDUFS6 F6	NDUFS7 F7	NDUFS8 F8	NDUFV1 F9	NDUFV2 F10	NDUFV3 F11	OXA1L F12
PPA1 G1	PPA2 G2	SDHA G3	SDHB G4	SDHC G5	SDHD G6	UQCR G7	UQCRC1 G8	UQCRC2 G9	UQCRFS1 G10	UQCRH G11	UQCRQ G12
B2M H1	HPRT1 H2	RPL13A H3	GAPDH H4	ACTB H5	HGDC H6	RTC 1 H7	RTC 2 H8	RTC 3 H9	PPC 1 H10	PPC 2 H11	PPC 3 H12

Figure 3.4 Layout of the Human Mitochondrial Energy Metabolism RT² Profiler PCR Array.
Housekeeping assay panel: wells H1 through H5 contained a housekeeping gene panel to normalize PCR array data. Genomic DNA controls (HGDC): well H6 contained a replicate genomic DNA controls that detects non-transcribed genomic DNA contamination with a high level of sensitivity. Reverse transcription controls (RTC): wells H7 through H9 contained replicate reverse transcription controls that tests the efficiency of the RT2 First Strand Kit reaction with a primer set detecting the template synthesized from the kit's built-in external RNA control. Positive PCR controls (PPC): Wells H10 through H12 contained replicate positive PCR controls that tested the efficiency of the polymerase chain reaction itself using a pre-dispensed artificial DNA sequence and the primer set that detects it. The sets of replicate control wells (GDC, RTC, & PPC) also tested for inter-well, intra-plate consistency.

Table 3.3 Panel of gene expression analyzed using The Human Mitochondria RT² Profiler PCR Array.

This array profiled the expression of 84 genes involved in the diverse cellular functions of mitochondrial biology. The genes monitored by this array included regulators of mitochondrial biogenesis, regulators and mediators of mitochondrial molecular transport and genes involved in apoptosis. Position indicates the location in the 96-well plate where the gene was assessed, Symbol denotes the gene identification, RefSeq denotes the Reference Sequence from the National Center for Biotechnology Information collection, Description gives a summary information about the gene identification and/or function.

Position	Symbol	Refseq	Description
A01	***AIFM2***	NM_032797	Apoptosis-inducing factor, mitochondrion-associated, 2
A02	***AIP***	NM_003977	Aryl hydrocarbon receptor interacting protein
A03	***BAK1***	NM_001188	BCL2-antagonist/killer 1
A04	***BBC3***	NM_014417	BCL2 binding component 3
A05	***BCL2***	NM_000633	B-cell CLL/lymphoma 2, apoptosis regulator
A06	***BCL2L1***	NM_138578	BCL2-like 1, apoptosis regulator BCLX
A07	***BID***	NM_001196	BH3 interacting domain death agonist
A08	***BNIP3***	NM_004052	BCL2/adenovirus E1B 19kDa interacting protein 3, pro-apoptotic factor
A09	***CDKN2A***	NM_000077	Cyclin-dependent kinase inhibitor 2A, inhibits CDK4
A10	***COX10***	NM_001303	COX10 cytochrome c oxidase assembly protein homolog
A11	***COX18***	NM_173827	COX18 cytochrome c oxidase assembly homolog
A12	***CPT1B***	NM_004377	Carnitine palmitoyltransferase 1B
B01	***CPT2***	NM_000098	Carnitine palmitoyltransferase 2
B02	***DNAJC19***	NM_145261	DnaJ (Hsp40) homolog, subfamily C, member 19, TIMM14
B03	***DNM1L***	NM_005690	Dynamin 1-like, mitochondrial and peroxisomal division
B04	***FIS1***	NM_016068	Mitochondrial fission 1 protein homolog
B05	***TIMM10B***	NM_012192	Translocase of inner mitochondrial membrane 10 homolog B
B06	***GRPEL1***	NM_025196	GrpE-like 1, mitochondrial protein import
B07	***HSP90AA1***	NM_001017963	Heat shock protein 90kDa alpha, class A member 1, folding of target proteins
B08	***HSPD1***	NM_002156	Heat shock 60kDa protein 1, chaperonin family, folding and assembly of proteins
B09	***IMMP1L***	NM_144981	Mitochondrial inner membrane protease subunit 1-like
B10	***IMMP2L***	NM_032549	Mitochondrial inner membrane protease Subunit 2-like
B11	***LRPPRC***	NM_133259	Leucine-rich PPR-motif containing, cytoskeletal organization and vesicular transport
B12	***MFN1***	NM_033540	Mitofusin 1, mediator of mitochondrial fusion
C01	***MFN2***	NM_014874	Mitofusin 2, mediator of mitochondrial fusion
C02	***MIPEP***	NM_005932	Mitochondrial intermediate peptidase, maturation of OXPHOS-related proteins
C03	***MSTO1***	NM_018116	Misato homolog 1, mitochondrial distribution and morphology regulator
C04	***MTX2***	NM_006554	Metaxin 2, mitochondrial outer membrane import complex protein 2
C05	***NEFL***	NM_006158	Neurofilament, light polypeptide, protein phosphatase 1
C06	***OPA1***	NM_130837	Optic atrophy 1, mitochondrial dynamin-like GTPase, related to mitochondrial network
C07	***PMAIP1***	NM_021127	Phorbol-12-myristate-13-acetate-induced protein 1, related to activation of caspases and apoptosis
C08	***RHOT1***	NM_018307	Ras homolog gene family, member T1, mitochondrial GTPase involved in mitochondrial trafficking
C09	***RHOT2***	NM_138769	Ras homolog gene family, member T2, mitochondrial GTPase involved in mitochondrial trafficking
C10	***SFN***	NM_006142	Stratifin
C11	***SH3GLB1***	NM_016009	SH3-domain GRB2-like endophilin B1, Bax-interacting Factor 1, apoptotic signaling pathway
C12	***SLC25A1***	NM_005984	Solute carrier family 25 (mitochondrial carrier; citrate transporter), member 1
D01	***SLC25A10***	NM_012140	Solute carrier family 25 (mitochondrial carrier; dicarboxylate transporter), member 10
D02	***SLC25A12***	NM_003705	Solute carrier Family 25 (aspartate/glutamate carrier), member 12, calcium carrier
D03	***SLC25A13***	NM_014251	Solute carrier Family 25 (aspartate/glutamate carrier), member 13

D04	***SLC25A14***	NM_003951	Solute carrier family 25 (mitochondrial carrier), member 14, UCP5
D05	***SLC25A15***	NM_014252	Solute carrier family 25 (mitochondrial carrier; ornithine transporter) member 15
D06	***SLC25A16***	NM_152707	Solute carrier family 25 (mitochondrial carrier), member 16
D07	***SLC25A17***	NM_006358	Solute carrier family 25 (mitochondrial carrier; peroxisomal membrane protein), member 17
D08	***SLC25A19***	NM_021734	Solute carrier family 25 (mitochondrial thiamine pyrophosphate carrier), member 19
D09	***SLC25A2***	NM_031947	Solute carrier family 25 (mitochondrial carrier; ornithine transporter) member 2, ORNT2
D10	***SLC25A20***	NM_000387	Solute carrier family 25 (carnitine/acylcarnitine translocase), member 20
D11	***SLC25A21***	NM_030631	Solute carrier family 25 (mitochondrial oxodicarboxylate carrier), member 21
D12	***SLC25A22***	NM_024698	Solute carrier family 25 (mitochondrial carrier: glutamate), member 22
E01	***SLC25A23***	NM_024103	Solute carrier family 25 (mitochondrial carrier; phosphate carrier), member 23
E02	***SLC25A24***	NM_013386	Solute carrier family 25 (mitochondrial carrier; phosphate carrier), member 24
E03	***SLC25A25***	NM_052901	Solute carrier family 25 (mitochondrial carrier; phosphate carrier), member 25
E04	***SLC25A27***	NM_004277	Solute carrier family 25, member 27, UCP4
E05	***SLC25A3***	NM_002635	Solute carrier family 25 (mitochondrial carrier; phosphate carrier), member 3
E06	***SLC25A30***	NM_001010875	Solute carrier family 25, member 30
E07	***SLC25A31***	NM_031291	Solute carrier family 25 (mitochondrial carrier; adenine nucleotide translocator), member 31, ANT4
E08	***SLC25A37***	NM_016612	Solute carrier family 25, (mitochondrial iron transporter), member 37
E09	***SLC25A4***	NM_001151	Solute carrier family 25 (mitochondrial carrier; adenine nucleotide translocator), member 4, ANT1
E10	***SLC25A5***	NM_001152	Solute carrier family 25 (mitochondrial carrier; adenine nucleotide translocator), member 5, ANT2
E11	***SOD1***	NM_000454	Superoxide dismutase 1, soluble, Cu/Zn superoxide dismutase
E12	***SOD2***	NM_000636	Superoxide dismutase 2, mitochondrial, Fe/Mn superoxide dismutase
F01	***STARD3***	NM_006804	StAR-related lipid transfer (START) domain containing 3, lipid trafficking protein
F02	***TAZ***	NM_000116	Tafazzin
F03	***TIMM10***	NM_012456	Translocase of inner mitochondrial membrane 10 homolog (yeast)
F04	***TIMM17A***	NM_006335	Translocase of inner mitochondrial membrane 17 homolog A (yeast)
F05	***TIMM17B***	NM_005834	Translocase of inner mitochondrial membrane 17 homolog B (yeast)
F06	***TIMM22***	NM_013337	Translocase of inner mitochondrial membrane 22 homolog (yeast)
F07	***TIMM23***	NM_006327	Translocase of inner mitochondrial membrane 23 homolog (yeast)
F08	***TIMM44***	NM_006351	Translocase of inner mitochondrial membrane 44 homolog (yeast)
F09	***TIMM50***	NM_001001563	Translocase of inner mitochondrial membrane 50 homolog (S. cerevisiae)
F10	***TIMM8A***	NM_004085	Translocase of inner mitochondrial membrane 8 homolog A (yeast)
F11	***TIMM8B***	NM_012459	Translocase of inner mitochondrial membrane 8 homolog B (yeast)
F12	***TIMM9***	NM_012460	Translocase of inner mitochondrial membrane 9 homolog (yeast)
G01	***TOMM20***	NM_014765	Translocase of outer mitochondrial membrane 20 homolog (yeast)
G02	***TOMM22***	NM_020243	Translocase of outer mitochondrial membrane 22 homolog (yeast)
G03	***TOMM34***	NM_006809	Translocase of outer mitochondrial membrane 34
G04	***TOMM40***	NM_006114	Translocase of outer mitochondrial membrane 40 homolog (yeast)
G05	***TOMM40L***	NM_032174	Translocase of outer mitochondrial membrane 40 homolog (yeast)-like
G06	***TOMM70A***	NM_014820	Translocase of outer mitochondrial membrane 70 homolog A (S. cerevisiae)
G07	***TP53***	NM_000546	Tumor protein p53, P53 tumor suppressor
G08	***TSPO***	NM_000714	Translocator protein (18kDa), transport of cholesterol
G09	***UCP1***	NM_021833	Uncoupling protein 1 (mitochondrial, proton carrier), SLC25A7, proton leak
G10	***UCP2***	NM_003355	Uncoupling protein 2 (mitochondrial, proton carrier), SLC25A8, proton leak
G11	***UCP3***	NM_003356	Uncoupling protein 3 (mitochondrial, proton carrier), SLC25A9, proton leak
G12	***UXT***	NM_004182	Ubiquitously-expressed transcript
H01	***B2M***	NM_004048	Beta-2-microglobulin
H02	***HPRT1***	NM_000194	Hypoxanthine phosphoribosyltransferase 1
H03	***RPL13A***	NM_012423	Ribosomal protein L13a
H04	***GAPDH***	NM_002046	Glyceraldehyde-3-phosphate dehydrogenase
H05	***ACTB***	NM_001101	Actin, beta

H06	***HGDC***	SA_00105	Human Genomic DNA Contamination
H07	***RTC***	SA_00104	Reverse Transcription Control
H08	***RTC***	SA_00104	Reverse Transcription Control
H09	***RTC***	SA_00104	Reverse Transcription Control
H10	***PPC***	SA_00103	Positive PCR Control
H11	***PPC***	SA_00103	Positive PCR Control
H12	***PPC***	SA_00103	Positive PCR Control

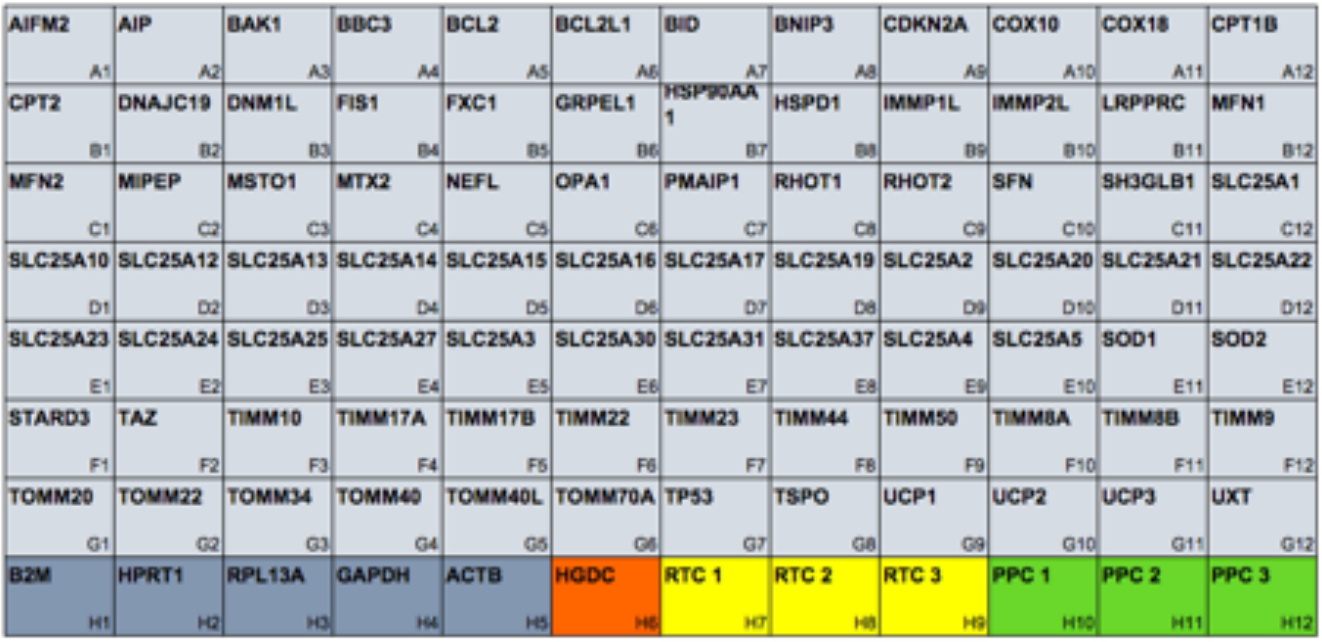

Figure 3.5 Layout of the Human Mitochondria RT² Profiler PCR Array.
Housekeeping assay panel: wells H1 through H5 contained a housekeeping gene panel to normalize PCR array data. Genomic DNA controls (HGDC): well H6 contained a replicate genomic DNA controls that detects non-transcribed genomic DNA contamination with a high level of sensitivity. Reverse transcription controls (RTC): wells H7 through H9 contained replicate reverse transcription controls that tests the efficiency of the RT2 First Strand Kit reaction with a primer set detecting the template synthesized from the kit's built-in external RNA control. Positive PCR controls (PPC): Wells H10 through H12 contained replicate positive PCR controls that tested the efficiency of the polymerase chain reaction itself using a pre-dispensed artificial DNA sequence and the primer set that detects it. The sets of replicate control wells (GDC, RTC, & PPC) also tested for inter-well, intra-plate consistency.

3.7 Protein extraction and quantification

A small piece of frozen tissue (≈30 mg) was used for whole tissue protein extraction. All the extraction procedures were performed on ice. Tissue was homogenized in a 20% (w/v) RIPA buffer (150 mM NaCl, 50 mM Tris pH 8.0 (HCl), 0.5% sodium deoxycholate (DOC), 1% IGEPAL (CA-630) and 0.1% sodium dodecyl sulfate (SDS)), supplemented with 5 µl/100 mg (tissue) of protease inhibitors cocktail (P8340, Sigma-Aldrich) and sodium orthovanadate, a phosphatase inhibitor, using an electric homogenizer PowerGen Model 125 (ThermoFischer Scientific, Fisher Scientific). The suspension was kept on ice for 5 min and then centrifuged at 14,000 g for 5 min at 4ºC to remove cellular debris. The pellet was discarded and protein concentration in the supernatant was determined by the Bicinchoninic acid assay (BCA) using the commercial Pierce BCA assay kit protocol (#9981, ThermoFischer Scientific, Fisher Scientific), using bovine serum albumin (BSA type V, Sigma-Aldrich) ranging from 0.25 to 2 mg/ml as standard. The amount of protein was calculated after determining the absorbance of the dye at 545 nm in a Victor X3 plate reader (PerkinElmer, Waltham, Massachusetts, USA). Standards and unknown samples were performed in triplicates. After protein determination, all the proteins were diluted for the same final concentration with RIPA and stored at -80ºC until forward use.

3.8 Protein analysis by Western blot

Initially, extracted proteins were solubilized to achieve a working concentration of 1mg/ml or 2 mg/ml of protein with Laemmli buffer (62.5 mM Tris pH 6.8 (HCl), 50% glycerol, 2% SDS, 0.005% bromophenol blue, supplemented with 5% β-mercaptoethano) and boiled for 5 min in a water bath and then centrifuged at 14,000 g for 5 min to remove cellular debris. Equivalent amounts of total protein (10 µg per lane) were loaded in a 10-20% gradient Tris-HCl polyacrylamide gel as well two distinct molecular weight standard for molecular weight estimation and for monitoring the electrophoresis, the Precision Plus Protein Dual Color Standards (Bio-Rad) and the SeeBlue Plus2 Pre-Stained Standard (ThermoFischer Scientific, Invitrogen). Electrophoresis was carried at room temperature in a Criterion system (Bio-Rad) using 150 V until the sample buffer (blue) reached the bottom of the gel

(≈ 90 min).

After separation of proteins by SDS-PAGE, proteins were electrophoretically transferred in a TransBlot Cell system (Bio-Rad) to a polyvinylidene difluoride (PVDF) membrane previously activated, a constant amperage (0.5 A) during 2 h at 4ºC using a CAPS transfer buffer (10 mM 3-(Cyclohexylamino)-1-propanesulfonic acid pH 11 (NaOH), 10% methanol). Good electrophoretic transfer was indicated by the complete transfer of prestained molecular weight markers below 100 kDa and by Ponceau staining. Ponceau results were also used to confirm equal amount of protein loading and to normalize the data.

Subsequently, after Ponceau removal the membranes were blocked in 5% non-fat milk/PBS overnight at 4ºC with agitation. Before incubation with primary antibodies the membrane was washed for 10 min in PBS 0.05% Tween-20 (PBS-T). Primary antibodies in Table 3.4 were prepared in 1% non-fat milk/PBS to a final volume of 5 ml and incubated overnight at 4ºC.

After incubation with primary antibodies, membranes were washed with PBS-T solution three times, 5 min each and incubated with the correspondent alkaline phosphatase conjugated secondary antibodies (against the animal where the primary antibody was produced for 2 h at room temperature with stirring (see Table 3.5).

Finally, for immunodetection, membranes were washed three times for 5 min each with PBS-T, rinsed in PBS to remove any Tween-20, which could be inhibitory to the detection method, dried and incubated with enhanced chemifluorescence (ECF) system (#RPN5785, GE Healthcare, Little Chalfont, Buckinghamshire, UK) during a maximum of 5 min. The ECF substrate allows the formation of fluorescence at 540 nm to 560 nm when excited at approximately 450 nm and images were collected with a UVP BioSpectrum 500 Imaging System (UVP, Upland, California, USA). Density analysis of bands was carried out with VisionWorks.LS Image Acquisition and Analysis Software (UVP).
Resulting images were analyzed and densities were normalized to Ponceau [198]. The average value of the control males (C-M) group was assumed as one unit and the values of each sample were determined proportionally.

Table 3.4 Panel of antibodies used in immunodetection.
Symbol denotes the protein identification, Description gives a summary information about the protein identification and/or function, Acession number denotes the reference from The Universal Protein Resource (UniProt) and Dilution represent the incubation conditions for the respective primary antibody.

Symbol	Description	Acession number[a]	Manufecturer code		Host Species	MW (KDa)	Dilution
NDUFB8	NADH dehydrogenase 1 beta subcomplex subunit 8	O95169	abcam	ab110242	Mouse	20	1:500
SDHB	Succinate dehydrogenase complex subunit B	P21912	abcam	ab14714	Mouse	29	1:500
SDHC	Succinate dehydrogenase complex subunit C	Q99643	Santa Cruz	sc-49491	Goat	12	1:100
UQCRC1	Ubiquinol-cytochrome c reductase core protein II	P31930	abcam	ab110252	Mouse	49	1:500
UQCRC2	Ubiquinol-cytochrome c reductase core protein II	P22695	abcam	ab14745	Mouse	47	1:500
MT-CO2	Cytochrome c oxidase subunit 2	P00403	abcam	ab110258	Mouse	24	1:500
COX6C	Cytochrome c oxidase subunit Vic	P09669	abcam	ab150422	Rabbit	9	1:1000
ATP5A1	ATP synthase subunit alpha, mitochondrial	P25705	abcam	ab14748	Mouse	53	1:500
ATP5A	ATP synthase subunit alpha	P25705	abcam	ab110273	Mouse	55	1:500
Cyt c	Cytochrome c	P99999	abcam	ab110325	Mouse	12	1:500
VDAC1	Voltage-dependent anion-selective channel protein 1	P21796	abcam	ab14734	Mouse	39	1:500
Cyc D	Cyclophilin D	P30405	abcam	ab110324	Mouse	21	1:500
CS	Citrate synthase	O75390	abcam	ab129088	Rabbit	52	1:1000
CAT	Catalase	P04040	abcam	ab1877	Rabbit	59	1:1000
SOD1	Superoxide dismutase 1	P00441	Santa Cruz	sc-11407	Rabbit	23	1:100
Fis1	Mitochondrial fission 1 protein	Q9Y3D6	Santa Cruz	sc48865	Goat	17	1:500

[a] as provided by the manufacturer and available on http://www.uniprot.org
Antibodies were diluted in 1% non-fat milk in PBS supplemented with 0.02% sodium azide, as a preservative, to a final volume of 5 ml and stored at 4ºC for no longer than 3 months or use to a maximum, of 5 times.

Table 3.5 List of secondary antibodies used in immunodetection.

Symbol	Description	Manufacturer code		Host Species	Dilution
G@R	goat anti-rabbit IgG-AP	Santa Cruz	sc-2007	Goat	1:5000
G@M	goat anti-mouse IgG-AP	Santa Cruz	sc-2008	Goat	1:5000
R@G	rabbit anti-goat IgG-AP	Santa Cruz	sc-2771	Rabbit	1:5000

3.9 Tissue Immunohistochemistry

Tissue immunohistochemistry was performed by a standard avidin-biotin histochemical technique as previously described [199]. Initial titrations were performed with three different concentrations of primary antibody that contained the suggested dilution of the manufacturer. The final primary antibody concentration was adjusted to give the cleanest immunostaining achievable. Once the final dilution of the primary antibody was determined, all sections to be analyzed were immunostained in the same assay to assure identical conditions. Briefly, fixed tissues sections (5 μm) were deparaffinized with xylene and rehydrated in decreasing grades of ethanol to water (100, 95, 70, and 50%). Antigen retrieval was performed for 15 min using citrate buffer (0.01 M citrate buffer, pH 6.0) in a microwave and heated to boiling. After cooling for 15 min, the section was rinsed for 5 min in potassium PBS (KPBS; 0.04 M K_2HPO_4, 0.01 M KH_2PO_4, 0.154 M NaCl, pH 7.4) and washed for 10 min in a solution of 1.5% H_2O_2/methanol and then for 5 min in KPBS. Sections were placed in diluted (10%) normal serum for 10 min and covered with primary antibody (Table 3.6) overnight at 4ºC [cytochrome c oxidase subunit VIc (COX6C): mouse monoclonal antibody (sc-65240); mitofusin 2 (Mfn2): mouse monoclonal antibody (sc-100560); and translocase of inner mitochondrial membrane 9A homolog (Tim9A): mouse monoclonal antibody (sc-101285) from Santa Cruz Biotechnology (Dallas, Texas, USA); sirtuin 3 (SIRT3): rabbit monoclonal antibody (2627); sirtuin 3 (SIRT3): rabbit monoclonal antibody (5490) from Cell Signaling Technology (Danvers, Massachusetts, USA) and anti-cytochrome c isoform 1 (CYC1): rabbit polyclonal antibody (HPA001247) from Sigma-Aldrich (St. Louis, Missouri, USA)] and incubated for 1 h at room temperature with the secondary antibody. All biotinylated secondary antibodies were obtained from Vector Laboratories (Burlingame, California, USA): goat anti-rabbit (BA-1000) and horse anti-mouse (BA-2000). All were used at a 1:1,000 dilution. The appropriate negative controls were also run in the absence of the primary antibody but in the presence of normal serum. Three slides per animal were analyzed, and six pictures/slide per section (for kidney samples, two sections, cortex and medulla, were assumed) were randomly taken and analyzed with ImageJ software (National Institutes of Health, New York, USA) for fraction (area immunostained/area of the field of interest x 100%) and density (arbitrary density units).

Table 3.6 Panel of antibodies used in immunohistochemistry.
Symbol denotes the protein identification, Description gives a summary information about the protein identification and/or function, Acession number denotes the reference from The Universal Protein Resource (UniProt) and Dilution represent the incubation conditions for the respective primary antibody.

Symbol	Description	Accession number [a]	Manufacturer code		Host Species
CYC1	Cytochrome c-1, UQCR4	P08574	Sigma-Aldrich	HPA001247	Rabbit
COX6C	Cytochrome c oxidase subunit VIc	P09669	Santa Cruz	sc65240	Mouse
MFN2	Mitofusin 2	P25705	Santa Cruz	sc100560	Mouse
SIRT3	Sirtuin 3	Q9NTG7	Cell signaling	2627	Rabbit
SIRT3	Sirtuin 3	Q9NTG7	Cell signaling	5490	Rabbit
TIM9A	Translocase of inner mitochondrial membrane 9A	P25705	Santa Cruz	sc101285	Mouse

[a] as provided by the manufacturer and available on http://www.uniprot.org

3.10 Enzymatic activity of mitochondrial proteins

3.10.1 NADH dehydrogenase activity

Activity of complex I was measured by a method previously described by Long and collaborators [200] with some modifications. Succinctly, 30 μg of tissue homogenate was ressuspended in reaction buffer containing 25 mM KH_2PO_4 pH 7.5, 5 mM $MgCl_2$, 300 μM KCN, 4 μM antimycin A, 3 mg/ml BSA, 60 μM coenzyme Q1, 160 μM 2,6- dichlorophenolindophenol (DCPIP). Complex I activity was determined by the decrease in absorbance (600 nm) of DCPIP upon addition of 100 μM freshly-prepared NADH in a VICTOR X3 plate reader (PerkinElmer) at 37ºC. Enzymatic activity was determined through the mean of slopes obtained during the linear phase of duplicates. Particular mitochondrial complex I activity was computed as the difference among basal activity in the absence or presence of 10 μM rotenone, a specific inhibitor of complex I. Normalization was performed taking in consideration the protein concentration and the molar extinction coefficient of ε600 = 19.1 $mM^{-1}.cm^{-1}$. Complex I activity was expressed as nmol DCPIP/min/mg protein.

3.10.2 Succinate dehydrogenase activity

Activity of complex II/III was analyzed by a method previously defined by Tisdale [201] with minor modifications. Concisely, 100 μg of tissue homogenate was pre-

incubated in 200 µL of phosphate buffer (166 mM KH_2PO_4/K_2HPO_4, pH 7.4) supplemented with 100 mM KCN and 500 mM sodium succinate during 5 min at 37°C. Initiation of the reaction occurred by the addition of 120 µL of phosphate buffer supplemented with 2 mM oxidized cytochrome c (cyt c ox) plus 15 mM EDTA-dipotassium. Enzyme activity was measured through the mean of slopes obtained during the linear phase for duplicates. Complex II/III activity was determined by following the reduction of cyt c ox (increased absorbance at 550 nm), using a VICTOR X3 plate reader. Mitochondrial complex II/III specific activity was computed as the difference between basal activity in the absence or presence of 4 mM antimycin A (specific inhibitor of complex III). Normalization was performed taking in consideration the protein concentration and the molar extinction coefficient of ε550 = 18.5 $mM^{-1}.cm^{-1}$. Results were express as nmol cyt c ox/min/mg protein.

3.10.3 Ubiquinol cytochrome c oxidoreductase activity

Activity of complex III was analyzed by adaptation of the method described by Luo and collaborators [202]. Briefly, 100 µg of tissue homogenate was suspended in reaction buffer containing 25 mM KH_2PO_4 pH 7.5, 4 µM rotenone, 0.025% Tween-20, 100 µM fresh decylubiquinone solution at 37°C. Enzymatic activity was measured as an increase in absorbance of cyt c ox at 550 nm, upon addition of 75 µM cyt c ox in a VICTOR X3 plate reader. Enzyme activity was determined through the mean of slopes obtained during the linear phase for duplicates. For determination of the specific complex III activity, 2.5 mM antimycin A (complex III specific inhibitor) was used and the difference between basal activity in the absence or presence of antimycin A was determined. Normalization was performed taking in consideration the protein concentration and the molar extinction coefficient of ε550 = 18.5 $mM^{-1}.cm^{-1}$. Results were express as nmol cyt cox min/mg protein.

3.10.4 Cytochrome c oxidase activity

Activity of complex IV was measured by adaptation of the method previously described by Brautigan and collaborators [203]. Briefly, 25 µg of tissue homogenate was suspended in reaction buffer containing 50 mM KH_2PO_4 pH 7.0, 4 µM antimycin A, 0.05% n-dodecyl-β-D-maltoside at 37°C. Enzymatic activity was followed in a VICTOR X3 plate reader as a decrease in absorbance of reduced cytochrome c (cyt c

red) at 550 nm, upon addition of 57 μM freshly-prepared cyt c red. Enzyme activity was calculated through the mean of slopes obtained during the linear phase for duplicates. Cyanide, a complex IV specific inhibitor, was use for determination of mitochondrial complex IV specific activity that was computed as the difference between basal activity in the absence or presence of 10 mM of KCN. Normalization was performed taking in consideration the protein concentration and the molar extinction coefficient of ε550 = 18.5 $mM^{-1}.cm^{-1}$. Activity was expressed as nmol cyt c red min/mg protein.

3.10.5 Citrate synthase

Activity of citrate synthase was analyzed by adapting the method previously described by Core and collaborators [204]. Concisely, 25 μg of tissue homogenate was suspended in a reaction buffer containing 100 mM Tris pH 8.0 plus 200 μM Acetyl-CoA, 200 μM 5,5′- dithiobis-2-nitrobenzoic acid at 37°C. Enzymatic activity was measured by following the increase in absorbance (412 nm) upon addition of 100 μM freshly-prepared oxaloacetate in a VICTOR X3 plate reader at 37°C. Enzyme activity was calculated through the mean of slopes obtained during the linear phase for duplicates. Specific citrate synthase activity was determined by subtracting the basal activity in the presence of 0.1% Triton-X100. Normalization was performed taking in consideration the protein concentration and the molar extinction coefficient of ε412 = 13.6 mM−1 ·cm−1. Enzyme activity was expressed as nmol of oxaloacetate min/mg protein.

3.11 Analysis of adenine nucleotides

Adenine nucleotide levels were measured according to the method previously described by Santos and collaborators [205]. Briefly, by using an electric homogenizer, the tissue was homogenized in 0.3 M perchloric acid (equal parts of PBS and 0.6 M perchloric acid) and kept for 5 min on ice. The acid homogenates were centrifuged at 14,000 g for 10 min and at 4°C. Supernatants were transferred to 1.5 ml tubes and brought to neutral pH with 3 M KOH in 1.5 mM Tris. The pellets were ressuspended in 1 M NaOH and stored at -80ºC for future determination of protein concentration by BCA, using BSA standards. After neutralization of the

supernatants, the samples were centrifuged at 14,000 g, for 10 min at 4ºC, and stored at -80ºC until HPLC injection.

The supernatants were assayed for ATP, ADP, and AMP by separation in a reverse-phase high-performance liquid chromatography (HPLC), as described by Stocchi and collaborators [206]. The chromatographic apparatus used was a Beckman-System Gold (Beckman Instruments, Fullerton, California, USA), consisting of a binary pump (model 126) and a variable UV detector (model 166), controlled by a computer. The detection wavelength was 254 nm, and the column used was a LiChrospher 100 RP-18 (5 μm) from Merck. An isocratic elution with 100 mmol/l phosphate buffer (KH_2PO_4; pH 6.5) and 1.0% methanol was performed with a flow rate of 1 ml/min. The required time for each analysis was 6 min. Peak identity was determined by the retention time compared with standards. The amounts of nucleotides and metabolites were determined by a concentration standard curve. Concentration of adenylates was expressed as nmol/mg of protein and adenylate energy charge (AEC) was determined according to the formula (ATP + 1/2 ADP) /(ATP + ADP + AMP).

3.12 Oxidative stress evaluation

Oxidative stress was evaluated by measuring malondialdehyde (MDA) levels and oxidized glutathione (GSSG), while the antioxidant capacity was evaluated by determination of reduced glutathione (GSH) and vitamin E contents. The enzymatic activities of glutathione peroxidase (Gl-Px) and glutathione reductase (Gl-Red) were also determined.

3.12.1 Lipid peroxidation evaluation by malondialdehyde contents

Levels of lipid peroxidation were assessed by adaptation of the method previously described by Draper and collaborators [207] using fluorimetric determination (excitation at 515 nm and emission at 553 nm; FP-2020/2025, Jasco, Tokyo, Japan) of malondialdehyde adducts separated by high-performance liquid chromatography (HPLC; Gilson, Lewis Center, Ohio, USA) using the ClinRep complete kit (RECIPE, Munich, Germany). Results were expressed as μM of MDA.

3.12.2 Measurement of reduced glutathione and oxidized glutathione contents

Reduced and oxidized glutathione (GSH and GSSG) were evaluated by adaptation of the method previously described by Tsao and collaborators [208] operating an HPLC system (Gilson) with fluorimetric detection (excitation at 385 nm and emission at 515 nm; FP-2020/2025, Jasco), using the Immunodiagnostik kit (Immunodiagnostik AG, Bensheim, Germany). Results were expressed as μM of GSH and μM of GSSG.

3.12.3 Measurement of Vitamin E levels

Vitamin E present in tissue was extracted in n-hexane (Merck) and quantified by reverse-phase HPLC (Gilson), using an analytic column Spherisorb S10w (250 x 4.6 mm), eluted at 1.5 ml/min with n-hexane modified with 0.9% of methanol (Merck) and spectrophotometric detection at 287 nm. Results were expressed as μM of Vit E.

3.12.4 Determination of glutathione peroxidase activity

The activity of glutathione peroxidase (Gl-Px) was evaluated by adaptation of the method previously described by Palia and collaborators [209] and through means of spectrophotometry using tert-butylperoxide (Sigma-Aldrich) as a substrate the assay monitored the formation of oxidized glutathione through the quantification of the oxidation of NADPH (Sigma-Aldrich) to $NADP^+$ at 340 nm in a thermostatized spectrophotometer (UVIKON 933 double bean UV/Visible spectrophotometer, Kontron instruments, Milan, Italy). Results were expressed in international units of enzyme per liter (U/l).

3.12.5 Evaluation of glutathione reductase activity

Glutathione reductase (Gl-Red) activity was evaluated by adaptation of the method previously described by Goldberg and collaborators [210] operating spectrophotometry at 340 nm, using GSSG (Sigma) as a substrate and monitoring its reduction to GSH through the quantification of NADPH (Sigma) oxidation at 37ºC in a thermostatized spectrophotometer (UVIKON 933 double bean UV/Visible spectrophotometer). Gl-Red activity was expressed in international units of enzyme per liter (U/l).

3.13 Transmission Electron Microscopy

Samples were processed by the certificated Electron Microscopy Lab at the Department of Pathology at UTHSCSA using the Transmission Electron Microscope (TEM) JEOL 1230 (JEOL, Peabody, Massachusetts, USA). After the primary fixation at the cesarean section samples were rinsed with PBS and pos-fixed durin 30 min with 1% buffered Osmium Tetroxide, according to Zetterqvist (1956) [211]. Samples were dehydrated in increasing grades of ethanol (70, 95 and 100%) and placed in propylene oxide at the end of the dehydration. After being in propylene oxide during 20 min, samples were infiltrated with a mixture 1:1 of propylene oxide / resin followed by 30 min in 100% resin under 25 psi vacuum. Longitudinal pieces were flat-embedding in molds and filled to the top with resin. Resin was polymerized at 80ºC overnight. Tissues were sectioned in 0.5-1 μm sections and stained with T-blue during 10 seconds on a hot plate. Sections quality was checked using a light microscope. Cardiac sections were either left unstained or stained with uranyl acetate during 30 sec, followed by Reynold's Lead Citrate stain during 20 sec for imaging. A series of 5-6 images at 3,300x magnification demonstrating areas of interest were obtained.

3.14 Data analysis and statistics

The hypothesis to be tested in this study is that maternal nutrition reduction by 30% during gestation affects renal and cardiac mitochondria heritage and function of the progeny. A secondary question is whether these effects are dependent on the fetus's gender.

By definition the experimental unit is the unit which could be independently assigned to any treatment. In this study, each pregnant female baboon and the correspondent fetus were considered as an experimental unit. Outbred pregnant female baboons were randomly assigned to control or MNR groups. The resource equation method was used for determining the sample size where E = (total number of animals) – (number of treatment groups) and $10 < E < 20$. Whenever possible, we performed blind assessment of the diet effects and blind determination of the parameters to be statistically analyzed.

Data are expressed as mean ± standard error of the mean. Whenever possible, parametric tests were employed, assessed by the Kolmogorov-Smirnov normality test and Levene variance homogeneity test. If a normal distribution was absent or groups were considered to small, the equivalent non-parametric tests were employed, essentially the Mann-Whitney test. Statistical tests were performed considering a significance level of $\alpha=0.05$. PCR array data were analyzed using the ΔΔCt method and the web tools of SA Biosciences (SA Biosciences, Qiagen, http://www.sabiosciences.com/pcr/arrayanalysis.php). Statistical analyses were performed using SPSS version 17.0 (IBM corporation, Armonk, New York, USA) with significance set at $P<0.05$ by two independent investigators for diminish the influence of natural human biases and corroboration. Graphical representations were obtained using GraphPad Prism version 6.0 (GraphPad Software, San Diego, California, USA).

3.15 The 3 R's application

The authors are truthfully committed with animal wellbeing. During this study the reduction of animals used and the refinement of testing to reduced suffering were important goals. Refinement was performed by environmental enrichments, favoring group housing, performing more humane practices with less stressful and less painful procedures using training (route to the feeding cages), non-invasive monitoring (weighing procedure), pain killers and humane endpoints.

By applying an appropriated experimental design, truly independent replicates, blind assessment, the correct statistical analysis and collecting and stored several biological samples from each animal which were shared by several collaborations we do believe that we reduced the number of animals needed to get strong evidences of the maternal diet effects in fetuses.

In this study we did not perform animal replacement but we are making sincerely efforts so that in the future it will be possible to continue these studies in humans.

Chapter 4

Effects of moderate global maternal nutrient reduction on fetal baboon renal mitochondrial gene expression at 0.9 gestation

This chapter includes the material from an original paper that has being previously published in the American Journal of Physiology – Renal Physiology and is referred below:

Susana P. Pereira, Paulo J. Oliveira, Ludgero Tavares, António J. Moreno, Laura A, Cox, Peter W. Nathanielsz, Mark J. Nijland (2015). **Effects of Moderate Global Maternal Nutrient Reduction on Fetal Baboon Renal Mitochondrial Gene Expression at 0.9 Gestation**. American Journal of Physiology - Renal Physiology.

Acknowledgements

The author acknowledge the contributions by Peter W. Nathanielsz and Mark J. Nijland that developed the animal model; by Paulina Quezada, Greg Langone and Li Cun for immunohistochemistry, by Michelle Zavala and Ana Maria Silva for general assistance in the laboratory, by Leslie Myatt, Alina Maloyan, Nagarjun Kasaraneni, Chunming Guo, Balasubashini Muralimanoharan and James Mele by allowing access to equipment, by Ludgero C. Tavares for the statistics validation, and finally by Karen Moore and Susan Jenkins for bibliography and data archiving.

4.1 Introduction

Suboptimal prenatal development predisposes to adult onset diseases such as hypertension, diabetes, cardiovascular and renal disease [212–215]. Importantly, there is clear evidence that the developing nonhuman primate kidney is sensitive to decreased maternal nutrition [216]. Poor intrauterine nutrition is associated with reduced nephron number in both animals and humans [217–220]. Analysis of renal autopsies of adults born with low birth weight has shown substantial variation in renal composition [221]. Remarkably, little attention has been given to the possible involvement of mitochondria as putative mediators between maternal nutrient reduction and altered renal development in their offspring. This is surprising, because healthy nephron and organ function rely on polarized mitochondria abundant in epithelial cells [222]. Mitochondria not only produce energy by using the oxidative phosphorylation system, but are also a source of guanosine triphosphate (GTP) and amino acids, the hub of cell death signaling pathways, a reservoir of cell calcium and an important site for the production of reactive oxygen species [118,223–225]. Mitochondria also play a crucial role in numerous regulatory functions during oocyte maturation [226], fertilization, initiation and progression of preimplantation embryos [227]. A postmortem study [228] of muscles from premature neonates demonstrated a functional respiratory chain showing that mitochondria are functional during fetal development.

Dysfunctional mitochondrial OXPHOS is a key player in a variety of human disorders including primary mitochondrial diseases caused by mutations in mitochondrial and/or nuclear DNA[229] as well as in aging [230], drug toxicity [118,224,231,232], diabetes [233] and several neurodegenerative disorders [234]. Both the quality and quantity of mitochondria are essential prerequisites for successful embryo and fetal development [235]. For all these reasons we propose that regulation of mitochondrial metabolism during fetal development is not only important for neonatal life but also may have implications for health and disease in adulthood.

Baboons are valuable models for the study of complex physiological and disease processes because they exhibit similarity to human health and disease phenotypes. The baboon also exhibits a pattern of disease susceptibility and health complications that is very similar to that seen in humans [236]. Our previous study [237] demonstrated

that pregnant baboons that consumed 70% of the global *ad libitum* diet from 0.16 to 0.5 gestation had an 11% decrease in maternal body weight accompanied by intrauterine growth reduction and a similar decrease in fetal body weight, whereas the fetal kidney weight-to-body weight ratio was not significantly altered. However, this moderate level of MNR altered the subcellular histology of the kidney at 50% gestation by decreasing tubule density and altering renal transcriptome expression, with several transcripts for mitochondrial components being downregulated including subunits of the respiratory chain and ATP synthase [197,216].

In accordance with these previous observations, the aim of the present study was to determine the effects of a controlled and moderate global MNR on fetal baboon renal mitochondrial transcripts and proteins at term (0.9 gestation). We hypothesized that poor maternal nutrition during pregnancy impairs the mitochondrial transcriptome, potentially influencing kidney development and contributing to the development of renal disease in adult life.

4.2 Results

4.2.1 Biological changes resulting from MNR

Control and MNR groups did not differ in maternal body weight before pregnancy. However, at 0.9 gestation, *ad libitum*-fed control mothers weighed more than MNR mothers. The maternal control group gained 11.30 ± 3.05% of their body weight during pregnancy. In contrast, MNR mothers significantly lost weight (5.63 ± 3.89%). Maternal weight loss was more pronounced in MNR mothers carrying male fetuses (-10.51 ± 5.41% vs -0.76 ± 4.78%). Placental weight was also significantly decreased in MNR mothers (-19.55 ± 5.13%, Table 4.1).

At cesarean section, measurements of biomarkers for maternal renal function, such as BUN, creatinine, BUN creatine ratio, sodium (Na^+), potassium (K^+), and carbon dioxide (CO_2), were not altered by MNR, only serum chloride (Cl^-) content was significantly decreased in the MNR mothers carrying female fetuses. A statistical tendency was found for a diet-effect on serum triglycerides (P=0.056), namely for MNR mothers carrying male fetuses. In this group, an increase of 79% of circulating blood serum triglycerides was observed compared with mothers that received the control diet and carrying a male fetus. In terms of fetal morphometrics, MNR decreased the fetal body mass index by 16.7% (P=0.02). In addition, femoral length from MNR female fetuses was decreased compared with the control group (P=0.046). However, MNR did not alter fetal kidney weight or the kidney weight-to-body weight ratio, although the brain weight-to-body weight ratio increased significantly in MNR fetuses.

4.2.2 Fetal and maternal cortisol, glucose, and insulin levels

Circulating cortisol in *ad libitum*-fed control mothers was about 2.7 fold higher than in their offspring at 0.9 gestation (Figure 4.1). A proportional increase in cortisol was observed in both maternal and fetal blood serum in MNR baboons. However, this increase only reached statistical significance in the MNR mothers carrying male fetuses and in the serum of MNR fetuses, namely due to effects on MNR female fetuses. The results also show an analogous maternal-to-fetal circulating cortisol gradient in control and MNR pregnancies (Figure 4.1A).

Table 4.1 Maternal and fetal morphological and biochemical parameters at 0.9 gestation in control ad libitum-fed pregnancies and in the presence of maternal nutrient reduction (MNR) to 70% of the food eaten by the control mothers on a weight-adjusted basis.

	Genders combined		Male		Female		P-value by Mann-Whitney test				
	Control	MNR	Control	MNR	Control	MNR	Diet	Male C vs. MNR	Female C vs. MNR	Control M vs. F	MNR M vs. F
Number of animals/group	6	6	3	3	3	3					
Maternal characterization											
Weight preconception (Kg)	15.18 ± 0.95	14.93 ± 0.39	13.67 ± 0.61	15.14 ± 0.42	16.69 ± 1.36	14.72 ± 0.74	-	-	-	-	-
Weight at cesarean section (Kg)	16.80 ± 0.79	14.11 ± 0.77	15.91 ± 0.98	13.59 ± 1.19	17.70 ± 1.17	14.63 ± 1.12	0.037	-	-	-	-
Weight variation (%)	11.30 ± 3.05	-5.63 ± 3.89	16.27 ± 4.26	-10.51 ± 5.41	6.32 ± 1.87	-0.76 ± 0.47	0.01	0.05	-	0.05	-
Placental weight (g)	181.67 ± 7.77	145.00 ± 7.23	180.33 ±10.33	147.67 ± 14.86	183.00 ± 13.89	142.33 ± 5.78	0.01	0.05	0.05	-	-
Blood serum at cesarean section							-	-	-	-	-
Blood urea nitrogen (mg/dl)	8.83 ± 0.60	9.33 ± 1.02	8.00 ± 0.58	7.67 ± 0.33	9.67 ± 0.88	11.00 ± 1.53	-	-	-	-	-
Creatinine (mg/dl)	0.87 ± 0.05	1.02 ± 0.10	0.83 ± 0.09	0.93 ± 0.07	0.90 ± 0.06	1.10 ± 0.21	-	-	-	-	-
Blood urea nitrogen/Creatinine	10.31 ± 0.80	9.55 ± 1.41	9.72 ± 0.84	8.33 ± 0.88	10.90 ± 1.45	10.77 ± 2.77	-	-	-	-	-
Sodium (mEq/l)	140.67 ± 0.88	140.50 ± 1.09	140.33 ± 1.67	142.00 ± 1.15	141.00 ± 1.00	139.00 ± 1.53	-	-	-	-	-
Potassium (mEq/l)	3.60 ± 0.12	3.65 ± 0.15	3.77 ± 0.18	3.70 ± 0.10	3.43 ± 0.12	3.60 ± 0.32	-	-	-	-	-
Chloride (mEq/l)	111.83 ± 0.79	109.50 ± 1.41	112.33 ± 1.67	111.00 ± 2.52	111.33 ± 0.33	108.00 ± 1.15	-	-	0.046	-	-
Carbon dioxide (mEq/l)	22.00 ± 0.86	21.17 ± 1.08	23.00 ± 0.58	22.33 ± 0.67	21.00 ± 1.53	20.00 ± 2.00	-	-	-	-	-
Anion Gap (mEq/l)	10.43 ± 1.27	13.48 ± 1.49	8.77 ± 0.41	12.37 ± 2.24	12.10 ± 2.25	14.60 ± 2.21	-	-	-	-	-
Calcium (mg/dl)	8.46 ± 0.11	8.40 ± 0.13	8.43 ± 0.19	8.23 ± 0.03	8.50 ± 0.10	8.65 ± 0.25	-	-	-	-	-
Phosphorus (mg/dl)	3.34 ± 0.08	3.22 ± 0.13	3.33 ± 0.12	3.33 ± 0.18	3.35 ± 0.15	3.05 ± 0.15	-	-	-	-	-
Albumin (g/dl)	2.75 ± 0.15	2.72 ± 0.05	2.87 ± 0.03	2.73 ± 0.07	2.63 ± 0.32	2.70 ± 0.10	-	-	-	-	-
Total protein (g/dl)	6.35 ± 0.24	6.28 ± 0.20	6.43 ± 0.07	6.00 ± 0.25	6.27 ± 0.53	6.57 ± 0.24	-	-	-	-	-
Total bilirubin (mg/dl)	0.28 ± 0.06	0.32 ± 0.06	0.30 ± 0.10	0.30 ± 0.06	0.25 ± 0.05	0.35 ± 0.15	-	-	-	-	-
Alkaline phosphatase (U/l)	137.50 ± 28.62	178.67 ± 43.49	171.33 ± 53.35	163.33 ± 13.93	103.67 ± 10.27	194.00 ± 95.02	-	-	-	-	-
Alanine aminotransferase (U/l)	38.17 ± 6.94	58.50 ± 12.53	36.00 ± 10.02	53.33 ± 13.98	40.33 ± 11.67	63.67 ± 23.73	-	-	-	-	-
Aspartate aminotransferase (U/l)	22.17 ± 2.63	37.33 ± 6.98	22.00 ± 2.65	38.67 ± 11.79	22.33 ± 5.24	36.00 ± 10.15	-	-	-	-	-
Gamma-glutamyl transferase (U/l)	31.60 ± 1.69	32.40 ± 1.03	31.00 ± 2.65	32.67 ± 1.76	32.50 ± 2.50	32.00 ± 1.00	-	-	-	-	-
Cholesterol (mg/dl)	60.17 ± 7.02	64.17 ± 7.53	62.33 ± 14.31	57.33 ± 8.21	58.00 ± 6.08	71.00 ± 13.00	-	-	-	-	-
Triglycerides (mg/dl)	29.40 ± 3.91	51.80 ± 6.96	29.33 ± 5.67	52.67 ± 8.35	29.50 ± 7.50	50.50 ± 16.50	-	-	-	-	-
Lactate dehydrogenase (U/l)	190.40 ± 17.54	191.00 ± 15.88	167.33 ± 15.50	197.33 ± 28.09	225.00 ± 19.00	181.50 ± 2.50	-	-	-	-	-
Creatine phosphokinase (U/l)	291.00 ± 62.75	357.40 ± 128.24	376.67 ± 60.98	390.67 ± 230.36	162.50 ± 26.50	307.50 ± 33.50	-	-	-	-	-
Fetal characterization											
Weight (g)	755.00 ± 35.22	668.50 ± 33.41	784.33 ± 46.16	711.00 ± 55.19	725.67 ± 56.68	626.00 ± 27.01	-	-	-	-	-
Body length (cm)	36.42 ± 0.90	37.50 ± 1.02	37.33 ± 0.44	38.50 ± 1.26	35.50 ± 1.73	36.50 ± 1.61	-	-	-	-	-
Femur length (cm)	7.71 ± 0.28	7.25 ± 0.21	7.33 ± 0.17	7.67 ± 0.17	8.08 ± 0.46	6.83 ± 0.17	-	-	0.046	-	0.043
Body mass index (Kg/m^2)	5.70 ± 0.22	4.77 ± 0.20	5.65 ± 0.45	4.78 ± 0.15	5.76 ± 0.19	4.75 ± 0.42	0.025	-	0.05	-	-
Kidney weight (g)	3.54 ± 0.26	3.56 ± 0.27	3.78 ± 0.52	3.60 ± 0.17	3.30 ± 0.08	3.51 ± 0.59	-	-	-	-	-
Kidney weight/body weight (x1000)	4.71 ± 0.31	5.39 ± 0.53	4.80 ± 0.54	5.10 ± 0.33	4.62 ± 0.44	5.68 ± 1.11	-	-	-	-	-
Brain weight (g)	77.30 ± 3.63	77.69 ± 2.49	82.27 ± 4.45	77.59 ± 4.90	72.33 ± 4.63	77.79 ± 2.62	-	-	-	-	-
Brain weight/body weight (x1000)	103.00 ± 5.45	116.92 ± 3.86	106.13 ± 11.44	109.39 ± 1.94	99.93 ± 2.84	124.46 ± 3.71	0.037	-	-	-	0.05

Data are means ± SEM; n=3 (when separated by gender) or n=6 (genders combined) animals/group. Comparison between groups was performed using a non-parametric Mann-Whitney test. P-value less than 0.05 was considered significant.

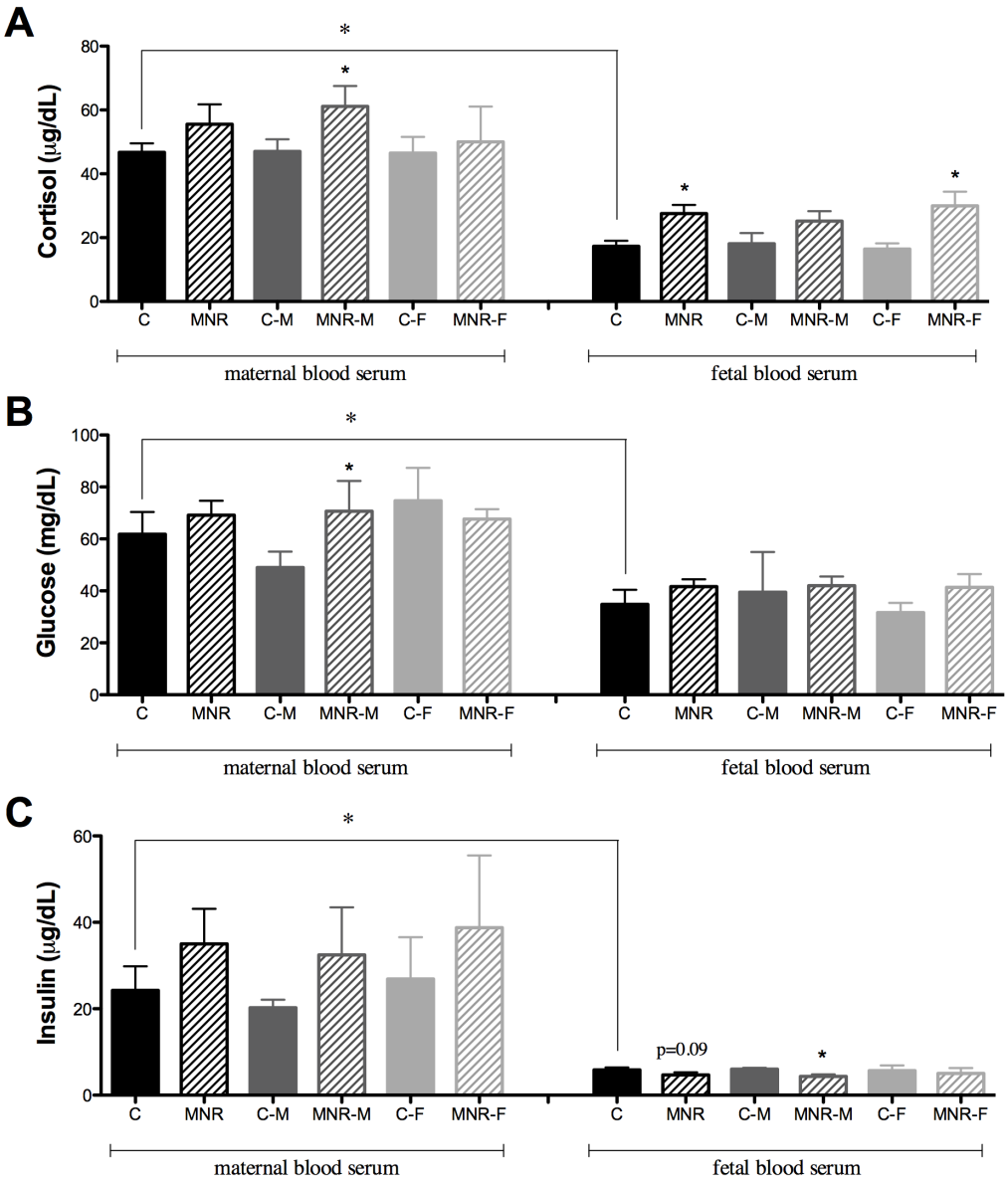

Figure 4.1 Cortisol, glucose, and insulin levels in maternal and fetal plasma of control (C) and maternal nutrient reduction (MNR) groups.
These parameters were determined in maternal and fetal plasma of control ad libitum-fed pregnancies and in the presence of MNR, characterized as 70% of the food consumed by control mothers on a weight-adjusted basis of baboons at 0.9 gestation. A: cortisol levels in maternal and fetal plasma of control and MNR baboons (male fetuses n=3; female fetuses n=3). C-M, male fetuses from control group; C-F, female fetuses from control group; MNR-M, male fetuses from MNR group; MNR-F, female fetuses from MNR group. B: glucose levels in maternal and fetal plasma of control and MNR (n=6) baboons (male fetuses n=3; female fetuses n=3). C: insulin levels in maternal and fetal plasma of control and MNR baboons (male fetuses n=3; female fetuses n=3). Means ± SEM; n=3 (when separated by gender) or n=6 (genders combined) animals/group. Comparison between groups was performed using a non-parametric Mann-Whitney test. P-value less than 0.05 was considered significant. *P<0.05 vs. respective controls or as indicated.

The maternal-to-fetal cortisol gradient was not different in MNR compared to control pregnancies.

Plasma glucose in control mothers fed ad libitum was 1.8 fold higher than that of their fetuses at 0.9 gestation ($P<0.05$). However, no difference was observed in glucose levels between control and MNR fetuses when genders were either combined or separated (Figure 4.1B). Only MNR mothers carrying male fetuses registered a significant increase in glucose levels. There was a trend for increased maternal insulin levels in all MNR mothers; however, due to variability in the data obtained, the difference did not reach significance. Insulin levels in control mothers were 4.1 fold greater than in fetuses (0.9 gestation). Diet effects were observed only in the fetal male insulin levels (Figure 4.1C).

4.2.3 MNR affects key mitochondrial genes in the fetus kidney

The Human Mitochondrial Energy Metabolism and the Human Mitochondria Pathway Arrays were used for expression profiling in fetal kidney RNA samples. The complete set of data is shown in Table 4.1 and summarized in Fig. 4.1. PCR arrays presented a residual percentage of absent calls (7.5% and 3% for the respectively array). The mitochondrial genes investigated showed diet-dependent effects, with a significant overall decreased expression of mitochondrial genes in the MNR fetuses compared with control fetuses, with the greatest alterations occurring when genders were combined (Fig. 4.2.E). There were 46 genes differentially expressed in the MNR group, with 93% of the alterations involving downregulation. Most of the downregulated transcripts encoded subunits of mitochondrial OXPHOS, including 18 of 33 subunits analyzed from complex I: *NDUFA1, NDUFA2, NDUFA4, NDUFA5, NDUFA7, NDUFA8, NDUFA10, NDUFA11, NDUFAB1, NDUFB5, NDUFB9, NDUFC1, NDUFC2, NDUFS3, NDUFS4, NDUFS5, NDUFS8* and *NDUFV3*; 2 of 4 subunits analyzed for complex II: *SDHA* and *SDHB*; 2 of 6 subunits analyzed for complex III: *UQCRC1* and *UQCRFS1*; 4 of 14 subunits analyzed for complex IV: *COX4I1*, *COX5A*, *COX5B* and *COX8C*; *OXA1L*, an essential factor for the activity and assembly for this complex; and 8 of 21 subunits analyzed for ATP synthase: *ATP4A, ATP4B, ATP5B, ATP5G1, ATP5J, ATP5O, ATP6V0A2* and *ATP6V1C2*. In addition, transcripts for regulators and mediators of mitochondrial molecular transport, namely small-molecule transporters

(*SLC25A15, SLC25A16, SLC25A23, SLC25A27, SLC25A31*) and two members of the inner membrane translocation system (*TIMM23* and *FXC1*) were also downregulated in the MNR group. Finally, two members of the inorganic pyrophosphatase family, which catalyze the hydrolysis of pyrophosphate to inorganic phosphate (*PPA1* and *PPA2*) and ultimately the mitochondrial apoptosis-inducing factor (*AIFM2*), which plays a role as a caspase-independent apoptotic factor, were also downregulated.

A significant sexual dimorphism was shown in the mitochondrial profile of the control fetuses. Female fetuses presented a higher content in transcripts for *NDUFV1*, a complex I subunit; *COX6A1*, a cytochrome c oxidase subunit; *ATP5C1*, an ATP synthase subunit; *IMMP1L*, a subunit of the mitochondrial inner membrane peptidase (IMP); *TIMM9*, an inner mitochondrial membrane protein translocase; *BID*, a member of the Bcl-2 family of cell death regulators and *SFN*, a p53-regulated inhibitor of G2/M progression. On the other hand, female fetuses contained decreased abundance of transcripts for *OPA1*, which is required for mitochondrial fusion and regulation of apoptosis; *SLC25A17*, a peroxisomal transporter for multiple cofactors such as coenzyme A (CoA), flavin adenine dinucleotide (FAD), flavin mononucleotide (FMN) and nucleotide adenosine monophosphate (AMP); *TIMM17A*, an essential component of the TIM complex, a complex that mediates the translocation of proteins across the mitochondrial inner membrane; *TOMM70A*, which encodes a component of the outer membrane translocase complex, and *SOD1*, the cytosolic superoxide dismutase.

Diet-induced transcript differences were also observed within the same gender. In summary, multiple components of the mitochondrial respiratory chain were reduced in MNR male fetuses, including two subunits of complex I (*NDUFA1, NDUFA4*), one subunit of complex II (*SDHB*), and one ATP synthase subunit of (*ATP6V1C2*). Decreased transcripts also included *SOD1*, as well as *TIMM23*, a gene encoding a component of the inner mitochondrial membrane import system. On the other hand, one complex IV subunit (*COX6A1*) was significantly increased (1.7 fold), as well as stratifin (*SFN*), which has been implicated in the regulation of a large spectrum of both general and specialized signaling pathways. In the MNR female fetus, the same trend was found, although with a slight difference in the subunits affected by maternal diet. MNR resulted in a significant decrease in the abundance of transcripts for the mitochondrial respiratory chain, including *NDUFS5* and *NDUFV3*, two

subunits from complex I, *COX6C* and *COX7B*, two subunits from complex IV, as well as ATP synthase subunit F6 (*ATP5J*). Other significant diet-induced downregulated gene-expression occurred for *MFN2*, which is involved in mitochondrial fusion; three solute mitochondrial carrier family 25 genes (*SLC25A16*, *SLC25A17*, and *SLC25A31* an adenine nucleotide translocator), pro-apoptotic Bcl-2-binding component 3 (*BBC3*), *BID*, a mediator of mitochondrial damage induced by caspase-8, and the STAR-related lipid transfer domain 3 (*STARD3*), which encodes for a lipid trafficking protein that may be involved in exporting cholesterol. The two transcripts that were significantly upregulated in the MNR female fetuses were cyclin-dependent kinase inhibitor 2A (*CDKN2A*), a stabilizer of the tumor suppressor protein p53, and one solute mitochondrial carrier family 25 gene (*SLC25A15*, coding for an ornithine transporter).

Figure 4.2 Renal gene expression analysis of control and MNR baboon fetuses at 0.9 gestation. (following page)
mRNA abundance for mitochondrial proteins was assessed by PCR array in whole kidney samples from baboon fetuses from mothers fed *ad libitum* (control group) or 70% of the control diet (MNR group) at 0.9 gestation. A: Sexual dimorphism in the mitochondrial profile of control fetusus B: and C: comparison of transcripts expression based on maternal diet for the same gender [male fetuses (B) and female fetuses (C)]. D: gender dimorphism in the mitochondrial profile of the MNR fetus and E: global diet-dependent effects in the mitochondrial expression profile. Transcripts related to oxidative phosphorylation system (OXPHOS), complex I (CI; NADH dehydrogenase, complex II (CII; succinate dehydrogenase), complex III (CIII; ubiquinol cytochrome c oxidoreductase), complex IV [CIV; cytochrome c oxidase (COX)], and complex V (CV; ATP synthase). Values were normalized to endogenous controls [hypoxanthine phosphoribosyltransferase 1 (*HPRT1*), ribosomal protein L13a (*RPL13A*), and Beta-actin (*ACTB*)] and expressed relative to their normalized values. Means ± SEM; n=3 (when separated by gender) or n=6 (genders combined) animals/group. All transcripts presented have $P<0.05$ vs. respective paired group. See the Table 4.2 from this section or the Material and Methods Table 3.2 and Table 3.3 for gene abbreviations used.

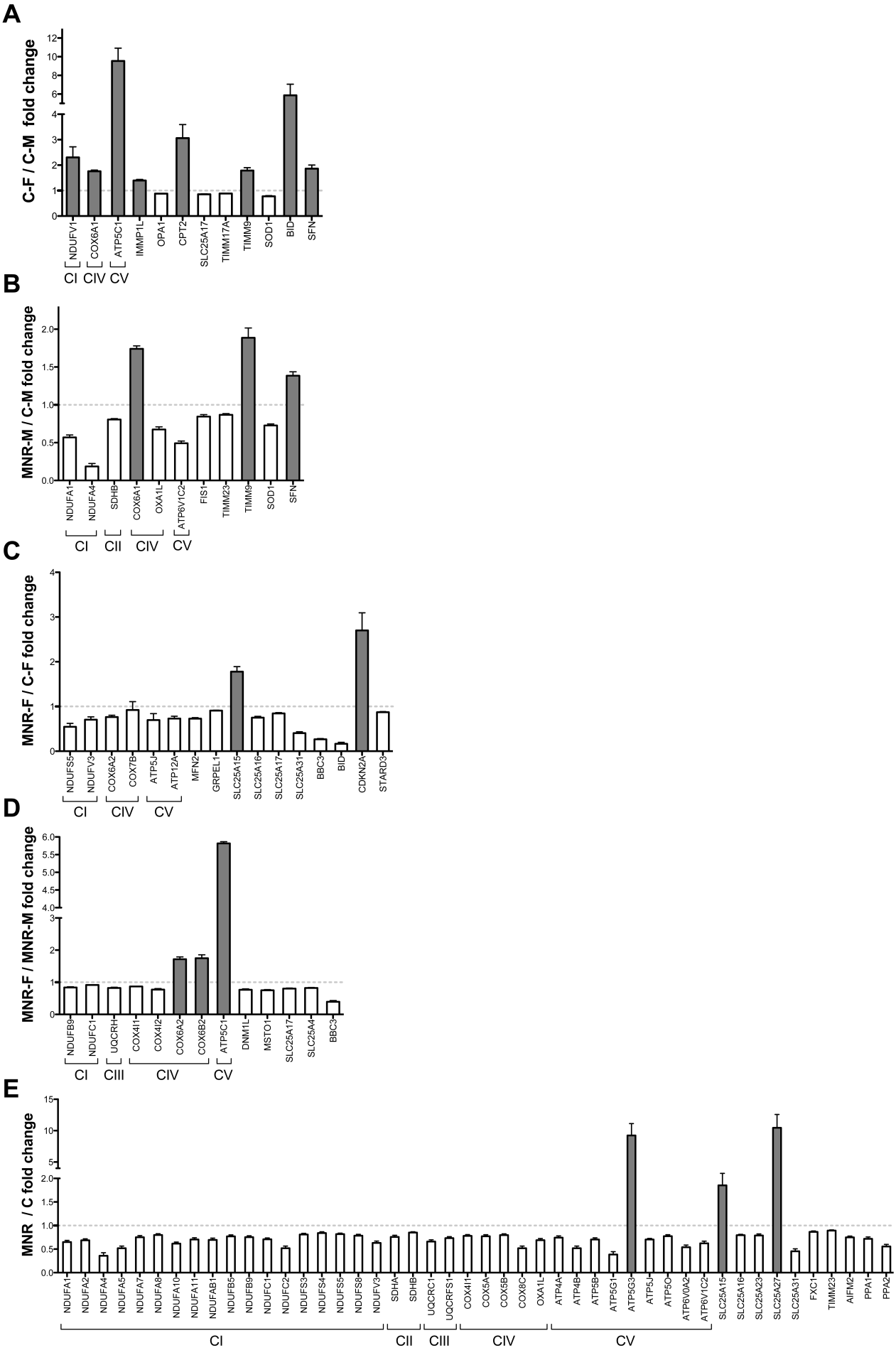
A
C-F / C-M fold change
NDUFV1
COX6A1
ATP5C1
IMMP1L
OPA1
CPT2
SLC25A17
TIMM17A
TIMM9
SOD1
BID
SFN
CI CIV CV
B
MNR-M / C-M fold change
NDUFA1
NDUFA4
SDHB
COX6A1
OXA1L
ATP6V1C2
FIS1
TIMM23
TIMM9
SOD1
SFN
CI CII CIV CV
C
MNR-F / C-F fold change
NDUFS5
NDUFV3
COX6A2
COX7B
ATP5J
ATP12A
MFN2
GRPEL1
SLC25A15
SLC25A16
SLC25A17
SLC25A31
BBC3
BID
CDKN2A
STARD3
CI CIV CV
D
MNR-F / MNR-M fold change
NDUFB9
NDUFC1
UQCRH
COX4I1
COX4I2
COX6A2
COX6B2
ATP5C1
DNM1L
MSTO1
SLC25A17
SLC25A4
BBC3
CI CIII CIV CV
E
MNR / C fold change
NDUFA1
NDUFA2
NDUFA4
NDUFA5
NDUFA7
NDUFA8
NDUFA10
NDUFA11
NDUFAB1
NDUFB5
NDUFB9
NDUFC1
NDUFC2
NDUFS3
NDUFS4
NDUFS5
NDUFS8
NDUFV3
SDHA
SDHB
UQCRC1
UQCRFS1
COX4I1
COX5A
COX5B
COX8C
OXA1L
ATP4A
ATP4B
ATP5B
ATP5G1
ATP5G3
ATP5J
ATP5O
ATP6V0A2
ATP6V1C2
SLC25A15
SLC25A16
SLC25A23
SLC25A27
SLC25A31
FXC1
TIMM23
AIFM2
PPA1
PPA2
CI CII CIII CIV CV

Table 4.2 mRNA abundance for mitochondrial proteins.
mRNA abundance was assessed by PCR array in whole kidney samples from baboon fetuses from mothers fed *ad libitum* (controls, C) or 70% of the control diet (maternal nutrient reduction, MNR) at 0.9 gestation. Symbol denotes the gene identification, RefSeq denotes the Reference Sequence from the National Center for Biotechnology Information collection, Description gives a summary information about the gene identification and/or function, Fold difference was calculate between the groups enunciated, positive values for up regulation and negative values for a down regulation. Fold differences relevant to the mitochondrial profile of the control fetus (control female, C-F vs. control male, C-M) were presented in the C-F vs. C-M section, as well the comparison of transcripts expression based on maternal diet for the same gender (in the MNR-M vs. C-M and MNR-F vs. C-F sections), the gender dimorphism in the mitochondrial profile of the MNR fetus (in the MNR-F vs. MNR-M section) and global diet-dependent effects in the mitochondrial expression profile (MNR vs. C section). The transcripts presented have either $0.05<p<0.1$ or $p<0.05$ in bold.

Symbol	Refseq	Description	Fold difference	P-value
		C-F vs. C-M		
NDUFB8	NM_005004	NADH dehydrogenase (ubiquinone) 1 beta subcomplex	2.656	0.075
NDUFV1	NM_007103	NADH dehydrogenase (ubiquinone) flavoprotein 1	**2.302**	**0.048**
COX6A1	NM_004373	Cytochrome c oxidase subunit VIa polypeptide 1	**1.758**	**0.001**
ATP5C1	NM_005174	ATP synthase, H+ transporting, mitochondrial F1 complex	**9.543**	**0.005**
IMMP1L	NM_144981	IMP1 inner mitochondrial membrane peptidase-like	**1.397**	**0.016**
OPA1	NM_130837	Optic atrophy 1	**-1.138**	**0.024**
CPT2	NM_000098	Carnitine palmitoyltransferase 2	3.063	0.061
SLC25A17	NM_006358	Solute carrier family 25 (mitochondrial carrier), member 17	**-1.170**	**0.037**
TIMM17A	NM_006335	Translocase of inner mitochondrial membrane 17	**-1.131**	**0.016**
TIMM9	NM_012460	Translocase of inner mitochondrial membrane 9	**1.787**	**0.010**
TOMM70A	NM_014820	Translocase of outer mitochondrial membrane 70	-1.155	0.052
SOD1	NM_000454	Superoxide dismutase 1, soluble	**-1.289**	**0.034**
SOD2	NM_000636	Superoxide dismutase 2, mitochondrial	1.679	0.076
BID	NM_001196	BH3 interacting domain death agonist	**5.864**	**0.030**
SFN	NM_006142	Stratifin	**1.863**	**0.050**
		MNR-M vs. C-M		
NDUFA1	NM_004541	NADH dehydrogenase (ubiquinone) 1 alpha subcomplex, 1.	**-1.755**	**0.044**
NDUFA2	NM_002488	NADH dehydrogenase (ubiquinone) 1 alpha subcomplex, 2.	-1.540	0.078
NDUFA4	NM_002489	NADH dehydrogenase (ubiquinone) 1 alpha subcomplex, 4.	**-5.377**	**0.045**
NDUFA8	NM_014222	NADH dehydrogenase (ubiquinone) 1 alpha subcomplex, 8.	-1.192	0.086
NDUFA10	NM_004544	NADH dehydrogenase (ubiquinone) 1 alpha subcomplex, 10.	-1.756	0.052
NDUFAB1	NM_005003	NADH dehydrogenase (ubiquinone) 1, alpha/beta subcomplex, 1.	-1.510	0.098
NDUFC1	NM_002494	NADH dehydrogenase (ubiquinone) 1,	-1.502	0.097

		subcomplex unknown, 1.		
NDUFS3	NM_004551	NADH dehydrogenase (ubiquinone) Fe-S protein 3.	-1.269	0.080
NDUFS5	NM_004552	NADH dehydrogenase (ubiquinone) Fe-S protein 5.	-1.250	0.051
NDUFV3	NM_021075	NADH dehydrogenase (ubiquinone) flavoprotein 3.	-1.290	0.080
SDHB	NM_003000	Succinate dehydrogenase complex, subunit B, iron sulfur (Ip)	**-1.240**	**0.006**
COX6A1	NM_004373	Cytochrome c oxidase subunit VIa polypeptide 1	**1.741**	**0.000**
OXA1L	NM_005015	Oxidase (cytochrome c) assembly 1-like	**-1.484**	**0.042**
ATP5B	NM_001686	ATP synthase, H+ transporting, mitochondrial F1 complex, beta polypeptide	-1.602	0.059
ATP5J	NM_001685	ATP synthase, H+ transporting, mitochondrial Fo complex, subunit F6	-1.406	0.085
ATP6V1C2	NM_144583	ATPase, H+ transporting, lysosomal 42kDa, V1 subunit C2	**-2.032**	**0.027**
OPA1	NM_130837	Optic atrophy 1	-1.152	0.087
FIS1	NM_016068	Fission 1 (mitochondrial outer membrane)	-1.185	0.080
SLC25A13	NM_014251	Solute carrier family 25, member 13	-1.271	0.099
SLC25A16	NM_152707	Solute carrier family 25 (mitochondrial carrier), member 16	-1.185	0.072
SLC25A17	NM_006358	Solute carrier family 25 (mitochondrial carrier), member 17	-1.112	0.073
TIMM23	NM_006327	Translocase of inner mitochondrial membrane 23	**-1.152**	**0.042**
TIMM9	NM_012460	Translocase of inner mitochondrial membrane 9	**1.886**	**0.014**
SOD1	NM_000454	Superoxide dismutase 1, soluble	**-1.375**	**0.009**
AIFM2	NM_032797	Apoptosis-inducing factor, mitochondrion-associated, 2	-1.222	0.072
SFN	NM_006142	Stratifin	**1.385**	**0.021**
		C-F vs. MNR-F		
NDUFA11	NM_175614	NADH dehydrogenase (ubiquinone) 1 alpha subcomplex, 11	-1.443	0.098
NDUFB9	NM_005005	NADH dehydrogenase (ubiquinone) 1 beta subcomplex, 9	-1.438	0.072
NDUFB10	NM_004548	NADH dehydrogenase (ubiquinone) 1 beta subcomplex, 10	-1.391	0.082
NDUFS5	NM_004552	NADH dehydrogenase (ubiquinone) Fe-S protein 5	**-1.193**	**0.042**
NDUFV3	NM_021075	NADH dehydrogenase (ubiquinone) flavoprotein 3	**-1.949**	**0.040**
SDHA	NM_004168	Succinate dehydrogenase complex, subunit A, flavoprotein	-1.356	0.087
UQCRC2	NM_003366	Ubiquinol-cytochrome c reductase core protein II	-1.393	0.088
COX6A2	NM_005205	Cytochrome c oxidase subunit VIa polypeptide 2	**-1.206**	**0.049**
COX6C	NM_004374	Cytochrome c oxidase subunit VIc	-1.686	0.075
COX7B	NM_001866	Cytochrome c oxidase subunit VIIb	**-1.304**	**0.050**
ATP4B	NM_000705	ATPase, H+/K+ exchanging, beta polypeptide	-1.761	0.071

ATP5H	NM_006356	ATP synthase, H+ transporting, mitochondrial Fo complex, subunit d	-1.249	0.069
ATP5J	NM_001685	ATP synthase, H+ transporting, mitochondrial Fo complex, subunit F6	**-1.440**	**0.047**
ATP12A	NM_001676	ATPase, H+/K+ transporting, nongastric, alpha polypeptide	**-1.162**	**0.036**
CPT1B	NM_004377	Carnitine palmitoyltransferase 1B (muscle)	-1.633	0.091
MFN2	NM_014874	Mitofusin 2	**-1.374**	**0.008**
DNM1L	NM_005690	Dynamin 1-like	-1.220	0.097
GRPEL1	NM_025196	GrpE-like 1, mitochondrial	**-1.102**	**0.021**
SLC25A3	NM_002635	Solute carrier family 25 (mitochondrial carrier; phosphate carrier), member 3	-1.945	0.083
SLC25A12	NM_003705	Solute carrier family 25 (mitochondrial carrier), member 12	-1.618	0.068
SLC25A15	NM_014252	Solute carrier family 25 (mitochondrial carrier; ornithine transporter) member 15	**1.777**	**0.036**
SLC25A16	NM_152707	Solute carrier family 25 (mitochondrial carrier), member 16	**-1.331**	**0.047**
SLC25A17	NM_006358	Solute carrier family 25 (mitochondrial carrier), member 17	**-1.183**	**0.033**
SLC25A31	NM_031291	Solute carrier family 25 (mitochondrial carrier; adenine nucleotide translocator), member 31	**-2.481**	**0.016**
AIFM2	NM_032797	Apoptosis-inducing factor, mitochondrion-associated, 2	-1.456	0.070
BBC3	NM_014417	BCL2 binding component 3	**-3.749**	**0.001**
BID	NM_001196	BH3 interacting domain death agonist	**-6.046**	**0.029**
CDKN2A	NM_000077	Cyclin-dependent kinase inhibitor 2A	**2.701**	**0.024**
STARD3	NM_006804	StAR-related lipid transfer (START) domain containing 3	**-1.147**	**0.023**
LHPP	NM_022126	Phospholysine phosphohistidine inorganic pyrophosphate phosphatase	-1.291	0.081
		MNR-F vs. MNR-M		
NDUFA8	NM_014222	NADH dehydrogenase (ubiquinone) 1 alpha subcomplex, 8	-1.188	0.067
NDUFB9	NM_005005	NADH dehydrogenase (ubiquinone) 1 beta subcomplex, 9	**-1.193**	**0.043**
NDUFC1	NM_002494	NADH dehydrogenase (ubiquinone) 1	**-1.091**	**0.033**
NDUFS4	NM_002495	NADH dehydrogenase (ubiquinone) Fe-S protein 4	-1.182	0.056
NDUFS5	NM_004552	NADH dehydrogenase (ubiquinone) Fe-S protein 5	-1.120	0.062
SDHA	NM_004168	Succinate dehydrogenase complex, subunit A, flavoprotein	-1.226	0.071
UQCRH	NM_006004	Ubiquinol-cytochrome c reductase hinge protein	**-1.218**	**0.034**
UQCRQ	NM_014402	Ubiquinol-cytochrome c reductase, complex III subunit VII	-1.453	0.233
COX4I1	NM_001861	Cytochrome c oxidase subunit IV isoform 1	**-1.151**	**0.004**
COX4I2	NM_032609	Cytochrome c oxidase subunit IV isoform 2	**-1.293**	**0.038**
COX6A2	NM_005205	Cytochrome c oxidase subunit VIa polypeptide 2	**1.718**	**0.004**

COX6B2	NM_144613	Cytochrome c oxidase subunit VIb polypeptide 2	**1.750**	**0.026**
COX7B	NM_001866	Cytochrome c oxidase subunit VIIb	-1.121	0.093
ATP5C1	NM_005174	ATP synthase, H+ transporting, mitochondrial F1 complex, gamma polypeptide 1	**5.818**	**0.002**
ATP5F1	NM_001688	ATP synthase, H+ transporting, mitochondrial Fo complex, subunit B1	1.235	0.090
ATP5O	NM_001697	ATP synthase, H+ transporting, mitochondrial F1 complex, O subunit	-1.171	0.059
MFN2	NM_014874	Mitofusin 2	-1.302	0.053
DNM1L	NM_005690	Dynamin 1-like	**-1.306**	**0.039**
CPT1B	NM_004377	Carnitine palmitoyltransferase 1B	-1.494	0.075
MSTO1	NM_018116	Misato homolog 1	**-1.330**	**0.021**
MIPEP	NM_005932	Mitochondrial intermediate peptidase	-1.380	0.062
RHOT1	NM_018307	Ras homolog gene family, member T1	-1.301	0.092
SLC25A17	NM_006358	Solute carrier family 25 (mitochondrial carrier), member 17	**-1.244**	**0.007**
SLC25A4	NM_001151	Solute carrier family 25 (mitochondrial carrier; adenine nucleotide translocator), member 4	**-1.216**	**0.012**
LRPPRC	NM_133259	Leucine-rich PPR-motif containing	-1.141	0.070
SOD1	NM_000454	Superoxide dismutase 1, soluble	1.132	0.099
BBC3	NM_014417	BCL2 binding component 3	**-2.537**	**0.030**
SH3GLB1	NM_016009	SH3-domain GRB2-like endophilin B1	-1.131	0.060

MNR vs. C				
NDUFA1	NM_004541	NADH dehydrogenase (ubiquinone) 1 alpha subcomplex, 1	**-1.540**	**0.014**
NDUFA2	NM_002488	NADH dehydrogenase (ubiquinone) 1 alpha subcomplex, 2	**-1.455**	**0.014**
NDUFA4	NM_002489	NADH dehydrogenase (ubiquinone) 1 alpha subcomplex, 4	**-2.782**	**0.008**
NDUFA5	NM_005000	NADH dehydrogenase (ubiquinone) 1 alpha subcomplex, 5	**-1.926**	**0.028**
NDUFA7	NM_005001	NADH dehydrogenase (ubiquinone) 1 alpha subcomplex, 7	**-1.332**	**0.043**
NDUFA8	NM_014222	NADH dehydrogenase (ubiquinone) 1 alpha subcomplex, 8	**-1.251**	**0.021**
NDUFA10	NM_004544	NADH dehydrogenase (ubiquinone) 1 alpha subcomplex, 10	**-1.623**	**0.009**
NDUFA11	NM_175614	NADH dehydrogenase (ubiquinone) 1 alpha subcomplex, 11	**-1.420**	**0.034**
NDUFAB1	NM_005003	NADH dehydrogenase (ubiquinone) 1, alpha/beta subcomplex, 1	**-1.436**	**0.026**
NDUFB5	NM_002492	NADH dehydrogenase (ubiquinone) 1 beta subcomplex, 5	**-1.298**	**0.035**
NDUFB9	NM_005005	NADH dehydrogenase (ubiquinone) 1 beta subcomplex, 9	**-1.327**	**0.023**
NDUFB10	NM_004548	NADH dehydrogenase (ubiquinone) 1 beta subcomplex, 10	-1.325	0.055
NDUFC1	NM_002494	NADH dehydrogenase (ubiquinone) 1	**-1.415**	**0.016**
NDUFC2	NM_004549	NADH dehydrogenase (ubiquinone) 1	**-1.926**	**0.028**
NDUFS1	NM_005006	NADH dehydrogenase (ubiquinone) Fe-S protein 1	-1.277	0.062
NDUFS3	NM_004551	NADH dehydrogenase (ubiquinone) Fe-S protein 3	**-1.236**	**0.029**

NDUFS4	NM_002495	NADH dehydrogenase (ubiquinone) Fe-S protein 4	**-1.188**	**0.049**
NDUFS5	NM_004552	NADH dehydrogenase (ubiquinone) Fe-S protein 5	**-1.221**	**0.011**
NDUFS8	NM_002496	NADH dehydrogenase (ubiquinone) Fe-S protein 8	**-1.274**	**0.038**
NDUFV2	NM_021074	NADH dehydrogenase (ubiquinone) flavoprotein 2	-1.208	0.075
NDUFV3	NM_021075	NADH dehydrogenase (ubiquinone) flavoprotein 3	**-1.586**	**0.004**
SDHA	NM_004168	Succinate dehydrogenase complex, subunit A, flavoprotein	**-1.321**	**0.038**
SDHB	NM_003000	Succinate dehydrogenase complex, subunit B, iron sulfur	**-1.176**	**0.012**
UQCRC1	NM_003365	Ubiquinol-cytochrome c reductase core protein I	**-1.516**	**0.032**
UQCRC2	NM_003366	Ubiquinol-cytochrome c reductase core protein II	-1.411	0.053
UQCRFS1	NM_006003	Ubiquinol-cytochrome c reductase, Rieske iron-sulfur polypeptide 1	**-1.366**	**0.024**
CYC1	NM_001916	Cytochrome c-1	-1.307	0.101
COX4I1	NM_001861	Cytochrome c oxidase subunit IV isoform 1	**-1.281**	**0.017**
COX4I2	NM_032609	Cytochrome c oxidase subunit IV isoform 2	**-1.245**	0.082
COX5A	NM_004255	Cytochrome c oxidase subunit Va	**-1.296**	**0.037**
COX5B	NM_001862	Cytochrome c oxidase subunit Vb	**-1.254**	**0.028**
COX6A1	NM_004373	Cytochrome c oxidase subunit VIa polypeptide 1	1.306	0.078
COX6B1	NM_001863	Cytochrome c oxidase subunit Vib polypeptide 1	-1.367	0.057
COX7B	NM_001866	Cytochrome c oxidase subunit VIIb	-1.188	0.072
COX8A	NM_004074	Cytochrome c oxidase subunit VIIIA	1.234	0.672
COX8C	NM_182971	Cytochrome c oxidase subunit VIIIC	**-1.926**	**0.028**
COX10	NM_001303	COX10 homolog, cytochrome c oxidase assembly protein	**-1.309**	0.063
OXA1L	NM_005015	Oxidase (cytochrome c) assembly 1-like	**-1.450**	**0.016**
ATP4A	NM_000704	ATPase, H+/K+ exchanging, alpha polypeptide	**-1.345**	**0.038**
ATP4B	NM_000705	ATPase, H+/K+ exchanging, beta polypeptide	**-1.926**	**0.028**
ATP5B	NM_001686	ATP synthase, H+ transporting, mitochondrial F1 complex, beta polypeptide	**-1.421**	**0.027**
ATP5G1	NM_005175	ATP synthase, H+ transporting, mitochondrial Fo complex, subunit C1	**-2.588**	**0.023**
ATP5G3	NM_001689	ATP synthase, H+ transporting, mitochondrial Fo complex, subunit C3	**9.231**	**0.018**
ATP5I	NM_007100	ATP synthase, H+ transporting, mitochondrial Fo complex, subunit E	-1.194	0.063
ATP5J	NM_001685	ATP synthase, H+ transporting, mitochondrial Fo complex, subunit F6	**-1.423**	**0.003**
ATP5O	NM_001697	ATP synthase, H+ transporting, mitochondrial F1 complex, O subunit	**-1.290**	**0.029**
ATP6V0A2	NM_012463	ATPase, H+ transporting, lysosomal V0 subunit a2	**-1.856**	**0.020**
ATP6V1C2	NM_144583	ATPase, H+ transporting, lysosomal,	**-1.606**	**0.028**

		V1 subunit C2		
SLC25A13	NM_014251	Solute carrier family 25, member 13 (citrin)	-1.148	0.085
SLC25A15	NM_014252	Solute carrier family 25 (mitochondrial carrier; ornithine transporter) member 15	**1.853**	**0.014**
SLC25A16	NM_152707	Solute carrier family 25 (mitochondrial carrier), member 16	**-1.256**	**0.003**
SLC25A17	NM_006358	Solute carrier family 25 (mitochondrial carrier), member 17	-1.147	0.069
SLC25A23	NM_024103	Solute carrier family 25 (mitochondrial carrier; phosphate carrier), member 23	**-1.269**	**0.050**
SLC25A27	NM_004277	Solute carrier family 25, member 27	**10.446**	**0.029**
SLC25A31	NM_031291	Solute carrier family 25 (mitochondrial carrier; adenine nucleotide translocator), member 31	**-2.199**	**0.035**
FXC1	NM_012192	Fracture callus 1 homolog	**-1.155**	**0.029**
TIMM23	NM_006327	Translocase of inner mitochondrial membrane 23	**-1.120**	**0.024**
TOMM20	NM_014765	Translocase of outer mitochondrial membrane 20	-1.159	0.062
TOMM34	NM_006809	Translocase of outer mitochondrial membrane 34	-1.339	0.082
TOMM70A	NM_014820	Translocase of outer mitochondrial membrane 70	-1.214	0.073
MIPEP	NM_005932	Mitochondrial intermediate peptidase	-1.211	0.097
OPA1	NM_130837	Optic atrophy 1	-1.096	0.072
AIFM2	NM_032797	Apoptosis-inducing factor, mitochondrion-associated, 2	**-1.334**	**0.007**
BBC3	NM_014417	BCL2 binding component 3	-1.836	0.056
CDKN2A	NM_000077	Cyclin-dependent kinase inhibitor 2A (inhibits CDK4)	1.751	0.088
SH3GLB1	NM_016009	SH3-domain GRB2-like endophilin B1	-1.125	0.082
UXT	NM_004182	Ubiquitously-expressed transcript	-1.109	0.078
PPA1	NM_021129	Pyrophosphatase (inorganic) 1	**-1.392**	**0.038**
PPA2	NM_176869	Pyrophosphatase (inorganic) 2	**-1.798**	**0.031**

4.2.4 MNR offspring present altered mitochondrial protein content

The tissue content of four mitochondrial proteins (COX6C, CYC1, MFN2, and TIMM9A) was also measured by immunohistochemistry. Due to the structural and functional diversity of the kidney accompanied by a wide variation in the local presence of different mitochondrial enzymes, we decided to quantify mitochondrial proteins in two regions of the kidney, the cortex (CX) and medulla (MD). In agreement with the observed decrease in mRNA expression of respiratory chain subunits, a decrease in COX6C, a subunit of complex IV, was measured in MNR male fetuses (Figure 4.3). Under control diet conditions, control female fetuses had a

1.82-fold decrease content of COX6C fraction stained (%) and a 1.14-fold decrease in density (AU) in the renal cortex compared to control male fetal samples (for details, see Figure 4.4). Notwithstanding, MNR female fetuses presented a significant increase in complex III subunit CYC1, detected by a increase of 1.37-fold in cortex fraction stained (%) and in density (AU; Figure 4.5).

There were no differences between diets or genders in the quantitative immunohistochemistry of MNF2 or TIMM9A in the renal tissue analyzed (Figure 4.6).

Figure 4.3 Quantitative immunohistochemistry of mitochondrial subunit COX6C in renal tissue of fetal baboon. (following page)
The fetuses analyzed were from mothers that were fed *ad libitum* (control group) or 70% of the control diet (MNR group). A: representative micrographs (magnification: x20) of cortex (CX) and medulla (MD) sections of male and female fetus. Immunoreactivity was expressed as fraction stained (in %; B) and density [C; in arbitrary units (AU)]. Data are expressed as mean and SEM; n=3 (when separated by gender) or n=6 (genders combined) animals/group. Comparison between groups was performed using a non-parametric Mann-Whitney test. P-value less than 0.05 was considered significant. *P<0.05 vs. respective controls or as indicated.

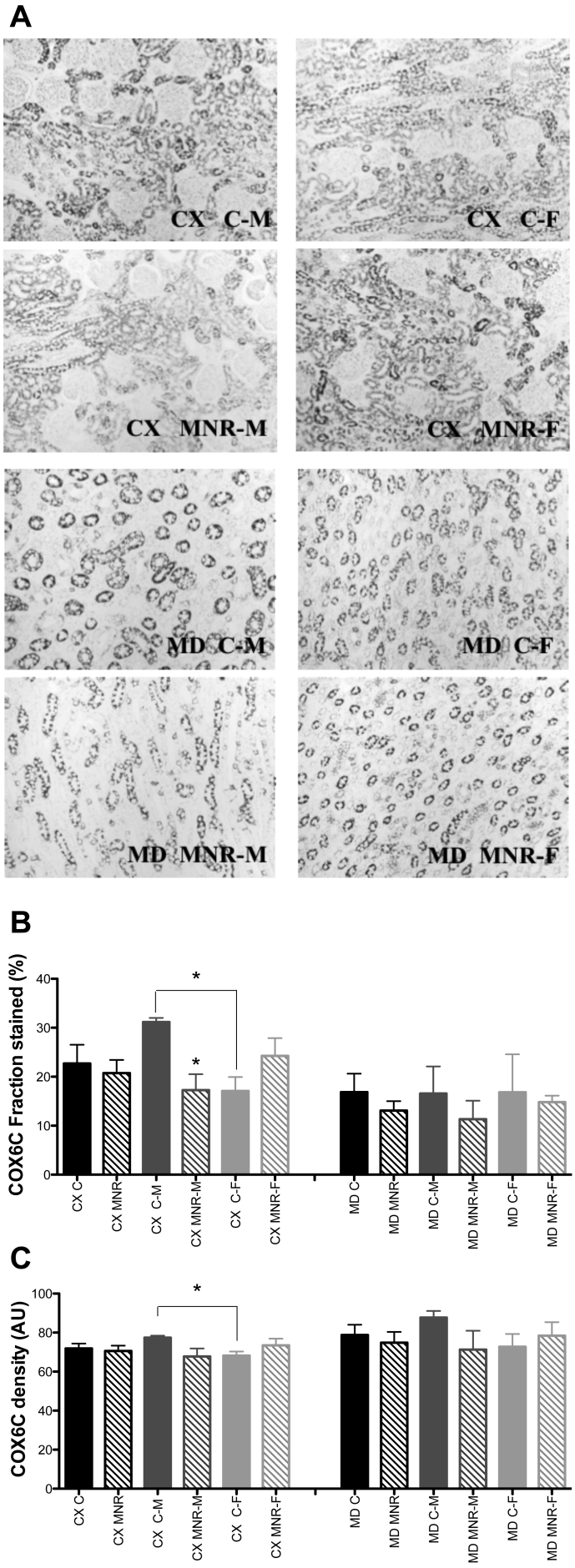
A
CX C-M
CX C-F
CX MNR-M
CX MNR-F
MD C-M
MD C-F
MD MNR-M
MD MNR-F
B
COX6C Fraction stained (%)
0
10
20
30
40
*
*
CX C
CX MNR
CX C-M
CX MNR-M
CX C-F
CX MNR-F
MD C
MD MNR
MD C-M
MD MNR-M
MD C-F
MD MNR-F
C
COX6C density (AU)
0
20
40
60
80
100
*
CX C
CX MNR
CX C-M
CX MNR-M
CX C-F
CX MNR-F
MD C
MD MNR
MD C-M
MD MNR-M
MD C-F
MD MNR-F

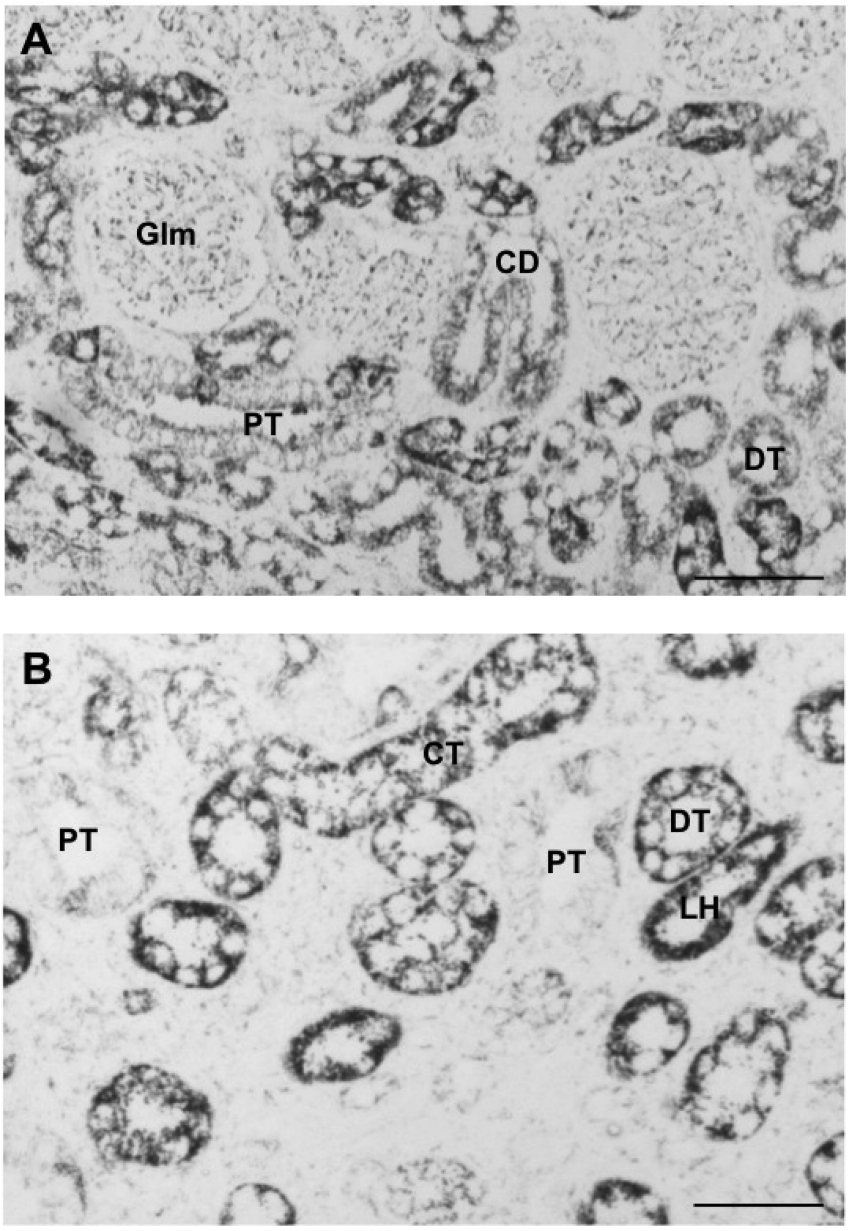

Figure 4.4 Magnification of immunohistochemistry images shown in Figure 4.3A. [CX (A), MD (B) of a control male fetuses]. A: immunolabeling for COX6C was associated with distal tubuli (DT), proximal tubuli (PT), collecting ducts (CD), and glomeruli (Glm) in cortex samples from a male fetal baboon from mothers that were fed *ad libitum*. B: COX6C was associated with distal tubuli (DT), collecting ducts (CD), limbs of Henle's Loop (HL), and proximal tubuli (PT) in medulla from control male kidney samples. However, the immunolabeling for COX6C was more consistent in DT in medulla section. Scale bar = 50 μm.

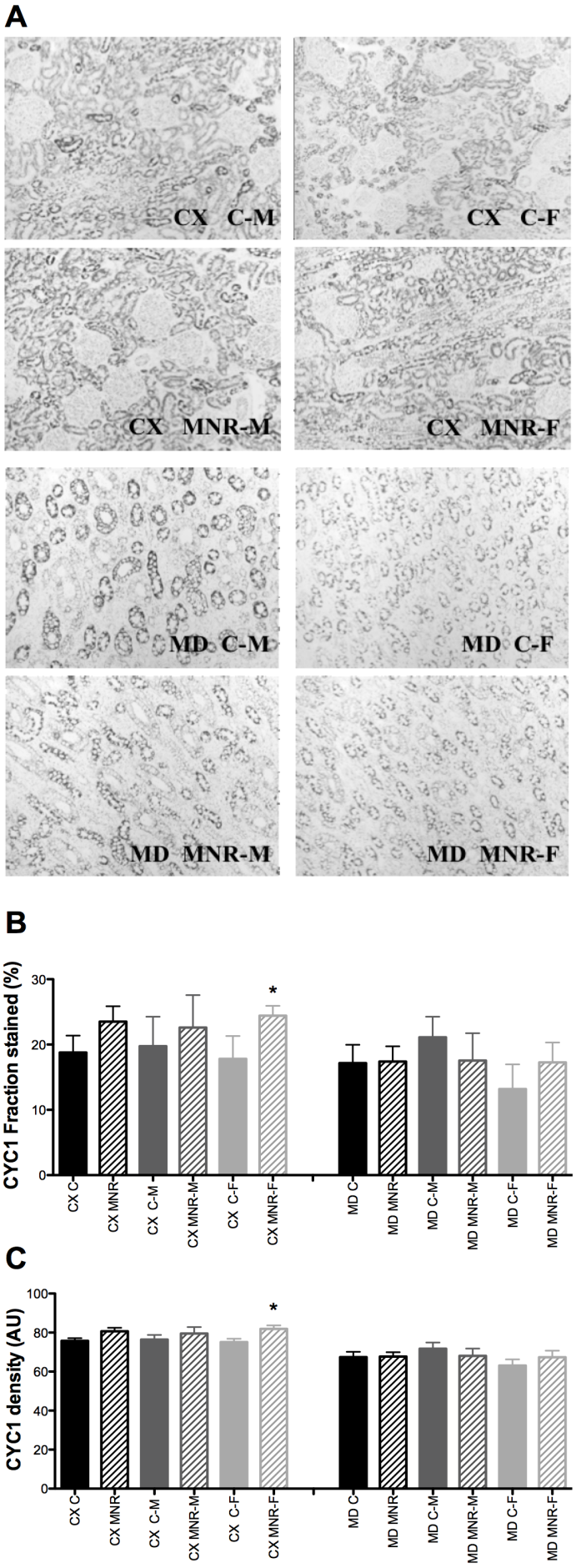
A
CX C-M
CX C-F
CX MNR-M
CX MNR-F
MD C-M
MD C-F
MD MNR-M
MD MNR-F
B
CYC1 Fraction stained (%)
30
20
10
0
*
CX C
CX MNR
CX C-M
CX MNR-M
CX C-F
CX MNR-F
MD C
MD MNR
MD C-M
MD MNR-M
MD C-F
MD MNR-F
C
CYC1 density (AU)
100
80
60
40
20
0
*
CX C
CX MNR
CX C-M
CX MNR-M
CX C-F
CX MNR-F
MD C
MD MNR
MD C-M
MD MNR-M
MD C-F
MD MNR-F

Figure 4.5 Quantitative immunohistochemistry of mitochondrial subunit CYC1 in renal tissue of fetal baboon. (previous page)
The fetuses analyzed were from mothers that were fed *ad libitum* (control group) or 70% the control diet (MNR group). A: representative micrographs (magnification: x20) of cortex (CX) and medulla (MD) sections of males and females fetuses. Immunoreactivity expressed as fraction stained (B; in %) and density (C; in AU). Data are expressed as mean and SEM; n=3 (when separated by gender) or n=6 (genders combined) animals/group. Comparison between groups was performed using a non-parametric Mann-Whitney test. P-value less than 0.05 was considered significant. *P<0.05 vs. respective controls.

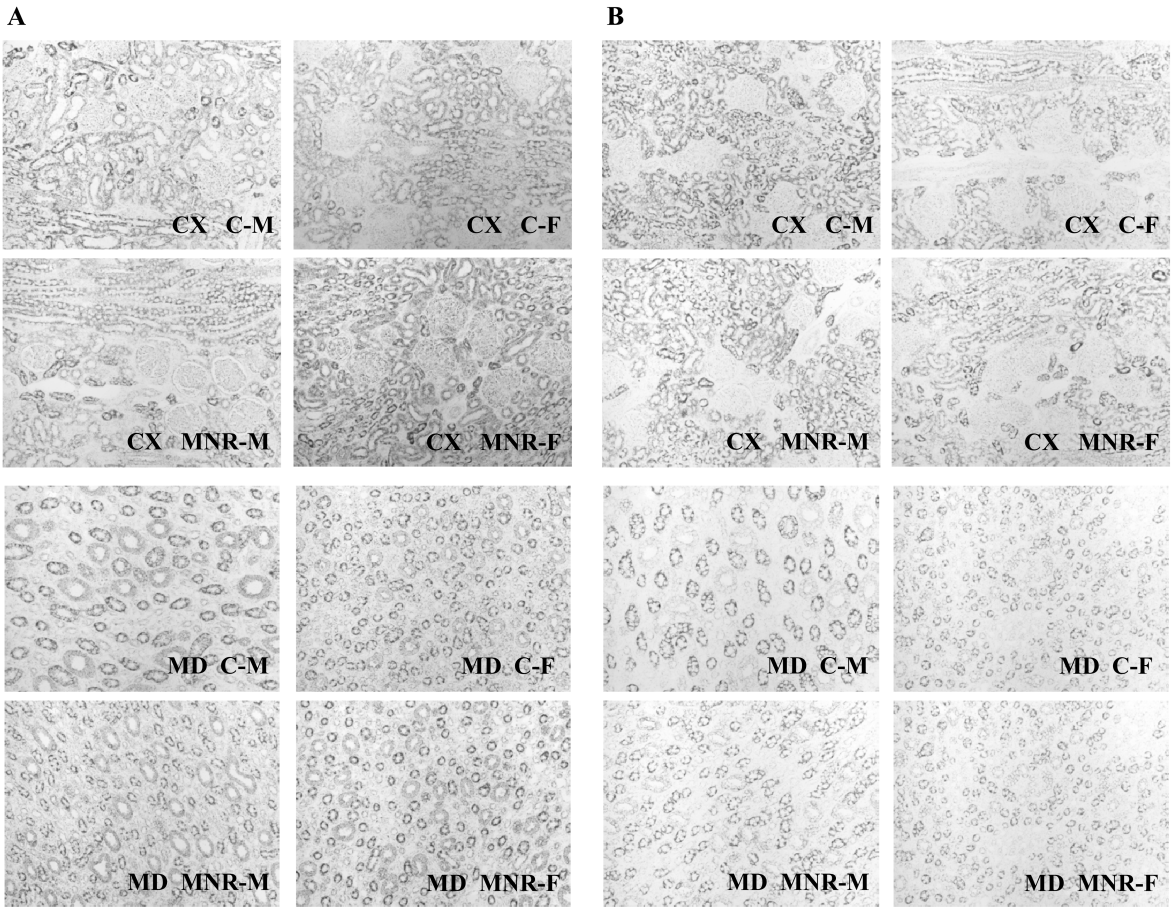

Figure 4.6 Representative immunohistochemistry of mitochondrial subunit MFN2 and TIMM9A.
(A) MFN2 and (B) TIMM9 in renal tissue of fetal baboon from mothers that were fed *ad libitum* (control group) or 70% of the control (MNR group). Micrographs (magnification: x20) of cortex (CX) and medulla (MD) sections of male and female fetuses are shown.

4.3 Discussion

4.3.1 The Baboon model in intrauterine programming studies

Several studies exist on developmental programming in altricial, polytocous rodent species [238–240] but few in precocial, monotocous species [197,241]. Much of prenatal renal development in primates, including humans and baboons, occurs postnatally in rodents [242,243]. This difference is important because the intrauterine environment differs from the postnatal environment in many different ways, which can significantly affect that developmental trajectory of development. Oxygen tension and hence potential for oxidative stress, metabolite concentrations such as glucose, and of particular importance, fetal glucocorticoid levels, which rise prenatally in precocial species [244,245] and postnatally in altricial species [245] can be factors of segregation. Studies in nonhuman primates are important since they allow for a more direct translation to the human developmental programming. To our knowledge, the model we present here is the first to test the concept of developmental programming as modified by reduced maternal nutrition. In our experimental animal model, a careful selection of mothers of similar phenotype before breeding was performed, which added power to the observations and were unable to be replicated in human studies.

Fetal baboon development closely resembles that of the human fetus, allowing targeted nutritional manipulations during specific periods of organogenesis. Most notably, development of the metanephros or "final" kidney occurs at a similar gestational time in humans and baboons. Kidney development in humans begins in the 9th week of gestation and ends around the 36th week of gestation [246]. This corresponds to 0.9 gestation of the human fetus, exactly the same time point analyzed in our baboon model. The evolutionary similarity of mitochondrial genes between baboons and humans was also evident by the efficacy of human primers in baboon samples. In addition, baboons and humans share a broad range of physiological similarities that make baboons particularly valuable for analysis of gene-gene and gene-environment interactions [236], while both breeding and environmental factors can still be carefully controlled to suit experimental purposes. Furthermore, baboons develop spontaneous diabetes and diabetic nephropathy with morphological

changes that resemble diabetic nephropathy found in humans [247]. Diabetic baboons have larger glomeruli, increased glomerular and tubular basement membranes thickness, and matrix expansion with increased deposition of fibronectin and laminin, thus making this animals an attractive, although expensive, model for human diabetic nephropathy [247] or hypertension [248].

4.3.2 Intrauterine programming of adult life phenotype by maternal diet in the baboon

The majority of studies on developmental programming by maternal nutrition has been performed in rodents, and much less is known about the impact of nutrient reduction on fetal primate development. The strength and relevance of the baboon fetal experiments we have performed lie not only in its phylogenetic and developmental proximity to humans but also in the moderate level of MNR used, which produces a level of IUGR (approximately 14% birth weight reduction) that is commonly seen in human pregnancy. We have previously demonstrated that consumption of 70% of a global *ad libitum* control diet by female baboons carefully selected to be of similar age and phenotype at conception resulted in impaired development of the fetal kidney [197,249], brain [250], liver [199] and pancreatic islets [251]. In addition, MNR during pregnancy and lactation programs offspring behavioral function [252] and metabolic responses, increasing insulin resistance and β-cell responsiveness, resulting in emergence of an overall phenotype that would predispose to later life type 2 diabetes [253]. We hypothesize that permanent alterations in gene expression related to mitochondrial function and communication, set in motion by a suboptimal intrauterine environment, contribute to the development of cardiovascular or kidney diseases later in life. The present study is the first to demonstrate significant alterations in mitochondrial gene expression profile in fetal baboon kidneys challenged by MNR *in utero*.

4.3.3 Morphological and biochemical data

IUGR associated with MNR affects organ development. In fact, nephron numbers are lower in IUGR neonates. One hypothesis is that when challenged by limited resources, energy resource allocation is prioritized for brain, cardiac and adrenal growth, whereas organs such as the kidneys and lungs receive lower priority [254]. This

allocation process is thought to be the root mechanism by which relative brain sparing and increased compromise in nonprotected organs takes place. A significant decrease in maternal weight gain during pregnancy was found for MNR mothers, which culminated in offspring with lower body mass indexes and with higher brain weight-to-body weight ratios. This diet effect was more visible for the MNR female fetuses, with a significant decrease in femur length. However, MNR did not significantly affect kidney weight or kidney weight-to-body weight ratio. These results indicate that the MNR protocol used in this work has a significant influence on body weight gain in the mother and influences fetal body mass index.

MNR significantly altered maternal and fetal endocrine factors, causing increased circulating cortisol and glucose in MNR mothers carrying male fetuses, significantly increasing circulating cortisol in the fetus independently of fetal gender (Figure 4.1). Maternal glucose metabolism was also impaired, since circulating glucose was significantly increased by MNR in mothers carrying male fetuses. Despite MNR promoting a decrease in fetal insulin in male fetuses, these changes did not appear to impact overall fetal glucose levels, since circulating fetal glucose was not significantly affected by MNR.

Increased circulating cortisol resulting from MNR is nonetheless important. Exposure of the fetus to glucocorticoid levels higher than required for the current stage of maturation triggers the expression of glucocorticoid target genes involved in energy metabolism and adipocyte differentiation, having been linked to the development of hyperglycemia, insulin resistance, and obesity later in life [255]. Glucocorticoid-induced gene demethylation likely also contributes to the "memory" of the developmental nutritional challenge [256].

Concerning markers of renal and hepatic functions, no significant alteration in serum alanine aminotransferase (ALT) or in the BUN or BUN/creatinine levels were found, suggesting no alterations in that metabolic pathway. In general, the lack of difference in total protein between control and MNR mothers may imply that MNR mothers manage to successfully maintain amino acid levels. Since the reduction in total caloric intake by MNR mothers was moderate compared with the control diet, we cannot eliminate the possibility that MNR mothers blunted the decrease in fetal nutrient availability through utilization of endogenous stores.

4.3.4 Mitochondrial transcripts are decreased in MNR fetuses

A modified embryonic-fetal developmental trajectory resulting in low birth weight has been associated with a reduced nephron endowment, hypertension, and renal diseases in adulthood [246,257,258]. Several molecular mechanisms have been suggested as contributing to impaired nephrogenesis [213]; however, little attention has been given to the involvement of mitochondria as mediators linking fetal MNR with later lifetime consequences.

The postnatal switch from glycolytic to oxidative metabolism is of crucial importance for all mammalian neonates and is essential for successful adaptation to extrauterine life [259]. After birth, more than 90% of ATP is produced by mitochondrial ATP synthase, which uses energy of the proton electrochemical gradient generated by respiratory chain complexes during substrate oxidation. The cellular capacity for energy provision relies on adequate biosynthesis of respiratory chain complexes and their proper assembly in the inner mitochondrial membrane. This process is under direct influence of numerous genes in nuclear and mitochondrial DNA [226].

Alterations of mitochondrial gene expression are likely important determinants for the development and function of major organ systems as well for susceptibility to disease.

A recent study from Fedovora et al. [260] using a model of chronic renal failure in male Sprague–Dawley rats observed mitochondrial impairments involving a 30% decrease in mitochondrial DNA copy number and an approximated 50% decrease in inner mitochondrial membrane proteins.

In a previous work [197], we found decreased tubule size in IUGR baboon fetal kidneys at 0.5 gestation, suggesting that IUGR alters kidney developmental trajectory. We also found that mammalian target of rapamycin signaling (mTOR), a key nutrient sensing pathway, was inhibited in IUGR 0.5 gestation fetal kidneys compared with control kidneys. These findings suggest that mTOR signaling via nutrient status influences tubule size [241]. Because alterations of mitochondrial function are important determinants of development and function for major organ systems, we investigated the role of mitochondrially related genes and proteins in the near-term baboon fetal kidney, i.e. are the effects of MNR observed at 0.5 gestation persistent at 0.9

gestation, and, if so, what are the potential underlying mechanisms?

In accordance, our transcriptomic analysis showed significant alterations in mitochondrially relevant transcripts in the MNR fetal kidney. A large number of transcripts encoding subunits of the respiratory chain, ATP synthase, and cytochrome c and other regulators and mediators of mitochondrial metabolite transport were found to be decreased by MNR. When examined using immunohistochemistry, changes were observed in protein abundance of COX6C, a COX subunit. Differences in gene expression do not always lead to altered protein and enzyme activity, and, as in our findings, protein and mRNA measurements are not always in agreement. However, these findings, when taken together, suggest that MNR kidney mitochondrial alterations can potentially significantly affect the renal energy balance and act as a primer for later disease during adulthood. The changes likely account, at least in part, for an impairment of mitochondrial function and ATP production in MNR fetuses. The passage from a predominantly *in utero* anaerobic to postbirth aerobic metabolism can potentially exacerbate the observed effects of altered expression of mitochondrial genes. This should be confirmed in the future using freshly obtained samples containing functional mitochondria. Moreover, sex differences are apparent early in fetal development, suggesting that innate mitochondrial differences between genders can give particularly useful insights to predict the development of hypertension later in life. In this regard, male subjects seem disadvantaged in the mitochondrial background, presenting lower content of several mitochondrial transcripts (Figure 4.2), suggesting hormone-dependent effects.

Gender dissimilarities in the progression of various renal diseases have been reported in animal and humans studies, with men at higher risk of developing renal diseases, with the tendency to develop it earlier in life and with a faster progression and deterioration of renal function than in women [261–266]. Apart from the genetically coded dissimilarities between the genders in renal structure and function, sex hormones may affect several of the routes implicated in the pathogenesis of renal disease development. Possible mechanisms include receptor-mediated effects of sex hormones on glomerular hemodynamics and cell proliferation as well as effects on the synthesis and release of cytokines, vasoactive agents, and growth factors. In addition, estrogens can also provide a protective effect in female subjects due to their antioxidant action [267].

Some studies concerning MNR have reported complementary results to our findings. For example, in term rat placentas, mitochondrial abnormalities are observed with reduced ATP levels found, despite increased mitochondrial biogenesis and activity [268]. Using a maternal low-protein diet rat model, the expression of malate dehydrogenase, as well as the mitochondrial DNA-encoded subunit 6 of the ATP synthase, was lower in the pancreatic islets, reducing the capacity of ATP production through mitochondrial oxidative metabolism. Interestingly, in agreement with our results, several consequences of protein restriction during fetal life were more marked in male offspring [269].

There is ample evidence that the intrauterine environment is extremely important for the future health of the individual. This has been shown for cardiovascular diseases, hypertension, obesity, type 2 diabetes and metabolic syndrome, as well as renal diseases, such as albuminuria and chronic kidney disease [213,254].

The findings presented here, for the first time, demonstrate the tissue-specific nature of mitochondrial protein development that may reflect differences in functional adaptation after birth. The divergence in mitochondrial response between tissues to maternal nutrient manipulations early in pregnancy further reflects these differential ontogenies.

It is also tempting to speculate that, by defining and delivering optimal maternal nutrition during critical time windows during fetal development, long-term health benefits for the offspring can be achieved.

Chapter 5

Effects of moderate global maternal nutrient reduction on fetal baboon cardiac mitochondria at 0.9 gestation

Acknowledgements

The author acknowledge the contributions by Peter W. Nathanielsz and Mark J. Nijland that developed the animal model; by Paulina Quezada, Greg Langone and Li Cun for immunohistochemistry, by Alina Maloyan for transmission electron microscopy, by Ana I. Duarte for the activity of mitochondrial enzymes, by Inês Baldeiras for the antioxidant and oxidant capacity analyzes, by Teresa Cunha-Oliveira for the determination of mitochondrial DNA, by Maria Sancha Santos for analyzing of adenine nucleotides, by Michelle Zavala and Ana Maria Silva for general assistance in the laboratory, by Leslie Myatt, Nagarjun Kasaraneni, Chunming Guo, Balasubashini Muralimanoharan and James Mele by allowing access to equipment, by Ludgero C. Tavares for the statistics validation and images correction, and finally by Karen Moore and Susan Jenkins for bibliography and data archiving.

5.1 Introduction

Cardiovascular disease is the leading cause of mortality worldwide [270]. A plethora of epidemiologic studies have demonstrated that adverse intrauterine environment can modulate the risk of developing cardiovascular disease later in adult life.

Low birth weight is defined as a birth weight below the 10th percentile, or 2 standard deviation below the mean for the gestational age, that may result from intrauterine growth restriction, preterm birth, or both. Therefore, infants born with low birth weight at term (< 2500 g) are considered to have IUGR. The global incidence of low birth weight is around 15.5% for all births, or over 20 million infants each year, according to United Nations Children´s Fund (UNICEF).

Low birth weigh is associated with an increased risk for coronary artery disease [271,272] as well as type 2 diabetes [273,274], hypertension [271], hypercholesterolemia [275] and hypercoagulopathies [276,277].

In their seminal work, Barker and collaborators described that fetuses born with low birth weight have more than a 2-fold increase in the prevalence of coronary artery disease as adults [278]. Barker´s findings have been corroborated by subsequent studies in different human populations [279–281]. It has been further demonstrated in several animal models that an insult during fetal development can induce permanent phenotypic and physiological effects in the organism. For example, in the developmental programming of adult cardiovascular disease models, including the maternal low-protein diet in rats [282] and a 48-h steroid infusion in the first trimester in sheep [283], the exposed fetuses were born with a normal cardiovascular phenotype but would later develop cardiac hypertrophy and hypertension in adult life [282,283].

Although there is a strong association between IUGR and cardiovascular disease, the direct effects of the exposure to maternal nutrient reduction on fetal heart metabolism and mitochondrial biology have not been investigated. Given the fact that the heart is the second largest oxygen-consuming organ within the body and that oxidation of fatty acids and glucose in mitochondria accounts for the vast majority of ATP generation in the healthy adult heart [284], mitochondria appears as a plausible target of MNR effects.

The mitochondrion contains an inner and an outer membrane which define a large matrix and the narrow intermembrane space. The outer membrane is permeable to

small molecules and contains well/regulated channels, whereas the inner membrane is strictly selective in terms of permeation to solutes which is controlled by the presence of several selective transporters that are critical for the exchange of molecules. Furthermore, the inner mitochondrial membrane is invaginated, creating cristae structures that allocated the respiratory chain proteins for the production of ATP. These cristae allow for the delimitation of microdomains of ATP, ADP, small soluble proteins, ions and nutrient molecules [5,285]. There are specific sites where the outer and inner mitochondrial membranes contact, and normally these loci are characterized by the presence of complexes such as the voltage dependent anion channel (VDAC), the mitochondrial creatine kinase, and the adenine nucleotide translocase (ANT) [5]. Mitochondria cannot be generated "de novo", as the increase in mitochondrial mass derive from the division of existing mitochondria. Mitochondrial enzymes are encoded by both nuclear and mitochondrial genes. All the enzymes of beta-oxidation and the TCA cycle, and most of the subunits of the OXPHOS are encoded by nuclear genes. In humans, the mtDNA is 16,569 base-pair, circular and double-stranded, encoding 37 polypeptides. Twenty four genes encode RNAs necessary for protein synthesis (22 transfer RNAs and 2 ribosome RNAs) and the remaining 13 genes encode for proteins that are critical subunits of the oxidative phosphorylation complexes I, III, IV and V [286]. Each mitochondrion has several mtDNA molecules ranging from 10^3 to 10^4, although the total copy number of the mitochondrial genome varies between cell type and development stage [286]. So the mtDNA can be replicated multiple times during each cell cycle. Therefore when mutations occurs this mechanism enhances their effects that ultimately could generate a dysfunctional oxidative phosphorylation system, leading to the accumulation of dysfunctional mitochondria [286,287]

There are multiple diseases associated with mitochondrial DNA depletions or alterations, including Alper's syndrome, progressive external ophthalmoplegia (PEO), and other recessive myopathies [288]. More notably, mtDNA alteration is also implicated in more common diseases such as type 2 diabetes [289], cancer [290], and neurodegenerative disorders such as Alzheimer's and Parkinson's disease [291].

In this study, we hypothesize that alterations in mitochondrial performance may be instrumental for the later appearance of cardiac disease displayed by IUGR offspring. This concept is supported by previous studies showing that mitochondrial dysfunction caused by mutations in mtDNA can lead to myocardial dysfunction [292–

[294]. Also, the reports of maternally-inherited familial cardiomyopathy [295,296] as well as of the cardiac involvement in primary mitochondrial diseases [287,297] sustain our hypothesis. Even more relevant for our rationale were the studies showing an association between abnormal mitochondrial function and obesity, diabetes and hypertension, the exact same biological consequences resulting from IUGR [170,298]. Nevertheless, mitochondria are also major sites for generation of oxygen free radicals, which have a central role in the pathogenesis of cardiovascular diseases [299]. In accordance with these previous observations, the goal of our study was to determine the effects of a 30% global maternal nutrient reduction on the fetal heart left ventricle. Hence, we investigated whether the reduction by 30% of global maternal nutrient intake in pregnant baboons conditions fetal development and reprograms heart metabolism by affecting cardiac mitochondria. Our secondary hypothesis was that the effects of MNR in the fetuses are gender-specific.

5.2 Results

5.2.1 Biological changes resulting from MNR

Control and MNR groups did not differ in maternal body weight before pregnancy (16.30 ± 0.73 kg vs. 16.64 ± 1.16 kg, Table 5.1). However, at 0.9 gestation, *ad libitum*-fed control mothers weighed more than MNR mothers. The maternal control group gained 12.84 ± 2.11% of their body weight during pregnancy. In contrast, MNR mothers significantly lost weight (-3.13 ± 3.02%). Maternal weight loss was more pronounced in MNR mothers carrying male fetuses (16.15 ± 3.17% vs. -7.06 ± 3.67%). Placental weight was also significantly decreased in MNR mothers (213.29 ± 14.35 g vs. 164.05 ± 11.165 g) and that effect was also more pronounced in MNR mothers carrying male fetuses, which displayed a decrease of 26.15%.

At cesarean section, measurements of biomarkers for maternal renal function (Table 5.1), such as BUN, creatinine, BUN creatine ratio, sodium (Na^+), potassium (K^+), and carbon dioxide (CO_2), were not altered by MNR. Nevertheless, serum chloride (Cl^-) content was significantly decreased in the MNR mothers carrying female fetuses, suggesting an imbalance of body fluids, namely in the body's acid-base balance. Aspartate aminotransferase (AST), a sensitive indicator of liver injury, was significantly augmented in MNR mothers. Triglycerides can be important for cardiovascular health and a tendency was found for a diet-effect on serum triglycerides, with MNR mothers registering an increase of 61.88% in these compounds. These results became even more relevant because creatine phosphokinase (CPK), a biomarker for stress or injury to the heart, the brain or the muscle tissue, also registered an increase of 27.19% for this group. Interestingly this enzyme is significant higher in control mothers carrying male fetuses.

Table 5.1 Notes (following page)

MNR, maternal nutrient reduction.

[a] maternal Blood serum at cesarean section was only analyzed in 3 C-M, 4 C-F, 3 MNR-M and 3 MNR-F, which resulted in n=7 in C group and n=6 in MNR group when genders were combined.

Comparison between groups was performed using a non-parametric Mann-Whitney test. P-value less than 0.05 was considered significant.

Table 5.1 Maternal and fetal morphological and biochemical parameters at 0.9 gestation in control *ad libitum*-fed pregnancies and in the presence of maternal nutrient reduction (MNR) to 70% of the food eaten by the control mothers on a weight-adjusted basis.

	Genders combined		Male		Female		P-value by Mann-Whitney test				
	Control	MNR	Control	MNR	Control	MNR	Diet	Male C vs MNR	Female C vs MNR	Control M vs F	MNR M vs F
Number of animals/group	12	12	6	6	6	6					
Maternal characterization											
Weight preconception (Kg)	16.30 ± 0.73	16.64 ± 1.16	15.95 ± 1.17	16.84 ± 1.73	16.64 ± 0.97	16.37 ± 1.74	-	-	-	-	-
Weight at cesarean section (Kg)	18.32 ± 0.74	16.43 ± 1.08	18.47 ± 1.24	15.91 ± 1.69	18.17 ± 0.91	16.96 ± 1.47	-	-	-	-	-
Weight variation (%)	12.84 ± 2.11	-3.13 ± 3.02	16.15 ± 3.17	-7.06 ± 3.67	9.53 ± 2.28	1.78 ± 4.23	0.001	0.006	-	-	-
Placental weight (g)	213.29 ± 14.35	164.05 ± 11.15	223.08 ±21.24	164.74 ± 13.28	203.50 ± 20.42	163.20 ± 21.26	0.019	0.045	-	-	-
Blood serum at cesarean section [a]							-	-	-	-	-
Blood urea nitrogen (mg/dl)	8.86 ± 0.51	9.33 ± 1.02	8.00 ± 0.58	7.67 ± 0.33	9.50 ± 0.65	11.00 ± 1.53	-	-	-	-	-
Creatinine (mg/dl)	0.89 ± 0.05	1.02 ± 0.10	0.83 ± 0.09	0.93 ± 0.07	0.93 ± 0.05	1.10 ± 0.21	-	-	-	-	-
Blood urea nitrogen/Creatinine	10.13 ± 0.70	9.55 ± 1.41	9.73 ± 0.84	8.33 ± 0.88	10.43 ± 1.13	10.77 ± 2.77	-	-	-	-	-
Sodium (mEq/l)	140.86 ± 0.77	140.50 ± 1.09	140.33 ± 1.67	142.00 ± 1.15	141.25 ± 0.75	139.00 ± 1.53	-	-	-	-	-
Potassium (mEq/l)	3.57 ± 0.11	3.65 ± 0.15	3.77 ± 0.18	3.70 ± 0.10	3.43 ± 0.09	3.60 ± 0.32	-	-	-	-	-
Chloride (mEq/l)	111.86 ± 0.67	109.50 ± 1.41	112.33 ± 1.67	111.00 ± 2.52	111.50 ± 0.29	108.00 ± 1.15	-	-	0.031	-	-
Carbon dioxide (mEq/l)	22.14 ± 0.74	21.17 ± 1.08	23.00 ± 0.58	22.33 ± 0.67	21.50 ± 1.19	20.00 ± 2.00	-	-	-	-	-
Anion Gap (mEq/l)	10.43 ± 1.07	13.48 ± 1.49	8.77 ± 0.41	12.37 ± 2.24	11.68 ± 1.65	14.60 ± 2.21	-	-	-	-	-
Calcium (mg/dl)	8.45 ± 0.09	8.40 ± 0.13	8.43 ± 0.19	8.23 ± 0.03	8.47 ± 0.07	8.65 ± 0.25	-	-	-	-	-
Phosphorus (mg/dl)	3.15 ± 0.20	3.22 ± 0.13	3.33 ± 0.12	3.33 ± 0.18	2.97 ± 0.39	3.05 ± 0.15	-	-	-	-	-
Albumin (g/dl)	2.84 ± 0.16	2.72 ± 0.05	2.87 ± 0.03	2.73 ± 0.07	2.83 ± 0.30	2.70 ± 0.10	-	-	-	-	-
Total protein (g/dl)	6.37 ± 0.21	6.28 ± 0.20	6.43 ± 0.07	6.00 ± 0.25	6.33 ± 0.38	6.57 ± 0.24	-	-	-	-	-
Total bilirubin (mg/dl)	0.27 ± 0.05	0.32 ± 0.06	0.30 ± 0.10	0.30 ± 0.06	0.23 ± 0.03	0.35 ± 0.15	-	-	-	-	-
Alkaline phosphatase (U/l)	130.14 ± 25.28	178.67 ± 43.49	171.33 ± 53.35	163.33 ± 13.93	99.25 ± 8.50	194.00 ± 95.02	-	-	-	-	-
Alanine aminotransferase (U/l)	45.14 ± 9.12	58.50 ± 12.53	36.00 ± 10.02	53.33 ± 13.98	52.00 ± 14.29	63.67 ± 23.73	-	-	-	-	-
Aspartate aminotransferase (U/l)	21.71 ± 2.26	37.33 ± 6.98	22.00 ± 2.65	38.67 ± 11.79	21.50 ± 3.80	36.00 ± 10.15	0.038	-	-	-	-
Gamma-glutamyl transferase (U/l)	31.50 ± 1.38	32.40 ± 1.03	31.00 ± 2.65	32.67 ± 1.76	32.00 ± 1.53	32.00 ± 1.00	-	-	-	-	-
Cholesterol (mg/dl)	60.57 ± 5.95	64.17 ± 7.53	62.33 ± 14.31	57.33 ± 8.21	59.25 ± 4.48	71.00 ± 13.00	-	-	-	-	-
Triglycerides (mg/dl)	32.00 ± 4.12	51.80 ± 6.96	29.33 ± 5.67	52.67 ± 8.35	34.67 ± 6.74	50.50 ± 16.50	-	-	-	-	-
Lactate dehydrogenase (U/l)	184.00 ± 15.69	191.00 ± 15.88	167.33 ± 15.50	197.33 ± 28.09	200.67 ± 26.69	181.50 ± 2.50	-	-	-	-	-
Creatine phosphokinase (U/l)	281.00 ± 52.20	357.40 ± 128.24	376.67 ± 60.98	390.67 ± 230.36	185.33 ± 27.49	307.50 ± 33.50	-	-	-	0.050	-
Fetal characterization											
Weight (g)	816.93 ± 33.93	716.67 ± 24.07	866.70 ± 47.63	726.90 ± 26.85	767.17 ± 42.51	706.44 ± 42.28	0.050	0.037	-	-	-
Body length (cm)	37.54 ± 0.84	38.08 ± 1.50	38.75 ± 1.28	36.83 ± 1.01	36.33 ± 0.92	39.33 ± 2.89	-	-	-	-	-
Femur length (cm)	7.44 ± 0.18	6.88 ± 0.16	7.33 ± 0.17	7.00 ± 0.32	7.54 ± 0.34	6.75 ± 0.11	0.032	-	-	-	-
Chest circumference (cm)	17.63 ± 0.26	16.75 ± 0.26	17.58 ± 0.40	16.58 ± 0.35	17.67 ± 0.38	16.92 ± 0.40	0.040				
Body mass index (Kg/m^2)	5.80 ± 0.18	5.11 ± 0.31	5.81 ± 0.34	5.40 ± 0.31	5.80 ± 0.18	4.82 ± 0.55	-	-	-	-	-
Heart weight (g)	4.90 ± 0.30	4.20 ± 0.22	4.99 ± 0.30	4.13 ± 0.26	4.81 ± 0.54	4.25 ± 0.36	-	-	-	-	-
Heart weight/body weight (x1000)	5.97 ± 0.22	5.35 ± 0.52	5.76 ± 0.20	4.72 ± 0.98	6.18 ± 0.39	5.98 ± 0.23	-	-	-	-	-
Brain weight (g)	78.86 ± 2.20	78.37 ± 1.52	82.19 ± 2.59	78.85 ± 2.46	76.08 ± 3.15	77.89 ± 2.01	-	-	-	-	-
Brain weight/body weight (x1000)	99.45 ± 3.76	110.41 ± 3.41	99.04 ± 7.77	108.71 ± 2.24	99.80 ± 3.40	112.11 ± 6.71	0.019	-	-	-	-

5.2.2 Maternal and fetal plasma concentrations of essential and non-essential amino acids

Our data showed an increase in maternal plasma amino acids at 0.9 gestation in the MNR group (Table 5.2). MNR increased plasma concentrations of the amino acids arginine (ARG), histidine (HIS), lysine (LYS), valine (VAL), asparagine (ASN) and serine (SER). Histidine was almost 2-fold increased in the maternal plasma of the MNR group, with a more pronounced effect in mothers carrying a male fetus (77.93 ± 2.78 μM vs. 189.02 ± 36.62 μM). Curiously, tyrosine (TYR) level was also 2-fold augmented in maternal plasma of the MNR group, however due to the variability in data, this change did not reach significance. The only exception was the significant diminution of the essential amino phenylalanine (PHE, 54.93 ± 7.34 μM vs. 34.50 ± 1.42 μM) in the maternal plasma of the MNR group.

In general, circulating amino acid concentrations in the control fetus were about 2-fold higher than in their mothers (Table 5.3). Still, the essential amino acid threonine (THR) showed the higher variation between fetal and maternal levels, reaching a 5.5 fold increase in the fetus. Only two amino acids, aspartic acid (ASP) and glutamic acid (GLU), showed the opposite tendency, being about 2-fold less in fetal samples. A diet effect was noted for the amino acid arginine (ARG, 101.48 ± 7.62 μM vs. 150.03 ± 16.64 μM) and glutamine (GLN, 714.61 ± 41.37 μM vs. 558.42 ± 37.21 μM), that was exacerbated in the female fetus. In male fetuses, the amino acid taurine (TAU) was significantly decreased in the MNR group. A fetal gender effect was also detected for the taurine amino acid in the MNR group.

Table 5.2 Maternal plasma amino acid profile (µM) at 0.9 gestation in control *ad libitum*-fed pregnancies and in the presence of maternal nutrient reduction (MNR) to 70% of the food eaten by the control mothers on a weight-adjusted basis.

		Genders combined		Male		Female		P-value by Mann-Whitney test				
		Control	MNR	Control	MNR	Control	MNR	Diet	Male C vs MNR	Female C vs MNR	Control M vs F	MNR M vs F
Number of animals/group		12	12	6	6	6	6					
Essential												
ARG	Arginine	35.26 ± 2.53	48.52 ± 3.67	34.43 ± 3.61	47.65 ± 6.55	36.09 ± 3.85	49.39 ± 3.99	0.006	0.037			
HIS	Histidine	77.93 ± 2.78	189.02 ± 36.62	80.49 ± 4.30	204.37 ± 61.36	75.37 ± 3.58	173.66 ± 45.19	0.008	0.025			
ILE	Isoleucine	42.79 ± 1.86	41.06 ± 2.61	44.18 ± 2.60	46.34 ± 3.22	41.39 ± 2.78	35.78 ± 2.91					
LEU	Leucine	65.62 ± 3.39	55.02 ± 4.14	67.50 ± 4.36	62.09 ± 5.37	63.74 ± 5.49	47.95 ± 5.17					
LYS	lysine	126.80 ± 6.81	154.10 ± 10.25	130.21 ± 8.96	162.78 ± 11.22	123.40 ± 10.91	145.43 ± 17.49	0.038				
MET	Methionine	21.88 ± 1.48	23.68 ± 2.40	22.56 ± 2.67	24.57 ± 4.37	21.20 ± 1.52	22.80 ± 2.43					
PHE	Phenylalanine	54.93 ± 7.43	34.50 ± 1.42	58.87 ± 10.87	35.05 ± 2.36	50.99 ± 10.62	33.95 ± 1.77	0.043				
THR	Threonine	79.83 ± 4.77	96.43 ± 9.30	29.01 ± 5.37	27.65 ± 5.23	24.43 ± 3.25	26.42 ± 4.12					
VAL	Valine	85.90 ± 4.49	98.57 ± 4.76	86.84 ± 7.89	103.53 ± 3.98	84.16 ± 5.09	93.61 ± 8.60	0.05				
Non-essential												
ALA	Alanine	164.38 ± 11.36	192.93 ± 12.69	178.92 ± 20.86	212.00 ± 20.71	149.84 ± 6.92	173.87 ± 11.61					
ASN	Asparagine	22.88 ± 1.38	29.88 ± 1.87	22.38 ± 2.70	31.65 ± 1.61	23.38 ± 1.00	28.11 ± 3.39	0.006	0.025			
ASP	Aspartic acid	10.91 ± 2.09	7.53 ± 0.97	13.98 ± 3.24	7.69 ± 1.08	7.84 ± 2.24	7.37 ± 1.73					
GLN	Glutamine	321.58 ± 18.02	303.40 ± 22.27	316.72 ± 28.97	313.34 ± 30.94	326.43 ± 24.08	293.46 ± 34.44					
GLU	Glutamic acid	74.12 ± 8.42	74.80 ± 8.39	85.62 ± 13.77	84.46 ± 11.83	62.61 ± 8.33	65.15 ± 11.52					
GLY	Glycine	241.26 ± 15.24	237.39 ± 15.86	247.98 ± 25.03	248.16± 26.73	234.54 ± 19.43	226.63 ± 18.61					
ORN	Ornithine	21.05 ± 5.13	15.81 ± 3.03	23.88 ± 8.21	13.94 ± 2.96	18.22 ± 6.71	17.67 ± 5.50					
SER	Serine	71.55 ± 4.04	96.23 ± 8.30	70.97 ± 3.78	106.47 ± 9.56	72.12 ± 7.59	85.99 ± 13.03	0.028	0.01			
TAU	Taurine	136.64 ± 13.02	122.31 ± 8.28	153.70 ± 22.45	115.65 ± 12.96	119.58 ± 11.17	128.96 ± 11.41					
TRP	Tryptophan	26.72 ± 3.07	27.04 ± 3.18	29.01 ± 5.37	27.65 ± 5.23	24.43 ± 3.25	26.42 ± 4.12					
TYR	Tyrosine	32.29 ± 2.20	113.20 ± 28.67	32.36 ± 3.20	106.09 ± 37.00	32.23 ± 3.33	120.31 ± 47.21					

Data are means ± SEM.

Table 5.3 Fetal plasma amino acid profile (µM) at 0.9 gestation in control *ad libitum*-fed pregnancies and in the presence of maternal nutrient reduction (MNR) to 70% of the food eaten by the control mothers on a weight-adjusted basis

		Genders combined		Male		Female			P-value by Mann-Whitney test			
		Control	MNR	Control	MNR	Control	MNR	Diet	Male C vs MNR	Female C vs MNR	Control M vs F	MNR M vs F
Number of animals/group		12	12	6	6	6	6					
Essential												
ARG	Arginine	101.48 ± 7.62	150.03± 16.64	98.81± 10.28	143.06 ± 29.96	103.70 ± 11.83	156.99 ± 17.38	0.023		0.025		
HIS	Histidine	149.36 ± 4.03	351.08 ± 68.27	155.33 ± 7.22	369.79 ± 110.77	144.38 ± 3.71	332.37 ± 89.99					
ILE	Isoleucine	65.94 ± 3.83	71.75 ± 3.58	66.88 ± 4.47	71.36 ± 5.32	65.16 ± 6.34	72.15 ± 5.30					
LEU	Leucine	89.30 ± 5.74	90.20 ± 6.11	90.24 ± 6.54	91.41 ± 8.69	88.52 ± 9.60	89.03 ± 9.39					
LYS	lysine	360.18 ± 20.43	435.35 ± 31.80	368.36 ± 30.29	439.76 ± 38.93	353.36 ± 29.96	430.94 ± 54.09					
MET	Methionine	47.61 ± 2.18	51.12 ± 5.48	42.96 ± 3.53	53.94 ± 10.21	47.81 ± 2.66	48.28 ± 4.98					
PHE	Phenylalanine	85.63 ± 7.90	63.96 ± 2.58	86.14 ± 10.78	62.77± 4.28	85.21 ± 12.31	65.15 ± 3.21					
THR	Threonine	144.23 ± 9.97	169.44 ± 16.97	129.05 ± 13.61	148.29 ± 25.11	156.88 ± 13.05	190.58 ± 21.40					
VAL	Valine	160.98 ± 7.59	184.33 ± 9.85	160.12 ± 10.41	181.93 ± 12.71	161.71 ± 11.79	186.73 ± 16.21					
Non-essential												
ALA	Alanine	341.09 ± 18.27	354.93 ± 27,35	353.85 ± 40.70	351.86 ± 36.39	330.45 ± 8.35	358.00 ± 44.31					
ASN	Asparagine	49,89 ± 4.18	49.82 ± 2.78	50.06± 7.82	50.90 ± 3.47	49.75 ± 4.82	48.73 ± 4.65					
ASP	Aspartic acid	6.57 ± 1.76	4.36 ± 0.69	6.57 ± 2.33	4.47 ± 1.15	6.58 ± 2.79	4.25 ± 0.88					
GLN	Glutamine	714.61 ± 41.37	558.42 ± 37.21	720.30 ± 65.88	572.69 ± 55.86	709.87 ± 58.06	544.15 ± 53.76	0.01		0.025		
GLU	Glutamic acid	44.60 ± 10.07	40.68 ± 4.60	51.65 ± 21.14	43.58 ± 8.12	38.73 ± 7.64	37.78 ± 4.89					
GLY	Glycine	425.79 ± 25.27	398.95 ± 20.11	418.33 ± 34.97	391.27 ± 33.24	432.01 ± 38.85	406.63 ± 25.52					
ORN	Ornithine	41.43 ± 4.91	58.78 ± 10.30	44.59 ± 9.67	61.03 ± 17.59	38.80 ± 4.79	56.52 ± 12.45					
SER	Serine	150.70 ± 7.51	175.28 ± 15.73	151.85 ± 15.42	192.62 ± 21.78	149.75 ± 6.92	157.94 ± 22.22					
TAU	Taurine	168.57 ± 8.40	140.61 ± 17.50	187.03 ± 14.45	110,17 ± 19,39	153.18 ± 3.92	171.04 ± 15.11		0.025			0.05
TRP	Tryptophan	49.77 ± 1.99	61.27 ± 5.31	48.22 ± 3.50	60.85 ± 8.09	51.06 ± 2.37	61.69 ± 7.66					
TYR	Tyrosine	55.84 ± 3.81	216.78 ± 56.13	53.89 ± 6.72	196.16 ± 69.07	57.46 ± 4.67	237.40 ± 94.45					

Data are means ± SEM.

5.2.3 Fetal and maternal cortisol, glucose, and insulin levels

Circulating cortisol in *ad libitum*-fed control mothers was about 2-fold greater than in their offspring at 0.9 gestation (Figure 5.1A, 40.70 ± 3.60 μg/l vs. 20.06 ± 2.04 μg/l). A proportional rise in cortisol was observed in both maternal and fetal blood serum in MNR baboons. However, this increase only reached statistical significance in the MNR mothers, particularly due to effects on MNR mothers carrying male fetuses. The maternal-to-fetal cortisol gradient was not different in MNR compared to control pregnancies with MNR fetuses similarly presenting half of the cortisol levels detected in their mothers.

Plasma glucose in control mothers fed *ad libitum* was 1.8-fold higher than that of their fetuses at 0.9 gestation (Figure 5.1B, 61.87 ± 7.21 mg/l vs. 33.83 ± 4.71 mg/l). However, no difference was observed in glucose levels between control and MNR fetuses when genders were either combined or separated (Figure 5.1B). Only MNR mothers carrying male fetuses showed a significant increase in glucose levels. There was a trend for increased maternal insulin levels in all MNR mothers compared to the fetuses, with insulin levels in control mothers were 1.8-fold greater than in fetuses at 0.9 gestation (Figure 5.1C). However, due to variability in the data obtained, the difference did not reach significance. The MNR treatment did not affect insulin levels in the maternal groups. However, MNR treatment reduced fetal insulin in male fetuses, while gender differences were observed for MNR males vs. MNR females (MNR-M vs. MNR-F) for maternal and fetal samples.

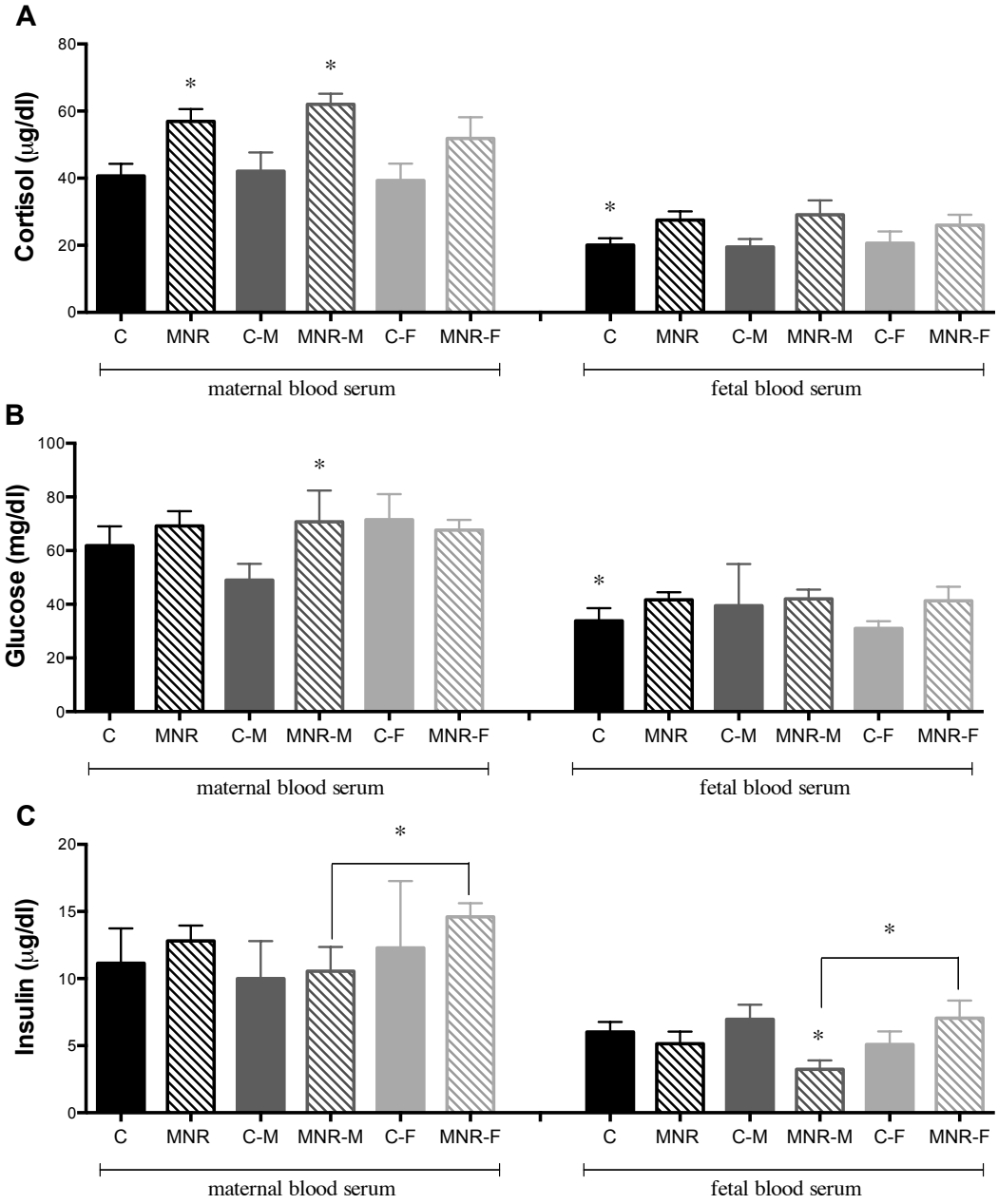

Figure 5.1 Cortisol, glucose, and insulin levels in maternal and fetal plasma of control (C) and maternal nutrient reduction (MNR) groups.

These parameters were determined in maternal and fetal plasma of control *ad libitum*-fed pregnancies and in the presence of MNR, characterized as 70% of the food consumed by control mothers on a weight-adjusted basis of baboons at 0.9 gestation. A: cortisol levels in maternal and fetal plasma of control and MNR baboons (male fetuses n=12; female fetuses n=12). C-M, male fetuses from control group (n=6); C-F, female fetuses from control group (n=6); MNR-M, male fetuses from MNR group (n=6); MNR-F, female fetuses from MNR group (n=6). B: glucose levels in maternal and fetal plasma of control and MNR baboons (C n=7; MNR n=6; C-M n=3; C-F n=4; MNR-M n=3; MNR-F n=3). C: insulin levels in maternal and fetal plasma of control and MNR baboons (C n=12; MNR n=12; C-M n=6; C-F n=6; MNR-M n=6; MNR-F n=6). Means ± SEM; Comparison between groups was performed using a non-parametric Mann-Whitney test. P-value less than 0.05 was considered significant. *P<0.05 vs. respective controls or as indicated.

5.2.4 Determination of mitochondrial DNA copy number in cardiac left ventricle by quantitative PCR

The first step in the evaluation of MNR effects on fetal mitochondrial fitness was the determination of the mtDNA copy number in a total of 23 samples from fetal cardiac left ventricle from control and MNR groups (Figure 5.2). The average mtDNA copy number in control group was 714.50 ± 84.89 copies per nucleus when using the mitochondrially encoded NADH dehydrogenase 1 (*ND1*) gene as reference and the nuclear encoded gene for beta-2-microglobulin (*B2M*) for normalization per nucleus. This amount is slightly different when the mitochondrially encoded NADH dehydrogenase 6 (*ND6*) gene was used as reference (1372.00 ± 206.70). However, both gave the same information, MNR induced an augment in mtDNA copy number in female fetuses. We found a relationship between MNR and increased mtDNA copy number per nucleus when using *ND1* but that difference was not uncovered when using *ND6*. Due to the significant increase registered in the MNR female fetuses, the number of mtDNA copies was significantly higher that in the MNR male fetuses, but once again, this observation was only significant using *ND1* as the mitochondrial reference gene.

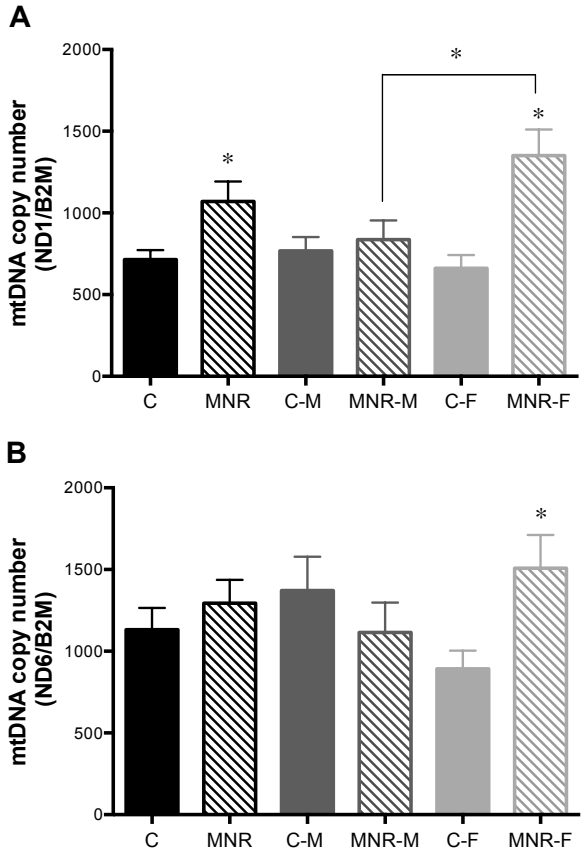

Figure 5.2. Variation of mitochondrial DNA (mtDNA) copy number in fetal cardiac left ventricle tissue from control (C) and maternal nutrient reduction (MNR) groups. mtDNA was determined in fetal cardiac tissue of control *ad libitum*-fed pregnancies and in the presence of MNR, characterized as 70% of the food consumed by control mothers on a weight-adjusted basis of baboons at 0.9 gestation. A: mtDNA copy number was calculated for control and MNR baboons fetuses as the ratio between the mitochondrially encoded NADH dehydrogenase 1 (ND1) gene and the nuclear encoded gene for beta-2-microglobulin (B2M). C-M, male fetuses from control group (n=6); C-F, female fetuses from control group (n=6); MNR-M, male fetuses from MNR group (n=6); MNR-F, female fetuses from MNR group (n=5). B: mtDNA copy number for control and MNR fetuses baboons determined using the mitochondrially encoded NADH dehydrogenase 6 (ND6) and the nuclear encoded gene for B2M (C n=12; MNR n=11; C-M n=6; C-F n=6; MNR-M n=6; MNR-F n=5). Means ± SEM; Comparison between groups was performed using a non-parametric Mann-Whitney test. P-value less than 0.05 was considered significant. *P<0.05 vs. respective controls or as indicated.

5.2.5 MNR affected the transcription of key mitochondrial genes in fetal cardiac left ventricle

We next investigated the mitochondrial effects of MNR by evaluating several transcripts related to the mitochondrial function. The Human Mitochondrial Energy Metabolism and the Human Mitochondria Pathway Arrays were used for expression

profiling in fetal cardiac left ventricle RNA samples. The complete set of data is shown in Table 5.4 and summarized in Figure 5.3, 5.4 and 5.5. PCR arrays presented a residual percentage of absent calls, approximately 10% of genes were not determined or were detectable but the gene's average threshold cycle was greater than the defined cut-off value (Ct = 35), these genes will appear colored as gray in Figure 5.3 and 5.4. The heat maps in Figure 5.3 and 5.4 provide a summary graphical representation of fold regulation expression data for maternal diet effects in fetus cardiac left ventricle (C vs. MNR, Figure 5.3) and for gender differences between the control fetuses (C-M vs. C-F, Figure 5.4). Qualitatively, our results support the notion that MNR increased several mitochondrial transcripts and that female fetuses had higher levels of mitochondrial transcripts. The statistical analyses confirmed that the mitochondrial transcripts investigated showed diet-dependent effects, with a significant overall increased mitochondrial-relevant transcripts in the MNR fetuses compared with control fetuses, with the greatest alterations occurring when genders were combined (Figure 5.5E). There were 21 transcripts differentially present in the MNR group, with 85% of the alterations showing upregulation. Most of the upregulated transcripts encoded subunits of mitochondrial OXPHOS system, including 3 of 33 subunits analyzed from complex I: *NDUFB6, NDUFB7,* and *NDUFV1*; 2 of 4 subunits analyzed for complex II: *SDHC* and *SDHD*; 1 of 6 subunits analyzed for complex III: *UQCR11*; and 5 of 21 subunits analyzed for ATP synthase: *ATP5A1, ATP5B, ATP5F1, ATP5G3* and *ATP5L*. In addition, transcripts for regulators and mediators of mitochondrial molecular transport, namely small-molecule transporters (*SLC25A24 and SLC25A27*); one member of the outer membrane translocation system (*TOMM34*); the mitochondrial outer membrane import complex protein 2 (*MTX2*); the mediator of mitochondrial fusion (*MFN2*); the heat shock protein 1 (*HSPD1*) and the one pro-apoptotic factor (*BNIP3*) were also upregulated in the MNR group. Finally, two members related to apoptosis pathway (*PMAIP1* and *TP53*) and one related with cholesterol transporter (*TSPO*) were downregulated.

A significant sexual dimorphism was present in the mitochondrial-related expression profile of the control fetuses. Female fetuses presented a higher content in transcripts for *NDUFB5* and *NDUFC1*, complex I subunits; *COX6C*, a cytochrome c oxidase subunit; *MSTO1*, a regulator of mitochondrial morphology and distribution; *SLC25A3*, *SLC25A4*, *SLC25A20*, regulators and mediators of

mitochondrial molecular transport and *SOD1* that encodes for the cytosolic superoxide dismutase. However, the gender differences were attenuated by maternal MNR with just one transcript being different between genders for this group, the subunit of complex I *NDUFB7*.

Diet-induced transcript differences were also observed within the same gender. In summary, multiple components of the mitochondrial respiratory chain were increased in MNR male fetuses, including two subunits of complex I (*NDUFA1, NDUFS6*), one subunit of complex II (*SDHD*), one subunit of complex III (*UQCR11*) and two ATP synthase subunits (*ATP5A1, ATP5G3*). Increased transcripts also included *SLC25A24*, *MTX2, HSPD1, BNIP3* as well as one member of the outer membrane translocase complex (*TOMM70A*).

In the MNR female fetus, MNR resulted in a significant increase in the abundance of two transcripts for the mitochondrial respiratory chain, including *NDUFB6* and *NDUFB7*. On the other hand, female fetuses exhibited a significant decrease in transcripts related to cell death pathways, such as the pro-apoptotic Bcl-2-binding component 3 (*BBC3*), *BID*, a mediator of mitochondrial damage induced by caspase-8, *PMAIP1*, which is related to the activation of caspases and apoptosis and *TP53*. Other significant diet-induced downregulated gene-expression occurred for *TIMM22,* an inner mitochondrial membrane protein translocase and *TSPO,* which has been connected with the transport of cholesterol.

Figure 5.3 Diet effects in gene expression profile.
Maternal nutrient reduction to 70% of the food eaten by the control mothers on a weight-adjusted basis leads to changes in gene expression profile on fetus cardiac left ventricle tissue. The heat map represents the transcriptome profile assessed in The Human Mitochondrial Energy Metabolism (top) and in the Human Mitochondria (bottom) pathway arrays in response to MNR when both genders were combined. Red and green indicate increased and decreased expression, respectively, relative to control group. Values were normalized to endogenous controls [hypoxanthine phosphoribosyltransferase 1 (*HPRT1*), ribosomal protein L13a (*RPL13A*), and Beta-actin (*ACTB*)] and expressed relative to their normalized values. n=12 (genders combined) animals/group. Cells in the heat map which are colored gray correspond to genes with erroneous fold changes, that is, this transcript average threshold cycle was either not determined or greater than the defined cut-off value (Ct = 35), in at least one of the groups, meaning that its expression was undetected, making this fold-change result erroneous and un-interpretable. See the Material and Methods Table 3.2 and Table 3.3 for gene abbreviations used.

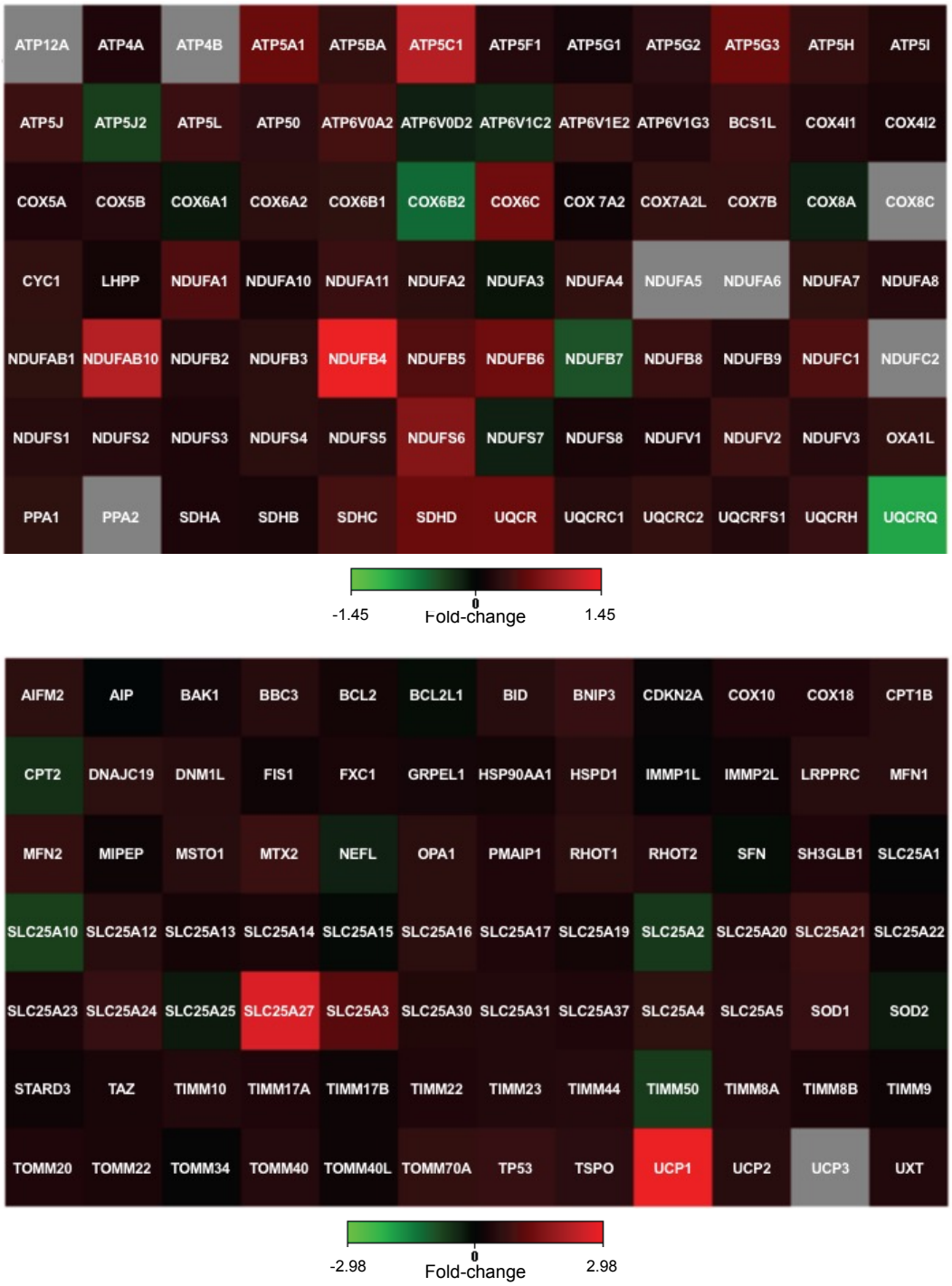

Figure 5.4 Gender effect in gene expression profile.
Expression profile comparison for control fetuses cardiac left ventricle tissue. The heat map represents the transcriptome profile assessed in The Human Mitochondrial Energy Metabolism (top) and in the Human Mitochondria (bottom) pathway arrays in response to fetus gender only for the control group. Red and green indicate increased and decreased expression, respectively, relative to control male fetuses. Values were normalized to endogenous controls [hypoxanthine phosphoribosyltransferase 1 (HPRT1), ribosomal protein L13a (RPL13A), and Beta-actin (ACTB)] and expressed relative to their normalized values. n=12 (genders combined) animals/group. Cells in the heat map which are colored gray correspond to genes with erroneous fold changes, that is, this transcript average threshold cycle was either not determined or greater than the defined cut-off value (Ct = 35), in at least one of the groups, meaning that its expression was undetected, making this fold-change result erroneous and un-interpretable. See the Material and Methods Table 3.2 and Table 3.3 for gene abbreviations used.

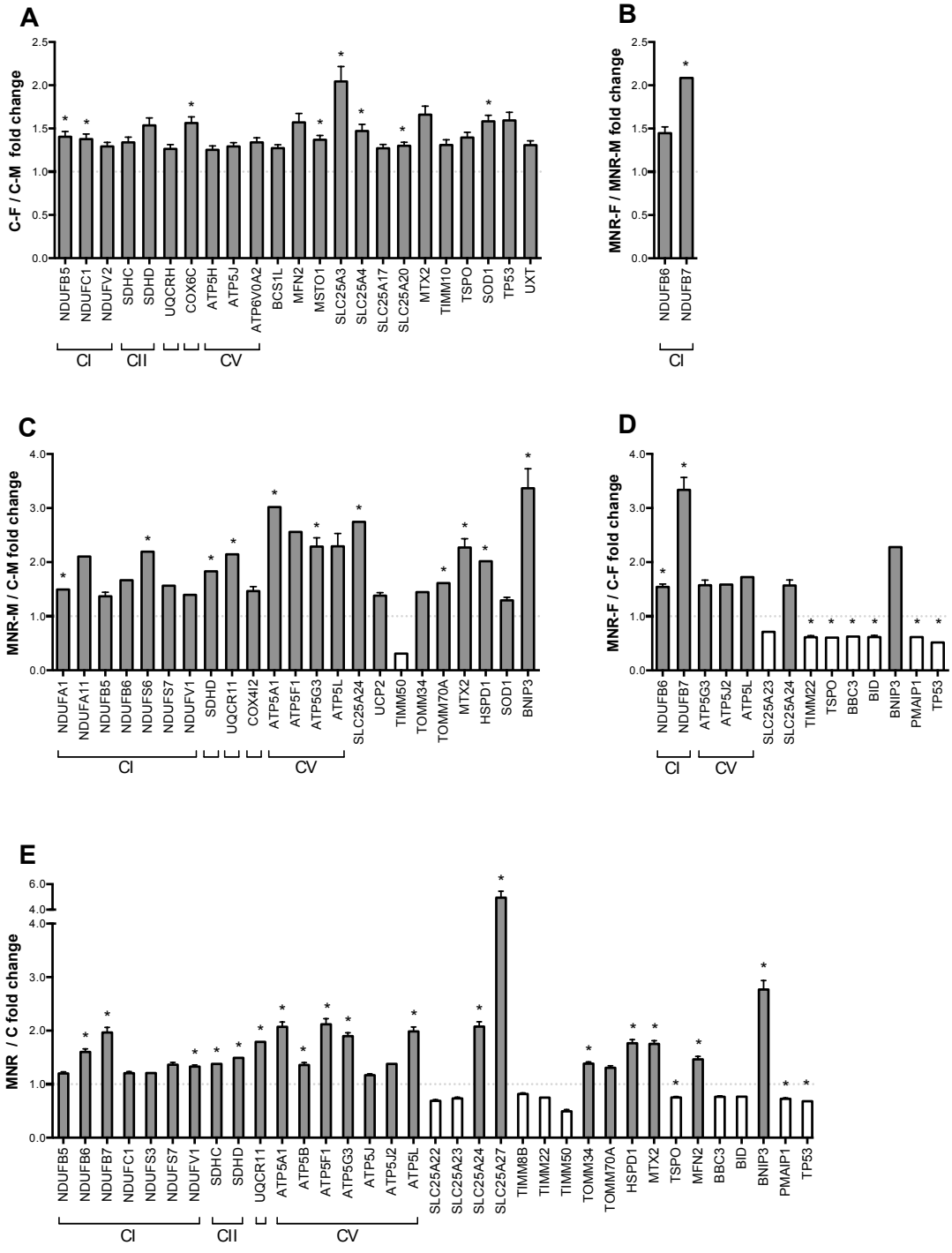

Figure 5.5 Cardiac left ventricle gene expression analysis.
Gene expression analysis of control and MNR baboon fetuses at 0.9 gestation. mRNA abundance for mitochondrial proteins was assessed by PCR array cardiac left ventricle samples from baboon fetuses from mothers fed *ad libitum* (control group) or 70% of the control diet (MNR group) at 0.9 gestation. A: Sexual dimorphism in the mitochondrial profile of control fetuses; B: and C: comparison of transcripts expression based on maternal diet for the same gender [male fetuses (B) and female fetuses (C)]; D: gender dimorphism in the mitochondrial profile of the MNR fetus and E: global diet-dependent effects in the mitochondrial gene expression profile. Transcripts related to oxidative phosphorylation system (OXPHOS), complex I (CI; NADH dehydrogenase), complex II (CII; succinate dehydrogenase), complex III (CIII; ubiquinol cytochrome c oxidoreductase), complex IV [CIV; cytochrome c oxidase (COX)], and complex V (CV; ATP synthase). Values were

normalized to endogenous controls [hypoxanthine phosphoribosyltransferase 1 (HPRT1), ribosomal protein L13a (RPL13A), and Beta-actin (ACTB)] and expressed relative to their normalized values. Means ± SEM; n=6 (when separated by gender) or n=12 (genders combined) animals/group. All transcripts presented have P<0.1 vs. respective paired group. *P<0.05 vs. respective controls. See the Table 5.4 or the Material and Methods Table 3.2 and Table 3.3 for gene abbreviations used.

Table 5.4. mRNA abundance of mitochondrial proteins was assessed by PCR array. mRNA levels in cardiac left ventricle samples from baboon fetuses originating from mothers fed *ad libitum* (controls, C) or 70% of the control diet (maternal nutrient reduction, MNR) at 0.9 gestation. Symbol denotes the gene identification, RefSeq denotes the Reference Sequence from the National Center for Biotechnology Information collection, Description gives a summary information about the gene identification and/or function, Fold difference was calculate between the groups enunciated, positive values for up regulation and negative values for a down regulation. Fold differences relevant to the mitochondrial profile of the control fetus (control female, C-F vs. control male, C-M) were presented in the C-F vs. C-M section, as well the comparison of transcripts expression based on maternal diet for the same gender (in the MNR-M vs. C-M and MNR-F vs. C-F sections), the gender dimorphism in the mitochondrial profile of the MNR fetus (in the MNR-F vs. MNR-M section) and global diet-dependent effects in the mitochondrial expression profile (MNR vs. C section). The transcripts presented have either 0.05<P<0.1 or P<0.05 in bold.

Symbol	Refseq	Description	Fold difference	P-value
		C-F vs. C-M		
ATP6V0A2	NM_012463	ATPase, H+ transporting, lysosomal V0 subunit a2	1,339	0,070
BCS1L	NM_004328	BCS1-like (S. cerevisiae)	1,272	0,053
COX6C	NM_004374	Cytochrome c oxidase subunit VIc	**1,563**	**0,010**
NDUFB5	NM_002492	NADH dehydrogenase (ubiquinone) 1 beta subcomplex, 5	**1,404**	**0,034**
NDUFC1	NM_002494	NADH dehydrogenase (ubiquinone) 1, subcomplex unknown, 1	**1,376**	**0,042**
SDHC	NM_003001	Succinate dehydrogenase complex, subunit C, integral membrane protein	1,339	0,089
SDHD	NM_003002	Succinate dehydrogenase complex, subunit D, integral membrane protein	1,537	0,066
UQCRH	NM_006004	Ubiquinol-cytochrome c reductase hinge protein	1,264	0,086
MFN2	NM_014874	Mitofusin 2, mediator of mitochondrial fusion	1,570	0,092
MSTO1	NM_018116	Misato homolog 1, mitochondrial distribution and morphology regulator	**1,370**	**0,034**
MTX2	NM_006554	Metaxin 2, mitochondrial outer membrane import complex protein 2	1,661	0,068
SLC25A17	NM_006358	Solute carrier family 25 (mitochondrial carrier; peroxisomal membrane protein), member 17	1,271	0,073
SLC25A20	NM_000387	Solute carrier family 25 (carnitine/acylcarnitine translocase), member 20	**1,300**	**0,045**

SLC25A3	NM_002635	Solute carrier family 25 (mitochondrial carrier; phosphate carrier), member 3	**2,044**	**0,016**
SLC25A4	NM_001151	Solute carrier family 25 (mitochondrial carrier; adenine nucleotide translocator), member 4, ANT1	**1,471**	**0,049**
SOD1	NM_000454	Superoxide dismutase 1, soluble, Cu/Zn superoxide dismutase	**1,583**	**0,015**
TIMM10	NM_012456	Translocase of inner mitochondrial membrane 10 homolog (yeast)	1,309	0,099
TP53	NM_000546	Tumor protein p53, P53 tumor suppressor	1,593	0,070
TSPO	NM_000714	Translocator protein (18kDa), transport of cholesterol	1,395	0,083
UXT	NM_004182	Ubiquitously-expressed transcript	1,308	0,060
		MNR-M vs. C-M		
ATP5A1	NM_004046	ATP synthase, H+ transporting, mitochondrial F1 complex, alpha subunit 1	**3,019**	**0,012**
ATP5G3	NM_001689	ATP synthase, H+ transporting, mitochondrial Fo complex, subunit C3	**2,287**	**0,010**
ATP5L	NM_006476	ATP synthase, H+ transporting, mitochondrial Fo complex, subunit G	2,294	0,058
COX4I2	NM_032609	Cytochrome c oxidase subunit IV isoform 2	1,464	0,071
NDUFA1	NM_004541	NADH dehydrogenase (ubiquinone) 1 alpha subcomplex, 1	**1,495**	**0,041**
NDUFA11	NM_175614	NADH dehydrogenase (ubiquinone) 1 alpha subcomplex, 11	2,103	0,070
NDUFB5	NM_002492	NADH dehydrogenase (ubiquinone) 1 beta subcomplex, 5	1,368	0,079
NDUFB6	NM_182739	NADH dehydrogenase (ubiquinone) 1 beta subcomplex, 6	1,666	0,084
NDUFS6	NM_004553	NADH dehydrogenase (ubiquinone) Fe-S protein 6	**2,194**	**0,027**
NDUFS7	NM_024407	NADH dehydrogenase (ubiquinone) Fe-S protein 7	1,563	0,094
NDUFV1	NM_007103	NADH dehydrogenase (ubiquinone) flavoprotein 1	1,396	0,081
SDHD	NM_003002	Succinate dehydrogenase complex, subunit D, integral membrane protein	**1,830**	**0,047**
UQCR11	NM_006830	Ubiquinol-cytochrome c reductase, complex III subunit XI	**2,145**	**0,026**
BNIP3	NM_004052	BCL2/adenovirus E1B 19kDa interacting protein 3, pro-apoptotic factor	**3,367**	**0,023**
HSPD1	NM_002156	Heat shock 60kDa protein 1, chaperonin family, folding and assembly of proteins	**2,018**	**0,018**
MTX2	NM_006554	Metaxin 2, mitochondrial outer membrane import complex protein 2	**2,271**	**0,019**
SLC25A24	NM_013386	Solute carrier family 25 (mitochondrial carrier; phosphate carrier), member 24	**2,745**	**0,019**

SOD1	NM_000454	Superoxide dismutase 1, soluble, Cu/Zn superoxide dismutase	1,293	0,098
TIMM50	NM_001001563	Translocase of inner mitochondrial membrane 50 homolog (S. cerevisiae)	-3,232	0,053
TOMM34	NM_006809	Translocase of outer mitochondrial membrane 34	1,446	0,099
TOMM70A	NM_014820	Translocase of outer mitochondrial membrane 70 homolog A (S. cerevisiae)	**1,612**	**0,048**
UCP2	NM_003355	Uncoupling protein 2 (mitochondrial, proton carrier), SLC25A8, proton leak	1,380	0,073
		MNR-F vs. C-F		
ATP5G3	NM_001689	ATP synthase, H+ transporting, mitochondrial Fo complex, subunit C3	1,575	0,093
ATP5J2	NM_004889	ATP synthase, H+ transporting, mitochondrial Fo complex, subunit F2	1,586	0,082
ATP5L	NM_006476	ATP synthase, H+ transporting, mitochondrial Fo complex, subunit G	**1,721**	**0,037**
NDUFB6	NM_182739	NADH dehydrogenase (ubiquinone) 1 beta subcomplex, 6	**1,542**	**0,008**
NDUFB7	NM_004146	NADH dehydrogenase (ubiquinone) 1 beta subcomplex, 7	**3,336**	**0,001**
BBC3	NM_014417	BCL2 binding component 3	**-1,596**	**0,032**
BID	NM_001196	BH3 interacting domain death agonist	**-1,622**	**0,028**
BNIP3	NM_004052	BCL2/adenovirus E1B 19kDa interacting protein 3, pro-apoptotic factor	2,278	0,098
PMAIP1	NM_021127	Phorbol-12-myristate-13-acetate-induced protein 1, related to activation of caspases and apoptosis	**-1,624**	**0,025**
SLC25A23	NM_024103	Solute carrier family 25 (mitochondrial carrier; phosphate carrier), member 23	-1,405	0,080
SLC25A24	NM_013386	Solute carrier family 25 (mitochondrial carrier; phosphate carrier), member 24	1,570	0,052
TIMM22	NM_013337	Translocase of inner mitochondrial membrane 22 homolog (yeast)	**-1,631**	**0,024**
TP53	NM_000546	Tumor protein p53, P53 tumor suppressor	**-1,933**	**0,021**
TSPO	NM_000714	Translocator protein (18kDa), transport of cholesterol	**-1,651**	**0,020**
		MNR-F vs. MNR-M		
NDUFB6	NM_182739	NADH dehydrogenase (ubiquinone) 1 beta subcomplex, 6	1,447	0,057
NDUFB7	NM_004146	NADH dehydrogenase (ubiquinone) 1 beta subcomplex, 7	**2,084**	**0,014**
		MNR vs. C		
ATP5A1	NM_004046	ATP synthase, H+ transporting, mitochondrial F1 complex, alpha subunit 1	**2,071**	**0,004**

ATP5B	NM_001686	ATP synthase, H+ transporting, mitochondrial F1 complex, beta polypeptide	**1,360**	**0,048**
ATP5F1	NM_001688	ATP synthase, H+ transporting, mitochondrial Fo complex, subunit B1	**2,120**	**0,024**
ATP5G3	NM_001689	ATP synthase, H+ transporting, mitochondrial Fo complex, subunit C3	**1,898**	**0,002**
ATP5J	NM_001685	ATP synthase, H+ transporting, mitochondrial Fo complex, subunit F6	1,168	0,094
ATP5J2	NM_004889	ATP synthase, H+ transporting, mitochondrial Fo complex, subunit F2	1,380	0,069
ATP5L	NM_006476	ATP synthase, H+ transporting, mitochondrial Fo complex, subunit G	**1,987**	**0,003**
NDUFB5	NM_002492	NADH dehydrogenase (ubiquinone) 1 beta subcomplex, 5	1,202	0,088
NDUFB6	NM_182739	NADH dehydrogenase (ubiquinone) 1 beta subcomplex, 6	**1,603**	**0,004**
NDUFB7	NM_004146	NADH dehydrogenase (ubiquinone) 1 beta subcomplex, 7	**1,966**	**0,013**
NDUFC1	NM_002494	NADH dehydrogenase (ubiquinone) 1, subcomplex unknown, 1	1,207	0,090
NDUFS3	NM_004551	NADH dehydrogenase (ubiquinone) Fe-S protein 3	1,209	0,066
NDUFS7	NM_024407	NADH dehydrogenase (ubiquinone) Fe-S protein 7	1,363	0,051
NDUFV1	NM_007103	NADH dehydrogenase (ubiquinone) flavoprotein 1	**1,328**	**0,012**
SDHC	NM_003001	Succinate dehydrogenase complex, subunit C, integral membrane protein	**1,379**	**0,040**
SDHD	NM_003002	Succinate dehydrogenase complex, subunit D, integral membrane protein	**1,491**	**0,027**
UQCR11	NM_006830	Ubiquinol-cytochrome c reductase, complex III subunit XI	**1,790**	**0,023**
BBC3	NM_014417	BCL2 binding component 3	-1,309	0,054
BID	NM_001196	BH3 interacting domain death agonist	-1,304	0,066
BNIP3	NM_004052	BCL2/adenovirus E1B 19kDa interacting protein 3, pro-apoptotic factor	**2,770**	**0,003**
HSPD1	NM_002156	Heat shock 60kDa protein 1, chaperonin family, folding and assembly of proteins	**1,766**	**0,009**
MFN2	NM_014874	Mitofusin 2, mediator of mitochondrial fusion	**1,465**	**0,041**
MTX2	NM_006554	Metaxin 2, mitochondrial outer membrane import complex protein 2	**1,754**	**0,004**
PMAIP1	NM_021127	Phorbol-12-myristate-13-acetate-induced protein 1, related to activation of caspases and apoptosis	**-1,375**	**0,023**
SLC25A22	NM_024698	Solute carrier family 25 (mitochondrial carrier: glutamate),	**-1,449**	**0,045**

		member 22		
SLC25A23	NM_024103	Solute carrier family 25 (mitochondrial carrier; phosphate carrier), member 23	-1,363	0,061
SLC25A24	NM_013386	Solute carrier family 25 (mitochondrial carrier; phosphate carrier), member 24	**2,076**	**0,001**
SLC25A27	NM_004277	Solute carrier family 25, member 27, UCP4	**4,942**	**0,044**
TIMM22	NM_013337	Translocase of inner mitochondrial membrane 22 homolog (yeast)	-1,336	0,051
TIMM50	NM_001001563	Translocase of inner mitochondrial membrane 50 homolog (S. cerevisiae)	-2,031	0,062
TIMM8B	NM_012459	Translocase of inner mitochondrial membrane 8 homolog B (yeast)	-1,223	0,052
TOMM34	NM_006809	Translocase of outer mitochondrial membrane 34	**1,383**	**0,026**
TOMM70A	NM_014820	Translocase of outer mitochondrial membrane 70 homolog A (S. cerevisiae)	1,305	0,100
TP53	NM_000546	Tumor protein p53, P53 tumor suppressor	**-1,468**	**0,027**
TSPO	NM_000714	Translocator protein (18kDa), transport of cholesterol	**-1,332**	**0,041**

5.2.6 MNR offspring presented altered mitochondrial protein content

After detecting alterations in mtDNA and mRNA levels, we next investigated MNR effects on offspring specific mitochondrial proteins content. Ultimately, we would like to assess whether the changes at the transcript levels were translated to the protein level, so we performed Western blot and immunohistochemistry analysis.

In agreement with the observed increase in mRNA expression of the respiratory chain subunits, Western blot analysis (Table 5.5 and Figure 5.6) revealed an increase in mitochondrial proteins in the fetal MNR group, which was particularly evident for components of the mitochondrial respiratory chain, such as subunits of complex I (NDUFB8), complex II (UQCRC1) and cytochrome c (Cyt c), an electron transporter of the mitochondrial electron transport chain and a major player in cell death regulation. VDAC1, an isoform of the voltage-dependent anion-selective channel that behaves as a general diffusion pore for small hydrophilic molecules facilitating the exchange of ions and molecules between mitochondria and cytosol, and cyclophilin D (Cyc D), which is a modulator of the mitochondrial permeability transition pore that is located in the mitochondrial matrix were also increased in the MNR group. However, the major increase was observed for the mitochondrial

fission 1 protein (Fis1, 0.89 ± 0.08 vs. 1.33 ± 0.16), that is implicated in mitochondrial fission and regulation of mitochondrial morphology, cell cycle and apoptosis with this protein being 1.5-fold increased in the MNR group.

Diet-induced proteins differences were also observed within the same gender. In summary, from the 14 components of the mitochondria that were detectable, 11 were increased in MNR male fetuses and only two in the MNR female fetuses (COX6C and Fis1), denoting a more pronounced effect of the MNR on the male fetuses. It is important to take in consideration the pronounced gender dimorphism was already present in the control fetuses, with the female fetuses displaying a higher amount of nine mitochondrial proteins (UQCRC1, UQCRC2, MT-CO2, ATP5A1, ATP5A, Cyt c, VDAC, CyC D and CAT). Interestingly, MNR attenuated this gender-related difference by decreasing to four the number of the mitochondrial proteins that were distinct between genders in the MNR groups (NDUFB8, COX6C, CAT and FIS1).

Besides Western blot analysis, the tissue content of four mitochondrial proteins (COX6C, CYC1, MFN2, and TIMM9A) was also measured by immunohistochemistry (Figure 5.7 and Figure 5.8). In agreement with the overall mitochondrial proteins pattern, an increase in mitofusin 2 (MFN2), a mitochondrial membrane protein that participates in the mitochondrial fusion contributing to the maintenance and operation of the mitochondrial network, was measured in the left ventricle of MNR female fetuses (Figure 5.7). Although, under control diet conditions, female fetuses had decreased content of MFN2 when compared to male fetal samples (fraction stained (%) and in density (AU)). There were no differences between diets or genders in the quantitative immunohistochemistry of CYC1, COX6C or TIMM9A in the analyzed cardiac tissue (Figure 5.8).

Table 5.5 Effects of maternal diet on content level of mitochondrial proteins at 0.9 gestation in control *ad libitum*-fed pregnancies and in the presence of maternal nutrient reduction (MNR), considered as 70% of the food eaten by the control mothers on a weight-adjusted basis.

	Genders combined		Male		Female		P-value by Mann-Whitney test				
	Control	MNR	Control	MNR	Control	MNR	Diet	Male C vs MNR	Female C vs MNR	Control M vs F	MNR M vs F
Number of animals/group	12	12	6	6	6	6					
NDUFB8	1.11 ± 0.05	1.20 ± 0.05	1.00 ± 0.03	1.12 ± 0.01	1.21 ± 0.08	1.28 ± 0.10	0.033	0.010	-	-	0.037
UQCRC1	1.06 ± 0.03	1.17 ± 0.04	1.00 ± 0.02	1.09 ± 0.02	1.12 ± 0.03	1.24 ± 0.08	0.038	0.010	-	0.016	-
UQCRC2	1.12 ± 0.05	1.22 ± 0.05	1.00 ± 0.03	1.14 ± 0.01	1.24 ± 0.07	1.30 ± 0.09	-	0.016	-	0.016	-
MT-CO2	1.11 ± 0.05	1.20 ± 0.06	1.00 ± 0.03	1.11 ± 0.02	1.21 ± 0.08	1.29 ± 0.11	-	0.010	-	0.037	-
COX6C [a]	0.99 ± 0.01	1.01 ± 0.01	1.00 ± 0.01	0.99 ± 0.01	0.98 ± 0.01	1.03 ± 0.01	-	-	0.050-	-	0.050
ATP5A1	1.07 ± 0.03	1.17 ± 0.05	1.00 ± 0.02	1.10 ± 0.02	1.14 ± 0.04	1.24 ± 0.09	-	0.025	-	0.006	-
ATP5A	1.11 ± 0.05	1.21 ± 0.05	1.00 ± 0.03	1.13 ± 0.02	1.22 ± 0.06	1.30 ± 0.09	-	0.016	-	0.010	-
Cyt c	1.08 ± 0.04	1.20 ± 0.04	1.00 ± 0.02	1.13 ± 0.02	1.16 ± 0.04	1.27 ± 0.08	0.018	0.004	-	0.004	-
VDAC	1.08 ± 0.03	1.19 ± 0.05	1.00 ± 0.02	1.10 ± 0.02	1.16 ± 0.04	1.28 ± 0.09	0.043	0.006	-	0.004	-
Cyc D	1.07 ± 0.03	1.17 ± 0.04	1.00 ± 0.02	1.11 ± 0.02	1.13 ± 0.03	1.23 ± 0.07	0.050	0.010	-	0.010	-
CS [b]	0.90 ± 0.04	0.79 ± 0.04	1.00 ± 0.07	0.85 ± 0.03	0.83 ± 0.04	0.73 ± 0.06	-	-	-	-	-
CAT [a]	1.02 ± 0.01	1.05 ± 0.01	1.00 ± 0.01	1.07 ± 0.01	1.04 ± 0.05	1.03 ± 0.06	-	0.050	-	0.050	0.050
Fis1 [a]	0.89 ± 0.08	1.33 ± 0.16	1.00 ± 0.11	1.61 ± 0.15	0.78 ± 0.11	1.05 ± 0.19	0.019	0.037	0.050	-	0.050

Data were presented as arbitrary units and represent densitometry analysis of membranes immunoblot detection after image acquisition. Data are means ± SEM; n=6 (when separated by gender) or n=12 (genders combined) animals/group. Comparison between groups was performed using a non-parametric Mann-Whitney test. P-value less than 0.05 was considered significant

[a] for these proteins, the sample size is different from the one previously indicated, it is n=3 (when separated by gender) or n=6 (genders combined) animals/group

[b] for the CS protein, the sample size is different from the one previously indicated, it is n=4 (when separated by gender) or n=8 (genders combined) animals/group

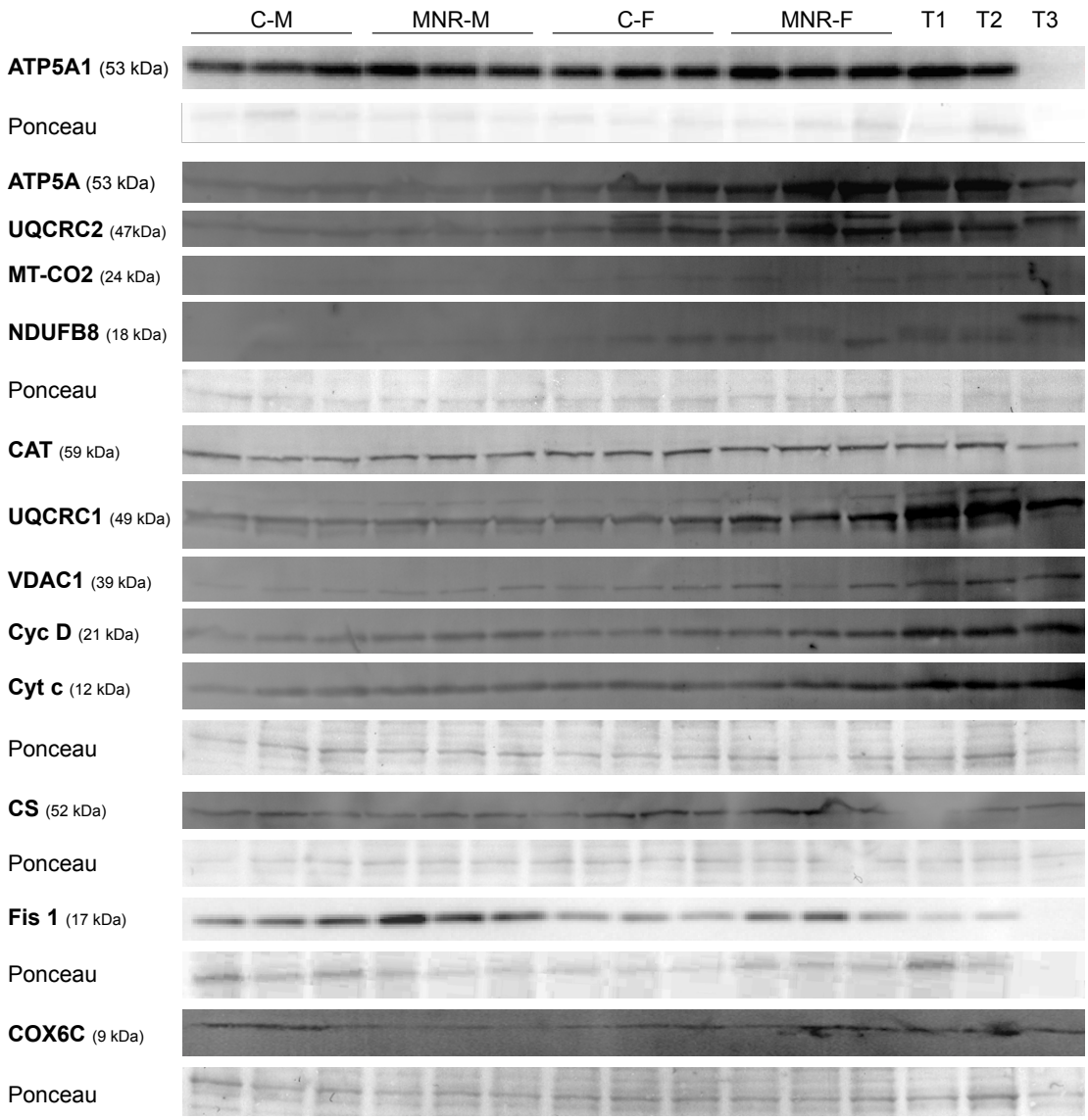

Figure 5.6 Representative protein immunoblot detection on fetal cardiac left ventricle tissue from control (C) and maternal nutrient reduction (MNR) groups.
Protein contents were determined in fetal cardiac tissue of control *ad libitum*-fed pregnancies and in the presence of MNR, characterized as 70% of the food consumed by control mothers on a weight-adjusted basis of baboons at 0.9 gestation. C-M, male fetuses from control group; C-F, female fetuses from control group; MNR-M, male fetuses from MNR group; MNR-F, female fetuses from MNR group; T1, left ventricle cardiac sample from an adult male baboon; T2, left ventricle cardiac sample from an adult female baboon; T3, cardiac human sample, not used in all membranes. Ponceau staining for the respective membrane was used for normalization and as a loading control since common protein used for that objective may be altered by the nutritional manipulations.

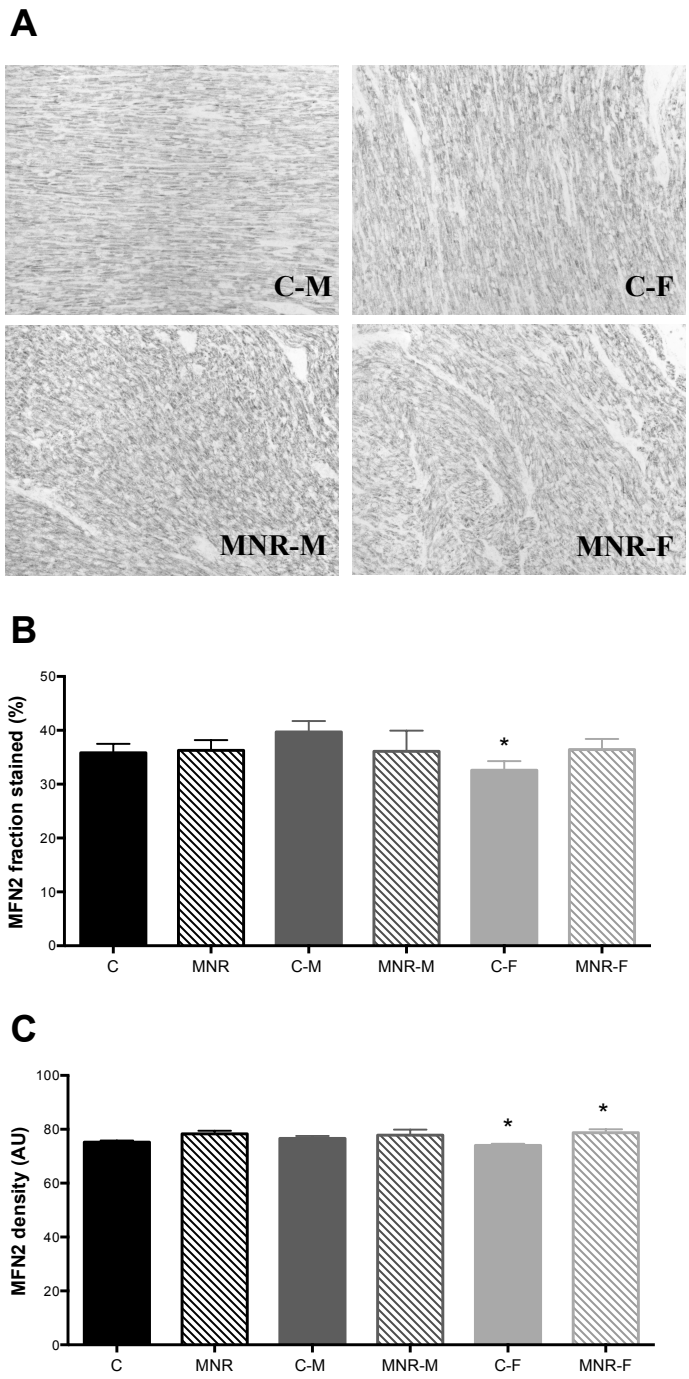

Figure 5.7 Quantitative immunohistochemistry of mitochondrial protein MFN2 in cardiac left ventricle tissue of fetal baboon.

The fetuses analyzed were from mothers that were fed *ad libitum* (control group) or fed with 70% of the control diet (MNR group). A: representative micrographs (magnification: x20) from cardiac sections of C-M, male fetuses from control group; C-F, female fetuses from control group; MNR-M, male fetuses from MNR group; MNR-F, female fetuses from MNR group. Immunoreactivity was expressed as fraction stained (in %; B) and density [C; in arbitrary units (AU)]. Data are expressed as mean and SEM; n=5 (when separated by gender) or n=10 (genders combined) animals/group. Comparison between groups was performed using a non-parametric Mann-Whitney test. P-value less than 0.05 was considered significant. *P<0.05 vs. respective controls.

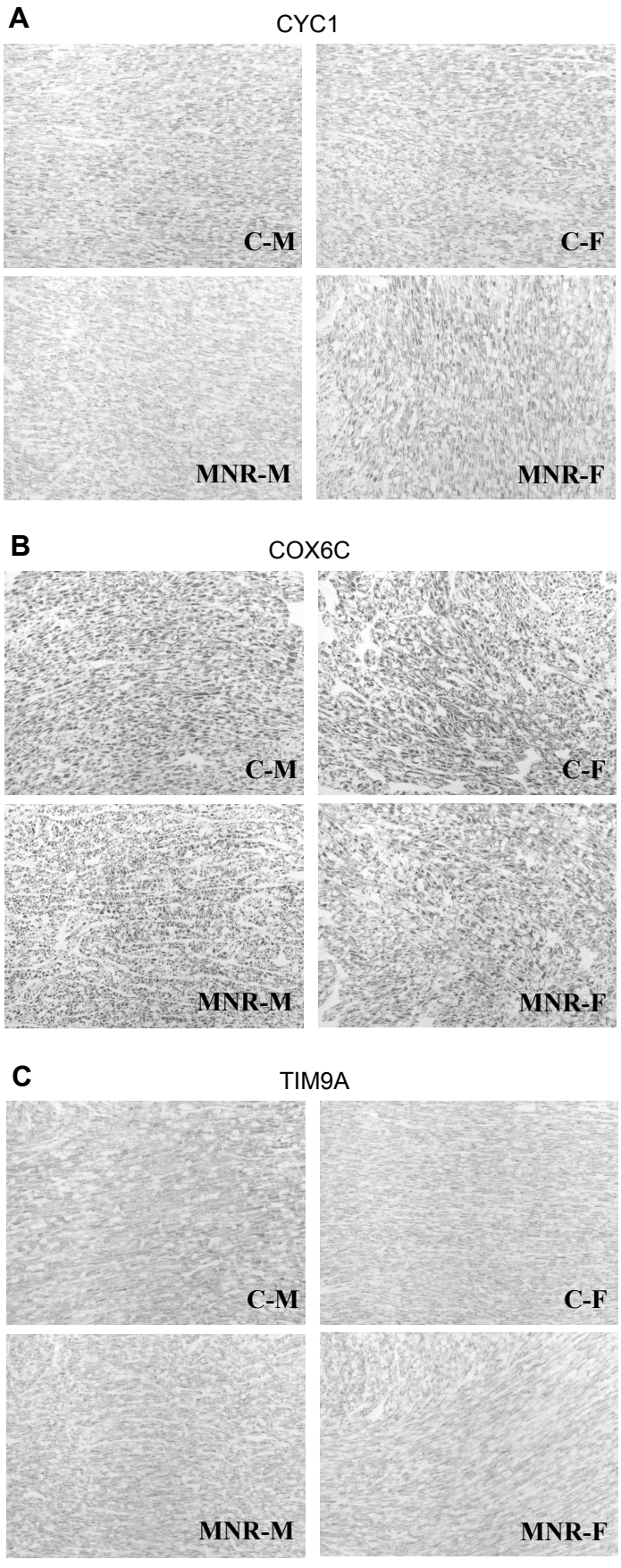

Figure 5.8. Representative immunohistochemistry of mitochondrial subunit CYC1, COX6C and TIMM9A.
The mitochondrial subunits CYC1 (A), COX6C (B) and TIMM9A (B) were analyzed in cardiac left ventricle tissue of fetal baboon from mothers that were fed *ad libitum* (control group) or fed with 70% of the control (MNR group). C-M, male fetuses from control group; C-F, female fetuses from control group; MNR-M, male fetuses from MNR group; MNR-F, female fetuses from MNR group. Micrographs (magnification: x20).

5.2.7 MNR impaired the activity of cardiac mitochondrial proteins in the offspring

The next step was the evaluation of the activity of selected enzymes involved in mitochondrial metabolic pathways (Table 5.6). We started by measuring the activity of citrate synthase (CS), a mitochondrial matrix enzyme, commonly used as a mitochondrial marker and as a normalization factor for mitochondrial mass between experimental groups. MNR decreased the activity of citrate synthase; the value of the control group was almost 1.8-fold higher than the MNR group (1798.74 ± 145.87 nmol/min/mg protein vs. 1011.39 ± 189.87 nmol/min/mg protein), for female fetuses the maternal reduced diet had a larger effect, reaching a 2-fold difference between C-F and MNR-F (1526.98 ± 187.18 nmol/min/mg protein vs. 741.41 ± 97.94 nmol/min/mg protein). Citrate synthase activity also varied among genders in the control group. Considering that the decrease in citrate synthase activity may reflect inherent mitochondrial dysfunction caused by maternal nutrient reduction, we decided to express the activities of mitochondrial respiratory chain complexes before and after normalization with citrate synthase.

The activity of mitochondrial respiratory chain complex was also measured for the same samples. Mitochondrial complex I, complex II/III and complex IV activities were significantly decreased in the MNR group, with complex II/III being the most severely affected by the reduced maternal diet, presenting a decrease of 80% in its activity. By analyzing the MNR effects for the male fetuses, we found that complex I and complex II/III activities were significantly decreased, with complex II/III activity reaching a 4.5-fold decline. Conversely, complex IV activity was 3.5-fold increased for the same group. We found a similar pattern in female fetuses, with MNR inducing a 6.4-fold decrease in the activity of complex II/III and a 10.4-fold increase in complex IV activity. Once again, a gender dimorphism was already present in control groups, with female fetuses presenting a higher activity for complex III and a decreased activity for complex II/III when compared with the male fetuses. The MNR completely abolished these gender-related differences between fetuses.

After the normalization with citrate synthase activity, we were still able to detect an effect of maternal diet in fetal mitochondrial respiratory chain activities, leading to a significant decrease in complex II/III activity and an increase in complex IV activity. However, only complex III activity remained distinct between genders in the control

group (C-M vs. C-F).

5.2.8 MNR caused a decline in fetal cardiac tissue energy state as determined by adenine nucleotides content

We further determined possible differences in adenine nucleotide levels in control and MNR fetuses (Table 5.7). Although no significant differences were observed in mitochondrial ADP and AMP levels, a decrease of 73% in ATP levels occurred in MNR fetuses when compared to controls. Moreover, this result was mostly due to the effect of MNR in male fetus. Diet-induced reduction of adenylate energy charge (AEC) was also observed for male fetuses. Once again, gender dimorphism was noted in control groups, with males exhibiting 5.2-fold higher ATP content and an increase of 2.2-fold in adenylate energy charge.

5.2.9 MNR increased lipid peroxidation in the fetal cardiac tissue

We next evaluated antioxidant and oxidant balance in the cardiac left ventricle from fetuses. Oxidative stress was evaluated based on oxidative lesion of lipids caused by ROS production (MDA content) and by measuring antioxidant enzymes and molecules, including activity of glutathione peroxidase (Gl-Px), glutathione reductase (Gl-Red) and the quantification of reduced and oxidized glutathione (GSH and GSSG) and vitamin E (Table 5.8).

MNR animals presented an increase of 40% in MDA levels, a biomarker of lipid damage by oxidative stress, indicating an oxidative environment in the cardiac left ventricle tissue. Likewise, this result was mostly due to the effect of MNR in male fetuses, since MDA was 60% increased in MNR-M. Another dissimilarity detected regarded the effect in the levels of GSH between fetuses of the MNR group, with the MNR-F group exhibiting 2.4-fold more GSH than MNR-M. Nevertheless, when comparing the GSH values for the controls, it appears that MNR induced a decrease in that antioxidant compound in males and an increase in female fetuses. Still, the variations did not reach significance when considering the diet effect.

Table 5.6 Effects of maternal diet on enzymatic activity of mitochondrial respiratory chain complex and citrate synthase at 0.9 gestation in control *ad libitum*-fed pregnancies and in the presence of maternal nutrient reduction (MNR), considered as a 70% reduction of the food eaten by the control mothers on a weight-adjusted basis.

	Genders combined		Male		Female		P-value by Mann-Whitney test				
	Control	MNR	Control	MNR	Control	MNR	Diet	Male C vsMNR	Female C vsMNR	Control M vs F	MNR M vs F
Number of animals/group	10	10	5	5	5	5					
Citrate Synthase (nmol/min/mg)	1798.74 ± 145.87	1011.39 ± 189.87	2070.50 ± 154.22	1281.36 ± 340.87	1526.98 ± 187.18	741.41 ± 97.94	0.008	-	0.016	0.047	-
Complex I (nmol/min/mg)	1813.93 ± 83.92	1339.23 ± 131.09	1955.08 ± 124.61	1441.08 ± 142.63	1672.77 ± 78.76	1237.38 ± 227.59	0.013	0.028	-	-	-
Complex II / III (nmol/min/mg)	838.66 ± 142.71	170.51 ± 65.99	1156.56 ± 78.51	259.86 ± 123.21	520.76 ± 186.98	81.16 ± 20.69	0.001	0.009	0.009	0.047	-
Complex III (nmol/min/mg)	1264.97 ± 153.20	1111.03 ± 278.06	929.00 ± 108.00	833.76 ± 291.07	1600.94 ± 193.68	1388.29 ± 474.09	-	-	-	0.028	-
Complex IV (nmol/min/mg)	153.84 ± 55.10	844.60 ± 51.13	218.19 ± 89.63	760.85 ± 68.68	89.49 ± 59.64	928.35 ± 59.50	<0.001	0.016	0.009	-	-
ComplEx I / Citrate Synthase	1.09 ± 0.14	1.58 ± 0.22	0.979 ± 0.11	1.44 ± 0.37	1.22 ± 0.25	1.71± 0.26	-	-	-	-	-
(Complex II / III) / Citrate Synthase	0.47 ± 0.07	0.19 ± 0.06	0.58 ± 0.08	0.24 ± 0.11	0.35 ± 0.11	0.14 ± 0.04	0.013	-	-	-	-
Compex III / Citrate Synthase	0.82 ± 0.19	1.66 ± 0.53	0.45 ± 0.04	0.99 ± 0.39	1.18 ± 0.32	2.34 ± 0.94	-	-	-	0.009	-
Complex IV / Citrate Synthase	0.085 ± 0.03	1.08 ± 0.18	0.11 ± 0.04	0.80 ± 0.24	0.063 ± 0.04	1.36 ± 0.24	<0.001	0.009	0.009	-	-

Data are means ± SEM; n=5 (when separated by gender) or =10 (genders combined) animals/group. Comparison between groups was performed using a non-parametric Mann-Whitney test. P-value less than 0.05 was considered significant.

Table 5.7 Changes in the fetal left ventricle tissue adenine nucleotides and energy charge at 0.9 gestation in control *ad libitum*-fed pregnancies and in the presence of maternal nutrient reduction (MNR), considered as a 70% reduction of the food eaten by the control mothers on a weight-adjusted basis.

	Genders combined		Male		Female		P-value by Mann-Whitney test				
	Control	MNR	Control	MNR	Control	MNR	Diet	Male C vs MNR	Female C vs MNR	Control M vs F	MNR M vs F
Number of animals/group	12	12	6	6	6	6					
ATP (nmol/mg)	3.16 ± 2.24	0.70 ± 0.05	5.10 ± 4.08	0.76 ± 0.08	0.82 ± 0.08	0.63 ± 0.05	0.028	-	-	-	-
ADP (nmol/mg)	11.24 ± 2.78	7.90 ± 0.73	13.95 ± 4.89	8.68 ± 0.76	7.99 ± 1.28	6.97 ± 1.29	-	-	-	-	-
AMP (nmol/mg)	74.82 ± 7.65	77.46 ± 6.76	69.48 ± 12.82	84.31 ± 8.08	81.23 ± 7.54	69.24 ± 11.07	-	-	-	-	-
TAN (nmol/mg)	89.22 ± 8.10	86.06 ± 7.04	88.53 ± 13.89	93.75 ± 7.45	90.04 ± 8.42	76.84 ± 12.26	-	-	-	-	-
AEC	0.09 ± 0.03	0.06± 0.006	0.13 ± 0.06	0.05 ± 0.01	0.05 ± 0.005	0.06 ± 0.002	-	0.05	-	0.033	-

Abbreviations: ATP - adenosine triphosphate; ADP - adenosine diphosphate; AMP - adenosine diphosphate; TAN - total adenine nucleotide pool; adenylate energy charge

Data are means ± SEM; n=6 (when separated by gender) or =12 (genders combined) animals/group. Comparison between groups was performed using a non-parametric Mann-Whitney test. P-value less than 0.05 was considered significant.

Table 5.8 Effects of maternal diet on indicators of antioxidant capacity and oxidative stress in fetal cardiac left ventricle from control *ad libitum*-fed pregnancies and in the presence of maternal nutrient reduction (MNR), based on a 70% reduction of the food eaten by the control mothers on a weight-adjusted basis at 0.9 gestation.

	Genders combined		Male		Female		P-value by Mann-Whitney test				
	Control	MNR	Control	MNR	Control	MNR	Diet	Male C vs MNR	Female C vs MNR	Control M vs F	MNR M vs F
Number of animals/group	10	10	5	5	5	5					
GSH (μM)	11.87 ± 2.50	13.36 ± 3.21	9.96 ± 1.90	7.90 ± 1.97	13.78 ± 4.76	18.82 ± 5.24	-	-	-	-	0.047
GSSG (μM)	4.44 ± 1.50	3.06 ± 0.91	3.44 ± 1.48	1.60 ± 0.46	5.43 ± 2.74	4.52 ± 1.57	-	-	-	-	-
GSH/GSSG	2.88 ± 0.55	6.96 ± 1.68	3.37 ± 0.84	5.98 ± 1.33	2.40 ± 0.74	7.94 ± 3.22	0.021				
Gl-Px (U/l)	28.54 ± 2.54	23.14 ± 1.48	26.67 ± 3.05	23.42 ± 1.80	30.40 ± 4.24	22.87 ± 2.55	-	-	-	-	-
Gl-Red (U/l)	78.59 ± 7.20	83.48 ± 5.12	79.18 ± 5.56	87.04 ± 6.27	77.99 ± 14.23	79.93 ± 8.50	-	-	-	-	-
Vit E (μM)	80.40 ± 12.38	49.87 ± 2.56	109.38 ± 16.32	54.98 ± 1.06	51.43 ± 1.74	44.76 ± 3.91	-	-	-	-	-
MDA (μM)	1.07 ± 0.11	1.51 ± 0.21	0.90 ± 0.12	1.43 ± 0.13	1.24 ± 0.16	1.59 ± 0.43	0.041	0.028	-	-	-

Data are means ± SEM; n=5 (when separated by gender) or =10 (genders combined) animals/group. Comparison between groups was performed using a non-parametric Mann-Whitney test. P-value less than 0.05 was considered significant.

5.2.10 MNR altered mitochondrial morphology of cardiac left ventricle

Finally we used transmission electron microscopy to analyze the mitochondrial morphology and their overall organization within the left ventricle tissue (Figure 5.9 and Figure 5.10).

MNR resulted in drastically altered mitochondrial ultrastructure. (Figure 5.9). The ultrastructural variations in mitochondrial architecture occur mainly due to the differences in cristae amount and shape, which derived from the infolded inner mitochondrial membrane, in which protein complexes of oxidative phosphorylation and intermediate metabolism are embedded. Abundant cristae are found in mitochondria from control hearts, whereas MNR left ventricle samples displayed mitochondria with sparse cristae, disarrangement and distortion of cristae, partial or total cristolysis and electron-lucent matrix. MNR also appeared to induce an increase in mitochondria number, although this was not quantified.

Diet-induced mitochondrial morphological alterations were more prominent in the MNR male fetuses, presenting defective mitochondria with few cristae and some resembling onion-like structure, characterized by multi-layered inner membranes suggesting concentric spherical rings (the arrow in Figure 5.9 indicates a mitochondrion with multiple concentric sheets of the inner membrane). Although more images must be analyzed, it appears that multiple double-membrane structures exist in the two MNR groups. Though no evidence exists at this point, one may wonder if at least some of these structures represent autophagic vacuoles.

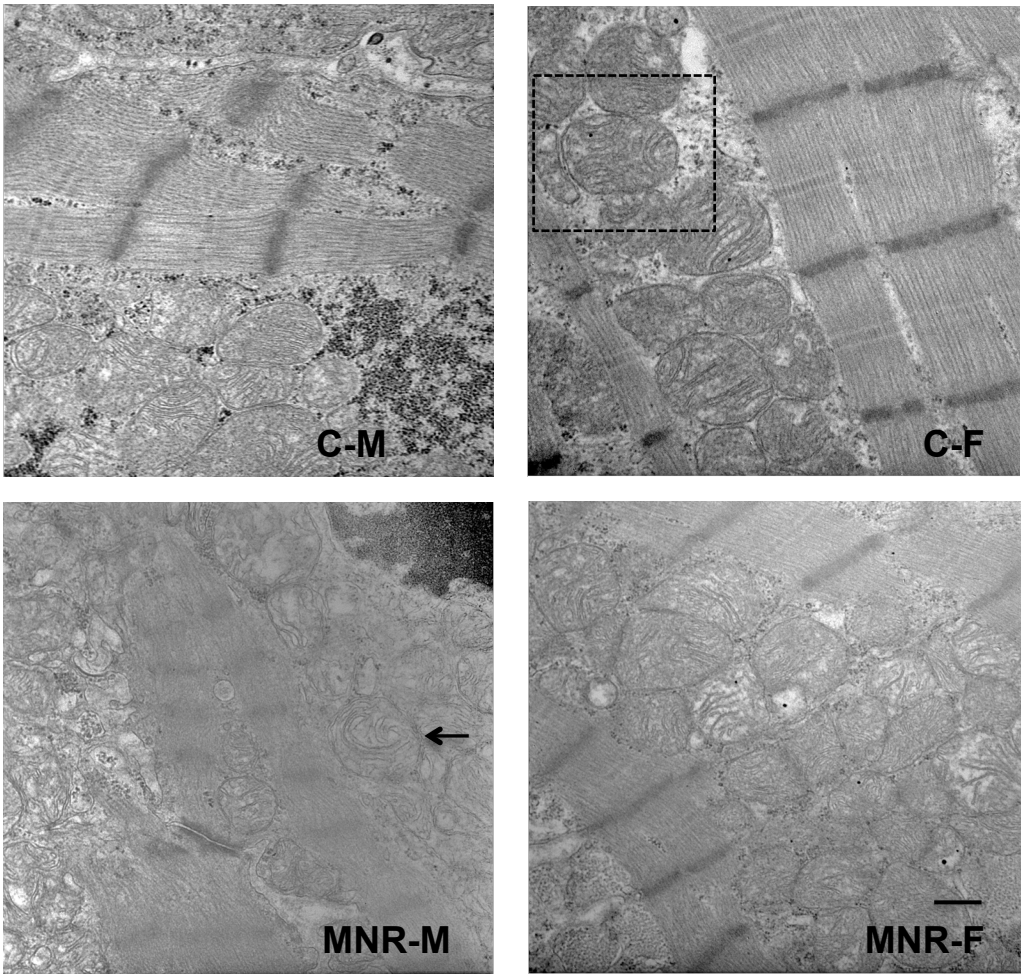

Figure 5.9 Representative transmission electron microscopy of cardiac left ventricle tissue of fetal baboon from mothers that were fed *ad libitum* (control group) or 70% of the control (MNR group).

C-M, male fetuses from control group; C-F, female fetuses from control group; MNR-M, male fetuses from MNR group; MNR-F, female fetuses from MNR group. Arrow indicates one mitochondrion with multiple concentric sheets of the inner membrane. Method of staining: uranyl acetate/lead citrate. Micrographs were taken with a magnification of 3,300x. Scale bar = 500 nm.

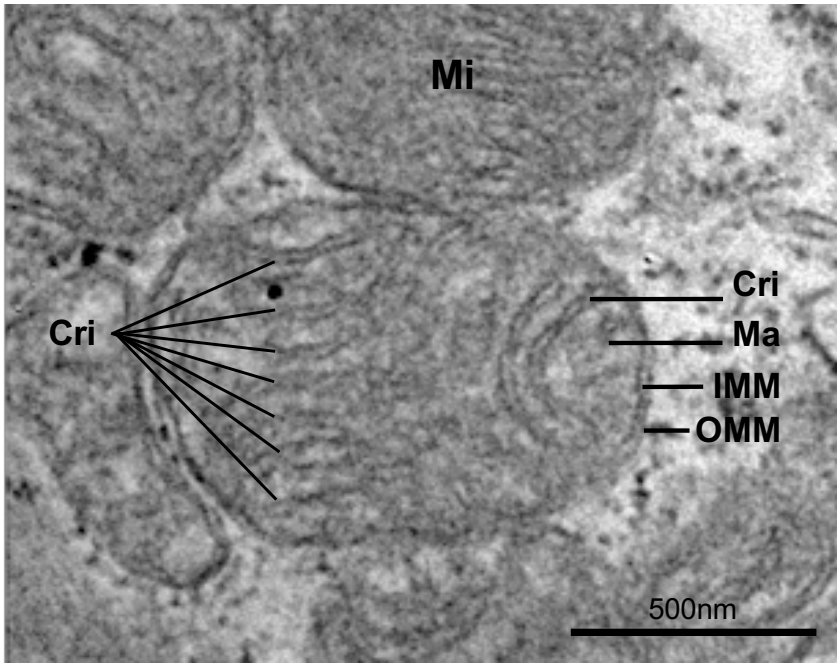

Figure 5.10. Magnification of the image shown in Figure 5.9 of a control female for detailed mitochondrial morphology.
Mitochondria are delimited by double membranes, enclosing the matrix (Ma), section that contains the mitochondrial DNA. The topology of the inner mitochondrial membrane (IMM) is dynamically controlled, allowing a vast variation in the morphology of the cristae (Cri). The outer mitochondrial membrane (OMM) is more uniform and establishes the organelle border. OMM, outer mitochondrial membrane; IMM, inner mitochondrial membrane; Ma, matrix; Cri, cristae; Mi, mitochondrion. Method of staining: uranyl acetate/lead citrate. Micrographs were taken with a magnification of 3,300x. Scale bar = 500 nm.

5.3 Discussion

5.3.1 Morphological and biochemical implications of MNR

During pregnancy, maternal metabolism undergoes a series of adaptations to sustain the needs of the developing fetus and placenta [300]. The present study demonstrates that MNR until 0.9 gestation altered multiple physiological outcomes in the fetal baboons cardiac left ventricle. Maternal weight gain was decreased in MNR mothers, as well the placental weight, being the effects more severe in MNR mothers carrying a male fetuses. MNR reduced the fetal weight, femur length and chest circumference of the MNR offspring. However, fetal heart weight or heart weight-to-body weight ratio were similar between the groups. Only brain weight-to-body weight ratio was increased in the MNR fetuses, which can be an indicator of the redistribution of fetal blood flow to favor the brain in response to reduced supply of nutrients. As a consequence, brain growth was maintained while other viscera atrophied. For humans, it is widely accepted that the determination of brain-to-liver weight ratio is a marker of nutritional growth restriction, with a normal value of 2.8:1, and values higher than 4 indicating asymmetrical intrauterine growth restriction [301,302]. Applying this calculation to our baboon model, we obtained a ratio of 3.31 in the control group and the value of 4.18 for the MNR group was obtained, suggesting fetal IUGR occurred in the MNR group; however, this indicator is not commonly used in NHP. We should also consider the epidemiologic evidence found by Barker in a birth cohort of more than 12,000 people in Finland, where those that later in life developed heart failure had small placentas, indicating that placental insufficiency may predispose the fetus for heart diseases later in life [303].

Adjustment of protein metabolism is also a vital component of maternal adaptation to pregnancy, since amino acids are substrates for protein synthesis, tissue formation and other biologically important molecules [304]. Typically, human maternal amino acid concentrations are diminished during pregnancy [305]. In accordance with what happens in human pregnancies, previous data published for our model also reported a decrease in circulating concentrations of several amino acids at 0.5 gestation compared with pre-pregnancy [306]. In human pregnancies, differences in maternal amino acid concentrations in pathologic conditions, such as spontaneous abortion [307], diabetes [308], or IUGR [309] have been reported. In a seminal work from Cetin and

collaborators, IUGR in human pregnancies was associated with increased maternal plasma amino acid concentrations for alanine, arginine, histidine, isoleucine, leucine, lysine, phenylalanine, tyrosine, and valine, comparing with normal pregnant women of the same gestational age [305]. In agreement with the reported elevation in the concentration of most essential amino acids in maternal plasma in women with IUGR [305] our MNR model evidenced similar effects, with a marked increase of arginine, histidine, isoleucine, lysine, and valine in maternal plasma from MNR group. In our model, asparagine and serine were also significantly increased in the MNR group, tyrosine was also 2.2-fold higher in the MNR group but did not reach the statistical significance. The only exception was phenylalanine that was decreased in the maternal plasma from the MNR group. It was surprising how well the maternal amino acid plasma profile of our model correlated with amino acids in maternal plasma in women with IUGR. The increased plasma concentrations of these amino acids can be a result from increased protein breakdown, such as a mobilization of maternal protein reserve normally from skeletal muscle, or reduced hepatic catabolism.

However, we should take in consideration that placental metabolism may be also impaired, resulting in a deficient amino acid transport to fetuses. Amino acids were actively transported by the placenta resulting in a fetal concentration of amino acids almost 2-fold higher than in maternal plasma, being this feto-maternal gradient in accordance with what has been described for human fetuses [309]. Despite all the maternal alterations, only two fetal amino acids were affected by MNR: arginine that was increased in MNR fetuses and glutamine that was decreased in the same group. Glutamine is the most abundant amino acid in the human body, being mainly produced in the muscles. Several important metabolic products are derived from glutamine, for example it is involved in the biosynthesis of DNA and RNA and the antioxidant glutathione contains glutamate (derived from glutamine). Glutamine is also involved in the regulation of the immune system and gut function, as well as in the removal of excess ammonia, keeping in this way the acid-base balance. Glutamine entrance into the citric acid cycle via alpha-ketoglutarate can be an important pathway for energy production. Considering the numerous metabolic processes where glutamine is a part of, it is not surprising that this imbalance can have adverse effects in numerous organ systems [310,311].

Glucose is a major energy substrate and essential for fetal metabolism and growth.

Glucose metabolism is regulated by a relatively complex set of mechanisms that tend to keep its concentration relatively constant [312–314]. Maternal glucose concentration can be maintained by enhancing rates of maternal glucose production or acquisition of glucose intolerance and insulin resistance until a certain level. Maternal glucose is transferred to the fetus through the placenta. Placental glucose uptake and transport are dependent on maternal glucose concentration, uterine blood flow and placental glucose utilization [312,313]. In our study, glucose level in control mothers fed *ad libitum* was almost 2-fold higher than that of their fetuses at 0.9 gestation. However, no difference was observed in glucose levels between control mothers fed *ad libitum* and MNR mothers when genders were combined. Only for mothers carrying male fetuses, MNR caused an increase in circulating glucose. However, the levels of glucose in their offspring remained unaltered. We need to take into consideration the fetal production of insulin by the emergent pancreas, which can contribute to an increase in glucose utilization in the insulin-sensitive developing tissues such as heart, skeletal muscle, liver and adipose tissue [253,312,315,316]. However, MNR-M fetuses exhibited a reduction in the insulin levels in plasma. In accordance with these findings, it was previously described that MNR decreased the size, number, and insulin staining density of pancreatic islets in this model [251]. On the other hand, no measurable effects of maternal nutrition on insulin maternal plasma were detected. Nonetheless, an association between increased insulin levels and MNR female fetuses for maternal and fetal blood plasmas was found. Ultimately, we should take in consideration that glucose uptake by fetal tissues is controlled by glucose transporters, whose expression can be influenced by changes in fetal glucose concentration and intrauterine conditions [312,317,318]. Another important aspect is that without the anabolic effect of insulin, no amount of substrate will induce optimal growth [319]. Despite the limited fetal effects of MNR at 0.9 gestation, a seminal validation of this model was described by Choi and collaborators when a manifestation of insulin resistance in juvenile baboon offspring of MNR mothers was found associated with an overall phenotype that would later influence type 2 diabetes. Juvenile offspring showed an increased fasting glucose and fasting insulin as well beta cells responsiveness accompanied by decreased peripheral glucose disposal [253].

Fetal cortisol production is very low in early gestation, but it rises markedly shortly before birth [320]. Pregnant women also exhibit increasing plasma cortisol near term [321].

Cortisol promotes the maturation of fetal organ systems, including the lungs, heart, liver, thyroid, and gut, needed for extrauterine life [320,322]. In the current study, circulating cortisol concentrations in control mothers fed *ad libitum* were about 2-fold higher than in their offspring at 0.9 gestation. Proportional increases in cortisol were observed in both maternal and fetal plasma in MNR baboons, thereby maintaining a similar maternal-to-fetal circulating cortisol gradient in control and MNR pregnancies. However, MNR significantly increased the maternal circulation cortisol levels, in special for the MNR mothers carrying male fetuses. Excess cortisol levels had been previously associated with metabolic syndrome [255], so increased maternal cortisol can predispose MNR fetuses to the development of hyperglycemia, insulin resistance and obesity later in life.

5.3.2 Mitochondrial DNA was increased in MNR fetuses

The present study was focused into the cardiac left ventricle because it is the thickest heart chamber being responsible in the adult life for pumping oxygenated blood to tissues all over the body. By contrast, the right ventricle solely pumps blood to the lungs. This choice was also done because the cardiac left ventricle exhibited a relatively high rate of oxygen consumption (approximately twice that of the right ventricle). Moreover, left ventricle hypertrophy and increased ventricular wall thickness are generally agreed to be powerful and independent risk factors for coronary heart disease, stroke and sudden death, and ultimately because the cardiac left ventricle has been most frequently studied in clinical and animals models [323]. On the other hand, analysis of fetal human hearts of third gestational trimester did not show a significant difference between any of the stereological parameters of the human fetal myocardial structures evaluated comparing right and left ventricular myocardium [324]. Nevertheless, for a non-human model, the fetal sheep, Smolich and collaborators described morphological differences for cardiac left and right ventricles for late-gestation fetuses, with the right ventricle exhibiting larger myocytes. However, after birth a dominance of the left ventricle emerges and that dissimilarity disappeared after the first postnatal week. Eight weeks after birth, morphometrics changed and left ventricle myocardium presented larger myocytes and a lower myocytes-to-capillary ratio [325]. So, we believe that the effects of the MNR programming would be exacerbated with the passage from an anaerobic life, such as

in utero, to an aerobic metabolism after birth, in which ATP synthesis through TCA in mitochondria becomes predominant. By using cardiac left ventricle, that has been described to be affected in cardiovascular diseases in adults, we potentiated our chances of identifying MNR-related developing program on fetus for later emergence of cardiac diseases. We will namely test the possibility of this phenotype being imprinted by mitochondrial adaptations already present in the fetus. It is relevant to use a more active tissue, since organs with higher metabolic demands are more likely to have manifestations of mitochondrial dysfunction by exacerbating the mitochondrial defects.

Mitochondria are implicated in numerous critical functions for the fetal heart development, such as ATP production, reduction of oxidative stress, calcium homeostasis, control of cell apoptosis and production of hormones [225,326]. The first mitochondrial indicator that we measured was the mtDNA content. We used a quantitative PCR-based assay to accurately determine total mtDNA copy number relative to the diploid chromosomal DNA content in a series of fetal cardiac left ventricle samples. Since a limited number of publications on baboon mtDNA is available [327–329], prior to selecting any region of the mtDNA to act as a reliable marker of mtDNA copy number, we designed several sets of primers for four short regions (*CYTB*, *D-loop*, *ND1* and *ND6*) for mtDNA and three region of the nDNA (*B2M*, *HBB* and *RNA16S*) and amplified them by PCR for seven left ventricle cardiac DNA extracts, randomly selected to include at least one animal for each group. The sample with higher DNA yield was used to create a serial dilution of 10x to determine the efficiency of amplification. Taking in consideration the reaction efficiency, we selected two sets of primers for mtDNA-encoded genes that have better performance and Cts values in the expected range, taking into account the experience of mtDNA analysis for other species and human cells. From these, *ND1* and *ND6* seemed to be the better indicators. It should be noted that the selected genes *ND1* and *ND6* are encoded each one by a different chain of mtDNA (heavy and light strand respectively). From the nuclear genes, we selected *B2M*, widely used as a reference for nuclear gene of mtDNA copy number in other species. Standards were prepared for absolute quantification of mtDNA and nDNA copies, the results show that *B2M* is approximately half of the copies of *HBB*, suggesting that *HBB* has more than one allele or the primers are amplifying more than one genomic product. A blast analysis, comparing the sequence of the *HBB* primers with the *Papio* spp.

genome data base, showed that these primers originated two genomic products, although it appears as only amplifying a product in the cDNA database for the genus *Papio* spp., which was used when designing primers. So, for mtDNA estimation per nuclei, we selected *B2M* as nuclear reference, since the used primers only amplified a gene product, as confirmed by analysis of the *Papio* spp. genome data base. *B2M* is an example of a single copy gene of known sequence that conveniently acts as a marker of diploid content (2N).

On average, each cell contains thousands of mtDNA molecules [330–332]. Using *ND1* as mtDNA reference and *B2M* as nDNA reference, we determined 714 ± 58 mtDNA copies per nuclei in the fetal control cardiac left ventricle and a significant increase in the MNR group 1070 ± 122 mtDNA/nDNA. This increase was mainly due to the effect of MNR in the mothers carrying a female fetuses.

The results obtained are in the same range as those previously published, namely a mean of 1811 ± 546 mtDNA copy number per diploid nuclear genome for human muscle tissues from 16 healthy humans aged 2-45 years [333]. In a study from Miller and collaborators [332] the human myocardium was found to contain approximately twice the number of mtDNA genomes per diploid nucleus as detected for skeletal muscle. mtDNA copy number in the human skeletal muscle age 1 h to 95 years was 3650 ± 620 mtDNA of copies/nDNA and was 6970 ± 920 mtDNA copies per diploid nuclear genome in the cardiac muscle, namely the right atrial myocardium aged 3 weeks to 80 years. However, we should take in consideration that these authors performed a correction, indicating that "the relative copy number of mtDNA genome per diploid nuclear genome in a given tissue extract was readily computed by taking twice the ratio of the mtDNA and beta-globin plasmid equivalent values" [332]. This means that for a direct comparison we should multiply our values by two. When performing absolute quantifications and comparisons we should take in consideration the fact that neonatal human myocardium (0 - 1 year old) exhibited around 68% mononucleated cardiomyocytes that remain unchanged throughout life [120]. In conclusion, humans do not display the transition to predominantly binucleated cardiomyocytes which is known to occur in murine models after birth [334,335]. Another aspect to take into consideration is ploidy. Mollova and collaborators found that at the age of 0–1 year, 16.3 ± 5.2% of mononucleated human cardiomyocytes were hyperploid (>2N), which increased to 39.5 ± 5.2% between 10 to 20 years old and intensified to 54.2 ± 5.8% above 40 years old [120].

These results illustrated that human cardiomyocytes undergo significant changes in their nuclear ploidy after birth presenting cardiomyocytes with a total nuclear DNA content higher than 2N. Because the number of nucleus and ploidy can significantly affect the number of copies for the same nuclear gene, we decided not to correct our values of nDNA since none of the referred characterizations were performed for the baboon heart. However, we consider important to alert to these differences between species and warrant caution when comparing absolute values of cardiac mtDNA between species and different developmental stages. Nevertheless, it is still valid to perform a comparative analysis between the MNR group and control to assess the effect of MNR in our study, although not performing the corrections that are sometimes made in humans. Still, since we would like to validate the baboon as a good model for studying human diseases, it would be beneficial to further investigate the necessary corrections for multi-nucleated cells.

The work form Mollova and collaborators altered the general paradigm that human heart grows exclusively by enlargement of cardiomyocytes. Using healthy hearts from humans 0-59 years old they found that between the first 20 years of life the number of cardiomyocytes increased 3.4-fold in the left ventricle, proving that cardiomyocytes proliferation contributes to developmental of heart growth in young humans [120].

5.3.3 MNR impaired the activity of mitochondrial respiratory chain proteins and energy charge

Mitochondrial function and integrity depends on the presence and balance of different metabolic pathways. For example, the activities of respiratory chain enzymes, tricarboxylic acid cycle, and fatty acid oxidation are interconnected. Oxidative phosphorylation occurs through five multienzyme complexes: complex I, also known as NADH dehydrogenase, that oxidizes NADH produced by the tricarboxylic acid cycle; complex II, succinate dehydrogenase; complex III, ubiquinol cytochrome c oxidoreductase which oxidizes ubiquinol produced by succinate dehydrogenase or complex I, complex IV, cytochrome c oxidase and complex V, also designated as ATP synthase [23]. Mitochondrial energy production is already present in several human fetal tissues during development [336,337]. Minai and collaborators [337] described that fetal OXPHOS complexes are fully assembled and

enzymatically functional in the human heart, though with lower activity than those registered after birth.

In the present study, we showed that *in utero* undernutrition in baboons resulted in increased mtDNA content with a significant increase in several mitochondrial transcripts encoding for OXPHOS subunits, transcripts associated with the proteins translocators in the mitochondrial membranes, the TIM and TOM complexes and others related to the transport of small molecules. These transcriptional alterations were associated with an overall increase in mitochondrial proteins assessed by Western blot. All this indicators point out to an increase in mitochondrial content and an expected improvement in mitochondria function. However, the activity of mitochondrial proteins was significantly decreased in the MNR fetuses, accompanied by a decreased ATP content and an increased oxidative stress reported by an augmented MDA levels. It seems like the reduction of the activity of mitochondrial enzymes and ATP production was not due to a decrease in mitochondrial content or the expression of the respiratory chain complexes. The observed differences can be due to a decrease in their activity or post-translational modifications. These differences can also be in part due to structural changes in the mitochondria morphology.

Our finding of decreased activity of mitochondrial proteins and ATP content is consistent with the altered energetics reported in heart tissue of patients with cardiac diseases and diabetes. It has been shown that mitochondria from diabetic human heart have impaired capacity to oxidize palmitoylcarnitine [338]. Furthermore, there is a decrease in myocardial energy production in heart failure patients [339]. Therefore, our results suggest that the decreased activity of mitochondria in the heart of *in utero* undernourished offspring may contribute to the increase risk of cardiovascular and other metabolic diseases.

Studies have shown that IUGR fetuses and neonates show changes in cardiac morphology and function [340,341], which combined with our findings suggest that IUGR may be associated with cardiac metabolic adaptations *in utero* that become detrimental in later life. Interestingly, in individuals with type 2 diabetes, mitochondrial metabolism was impaired in cardiac and skeletal muscle raising the hypothesis of using less invasive approaches to determine MNR effects. The present study was limited to the left ventricle, so it remains to be determined whether impaired energetics exist in other regions of the heart.

5.3.4 MNR altered the fetal cardiac mitochondrial morphology

Mitochondrial morphology is regulated by continuous fusion and fission events that are essential for maintaining a normal mitochondrial function. Mitochondrial fusion consist in a single mitochondrion being formed from existing isolated and independent mitochondrion, while mitochondrial fission refers to the separation of a single mitochondrion into two or more daughter organelles [342].

Mitochondrial fission and fusion machinery is crucial for the division, dynamics, distribution, and morphology of this organelle [343]. The principal components of this machinery include Opa1, Mfn1 and Mnf2, responsible for mitochondrial fusion and Fis1, Mtp18, and Drp1 or DNM1L, related with mitochondrial fission. In our study, we found elevated levels of mitofusin 2 transcripts in the cardiac left ventricle of MNR fetuses, which were accompanied by increased protein detected by immunohistochemistry for the MNR female fetuses. Mitofusin 2 is located in the outer mitochondrial membrane and its primary function is to induce the fusion of this membrane. Mitofusin 2 has also been implicated as a mitochondrial assembly regulator factor [344]. Perturbation of the fission/fusion balance causes mitochondrial deformation and has been found to be associated with numerous human diseases [29,37]. Genetic deregulation of the mitochondrial fusion protein mitofusin 2 has been associated with obesity and type 2 diabetes [344], as well with vascular proliferative disorders [345].

In order to assess putative modifications in mitochondrial morphology, we used transmission electron microscopy. We found considerable alterations in the mitochondrial ultrastructure for the MNR fetuses. The ultrastructural variations in mitochondrial architecture occur mainly due to the differences in the amount and shape of cristae. Abundant cristae were found in mitochondria from control tissues, whereas MNR tissues displayed mitochondria with sparse cristae, disarrangement and distortion of cristae, partial or total cristolysis and electron-lucent matrix. Mitochondrial cristolysis has been linked to loss of the mitochondrial inner membrane potential and serious defects in the respiratory chain [346]. Since the enzymes involved in oxidative phosphorylation are located in the inner mitochondrial membrane, its surface area and number of cristae are generally

correlated with the grade of metabolic activity exhibited by a cell [347]. In reality, Gilkerson and collaborators [348], predicted that the cristal membrane of mitochondria is the principal site of oxidative phosphorylation of the bovine heart tissue, using immunolabeling and transmission electron microscopy, and abnormalities in mitochondrial morphology, reflected as disorganized cristae within the mitochondria, have been described in cardiac and skeletal muscle biopsies from left ventricular non-compaction cardiomyopathy (LVNC) patients [349]. Although an abnormal mitochondria phenotype consisted in ultrastructural alterations seen by electron microscopy, we suspect that the identified ultrastructural alterations underlie a relevant impact on mitochondrial energetics in MNR conditions. Indeed, the prevalent existence of partial or total cristolysis observed in the MNR fetuses in this study supports the idea that the capacity of fetal cardiac left ventricle to generate energy by mitochondrial OXPHOS would be critically compromised, consequently these cardiomyocytes would be destined to a low bioenergetic state, what is in conformity with the low adenine nucleotides and energy charge found in the MNR fetal tissue.

5.3.5 Mito-GENDER?

In this study, we also reported that the effects of MNR demonstrated a gender specificity with different outputs depending on the fetuses gender. For example, only MNR male fetuses displayed a decrease in insulin levels, and only mothers that were carrying a MNR male fetuses had an increase in cortisol and glucose in circulation. On the other hand, MNR induced an increase in mtDNA of MNR female fetuses that was not observed for the MNR male fetuses. However, MNR male fetuses also exhibited an increase in mitochondrial transcripts and proteins. Conversely, the energy charge of the fetal cardiac left ventricle for the MNR male fetuses was significantly depleted, and remains unaffected by MNR for the female fetuses. It is also relevant to mention that the MNR male fetuses registered a 59% increase in MDA levels. Taking together, all the information seems to indicate that MNR male fetuses were more severely affected by the manipulation of maternal diet. These findings were in accordance with the numerous studies documenting gender differences, namely for the incidence and severity of cardiovascular diseases such as heart failure, cardiac hypertrophy, sudden cardiac death and coronary artery disease

[261]. These differences can be in part associated to mitochondrial mechanism underlying these dissimilarities. Mitochondria provides more than 90% of the energy essential for cardiac tissue to perform physiological and biochemical functions, so if mitochondria were affected, the capacity for energy production would be compromised, as we found for the MNR male fetuses. By other side, mitochondria are also a major site for generation of oxygen free radicals, which perform a central role in the pathogenesis of cardiovascular diseases [299], and MNR male fetuses already exhibited higher levels of MDA. Additionally, women show delayed progress of atherosclerosis, lower occurrence of heart failure [350–352], and acquire heart disease later in life than men [353,354]. It is believed that steroid sex hormones perform a substantial role in sexual dimorphism in cardiovascular diseases [355,356]. Also, intrinsic dissimilarities in cardiac morphology and function observed in healthy humans and animal model systems have been advanced as plausible risk factors for sex-associated vulnerability to cardiovascular diseases [357]. In females, hearts are smaller than males [358]. However, for our model at the 0.9 gestation we did not find that difference. Also, hearts from females show greater contractility [357], and better calcium handling [359], functions for which the mitochondria plays an important role. Although there are many studies describing sex-related cardiovascular risk, the molecular basis underlying the differences in the development of cardiovascular diseases between the genders is not yet well-defined and we would like to point out mitochondria as a possible contributor, since mitochondria are crucial for major features of cardiomyocytes, such as, excitability, contractility and conductibility [360] and ultimately the rate and force of contraction of heart relies on ATP utilization [360].

Our data support the view that challenges in pregnancy can have differential effects in the presence of a male or female fetus, reinforcing the need to observe effects taking in consideration the fetal gender.

Our data also demonstrate that maternal nutrient reduction alters mitochondrial metabolism in the fetal heart, which can influence the cardiovascular health and disease risk in the offspring. This relevant study is unique and warrants important translational findings for cardiovascular health in humans.

Chapter 6

Conclusion

"Do you ever get the feeling like you already know the entire contents of the universe somewhere inside of your head, as if you were born with a complete map of this world already grafted onto the folds of your cerebellum and you are just spending your entire life figuring out how to access this map?"

by Reif Larsen

Final conclusions

The findings presented here demonstrate that MNR until 0.9 gestation in a nonhuman primate model had the ability to modulate the offspring mitochondrial legacy. However, the effects exhibited a tissue-specific nature in mitochondrial effects, that may reflect differences in functional adaptation after birth. The divergence in mitochondrial response between tissues to maternal nutrient manipulation early in pregnancy, further reflects these differential ontogenies.

Taken together, these findings suggest that a programmed low mitochondrial content in the nephron likely constitutes a "first hit" to the kidney, which subsequently can cause a reduction in the intrinsic reserve to compensate to an imposed renal challenge or injury.

We have shown here for the first time that *in utero* MNR resulted in dysfunctional cardiac mitochondrial performance with morphological alterations. These findings support the hypothesis that MNR is implicated with a maladaptive programming process and dysfunctional cardiac energetics in the offspring.

The present work also demonstrated clear gender differences in the effects of MNR. Our findings suggest a pronounced sensitivity of male for detrimental effects in mitochondrial performance, presenting lower energy charge and higher oxidative stress. This can in part be the root of the differential gender-related risk for cardiovascular and renal disease.

Some authors described that physical activity in adult men is able to reduce the risk of metabolic syndrome associated with smallness at birth, which suggests that these risks can be attenuated. So, ideally LBW babies should be closely monitored and considered for mitochondrial impairments tests to attempt to prevent the advance of more serious diseases. It would be possible to modulate mitochondrial function by exercise, nutrition or pharmacologically. While the "treatment time" does not arrive, an investment should be made to prevent IUGR, because the effects of developmental programming suggest that early attention paid to reducing the long term disease risk will produce greatest benefit for the individuals. Attention to maternal health must start with young girls, ensuring that they have adequate access to nutrition to optimize they growth. Social change that addresses nutritional education, especially in younger ages, teenage pregnancy must be advocated for, and

access to family planning and prenatal care must be improved globally. Optimization of early nutrition to all children, monitoring growth velocity and percentiles, and encouragement of physical activity are important public health goals that can be implemented and should reduce the risk of hypertension and cardiac and renal diseases in future generations.

The results from the present work are critical in the process of understanding *in utero* metabolic reprogramming and long-term disease incidence in the offspring. This work is clear translational and responds to many social changes.

Figure 6.1 represent some of the factors that can modulate the effects of maternal nutrition reduction in the fetuses, and our work highly propose that mitochondrial can be one of the important players.

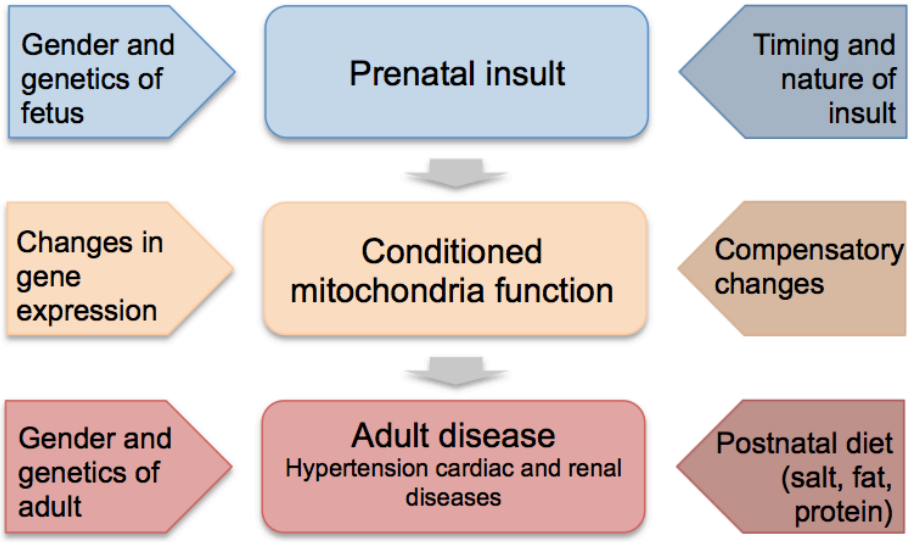

Figure 6.1 Factors which may impact on the final disease outcome following a prenatal insult.
It should be noted that other organs and systems may interact with renal and cardiac changes to exacerbate or ameliorate the onset of disease and that Developmental abnormalities that arise during the embryonic period can manifest themselves much later during gestation or even during postnatal life, particularly if the defects are not major.

Chapter 7

Further experimental work not included in this thesis

This chapter includes the summaries of further experimental work performed by the author during her registration as graduated student, however by decision of the author that work was not included as full length chapters in this thesis.

Acknowledgements

The author acknowledge the contributions by Peter W. Nathanielsz and Mark J. Nijland that developed the animal model; by Paulina Quezada, Greg Langone and Li Cun for immunohistochemistry, by Michelle Zavala and Ana Maria Silva for general assistance in the laboratory, by Leslie Myatt, Alina Maloyan, Nagarjun Kasaraneni, Chunming Guo, Balasubashini Muralimanoharan and James Mele by allowing access to equipment, by Ludgero C. Tavares for the statistics validation, and finally by Karen Moore and Susan Jenkins for bibliography and data archiving.

7.1 Effect of 30% maternal nutrition reduction on cardiac gene expression relevant to mitochondrial oxidative phosphorylation in the fetal baboon at 0.5 gestation

Malnutrition has been associated with alterations in cardiac metabolism and performance. Disruption of myocardial bioenergetics can be clinically devastating. Mitochondrial dysfunction has been related to more than 50 distinct diseases ranging from neonatal fatalities to cardiac dysfunction or neurodegeneration in the adult, and is a likely contributor to cancer and type 2 diabetes. In the heart, the pre-disposition to mitochondrial bioenergetic failure can start well before birth, when signaling pathways maturation is being achieved.

The hypothesis of the present work is that MNR alters the cardiac mitochondrial transcriptional profile at 0.5G.

Pregnant baboons of similar body weight were fed *ad libitum* (C, n=5) or, starting at 0.16 G, 70% of *ad libitum* fed C (MNR, n=5). Samples from the fetal cardiac left ventricle (LV) were obtained by c-section at 0.5 G and stored at -80°C. Quantitative PCR array was used to determine mRNA expression.

At 0.5G, several transcripts relevant to heart mitochondrial bioenergetics were decreased in the female (F) fetus, while only two transcripts were down-regulated in male (M) fetuses. Seven of the transcripts altered in F relate to mitochondrial Complex I (NDUFS2, NDUFS3, NDUFA11, NDUFA3, NDUFB2, NDUFB3, NDUFA10), one to Complex II (SDHB), one with Complex III (UQCRC1), one to Complex IV (COX4I1) and two in complex V (ATP4A, ATP6V1G3). Only two mitochondrial transcripts were different between the sexes in C fetuses, NDUFB10 and ATP5A1, and both were up-regulated in F.

MNR at 0.5 G had a marked effect on components of the mitochondrial oxidative phosphorylation apparatus, particularly in F fetuses. The data indicates that MNR promotes alterations in oxidative phosphorylation transcripts in the heart which can impact normal myocyte differentiation and cardiac development.

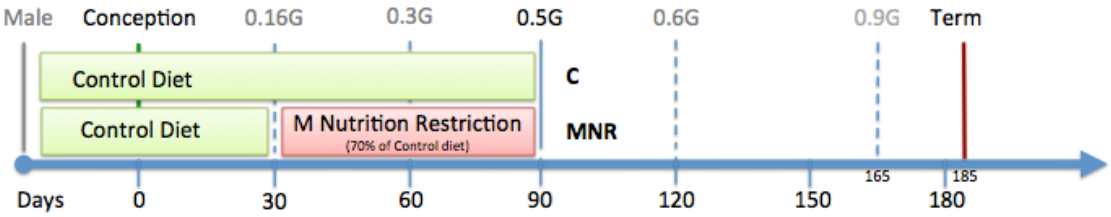

Figure 7.1 Timeline of maternal nutrition during baboon fetal development until 0.5 gestation (90 days).

7.2 Implications of maternal nutrient reduction on fetal nonhuman primate cardiac mitochondria at 0.65 gestation

Epidemiologic studies link poor maternal nutrition to later life cardiovascular disease. We examined the effect of Maternal Nutrient Reduction (MNR) on mitochondrial transcript expression, content and function of cardiac left ventricular mitochondrial protein changes in fetal baboons at 0.65G.

Pregnant baboons ate *ad libitum* (C, n=10) or, from 0.16G, fed 70% C diet (MNR, n=9). Samples were obtained by *c*-section at 0.65G and stored at -80°C. mRNAs were analyzed by qPCR and protein by Western Blotting. Enzymatic activities of citrate synthase and of respiratory chain enzymes (Complex I, Complex II/Complex III, Complex III and Complex IV) were spectrohotometrically determined. Antioxidant capacity and oxidative stress were evaluated by GSH, GSSG, GSH/GSSG, GI-Px, Gl-Red, Vit E and MDA. Adenine nucleotides were quantified by HPLC. Significance reported was $p<0.05$.

Maternal body weight at *c*-section was similar between C and MNR mothers (16.6 ± 0.44 Kg vs. 16.4 ± 0.76 Kg). However, fetal body length of C female (F) vs. MNR F (26.6 ± 0.25 cm vs. 25.0 ± 0.76 cm) was longer. MNR did not affect fetal heart weight or heart:body weight ratio. At 0.65G, several transcripts relevant to cardiac mitochondrial bioenergetics were altered in MNR fetuses in a sex dependent fashion, 11 transcripts down-regulated in Females (F) while only 3 transcripts were down-regulated in males (M). Up regulation of several transcripts in the mitochondrial carrier family (SLC25A19, SLC25A23, SLC25A37, TIMM44, TOMM40 and TOMM40L) occurred in males. UCP1 increased in both genders. Protein analysis showed citrate synthase, NDUFB8 and TOMM20 increased in MNR. In contrast, citrate synthase enzyme activity significantly decreased in MNR fetuses (648.8±73.18 nmol/min/mg protein vs. 278.9 ± 71.34 nmol/min/mg protein) whereas Complex I/citrate synthase increased (2.3 ± 0.34 vs. 12.7 ± 4.41). Total adenine nucleotides, ADP and AMP were decreased in MNR group. No alterations were found antioxidant capacity factors or MDA.

Our study provides evidence of an association between MNR and fetal cardiac mitochondrial remodeling and transcription and translation changes, which may impact heart development and predispose for metabolic disturbances later in life.

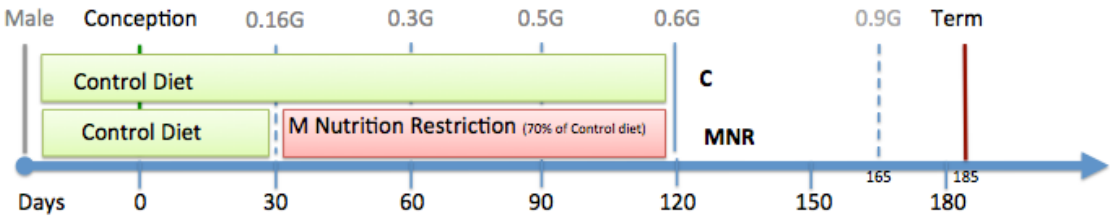

Figure 7.2 Timeline of maternal nutrition during baboon fetal development until 0.65 gestation (120 days).

7.3 The impact of maternal nutrition excess (MNE) on fetal cardiac mitochondrial transcripts and protein at 0.9 gestation in nonhuman primates (NHP)

Maternal obesity predisposes offspring to metabolic dysfunction and type 2 diabetes, with implications in organ dysfunction, namely in the cardiovascular system. We hypothesize that maternal nutrient excess (MNE) during gestation can impact mitochondrial biogenesis and function.

Female baboons were fed regular chow (12% energy fat, n=12) or MNE diet (45% energy fat and ad libitum fructose sodas, n=5).

At conception, MNE mothers were more obese and weighed more than regular chow controls. MNE fetuses were lighter (816.9±33.9g vs. 675.2±35.7g) and presented a lower BMI. At 0.9G, MNE did not affect fetal heart weight or heart:body weight ratio. Transcriptome analysis of the free wall of the cardiac left ventricle of MNE 0.9G fetuses showed 3,033 diferently expressed genes, with more than 100 related with mitochondria. Transcripts for Complex I (NDUFB3 and NDUFB6), Complex II (SDHC), Complex IV (COX6C and COX7C), Complex IV (ATP6VOA2 and ATP5A1) and the phosphate carrier were decreased in the MNE fetus. Variations in mRNA levels were accompanied by decreased protein levels of subunits from Complex III (CIII-core I), Complex IV (COX-II), Complex V (CV α), as well as cyclophilin D.

MNE induces 0.9G mitochondrial transcriptional and protein alterations in the cardiac left ventricle, which may impact normal heart development and predispose for metabolic disturbances later in life.

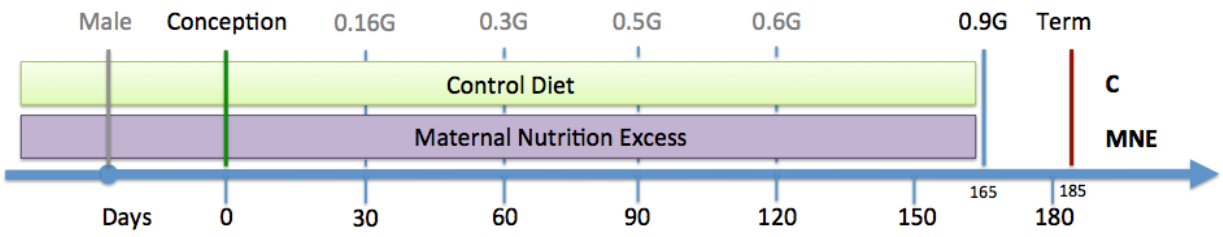

Figure 7.3 Timeline of maternal nutrition during baboon fetal development until 0.9 gestation (165 days).

"I would not know what to say to you, except this: there was never a map that got it all right…"

by Reif Larsen

Bibliography

1. Cross, J. C., Werb, Z. & Fisher, S. J. Implantation and the placenta: key pieces of the development puzzle. *Science* **266,** 1508–1518 (1994).

2. Wennekamp, S., Mesecke, S., Nédélec, F. & Hiiragi, T. A self-organization framework for symmetry breaking in the mammalian embryo. *Nat. Rev. Mol. Cell Biol.* **14,** 452–9 (2013).

3. Mitchell, P. Coupling of phosphorylation to electron and hydrogen transfer by a chemi-osmotic type of mechanism. *Nature* **191,** 144–148 (1961).

4. Benard, G. & Rossignol, R. Ultrastructure of the mitochondrion and its bearing on function and bioenergetics. *Antioxid. Redox Signal.* **10,** 1313–42 (2008).

5. Pereira, C. *et al.* Investigating drug-induced mitochondrial toxicity: a biosensor to increase drug safety? *Curr. Drug Saf.* **4,** 34–54 (2009).

6. Yi, M., Weaver, D. & Hajnóczky, G. Control of mitochondrial motility and distribution by the calcium signal: A homeostatic circuit. *J. Cell Biol.* **167,** 661–672 (2004).

7. Liu, X., Kim, C. N., Yang, J., Jemmerson, R. & Wang, X. Induction of apoptotic program in cell-free extracts: Requirement for dATP and cytochrome c. *Cell* **86,** 147–157 (1996).

8. Kroemer, G. Mitochondrial control of apoptosis: an overview. *Biochem. Soc. Symp.* **66,** 1–15 (1999).

9. Costantini, P., Jacotot, E., Decaudin, D. & Kroemer, G. Mitochondrion as a novel target of anticancer chemotherapy. *J. Natl. Cancer Inst.* **92,** 1042–1053 (2000).

10. Armstrong, J. S. Mitochondrial medicine: pharmacological targeting of mitochondria in disease. *Br. J. Pharmacol.* **151,** 1154–1165 (2007).

11. Iacobazzi, V., Castegna, A., Infantino, V. & Andria, G. Mitochondrial DNA methylation as a next-generation biomarker and diagnostic tool. *Mol. Genet. Metab.* **110,** 25–34 (2013).

12. Krishnan, K. J. & Turnbull, D. M. Mitochondrial DNA and genetic disease. *Essays Biochem.* **47,** 139–51 (2010).

13. Zeviani, M., Bonilla, E., DeVivo, D. C. & DiMauro, S. Mitochondrial diseases.

Neurol. Clin. **7,** 123–156 (1989).

14. DiMauro, S. & Moraes, C. T. Mitochondrial encephalomyopathies. *Arch. Neurol.* **50,** 1197–208 (1993).

15. Singhal, N., Gupta, B. S., Saigal, R., Makkar, J. & Mathur, R. Mitochondrial diseases: an overview of genetics, pathogenesis, clinical features and an approach to diagnosis and treatment. *J. Postgrad. Med.* **46,** 224–230 (2000).

16. Lightowlers, R. N., Taylor, R. W. & Turnbull, D. M. Mutations causing mitochondrial disease: What is new and what challenges remain? *Science.* **349,** 1494–1499 (2015).

17. Taylor, R. W. & Turnbull, D. M. Mitochondrial DNA mutations in human disease. *Nat. Rev. Genet.* **6,** 389–402 (2005).

18. Lodish, H. *et al. Molecular Cell Biology, 4th edition*. (2000).

19. Kennady, P. K., Ormerod, M. G., Singh, S. & Pande, G. Variation of mitochondrial size during the cell cycle: A multiparameter flow cytometric and microscopic study. *Cytometry. A* **62,** 97–108 (2004).

20. Rostovtseva, T. K. & Bezrukov, S. M. VDAC regulation: role of cytosolic proteins and mitochondrial lipids. *J. Bioenerg. Biomembr.* **40,** 163–70 (2008).

21. Halestrap, A. P. & Brenner, C. The adenine nucleotide translocase: a central component of the mitochondrial permeability transition pore and key player in cell death. *Curr. Med. Chem.* **10,** 1507–1525 (2003).

22. Giorgio, V. *et al.* Dimers of mitochondrial ATP synthase form the permeability transition pore. *Proc. Natl. Acad. Sci. U. S. A.* **110,** 5887–92 (2013).

23. Pereira, S. P., Pereira, G. C., Moreno, A. J. & Oliveira, P. J. Can drug safety be predicted and animal experiments reduced by using isolated mitochondrial fractions? *Altern. Lab. Anim.* **37,** 355–65 (2009).

24. Westermann, B. Mitochondrial fusion and fission in cell life and death. *Nat. Rev. Mol. Cell Biol.* **11,** 872–884 (2010).

25. Nakada, K., Inoue, K. & Hayashi, J. Interaction theory of mammalian mitochondria. *Biochem. Biophys. Res. Commun.* **288,** 743–746 (2001).

26. Romanello, V. *et al.* Mitochondrial fission and remodelling contributes to muscle atrophy. *EMBO J.* **29,** 1774–85 (2010).

27. Hom, J., Yu, T., Yoon, Y., Porter, G. & Sheu, S.-S. Regulation of mitochondrial fission by intracellular Ca(2+) in rat ventricular myocytes. *Biochim. Biophys. Acta* **1797,** 913–921 (2010).

28. Scott, I. & Youle, R. J. Mitochondrial fission and fusion. *Essays Biochem.* **47,** 85–98 (2010).

29. Huang, P., Galloway, C. a & Yoon, Y. Control of mitochondrial morphology through differential interactions of mitochondrial fusion and fission proteins. *PLoS One* **6,** e20655 (2011).

30. Twig, G., Hyde, B. & Shirihai, O. S. Mitochondrial fusion, fission and autophagy as a quality control axis: The bioenergetic view. *Biochim. Biophys. Acta - Bioenerg.* **1777,** 1092–1097 (2008).

31. Roy, M., Reddy, P. H., Iijima, M. & Sesaki, H. Mitochondrial division and fusion in metabolism. *Curr. Opin. Cell Biol.* **33,** 111–8 (2015).

32. Drake, J. C., Wilson, R. J. & Yan, Z. Molecular mechanisms for mitochondrial adaptation to exercise training in skeletal muscle. *FASEB J.* 1–10 (2015)

33. Putti, R., Sica, R., Migliaccio, V. & Lionetti, L. Diet impact on mitochondrial bioenergetics and dynamics. *Front. Physiol.* **6,** 109 (2015).

34. Dorn, G. W. Mitochondrial dynamism and heart disease: changing shape and shaping change. *EMBO Mol. Med.* **7,** 865–77 (2015).

35. Hales, K. G. The machinery of mitochondrial fusion, division, and distribution, and emerging connections to apoptosis. *Mitochondrion* **4,** 285–308 (2004).

36. Szabadkai, G. *et al.* Drp-1-dependent division of the mitochondrial network blocks intraorganellar Ca2+ waves and protects against Ca 2+-mediated apoptosis. *Mol. Cell* **16,** 59–68 (2004).

37. Chen, H. & Chan, D. C. Emerging functions of mammalian mitochondrial fusion and fission. *Hum. Mol. Genet.* **14,** 283–289 (2005).

38. Mozdy, A. D., McCaffery, J. M. & Shaw, J. M. Dnm1p GTPase-mediated mitochondrial fission is a multi-step process requiring the novel integral membrane component Fis1p. *J. Cell Biol.* **151,** 367–379 (2000).

39. Zungu, M., Schisler, J. & Willis, M. S. All the little pieces. Regulation of mitochondrial fusion and fission by ubiquitin and small ubiquitin-like modifer and their potential relevance in the heart. *Circ J* **75,** 2513–2521 (2011).

40. Bowes, T. & Gupta, R. S. Novel mitochondrial extensions provide evidence for a link between microtubule-directed movement and mitochondrial fission.

Biochem. Biophys. Res. Commun. **376,** 40–45 (2008).

41. Beraud, N. *et al.* Mitochondrial dynamics in heart cells: Very low amplitude high frequency fluctuations in adult cardiomyocytes and flow motion in non beating Hl-1 cells. *J. Bioenerg. Biomembr.* **41,** 195–214 (2009).

42. Parra, V. *et al.* Changes in mitochondrial dynamics during ceramide-induced cardiomyocyte early apoptosis. *Cardiovasc. Res.* **77,** 387–397 (2008).

43. Brady, N. R., Hamacher-Brady, A. & Gottlieb, R. A. Proapoptotic BCL-2 family members and mitochondrial dysfunction during ischemia/reperfusion injury, a study employing cardiac HL-1 cells and GFP biosensors. *Biochim. Biophys. Acta - Bioenerg.* **1757,** 667–678 (2006).

44. Song, M., Mihara, K., Chen, Y., Scorrano, L. & Dorn, G. W. Mitochondrial Fission and Fusion Factors Reciprocally Orchestrate Mitophagic Culling in Mouse Hearts and Cultured Fibroblasts. *Cell Metab.* **21,** 273–285 (2015).

45. Kasahara, A., Cipolat, S., Chen, Y., Dorn, G. W. & Scorrano, L. Mitochondrial Fusion Directs Cardiomyocyte Differentiation via Calcineurin and Notch Signaling. *Science (80-.).* **342,** 734–737 (2013).

46. Papanicolaou, K. N. *et al.* Mitofusins 1 and 2 are essential for postnatal metabolic remodeling in heart. *Circ. Res.* **111,** 1012–1026 (2012).

47. Chance, B. & Williams, G. R. The respiratory chain and oxidative phosphorylation. *Adv. Enzymol. Relat. Areas Mol. Biol.* **17,** 65–134 (1956).

48. Rich, P. R. The molecular machinery of Keilin's respiratory chain. *Biochem. Soc. Trans.* **31,** 1095–1105 (2003).

49. Bellance, N., Lestienne, P. & Rossignol, R. Mitochondria: from bioenergetics to the metabolic regulation of carcinogenesis. *Front. Biosci.* **14,** 4015–4034 (2009).

50. Turrens, J. F. Mitochondrial formation of reactive oxygen species. *J. Physiol.* **552,** 335–344 (2003).

51. Chance, B., Sies, H. & Boveris, A. Hydroperoxide metabolism in mammalian organs. *Physiol. Rev.* **59,** 527–605 (1979).

52. Lenaz, G. The mitochondrial production of reactive oxygen species: mechanisms and implications in human pathology. *IUBMB Life* **52,** 159–164 (2001).

53. Fariss, M. W., Chan, C. B., Patel, M., Van Houten, B. & Orrenius, S. Role of mitochondria in toxic oxidative stress. *Mol. Interv.* **5,** 94–111 (2005).

54. Hamanaka, R. B. & Chandel, N. S. Mitochondrial reactive oxygen species regulate cellular signaling and dictate biological outcomes. *Trends Biochem. Sci.* **35,** 505–513 (2010).

55. Cui, H., Kong, Y. & Zhang, H. Oxidative Stress, Mitochondrial Dysfunction, and Aging. *J. Signal Transduct.* **2012,** 1–13 (2012).

56. Abbà, S., Khouja, H. R., Martino, E., Archer, D. B. & Perotto, S. SOD1-targeted gene disruption in the ericoid mycorrhizal fungus Oidiodendron maius reduces conidiation and the capacity for mycorrhization. *Mol. Plant. Microbe. Interact.* **22,** 1412–1421 (2009).

57. Asimakis, G. K., Lick, S. & Patterson, C. Postischemic recovery of contractile function is impaired in SOD2+/- but not SOD1+/- mouse hearts. *Circulation* **105,** 981–986 (2002).

58. Candas, D. & Li, J. J. MnSOD in oxidative stress response-potential regulation via mitochondrial protein influx. *Antioxid. Redox Signal.* **20,** 1599–617 (2014).

59. Jung, I., Kim, T. Y. & Kim-Ha, J. Identification of Drosophila SOD3 and its protective role against phototoxic damage to cells. *FEBS Lett.* **585,** 1973–1978 (2011).

60. Andreassen, O. A. *et al.* Partial deficiency of manganese superoxide dismutase exacerbates a transgenic mouse model of amyotrophic lateral sclerosis. *Ann. Neurol.* **47,** 447–455 (2000).

61. Aniya, Y. & Imaizumi, N. Mitochondrial glutathione transferases involving a new function for membrane permeability transition pore regulation. *Drug Metab. Rev.* **43,** 292–299 (2011).

62. Marí, M. *et al.* Mitochondrial glutathione: Features, regulation and role in disease. *Biochim. Biophys. Acta - Gen. Subj.* **1830,** 3317–3328 (2013).

63. Hansen, J. M., Go, Y. M. & Jones, D. P. Nuclear and mitochondrial compartmentation of oxidative stress and redox signaling. *Annu. Rev. Pharmacol. Toxicol.* **46,** 215–234 (2006).

64. Meredith, M. J. & Reed, D. J. Status of the mitochondrial pool of glutathione in the isolated hepatocyte. *J. Biol. Chem.* **257,** 3747–3753 (1982).

65. Marí, M., Morales, A., Colell, A., García-Ruiz, C. & Fernández-Checa, J. C. Mitochondrial glutathione, a key survival antioxidant. *Antioxid. Redox Signal.* **11,** 2685–2700 (2009).

66. Blokhina, O., Virolainen, E. & Fagerstedt, K. V. Antioxidants, oxidative damage and oxygen deprivation stress: A review. *Ann. Bot.* **91,** 179–194 (2003).

67. Fernandes, P. N. *et al.* Oxidative stress response in eukaryotes: effect of glutathione, superoxide dismutase and catalase on adaptation to peroxide and menadione stresses in Saccharomyces cerevisiae. *Redox Rep.* **12,** 236–244 (2007).

68. Ribas, V., García-Ruiz, C. & Fernández-Checa, J. C. Glutathione and mitochondria. *Front. Pharmacol.* **5 JUL,** 1–19 (2014).

69. Chan, S. H. H., Tai, M. H., Li, C. Y. & Chan, J. Y. H. Reduction in molecular synthesis or enzyme activity of superoxide dismutases and catalase contributes to oxidative stress and neurogenic hypertension in spontaneously hypertensive rats. *Free Radic. Biol. Med.* **40,** 2028–2039 (2006).

70. Salvi, M. *et al.* Catalase takes part in rat liver mitochondria oxidative stress defense. *J. Biol. Chem.* **282,** 24407–24415 (2007).

71. Finkel, T. & Holbrook, N. J. Oxidants, oxidative stress and the biology of ageing. *Nature* **408,** 239–247 (2000).

72. Berridge, M. J., Lipp, P. & Bootman, M. D. The versatility and universality of calcium signalling. *Nat. Rev. Mol. Cell Biol.* **1,** 11–21 (2000).

73. Rizzuto, R. *et al.* Close contacts with the endoplasmic reticulum as determinants of mitochondrial Ca2+ responses. *Science* **280,** 1763–1766 (1998).

74. Brini, M. Ca2+ signalling in mitochondria: Mechanism and role in physiology and pathology. *Cell Calcium* **34,** 399–405 (2003).

75. Rottenberg, H. & Marbach, M. The Na(+)-independent Ca2+ efflux system in mitochondria is a Ca2+/2H+ exchange system. *FEBS Lett.* **274,** 65–68 (1990).

76. Carafoli, E., Crompton, M., Caroni, P., Schwerzmann, K. & Roos, I. The cycling of calcium across the inner mitochondrial membrane. **608,** 599–608 (1980).

77. Mackenzie, L., Roderick, H. L., Berridge, M. J., Conway, S. J. & Bootman, M. D. The spatial pattern of atrial cardiomyocyte calcium signalling modulates contraction. *J. Cell Sci.* **117,** 6327–6337 (2004).

78. Jouaville, L. S., Pinton, P., Bastianutto, C., Rutter, G. A. & Rizzuto, R. Regulation of mitochondrial ATP synthesis by calcium: evidence for a long-term metabolic priming. *Proc. Natl. Acad. Sci. U. S. A.* **96,** 13807–13812 (1999).

79. Pinton, P., Giorgi, C., Siviero, R., Zecchini, E. & Rizzuto, R. Calcium and apoptosis: ER-mitochondria Ca2+ transfer in the control of apoptosis. *Oncogene* **27,** 6407–6418 (2008).

80. Vandecasteele, G., Szabadkai, G. & Rizzuto, R. Mitochondrial calcium homeostasis: mechanisms and molecules. *IUBMB Life* **52,** 213–219 (2001).

81. Giorgi, C. *et al.* Mitochondrial calcium homeostasis as potential target for mitochondrial medicine. *Mitochondrion* **12,** 77–85 (2012).

82. Hunter, D. R. & Haworth, R. A. The Ca2+ induced membrane transition in mitochondria. I. The protective mechanisms. *Arch. Biochem. Biophys.* **195,** 453–9 (1979).

83. Kakkar, P. & Singh, B. K. Mitochondria: A hub of redox activities and cellular distress control. *Mol. Cell. Biochem.* **305,** 235–253 (2007).

84. Rasola, A. & Bernardi, P. The mitochondrial permeability transition pore and its involvement in cell death and in disease pathogenesis. *Apoptosis* **12,** 815–833 (2007).

85. Bernardi, P. & Rasola, A. Calcium and cell death: the mitochondrial connection. *Subcell. Biochem.* **45,** 481–506 (2007).

86. Baines, C. P. The molecular composition of the mitochondrial permeability transition pore. *J. Mol. Cell. Cardiol.* **46,** 850–857 (2009).

87. Bernardi, P. Mitochondrial transport of cations: channels, exchangers, and permeability transition. *Physiol. Rev.* **79,** 1127–1155 (1999).

88. Kroemer, G. & Reed, J. C. Mitochondrial control of cell death. *Nat. Med.* **6,** 513–519 (2000).

89. Halestrap, A. P., Doran, E., Gillespie, J. P. & O'Toole, A. Mitochondria and cell death. *Biochem. Soc. Trans.* **28,** 170–7 (2000).

90. Petronilli, V., Penzo, D., Scorrano, L., Bernardi, P. & Di Lisa, F. The mitochondrial permeability transition, release of cytochrome c and cell death. Correlation with the duration of pore openings in situ. *J. Biol. Chem.* **276,** 12030–12034 (2001).

91. Pinton, P. *et al.* A role for calcium in Bcl-2 action? *Biochimie* **84,** 195–201 (2002).

92. Pinton, P. *et al.* The Ca2+ concentration of the endoplasmic reticulum is a key determinant of ceramide-induced apoptosis: Significance for the molecular mechanism of Bcl-2 action. *EMBO J.* **20,** 2690–2701 (2001).

93. Biagioli, M. *et al.* Endoplasmic reticulum stress and alteration in calcium homeostasis are involved in cadmium-induced apoptosis. *Cell Calcium* **43,** 184–195 (2008).

94. Zamzami, N. *et al.* Reduction in mitochondrial potential constitutes an early irreversible step of programmed lymphocyte death in vivo. *J. Exp. Med.* **181,** 1661–1672 (1995).

95. Kelekar, A. & Thompson, C. B. Bcl-2-family proteins: The role of the BH3 domain in apoptosis. *Trends Cell Biol.* **8,** 324–330 (1998).

96. Harris, M. H. & Thompson, C. B. The role of the Bcl-2 family in the regulation of outer mitochondrial membrane permeability. *Cell Death Differ.* **7,** 1182–1191 (2000).

97. Gross, A., McDonnell, J. M. & Korsmeyer, S. J. BCL-2 family members and the mitochondria in apoptosis. *Genes Dev.* **13,** 1899–1911 (1999).

98. Green, D. R. & Kroemer, G. The pathophysiology of mitochondrial cell death. *Science* **305,** 626–629 (2004).

99. Bursch, W. The autophagosomal-lysosomal compartment in programmed cell death. *Cell Death Differ.* **8,** 569–581 (2001).

100. Lemasters, J. J. Selective mitochondrial autophagy, or mitophagy, as a targeted defense against oxidative stress, mitochondrial dysfunction, and aging. *Rejuvenation Res.* **8,** 3–5 (2005).

101. Rodriguez-Enriquez, S., Kim, I., Currin, R. T. & Lemasters, J. J. Tracker dyes to probe mitochondrial autophagy (mitophagy) in rat hepatocytes. *Autophagy* **2,** 39–46 (2006).

102. Kim, I., Rodriguez-Enriquez, S. & Lemasters, J. J. Selective degradation of mitochondria by mitophagy. *Arch. Biochem. Biophys.* **462,** 245–253 (2007).

103. Scherz-Shouval, R. & Elazar, Z. ROS, mitochondria and the regulation of autophagy. *Trends Cell Biol.* **17,** 422–427 (2007).

104. Elmore, S. P., Qian, T., Grissom, S. F. & Lemasters, J. J. The mitochondrial permeability transition initiates autophagy in rat hepatocytes. *FASEB J.* **15,** 2286–2287 (2001).

105. Xue, L., Fletcher, G. C. & Tolkovsky, a. M. Mitochondria are selectively eliminated from eukaryotic cells after blockade of caspases during apoptosis. *Curr. Biol.* **11,** 361–365 (2001).

106. Tatsuta, T. & Langer, T. Quality control of mitochondria: protection against neurodegeneration and ageing. *EMBO J.* **27,** 306–314 (2008).

107. Sheridan, C., Delivani, P., Cullen, S. P. & Martin, S. J. Bax- or Bak-Induced Mitochondrial Fission Can Be Uncoupled from Cytochrome c Release. *Mol. Cell* **31,** 570–585 (2008).

108. Huang, C. *et al.* Preconditioning involves selective mitophagy mediated by parkin and p62/SQSTM1. *PLoS One* **6,** (2011).

109. Andres, A. M. *et al.* Mitophagy is Required for Acute Cardioprotection by Simvastatin. *Antioxid. Redox Signal.* **11,** 1960–1973 (2013).

110. Almind, K., Manieri, M., Sivitz, W. I., Cinti, S. & Kahn, C. R. Ectopic brown adipose tissue in muscle provides a mechanism for differences in risk of metabolic syndrome in mice. *Proc Natl Acad Sci U S A* **104,** 2366–2371 (2007).

111. Chem, J. B. Essential Role of a Mitochondrial Protein in Steroid Hormone Synthesis Debunked. *J. Biol. Chem.* **289,** 27455–27455 (2014).

112. Bosch, M., Marí, M., Gross, S. P., Fernández-Checa, J. C. & Pol, A. Mitochondrial cholesterol: A connection between caveolin, metabolism, and disease. *Traffic* **12,** 1483–1489 (2011).

113. Garcia-Euiz, C. *et al.* Mitochondrial cholesterol in health and disease. *Histol. Histopathol.* **24,** 117–132 (2009).

114. Nakagawa, T. & Guarente, L. Urea cycle regulation by mitochondrial sirtuin, SIRT5. *Aging (Albany. NY).* **1,** 578–581 (2009).

115. Newmeyer, D. D. & Ferguson-Miller, S. Mitochondria: Releasing power for life and unleashing the machineries of death. *Cell* **112,** 481–490 (2003).

116. Kuznetsov, A. V., Janakiraman, M., Margreiter, R. & Troppmair, J. Regulating cell survival by controlling cellular energy production: Novel functions for ancient signaling pathways? *FEBS Lett.* **577,** 1–4 (2004).

117. Karbowski, M., Norris, K. L., Cleland, M. M., Jeong, S.-Y. & Youle, R. J. Role of Bax and Bak in mitochondrial morphogenesis. *Nature* **443,** 658–662 (2006).

118. Pereira, G. C. *et al.* Mitochondrionopathy phenotype in doxorubicin-treated Wistar rats depends on treatment protocol and is cardiac-specific. *PLoS One* **7,** e38867 (2012).

119. *Fetal growth and development.* (Cambridge University Press, 2001).

120. Mollova, M. *et al.* Cardiomyocyte proliferation contributes to heart growth in young humans. *Proc. Natl. Acad. Sci. U. S. A.* **110,** 1446–51 (2013).

121. Hom, J. R. *et al.* The permeability transition pore controls cardiac mitochondrial maturation and myocyte differentiation. *Dev. Cell* **21,** 469–478 (2011).

122. Dennery, P. A. Effects of oxidative stress on embryonic development. *Birth Defects Res. Part C - Embryo Today Rev.* **81,** 155–162 (2007).

123. Chen, Y., Liu, Y. & Dorn, G. W. Mitochondrial fusion is essential for organelle function and cardiac homeostasis. *Circ. Res.* **109,** 1327–1331 (2011).

124. Dorn, G. W. Mitochondrial dynamics in heart disease. *Biochim. Biophys. Acta - Mol. Cell Res.* **1833,** 233–241 (2013).

125. Saks, V. A., Ventura-Clapier, R., Leverve, X., Rossi, A. & Rigoulet, M. What do we not know of cellular bioenergetics?--a general view on the state of the art. *Mol. Cell. Biochem.* **184,** 3–9 (1998).

126. Huss, J. M. & Kelly, D. P. Review series Mitochondrial energy metabolism in heart failure : a question of balance. *J. Clin. Invest.* **115,** 547–555 (2005).

127. Weiss, R. G. & Maslov, M. Normal myocardial metabolism: Fueling cardiac contraction. *Adv. Stud. Med.* **4,** 457–463 (2004).

128. Power, A. *et al.* Uncoupling of oxidative phosphorylation and ATP synthase reversal within the hyperthermic heart. *Physiol. Rep.* **2,** e12138–e12138 (2014).

129. Ziegler, A., Zaugg, C. E., Buser, P. T., Seelig, J. & Künnecke, B. Non-invasive measurements of myocardial carbon metabolism using in vivo 13C NMR spectroscopy. *NMR Biomed.* **15,** 222–234 (2002).

130. Stanley, W. W. C., Recchia, F. A. & Lopaschuk, G. D. Myocardial Substrate Metabolism in the Normal and Failing Heart. *Physiol.* … **85,** 1093–1129 (2005).

131. Gertz, E. W., Wisneski, J. A., Stanley, W. C. & Neese, R. A. Myocardial substrate utilization during exercise in humans. Dual carbon-labeled carbohydrate isotope experiments. *J. Clin. Invest.* **82,** 2017–2025 (1988).

132. Lopaschuk, G. D., Ussher, J. R., Folmes, C. D. L., Jaswal, J. S. & Stanley, W. C. Myocardial fatty acid metabolism in health and disease. *Physiol. Rev.* **90,** 207–258 (2010).

133. Sato, K. *et al.* Insulin, ketone bodies, and mitochondrial energy transduction. *FASEB J.* **9,** 651–658 (1995).

134. Abel, E. D. Glucose transport in the heart. *Front. Biosci.* **9,** 201–215 (2004).

135. Depre, C., Vanoverschelde, J. L. & Taegtmeyer, H. Glucose for the heart. *Circulation* **99,** 578–588 (1999).

136. Kobayashi, K. & Neely, J. R. Control of maximum rates of glycolysis in rat cardiac muscle. *Circ. Res.* **44,** 166–175 (1979).

137. Patel, T. B. & Olson, M. S. Regulation of pyruvate dehydrogenase complex in ischemic rat heart. *Am. J. Physiol.* **246,** H858–H864 (1984).

138. Kerbey, A. L. *et al.* Regulation of pyruvate dehydrogenase in rat heart. Mechanism of regulation of proportions of dephosphorylated and phosphorylated enzyme by oxidation of fatty acids and ketone bodies and of effects of diabetes: role of coenzyme A, acetyl-coenzyme A and red. *Biochem. J.* **154,** 327–348 (1976).

139. Lopaschuk, G. D., Collins-Nakai, R. L. & Itoi, T. Developmental changes in energy substrate use by the heart. *Cardiovasc. Res.* **26,** 1172–1180 (1992).

140. Sheldon, C. A., Friedman, W. F. & Sybers, H. D. Scanning electron microscopy of fetal and neonatal lamb cardiac cells. *J. Mol. Cell. Cardiol.* **8,** 853–862 (1976).

141. Song, M. *et al.* Super-suppression of mitochondrial reactive oxygen species signaling impairs compensatory autophagy in primary mitophagic cardiomyopathy. *Circ. Res.* **115,** 348–353 (2014).

142. Dorn, G. W. & Kitsis, R. N. The Mitochondrial Dynamism-Mitophagy-Cell Death Interactome: Multiple Roles Performed by Members of a Mitochondrial Molecular Ensemble. *Circ. Res.* **116,** 167–182 (2014).

143. Cho, S. W. *et al.* Dual modulation of the mitochondrial permeability transition pore and redox signaling synergistically promotes cardiomyocyte differentiation from pluripotent stem cells. *J. Am. Heart Assoc.* **3,** (2014).

144. Seidman, C. E. & Seidman, J. G. Identifying sarcomere gene mutations in hypertrophic cardiomyopathy: A personal history. *Circ. Res.* **108,** 743–750 (2011).

145. Prieur, B. *et al.* Perinatal maturation of rat kidney mitochondria. *Biochem. J.* **305 (Pt 2,** 675–80 (1995).

146. Ishimoto, Y. & Inagi, R. Mitochondria: a therapeutic target in acute kidney injury. *Nephrol. Dial. Transplant.* gfv317 (2015).

147. Kuwertz-Bröking, E. *et al.* Renal Fanconi syndrome: first sign of partial respiratory chain complex IV deficiency. *Pediatr. Nephrol.* **14,** 495–498 (2000).

148. Emma, F. *et al.* 'Bartter-like' phenotype in Kearns-Sayre syndrome. *Pediatr. Nephrol.* **21,** 355–60 (2006).

149. Goldenberg, A. *et al.* Respiratory chain deficiency presenting as congenital nephrotic syndrome. *Pediatr. Nephrol.* **20,** 465–9 (2005).

150. Elgadi, K. M., Meguid, R. A., Qian, M., Souba, W. W. & Abcouwer, S. F. Cloning and analysis of unique human glutaminase isoforms generated by tissue-specific alternative splicing. *Physiol. Genomics* **1,** 51–62 (1999).

151. Kravos, M. & Malesic, I. Glutamate dehydrogenase activity in leukocytes and ageing. *Neurodegener. Dis.* **7,** 239–42 (2010).

152. Soltoff, S. P. ATP and the regulation of renal cell function. *Annu. Rev. Physiol.* **48,** 9–31 (1986).

153. Linkermann, A. *et al.* Regulated cell death in AKI. *J. Am. Soc. Nephrol.* **25,** 2689–701 (2014).

154. Thadhani, R., Pascual, M. & Bonventre, J. V. Acute renal failure. *N. Engl. J. Med.* **334,** 1448–60 (1996).

155. Venkatachalam, M. A. & Weinberg, J. M. The tubule pathology of septic acute kidney injury: a neglected area of research comes of age. *Kidney Int.* **81,** 338–40 (2012).

156. Cebrian, C., Asai, N., D'Agati, V. & Costantini, F. The number of fetal nephron progenitor cells limits ureteric branching and adult nephron endowment. *Cell Rep.* **7,** 127–137 (2014).

157. Brenner, B. M., Garcia, D. L. & Anderson, S. Glomeruli and blood pressure. Less of one, more the other? *Am J Hypertens* **1,** 335–347 (1988).

158. Keller, G., Zimmer, G., Mall, G., Ritz, E. & Amann, K. Nephron number in patients with primary hypertension. *N. Engl. J. Med.* **348,** 101–8 (2003).

159. Wrottesley, S. V., Lamper, C. & Pisa, P. T. Review of the importance of nutrition during the first 1000 days: maternal nutritional status and its associations with fetal growth and birth, neonatal and infant outcomes among African women. *J. Dev. Orig. Health Dis.* 1–19 (2015).

160. Wood-Bradley, R., Barrand, S., Giot, A. & Armitage, J. Understanding the Role of Maternal Diet on Kidney Development; an Opportunity to Improve Cardiovascular and Renal Health for Future Generations. *Nutrients* **7,** 1881–1905 (2015).

161. Christian, P., Lee, S. & Angel, M. Risk of childhood undernutrition related to small-for-gestational age and preterm birth in low- and middle-income countries. *Int. J.* … **42,** (2013).

162. Imdad, A. & Bhutta, Z. A. Nutritional management of the low birth weight/preterm infant in community settings: a perspective from the developing world. *J. Pediatr.* **162,** S107–14 (2013).

163. Gilbert, J. S., Cox, L. A., Mitchell, G. & Nijland, M. J. Nutrient-restricted fetus and the cardio-renal connection in hypertensive offspring. *Expert Rev. Cardiovasc. Ther.* **4,** 227–237 (2006).

164. Ninomiya, T. *et al.* Chronic kidney disease and cardiovascular disease in a general Japanese population: The Hisayama Study. *Kidney Int.* **68,** 228–236 (2005).

165. Forsdahl, A. Living conditions in childhood and subsequent development of risk factors for arteriosclerotic heart disease. The cardiovascular survey in Finnmark 1974-75. *J. Epidemiol. Community Health* **32,** 34–37 (1978).

166. Wadsworth, M. E., Cripps, H. A., Midwinter, R. E. & Colley, J. R. Blood pressure in a national birth cohort at the age of 36 related to social and familial factors, smoking, and body mass. *Br. Med. J. (Clin. Res. Ed).* **291,** 1534–1538 (1985).

167. Barker, D. J., Osmond, C., Simmonds, S. J. & Wield, G. A. The relation of small head circumference and thinness at birth to death from cardiovascular disease in adult life. *Bmj* **306,** 422–6 (1993).

168. Rich-Edwards, J. W. *et al.* Birth weight and risk of cardiovascular disease in a cohort of women followed up since 1976. *BMJ* **315,** 396–400 (1997).

169. Jarvelin, M. R. *et al.* Early Life Factors and Blood Pressure at Age 31 Years in the 1966 Northern Finland Birth Cohort. *Hypertension* **44,** 838–846 (2004).

170. Carolan-Olah, M., Duarte-Gardea, M. & Lechuga, J. A critical review: early life nutrition and prenatal programming for adult disease. *J. Clin. Nurs.* n/a–n/a (2015). doi:10.1111/jocn.12951

171. Gluckman, P. D. & Hanson, M. A. Developmental origins of disease paradigm: a mechanistic and evolutionary perspective. *Pediatr. Res.* **56,** 311–7 (2004).

172. Bol, V., Desjardins, F., Reusens, B., Balligand, J. L. & Remacle, C. Does early mismatched nutrition predispose to hypertension and atherosclerosis, in male mice? *PLoS One* **5,** (2010).

173. Christian, P., Mullany, L. C., Hurley, K. M., Katz, J. & Black, R. E. Nutrition and maternal, neonatal, and child health. *Semin. Perinatol.* **39,** 361–372 (2015).

174. Valero De Bernabé, J. *et al.* Risk factors for low birth weight: a review. *Eur. J. Obstet. Gynecol. Reprod. Biol.* **116,** 3–15 (2004).

175. Stewart, D. E., Raskin, J., Garfinkel, P. E., MacDonald, O. L. & Robinson, G. E. Anorexia nervosa, bulimia, and pregnancy. *Am. J. Obstet. Gynecol.* **157,** 1194–8 (1987).

176. King, J. C. The risk of maternal nutritional depletion and poor outcomes increases in early or closely spaced pregnancies. *J. Nutr.* **133,** 1732S–1736S

(2003).

177. Hickey, C. A. *et al.* Low prenatal weight gain among adult WIC participants delivering term singleton infants: variation by maternal and program participation characteristics. *Matern. Child Health J.* **3,** 129–40 (1999).

178. Hurley, K. M., Caulfield, L. E., Sacco, L. M., Costigan, K. A. & Dipietro, J. A. Psychosocial influences in dietary patterns during pregnancy. *J. Am. Diet. Assoc.* **105,** 963–6 (2005).

179. Palmer, J. L., Jennings, G. E. & Massey, L. Development of an assessment form: attitude toward weight gain during pregnancy. *J. Am. Diet. Assoc.* **85,** 946–9 (1985).

180. Conti, J., Abraham, S. & Taylor, A. Eating behavior and pregnancy outcome. *J. Psychosom. Res.* **44,** 465–77 (1998).

181. Fairburn, C. G. & Welch, S. L. The impact of pregnancy on eating habits and attitudes to shape and weight. *Int. J. Eat. Disord* **9,** 153–160 (1990).

182. Abraham, S., King, W. & Llewellyn-Jones, D. Attitudes to body weight, weight gain and eating behavior in pregnancy. *J. Psychosom. Obstet. Gynaecol.* **15,** 189–95 (1994).

183. Henriksen, T. & Clausen, T. The fetal origins hypothesis: placental insufficiency and inheritance versus maternal malnutrition in well-nourished populations. *Acta Obstet. Gynecol. Scand.* **81,** 112–4 (2002).

184. Witlin, A. & Sibai, B. Hypertension in pregnancy: current concepts of preeclampsia. *Annu. Rev. Med.* **48,** 115–127 (1997).

185. Alexander, B., Hendon, A., Ferril, G. & Dwyer, T. Renal Denervation Abolishes Hypertension in Low-Birth-Weight Offspring From Pregnant Rats With Reduced Uterine Perfusion. *Hypertension* **45,** 754–758 (2005).

186. Veerareddy, S., Campbell, M. E., Williams, S. J., Baker, P. N. & Davidge, S. T. Myogenic reactivity is enhanced in rat radial uterine arteries in a model of maternal undernutrition. *Am. J. Obstet. Gynecol.* **191,** 334–9 (2004).

187. Guillamón, M. D. L. H. & Clau, L. B. The sheep as a large animal experimental model in respiratory diseases research. *Arch. Bronconeumol.* **46,** 499–501 (2010).

188. Gardner, D. S., Jackson, A. A. & Langley-Evans, S. C. The effect of prenatal diet and glucocorticoids on growth and systolic blood pressure in the rat. *Proc. Nutr. Soc.* **57,** 235–40 (1998).

189. Phillips, K. A. *et al.* Why primate models matter. *Am. J. Primatol.* **827,** 1–27

(2014).

190. Cox, L. A. *et al.* Baboons as a model to study genetics and epigenetics of human disease. *ILAR J.* **54,** 106–21 (2013).

191. Gubhaju, L. & Black, M. J. The baboon as a good model for studies of human kidney development. *Pediatr. Res.* **58,** 505–9 (2005).

192. Schlabritz-Loutsevitch, N. E. *et al.* Development of a system for individual feeding of baboons maintained in an outdoor group social environment. *J. Med. Primatol.* **33,** 117–126 (2004).

193. Nowak, R. M. *Walker's Mammals of the World.* (The Johns Hopkins University Press, 1999).

194. site 1. Monkey Diet 5038. *http://labdiet.com/* 16 (2015). at <http://labdiet.com/cs/groups/lolweb/@labdiet/documents/web_content/mdrf/mdi4/~edisp/ducm04_028407.pdf>

195. Schlabritz-Loutsevitch, N. E. *et al.* Normal concentrations of essential and toxic elements in pregnant baboons and fetuses (Papio species). *J. Med. Primatol.* **33,** 152–62 (2004).

196. Wu, A., Ying, Z. & Gomez-Pinilla, F. Dietary omega-3 fatty acids normalize BDNF levels, reduce oxidative damage, and counteract learning disability after traumatic brain injury in rats. *J. Neurotrauma* **21,** 1457–67 (2004).

197. Cox, L. *et al.* Effect of 30 per cent maternal nutrient restriction from 0.16 to 0.5 gestation on fetal baboon kidney gene expression. *J. Physiol.* **572,** 67–85 (2006).

198. Romero-Calvo, I. *et al.* Reversible Ponceau staining as a loading control alternative to actin in Western blots. *Anal. Biochem.* **401,** 318–320 (2010).

199. Li, C. *et al.* Effects of maternal global nutrient restriction on fetal baboon hepatic insulin-like growth factor system genes and gene products. *Endocrinology* **150,** 4634–42 (2009).

200. Long, J. *et al.* Comparison of two methods for assaying complex I activity in mitochondria isolated from rat liver, brain and heart. *Life Sci.* **85,** 276–280 (2009).

201. Tisdale, H. D. Preparation and properties of succinic-cytochrome c reductase (complex II-III). *Methods Enzymol.* **10,** 213–215 (1967).

202. Luo, C., Long, J. & Liu, J. An improved spectrophotometric method for a more specific and accurate assay of mitochondrial complex III activity. *Clin. Chim. Acta* **395,** 38–41 (2008).

203. Brautigan, D. L., Ferguson-Miller, S. & Margoliash, E. Mitochondrial cytochrome c: Preparation and activity of native and chemically modified cytochromes c. *Methods Enzymol.* **53,** 128–164 (1978).

204. Coore, H. G., Denton, R. M., Martin, B. R. & Randle, P. J. Regulation of adipose tissue pyruvate dehydrogenase by insulin and other hormones. *Biochem. J.* **125,** 115–127 (1971).

205. Santos, M. S., Moreno, A. J. & Carvalho, A. P. Relationships between ATP depletion, membrane potential, and the release of neurotransmitters in rat nerve terminals. An in vitro study under conditions that mimic anoxia, hypoglycemia, and ischemia. *Stroke.* **27,** 941–950 (1996).

206. Stocchi, V. *et al.* Simultaneous extraction and reverse-phase high-performance liquid chromatographic determination of adenine and pyridine nucleotides in human red blood cells. *Anal. Biochem.* **146,** 118–124 (1985).

207. Draper, H. H. & Hadley, M. Malondialdehyde determination as index of lipid peroxidation. *Methods Enzymol.* **186,** 421–431 (1990).

208. Tsao, S. M., Yin, M. C. & Liu, W. H. Oxidant stress and B vitamins status in patients with non-small cell lung cancer. *Nutr. Cancer* **59,** 8–13 (2007).

209. Paglia, D. E. & Valentine, W. N. Studies on the quantitative and qualitative characterization of erythrocyte glutathione peroxidase. *J. Lab. Clin. Med.* **70,** 158–169 (1967).

210. Goldberg, D. & Spooner, R. in *Methods Enzym. Anal.* (Bergmerye) 258–265 (Verlag Chemie Weinheim Academic Pres, 1983).

211. Malhotra, B. S. K. Experiments on fixation for electron microscopy. *Small* **103,** 5–15 (1962).

212. Zohdi, V. *et al.* Low Birth Weight due to Intrauterine Growth Restriction and/or Preterm Birth: Effects on Nephron Number and Long-Term Renal Health. *Int. J. Nephrol.* **2012,** 136942 (2012).

213. Chong, E. & Yosypiv, I. V. Developmental programming of hypertension and kidney disease. *Int. J. Nephrol.* **2012,** 760580 (2012).

214. Armitage, J. *et al.* Developmental programming of aortic and renal structure in offspring of rats fed fat-rich diets in pregnancy. *J Physiol* **565,** 171–84 (2005).

215. Moritz, K. M. *et al.* Review: Sex specific programming: a critical role for the renal renin-angiotensin system. *Placenta* **31 Suppl,** S40–6 (2010).

216. Nijland, M. J., Schlabritz-Loutsevitch, N. E., Hubbard, G. B., Nathanielsz, P. W. & Cox, L. A. Non-human primate fetal kidney transcriptome analysis

indicates mammalian target of rapamycin (mTOR) is a central nutrient-responsive pathway. *J Physiol* **579,** 643–56 (2007).

217. Lucas, S. R., Zaladek-Gil, F., Costa-Silva, V. L. & Miraglia, S. M. Function and morphometric evaluation of intrauterine undernutrition on kidney development of the progeny. *Braz. J. Med. Biol. Res.* **24,** 967–70 (1991).

218. Merlet-Bénichou, C., Vilar, J., Lelievre-Pegorier, M., Moreau, E. & Gilbert, T. Fetal nephron mass: its control and deficit. *Adv. Nephrol. Necker Hosp.* **26,** 19–45 (1997).

219. Keller, G., Zimmer, G. & Mall, G. Nephron number in patients with primary hypertension. *New Engl. J.* … 101–108 (2003).

220. White, S. L. *et al.* Is low birth weight an antecedent of CKD in later life? A systematic review of observational studies. *Am. J. Kidney Dis.* **54,** 248–61 (2009).

221. Hughson, M., Farris, A. B., Douglas-Denton, R., Hoy, W. E. & Bertram, J. F. Glomerular number and size in autopsy kidneys: the relationship to birth weight. *Kidney Int.* **63,** 2113–22 (2003).

222. Heyman, S. N., Rosenberger, C. & Rosen, S. Acute kidney injury: lessons from experimental models. *Contrib. Nephrol.* **169,** 286–96 (2011).

223. Machado, N. G., Baldeiras, I., Pereira, G. C., Pereira, S. P. & Oliveira, P. J. Sub-chronic administration of doxorubicin to Wistar rats results in oxidative stress and unaltered apoptotic signaling in the lung. *Chem. Biol. Interact.* **188,** 478–86 (2010).

224. Pereira, S. P. *et al.* Toxicity assessment of the herbicide metolachlor comparative effects on bacterial and mitochondrial model systems. *Toxicol Vitr.* **23,** 1585–90 (2009).

225. Pereira, S. P. *et al.* Dioxin-induced acute cardiac mitochondrial oxidative damage and increased activity of ATP-sensitive potassium channels in Wistar rats. *Environ. Pollut.* **180,** 281–90 (2013).

226. Cummins, J. M. The role of mitochondria in the establishment of oocyte functional competence. *Eur. J. Obstet. Gynecol. Reprod. Biol.* **115 Suppl,** S23–9 (2004).

227. Dumollard, R., Duchen, M. & Carroll, J. The role of mitochondrial function in the oocyte and embryo. *Curr. Top. Dev. Biol.* **77,** 21–49 (2007).

228. Honzik, T. *et al.* Activities of respiratory chain complexes and pyruvate dehydrogenase in isolated muscle mitochondria in premature neonates. *Early*

Hum. Dev. **84,** 269–76 (2008).

229. DiMauro, S. & Schon, E. A. Mitochondrial respiratory-chain diseases. *N. Engl. J. Med.* **348,** 2656–68 (2003).

230. Balaban, R. S., Nemoto, S. & Finkel, T. Mitochondria, oxidants, and aging. *Cell* **120,** 483–95 (2005).

231. Lebrecht, D., Setzer, B., Ketelsen, U. P., Haberstroh, J. & Walker, U. A. Time-dependent and tissue-specific accumulation of mtDNA and respiratory chain defects in chronic doxorubicin cardiomyopathy. *Circulation* **108,** 2423–9 (2003).

232. Fernandes, M. A. S. *et al.* Comparative effects of three 1,4-dihydropyridine derivatives [OSI-1210, OSI-1211 (etaftoron), and OSI-3802] on rat liver mitochondrial bioenergetics and on the physical properties of membrane lipid bilayers: relevance to the length of the alkoxyl chain in. *Chem. Biol. Interact.* **173,** 195–204 (2008).

233. Szendroedi, J., Phielix, E. & Roden, M. The role of mitochondria in insulin resistance and type 2 diabetes mellitus. *Nat. Rev. Endocrinol.* **8,** 92–103 (2012).

234. Lin, M. T. & Beal, M. F. Mitochondrial dysfunction and oxidative stress in neurodegenerative diseases. *Nature* **443,** 787–95 (2006).

235. Tachibana, M. *et al.* Mitochondrial gene replacement in primate offspring and embryonic stem cells. *Nature* **461,** 367–72 (2009).

236. Rogers, J. & Hixson, J. E. Baboons as an animal model for genetic studies of common human disease. *Am. J. Hum. Genet.* **61,** 489–93 (1997).

237. Li, C., McDonald, T., Wu, G., Nijland, M. & Nathanielsz, P. Intrauterine growth restriction alters term fetal baboon hypothalamic appetitive peptide balance. *J Endocrinol* **217,** 275–82 (2013).

238. Assis, T., Melo, E. & Filho, J. A. Effects of intrauterine malnutrition on the renal morphology of Wistar rats: a systematic review. *J. Morphol. Sci* **28,** 1–3 (2011).

239. Bouret, S. G. & Simerly, R. B. Developmental programming of hypothalamic feeding circuits. *Clin. Genet.* **70,** 295–301 (2006).

240. Engeham, S. *et al.* Mitochondrial Respiration Is Decreased in Rat Kidney Following Fetal Exposure to a MaternalLow-ProteinDiet. *J. Nutr. Metab.* **2012,** 989037 (2012).

241. Nijland, M. J., Schlabritz-Loutsevitch, N. E., Hubbard, G. B., Nathanielsz, P. W. & Cox, L. A. Non-human primate fetal kidney transcriptome analysis indicates mammalian target of rapamycin (mTOR) is a central nutrient-

responsive pathway. *J. Physiol.* **579,** 643–56 (2007).

242. Moritz, K. M. & Wintour, E. M. Functional development of the meso- and metanephros. *Pediatr. Nephrol.* **13,** 171–8 (1999).

243. Benz, K. & Amann, K. Maternal nutrition, low nephron number and arterial hypertension in later life. *Biochim. Biophys. Acta* **1802,** 1309–17 (2010).

244. Fowden, A. L., Giussani, D. A. & Forhead, A. J. Endocrine and metabolic programming during intrauterine development. *Early Hum. Dev.* **81,** 723–34 (2005).

245. Magyar, D. M. *et al.* Time-trend analysis of plasma cortisol concentrations in the fetal sheep in relation to parturition. *Endocrinology* **107,** 155–9 (1980).

246. Luyckx, V. & Brenner, B. Low birth weight, nephron number, and kidney disease. *Kidney Int.* **68,** 68–77 (2005).

247. Rincon-Choles, H. *et al.* Renal histopathology of a baboon model with type 2 diabetes. *Toxicol. Pathol.* **40,** 1020–30 (2012).

248. Turkkan, J. S. & Goldstein, D. S. Chronic effects of high salt intake and conflict stress on blood pressure in primates. A progress report. *Integr. Physiol. Behav. Sci.* **26,** 269–81

249. Nijland, M. J. *et al.* Epigenetic modification of fetal baboon hepatic phosphoenolpyruvate carboxykinase following exposure to moderately reduced nutrient availability. *J. Physiol.* **588,** 1349–1359 (2010).

250. Antonow-Schlorke, I. *et al.* Vulnerability of the fetal primate brain to moderate reduction in maternal global nutrient availability. *Proc. Natl. Acad. Sci. U. S. A.* **108,** 3011–6 (2011).

251. Drever, N., McDonald, T., Nathanielsz, P. & Li, C. IGF-II and insulin (ins) are decreased in the baboon fetal pancreas in response to global 30% maternal nutrient restriction (MNR) (Abstract). *Reprod Sci* **15,** 122A (2008).

252. Keenan, K. *et al.* Poor nutrition during pregnancy and lactation negatively affects neurodevelopment of the offspring: evidence from a translational primate model. *Am J Clin Nutr* **98,** 396–402 (2013).

253. Choi, J. *et al.* Emergence of insulin resistance in juvenile baboon offspring of mothers exposed to moderate maternal nutrient reduction. *Am. J. Physiol. Regul. Integr. Comp. Physiol.* **301,** R757–62 (2011).

254. Barker, D. J. P., Lampl, M., Roseboom, T. & Winder, N. Resource allocation in utero and health in later life. *Placenta* **33 Suppl 2,** e30–4 (2012).

255. Dallman, M. F. *et al.* Glucocorticoids, the etiology of obesity and the metabolic syndrome. *Curr. Alzheimer Res.* **4,** 199–204 (2007).

256. Wyrwoll, C. S., Mark, P. J. & Waddell, B. J. Developmental programming of renal glucocorticoid sensitivity and the renin-angiotensin system. *Hypertension* **50,** 579–584 (2007).

257. Osmond, C. & Barker, D. J. Fetal, infant, and childhood growth are predictors of coronary heart disease, diabetes, and hypertension in adult men and women. *Environ. Health Perspect.* **108 Suppl,** 545–53 (2000).

258. Luyckx, V., Shukha, K. & Brenner, B. Low Nephron Number and Its Clinical Consequences. *Rambam Maimonides Med. J.* **2,** 1–16 (2011).

259. Ferré, P. *et al.* Glucose utilization in vivo and insulin-sensitivity of rat brown adipose tissue in various physiological and pathological conditions. *Biochem. J.* **233,** 249–52 (1986).

260. Fedorova, L. V *et al.* Mitochondrial impairment in the five-sixth nephrectomy model of chronic renal failure: proteomic approach. *BMC nephrol* **14,** 209 (2013).

261. Gilbert, J. S. & Nijland, M. J. Sex differences in the developmental origins of hypertension and cardiorenal disease. *Am. J. Physiol. Regul. Integr. Comp. Physiol.* **295,** R1941–52 (2008).

262. Gretz, N., Zeier, M., Geberth, S., Strauch, M. & Ritz, E. Is gender a determinant for evolution of renal failure? A study in autosomal dominant polycystic kidney disease. *Am. J. Kidney Dis.* **14,** 178–83 (1989).

263. Iseki, K., Ikemiya, Y., Kinjo, K. & Inoue, T. Body mass index and the risk of development of end-stage renal disease in a screened cohort. *Kidney Int.* **65,** 1870–1876 (2004).

264. Sakemi, T., Toyoshima, H. & Morito, F. Testosterone eliminates the attenuating effect of castration on the progressive glomerular injury in hypercholesterolemic male Imai rats. *Nephron* **67,** 469–76 (1994).

265. Reyes, D., Lew, S. Q. & Kimmel, P. L. Gender differences in hypertension and kidney disease. *Med. Clin. North Am.* **89,** 613–30 (2005).

266. Li, S. *et al.* Low birth weight is associated with chronic kidney disease only in men. *Kidney Int.* **73,** 637–42 (2008).

267. Silbiger, S. R. & Neugarten, J. The impact of gender on the progression of chronic renal disease. *Am. J. Kidney Dis.* **25,** 515–533 (1995).

268. Mayeur, S. *et al.* Maternal calorie restriction modulates placental mitochondrial

biogenesis and bioenergetic efficiency: putative involvement in fetoplacental growth defects in rats. *Am. J. Physiol. Endocrinol. Metab.* **304,** E14–22 (2013).

269. Theys, N., Bouckenooghe, T., Ahn, M. T., Remacle, C. & Reusens, B. Maternal low-protein diet alters pancreatic islet mitochondrial function in a sex-specific manner in the adult rat. *Am. J. Physiol. Regul. Integr. Comp. Physiol.* **297,** R1516–25 (2009).

270. WHO. Global status report on noncommunicable diseases. *World Heal. Organ.* 176 (2010). doi:ISBN 978 92 4 156422 9

271. Barker, D. J., Osmond, C., Golding, J., Kuh, D. & Wadsworth, M. E. Growth in utero, blood pressure in childhood and adult life, and mortality from cardiovascular disease. *BMJ* **298,** 564–567 (1989).

272. Rich-Edwards, J. *et al.* Longitudinal study of birth weight and adult body mass index in predicting risk of coronary heart disease and stroke in women. *BMJ* **330,** 1115 (2005).

273. Barker, D. The fetal origins of type 2 diabetes mellitus. *Ann. Intern. Med.* **130,** 322–324 (1999).

274. Roseboom, T. J. in *Diapedia* **17,** 2–5 (Diapedia.org, 2013).

275. Barker, D. J., Martyn, C. N., Osmond, C., Hales, C. N. & Fall, C. H. Growth in utero and serum cholesterol concentrations in adult life. *BMJ* **307,** 1524–1527 (1993).

276. Roseboom, T. J. *et al.* Plasma fibrinogen and factor VII concentrations in adults after prenatal exposure to famine. *Br. J. Haematol.* **111,** 112–117 (2000).

277. Martyn, C. N., Meade, T. W., Stirling, Y. & Barker, D. J. Plasma concentrations of fibrinogen and factor VII in adult life and their relation to intra-uterine growth. *Br. J. Haematol.* **89,** 142–146 (1995).

278. Barker, D. J., Winter, P. D., Osmond, C., Margetts, B. & Simmonds, S. J. Weight in infancy and death from ischaemic heart disease. *Lancet* **2,** 577–580 (1989).

279. Curhan, G. C. *et al.* Birth weight and adult hypertension, diabetes mellitus, and obesity in US men. *Circulation* **94,** 3246–3250 (1996).

280. Leon, D. A. *et al.* Reduced fetal growth rate and increased risk of death from ischaemic heart disease: cohort study of 15 000 Swedish men and women born 1915-29. *BMJ* **317,** 241–245 (1998).

281. Crispi, F. *et al.* Fetal growth restriction results in remodeled and less efficient hearts in children. *Circulation* **121,** 2427–2436 (2010).

282. Langley-Evans, S. C. *et al.* Protein intake in pregnancy, placental glucocorticoid metabolism and the programming of hypertension in the rat. *Placenta* **17,** 169–172 (1996).

283. Dodic, M., May, C. N., Wintour, E. M. & Coghlan, J. P. An early prenatal exposure to excess glucocorticoid leads to hypertensive offspring in sheep. *Clin. Sci. (Lond).* **94,** 149–155 (1998).

284. Stanley, W. C. & Chandler, M. P. Energy metabolism in the normal and failing heart: Potential for therapeutic interventions. *Heart Fail. Rev.* **7,** 115–130 (2002).

285. Hom, J. & Sheu, S. S. Morphological dynamics of mitochondria--a special emphasis on cardiac muscle cells. *J. Mol. Cell. Cardiol.* **46,** 811–20 (2009).

286. Giles, R. E., Blanc, H., Cann, H. M. & Wallace, D. C. Maternal inheritance of human mitochondrial DNA. *Proc. Natl. Acad. Sci. U. S. A.* **77,** 6715–9 (1980).

287. Bates, M. G. D. *et al.* Cardiac involvement in mitochondrial DNA disease: Clinical spectrum, diagnosis, and management. *Eur. Heart J.* **33,** 3023–3033 (2012).

288. Copeland, W. C. Defects in mitochondrial DNA replication and human disease. *Crit. Rev. Biochem. Mol. Biol.* **47,** 64–74 (2012).

289. Rolo, A. P. & Palmeira, C. M. Diabetes and mitochondrial function: Role of hyperglycemia and oxidative stress. *Toxicol. Appl. Pharmacol.* **212,** 167–178 (2006).

290. Yu, M. Generation, function and diagnostic value of mitochondrial DNA copy number alterations in human cancers. *Life Sci.* **89,** 65–71 (2011).

291. Coskun, P. *et al.* A mitochondrial etiology of Alzheimer and Parkinson disease. *Biochim. Biophys. Acta - Gen. Subj.* **1820,** 553–564 (2012).

292. Marin-Garcia, J. & Goldenthal, M. J. Cardiomyopathy and abnormal mitochondrial function. *Cardiovasc. Res.* **28,** 456–463 (1994).

293. De Jonge, N. & Kirkels, J. H. in *Clin. Cardiogenetics* 123–128 (2011).

294. Ozawa, T. Mitochondrial cardiomyopathy. *Herz* **19,** 105–118 (1994).

295. Suomalainen, A. *et al.* Inherited idiopathic dilated cardiomyopathy with multiple deletions of mitochondrial DNA. *Lancet* **340,** 1319–1320 (1992).

296. Zeviani, M. *et al.* Maternally inherited myopathy and cardiomyopathy: association with mutation in mitochondrial DNA tRNA(Leu)(UUR). *Lancet* **338,** 143–147 (1991).

297. Anan, R. *et al.* Cardiac involvement in mitochondrial diseases. A study on 17 patients with documented mitochondrial DNA defects. *Circulation* **91,** 955–961 (1995).

298. Vijay, V. *et al.* Sexual dimorphism in the expression of mitochondria-related genes in rat heart at different ages. *PLoS One* **10,** e0117047 (2015).

299. Ballinger, S. W. Mitochondrial dysfunction in cardiovascular disease. *Free Radic. Biol. Med.* **38,** 1278–1295 (2005).

300. Rieger, D., Loskutoff, N. M. & Betteridge, K. J. Developmentally related changes in the uptake and metabolism of glucose, glutamine and pyruvate by cattle embryos produced in vitro. *Reprod. Fertil. Dev.* **4,** 547–557 (1992).

301. Gruenwald, P. & Minh, H. N. Evaluation of body and organ weights in perinatal pathology. II. Weight of body and placenta of surviving and of autopsied infants. *Am. J. Obstet. Gynecol.* **82,** 312–319 (1961).

302. Marton, T., Hargitai, B., Bowen, C. & Cox, P. M. Elevated Brain Weight/Liver Weight Ratio in Normal Body Weight Centile Term Perinatal Deaths: An Indicator of Terminal Intrauterine Malnourishment. *Pediatr. Dev. Pathol.* **16,** 267–271 (2013).

303. Barker, D. J. P. *et al.* The early origins of chronic heart failure: impaired placental growth and initiation of insulin resistance in childhood. *Eur. J. Heart Fail.* **12,** 819–25 (2010).

304. Kalhan, S. C. Protein metabolism in pregnancy. in *Am. J. Clin. Nutr.* **71,** (2000).

305. Cetin, I. *et al.* Maternal concentrations and fetal-maternal concentration differences of plasma amino acids in normal and intrauterine growth-restricted pregnancies. *Am. J. Obstet. Gynecol.* **174,** 1575–1583 (1996).

306. McDonald, T. J. *et al.* Effect of 30 % nutrient restriction in the first half of gestation on maternal and fetal baboon serum amino acid concentrations. *Br. J. Nutr.* 1–7 (2012).

307. Schoengold, D. M., DeFiore, R. H. & Parlett, R. C. Free amino acids in plasma throughout pregnancy. *Am. J. Obstet. Gynecol.* **131,** 490–499 (1978).

308. Kalkhoff, R. K. *et al.* Relationship between neonatal birth weight and maternal plasma amino acid profiles in lean and obese nondiabetic women and in type I diabetic pregnant women. *Metabolism.* **37,** 234–239 (1988).

309. Economides, D. L., Nicolaides, K. H., Gahl, W. A., Bernardini, I. & Evans, M. I. Plasma amino acids in appropriate- and small-for-gestational-age fetuses.

Am. J. Obstet. Gynecol. **161,** 1219–1227 (1989).

310. Neu, J., Shenoy, V. & Chakrabarti, R. Glutamine nutrition and metabolism: where do we go from here ? *FASEB J.* **10,** 829–837 (1996).

311. Oliveira, G. P., Dias, C. M., Pelosi, P. & Rocco, P. R. M. Understanding the mechanisms of glutamine action in critically ill patients. *An. Acad. Bras. Cienc.* **82,** 417–430 (2010).

312. Hay, W. W. Placental-fetal glucose exchange and fetal glucose metabolism. *Trans. Am. Clin. Climatol. Assoc.* **117,** 321–339; discussion 339–340 (2006).

313. Magnusson, A. L., Powell, T., Wennergren, M. & Jansson, T. Glucose metabolism in the human preterm and term placenta of IUGR fetuses. *Placenta* **25,** 337–346 (2004).

314. Manzoni, P., Baù, M. G. & Farina, D. Glucose regulation in young adults with very low birth weight. *N. Engl. J. Med.* **357,** 616; author reply 617 (2007).

315. Guo, C., Li, C., Myatt, L., Nathanielsz, P. W. & Sun, K. Sexually dimorphic effects of maternal nutrient reduction on expression of genes regulating cortisol metabolism in fetal baboon adipose and liver tissues. *Diabetes* **62,** 1175–1185 (2013).

316. Li, C. *et al.* Effects of maternal global nutrient restriction on fetal baboon hepatic insulin-like growth factor system genes and gene products. *Endocrinology* **150,** 4634–4642 (2009).

317. Kavitha, J. V. *et al.* Down-regulation of placental mTOR, insulin/IGF-I signaling, and nutrient transporters in response to maternal nutrient restriction in the baboon. *FASEB J.* **28,** 1294–1305 (2014).

318. Abel, E. D. D. Glucose transport in the heart. *Front. Biosci.* **9,** 201–215 (2004).

319. Nicolini, U. *et al.* Maternal-fetal glucose gradient in normal pregnancies and in pregnancies complicated by alloimmunization and fetal growth retardation. *Am. J. Obstet. Gynecol.* **161,** 924–927 (1989).

320. Mesiano, S. & Jaffe, R. B. Developmental and functional biology of the primate fetal adrenal cortex. *Endocr. Rev.* **18,** 378–403 (1997).

321. Mastorakos, G. & Ilias, I. Maternal and fetal hypothalamic-pituitary-adrenal axes during pregnancy and postpartum. *Ann. N. Y. Acad. Sci.* **997,** 136–149 (2003).

322. Rog-Zielinska, E. A., Richardson, R. V., Denvir, M. A. & Chapman, K. E. Glucocorticoids and foetal heart maturation; implications for prematurity and foetal programming. *J. Mol. Endocrinol.* **52,** (2013).

323. Zong, P., Tune, J. D. & Downey, H. F. Mechanisms of oxygen demand/supply balance in the right ventricle. *Exp. Biol. Med. (Maywood).* **230,** 507–519 (2005).

324. Xavier-Vidal, R. & Madi, K. Comparison between right and left ventricular myocardia during the human fetal period. Stereological evaluation. *Arq. Bras. Cardiol.* **72,** 581–592 (1999).

325. Smolich, J. J., Walker, A. M., Campbell, G. R. & Adamson, T. M. Left and right ventricular myocardial morphometry in fetal, neonatal, and adult sheep. *Am. J. Physiol.* **257,** H1–9 (1989).

326. Leduc, L., Levy, E., Bouity-Voubou, M. & Delvin, E. Fetal programming of atherosclerosis: Possible role of the mitochondria. *Eur. J. Obstet. Gynecol. Reprod. Biol.* **149,** 127–130 (2010).

327. Zinner, D., Groeneveld, L. F., Keller, C. & Roos, C. Mitochondrial phylogeography of baboons (Papio spp.): indication for introgressive hybridization? *BMC Evol. Biol.* **9,** 83 (2009).

328. Keller, C., Roos, C., Groeneveld, L. F., Fischer, J. & Zinner, D. Introgressive hybridization in Southern African baboons shapes patterns of mtDNA variation. *Am. J. Phys. Anthropol.* **142,** 125–136 (2010).

329. Rooney, J. P. *et al.* PCR Based Determination of Mitochondrial DNA Copy Number in Multiple Species. *Methods Mol. Biol.* **1241,** 23–38 (2015).

330. Van Blerkom, J. Mitochondria in early mammalian development. *Semin. Cell Dev. Biol.* **20,** 354–64 (2009).

331. Tranah, G. J. *et al.* Mitochondrial DNA variation in human metabolic rate and energy expenditure. *Mitochondrion* (2011). 5

332. Miller, F. J. Precise determination of mitochondrial DNA copy number in human skeletal and cardiac muscle by a PCR-based assay: lack of change of copy number with age. *Nucleic Acids Res.* **31,** 61e–61 (2003).

333. Barthélémy, C. *et al.* Late-onset mitochondrial DNA depletion: DNA copy number, multiple deletions, and compensation. *Ann. Neurol.* **49,** 607–617 (2001).

334. Soonpaa, M. H., Kim, K. K., Pajak, L., Franklin, M. & Field, L. J. Cardiomyocyte DNA synthesis and binucleation during murine development. *Am. J. Physiol.* **271,** H2183–H2189 (1996).

335. Li, F., Wang, X., Capasso, J. M. & Gerdes, A. M. Rapid transition of cardiac myocytes from hyperplasia to hypertrophy during postnatal development. *J.*

Mol. Cell. Cardiol. **28,** 1737–1746 (1996).

336. Marin-Garcia, J., Ananthakrishnan, R. & Goldenthal, M. J. Heart mitochondrial DNA and enzyme changes during early human development. *Mol. Cell. Biochem.* **210,** 47–52 (2000).

337. Minai, L. *et al.* Mitochondrial respiratory chain complex assembly and function during human fetal development. *Mol. Genet. Metab.* **94,** 120–6 (2008).

338. Anderson, E. J. *et al.* Substrate-Specific Derangements in Mitochondrial Metabolism and Redox Balance in the Atrium of the Type 2 Diabetic Human Heart. *J. Am. Coll. Cardiol.* **54,** 1891–1898 (2009).

339. Boudina, S. *et al.* Mitochondrial energetics in the heart in obesity-related diabetes: Direct evidence for increased uncoupled respiration and activation of uncoupling proteins. *Diabetes* **56,** 2457–2466 (2007).

340. Bahtiyar, M. O. & Copel, J. a. Cardiac Changes in the Intrauterine Growth-Restricted Fetus. *Semin. Perinatol.* **32,** 190–193 (2008).

341. Fouzas, S. *et al.* Neonatal cardiac dysfunction in intrauterine growth restriction. *Pediatr. Res.* **75,** 651–7 (2014).

342. Westermann, B. Merging mitochondria matters: cellular role and molecular machinery of mitochondrial fusion. *EMBO Rep.* **3,** 527–31 (2002).

343. Ong, S. B. & Hausenloy, D. J. Mitochondrial morphology and cardiovascular disease. *Cardiovasc. Res.* **88,** 16–29 (2010).

344. Bach, D. *et al.* Mitofusin-2 determines mitochondrial network architecture and mitochondrial metabolism: A novel regulatory mechanism altered in obesity. *J. Biol. Chem.* **278,** 17190–17197 (2003).

345. Chen, K. H. *et al.* Dysregulation of HSG triggers vascular proliferative disorders. *Nat. Cell Biol.* **6,** 872–883 (2004).

346. Arismendi-Morillo, G. Electron microscopy morphology of the mitochondrial network in gliomas and their vascular microenvironment. *Biochim. Biophys. Acta* **1807,** 602–608 (2010).

347. Modica-Napolitano, J. S. & Singh, K. K. Mitochondria as targets for detection and treatment of cancer. *Expert Rev. Mol. Med.* **4,** 1–19 (2002).

348. Gilkerson, R. W., Selker, J. M. L. & Capaldi, R. a. The cristal membrane of mitochondria is the principal site of oxidative phosphorylation. *FEBS Lett.* **546,** 355–358 (2003).

349. Pignatelli, R. H. *et al.* Clinical Characterization of Left Ventricular

Noncompaction in Children: A Relatively Common Form of Cardiomyopathy. *Circulation* **108,** 2672–2678 (2003).

350. Vassalle, C., Simoncini, T., Chedraui, P. & Pérez-López, F. R. Why sex matters: the biological mechanisms of cardiovascular disease. *Gynecol. Endocrinol.* **28,** 746–751 (2012).

351. Czubryt, M. P., Espira, L., Lamoureux, L. & Abrenica, B. The role of sex in cardiac function and disease. *Can. J. Physiol. Pharmacol.* **84,** 93–109 (2006).

352. Arnold, A. P., Chen, X. & Itoh, Y. Sex and Gender Differences in Pharmacology. *Sex Gend. Differ. Pharmacol.* **214,** 67–88 (2012).

353. Goldzieher, J. W. Cardiovascular disease in women. *Circulation* **89,** 2942 (1994).

354. Mosca, L. *et al.* Cardiovascular Disease in Women : A Statement for Healthcare Professionals From the American Heart Association. *Circulation* **96,** 2468–2482 (1997).

355. Mendelsohn, M. E. & Karas, R. H. Molecular and cellular basis of cardiovascular gender differences. *Science* **308,** 1583–1587 (2005).

356. Ostadal, B., Netuka, I., Maly, J., Besik, J. & Ostadalova, I. Gender differences in cardiac ischemic injury and protection--experimental aspects. *Exp. Biol. Med. (Maywood).* **234,** 1011–1019 (2009).

357. Merz, C. N., Moriel, M., Rozanski, A., Klein, J. & Berman, D. S. Gender-related differences in exercise ventricular function among healthy subjects and patients. *Am. Heart J.* **131,** 704–709 (1996).

358. Colom, B., Oliver, J., Roca, P. & Garcia-Palmer, F. J. Caloric restriction and gender modulate cardiac muscle mitochondrial H2O2 production and oxidative damage. *Cardiovasc. Res.* **74,** 456–465 (2007).

359. Regitz-Zagrosek, V., Oertelt-Prigione, S., Seeland, U. & Hetzer, R. Sex and gender differences in myocardial hypertrophy and heart failure. *Circ. J.* **74,** 1265–1273 (2010).

360. Zhu, H. & Wang, S. Mitochondria and left ventricular hypertrophy. *J. Geriatr. Cardiol.* **5,** 50–59 (2008).

Appendix

Copy right license agreements

A1. Nature publishing group license

NATURE PUBLISHING GROUP LICENSE
TERMS AND CONDITIONS

Sep 27, 2015

This is a License Agreement between Susana Pereira ("You") and Nature Publishing Group ("Nature Publishing Group") provided by Copyright Clearance Center ("CCC"). The license consists of your order details, the terms and conditions provided by Nature Publishing Group, and the payment terms and conditions.

All payments must be made in full to CCC. For payment instructions, please see information listed at the bottom of this form.

License Number	3716980805384
License date	Sep 27, 2015
Licensed content publisher	Nature Publishing Group
Licensed content publication	Nature Reviews Genetics
Licensed content title	Mitochondrial DNA mutations in human disease
Licensed content author	Robert W. Taylor and Doug M. Turnbull
Licensed content date	May 1, 2005
Volume number	6
Issue number	5
Type of Use	reuse in a dissertation / thesis
Requestor type	academic/educational
Format	print and electronic
Portion	figures/tables/illustrations
Number of figures/tables/illustrations	1
High-res required	no
Figures	Figure 1.1
Author of this NPG article	no
Your reference number	None
Title of your thesis / dissertation	PROGRAMMING OF FETAL CARDIO-RENAL MITOCHONDRIA BY MATERNAL NUTRITION
Expected completion date	Sep 2015
Estimated size (number of pages)	300
Customer Tax ID	PT501617582
Total	0.00 EUR
Terms and Conditions	

Terms and Conditions for Permissions

Nature Publishing Group hereby grants you a non-exclusive license to reproduce this material for this purpose, and for no other use,subject to the conditions below:

1. NPG warrants that it has, to the best of its knowledge, the rights to license reuse of this material. However, you should ensure that the material you are requesting is original to

A1. Nature publishing group license

Nature Publishing Group and does not carry the copyright of another entity (as credited in the published version). If the credit line on any part of the material you have requested indicates that it was reprinted or adapted by NPG with permission from another source, then you should also seek permission from that source to reuse the material.

2. Permission granted free of charge for material in print is also usually granted for any electronic version of that work, provided that the material is incidental to the work as a whole and that the electronic version is essentially equivalent to, or substitutes for, the print version.Where print permission has been granted for a fee, separate permission must be obtained for any additional, electronic re-use (unless, as in the case of a full paper, this has already been accounted for during your initial request in the calculation of a print run).NB: In all cases, web-based use of full-text articles must be authorized separately through the 'Use on a Web Site' option when requesting permission.

3. Permission granted for a first edition does not apply to second and subsequent editions and for editions in other languages (except for signatories to the STM Permissions Guidelines, or where the first edition permission was granted for free).

4. Nature Publishing Group's permission must be acknowledged next to the figure, table or abstract in print. In electronic form, this acknowledgement must be visible at the same time as the figure/table/abstract, and must be hyperlinked to the journal's homepage.

5. The credit line should read:
   Reprinted by permission from Macmillan Publishers Ltd: [JOURNAL NAME] (reference citation), copyright (year of publication)
   For AOP papers, the credit line should read:
   Reprinted by permission from Macmillan Publishers Ltd: [JOURNAL NAME], advance online publication, day month year (doi: 10.1038/sj.[JOURNAL ACRONYM].XXXXX)

   Note: For republication from the *British Journal of Cancer,* the following credit lines apply.
   Reprinted by permission from Macmillan Publishers Ltd on behalf of Cancer Research UK: [JOURNAL NAME] (reference citation), copyright (year of publication)For AOP papers, the credit line should read:
   Reprinted by permission from Macmillan Publishers Ltd on behalf of Cancer Research UK: [JOURNAL NAME], advance online publication, day month year (doi: 10.1038/sj.[JOURNAL ACRONYM].XXXXX)

6. Adaptations of single figures do not require NPG approval. However, the adaptation should be credited as follows:

   Adapted by permission from Macmillan Publishers Ltd: [JOURNAL NAME] (reference citation), copyright (year of publication)

   Note: For adaptation from the *British Journal of Cancer,* the following credit line applies.
   Adapted by permission from Macmillan Publishers Ltd on behalf of Cancer Research UK: [JOURNAL NAME] (reference citation), copyright (year of publication)

7. Translations of 401 words up to a whole article require NPG approval. Please visit http://www.macmillanmedicalcommunications.com for more information.Translations of up to a 400 words do not require NPG approval. The translation should be credited as follows:

   Translated by permission from Macmillan Publishers Ltd: [JOURNAL NAME] (reference citation), copyright (year of publication).

   Note: For translation from the *British Journal of Cancer,* the following credit line applies.
   Translated by permission from Macmillan Publishers Ltd on behalf of Cancer Research UK: [JOURNAL NAME] (reference citation), copyright (year of publication)

We are certain that all parties will benefit from this agreement and wish you the best in the

use of this material. Thank you.
Special Terms:
v1.1

A2. ATLA - Alternatives to laboratory animals licence

Gmail by Google

Susana Pereira <pereirasusan@gmail.com>

permission to use figure in ATLA paper

1 mensagem

Rita Seabra <Rita@frame.org.uk> 29 de setembro de 2015 às 08:56
Para: Susana Pereira <pereirasusan@gmail.com>
Cc: Susan Trigwell <Susan@frame.org.uk>

Dear Mrs Pereira,

We grant you permission to use the figures published in *ATLA* 37.4 (pp. 355-365) on the condition that the source is cited in an appropriate manner.

Best regards,

Rita

Rita Seabra

Publications Officer

If you'd like to get regular updates from FRAME you can **sign up for our email list** at http://eepurl.com/hvoVQ .

We promise not to swamp you with messages - about one every two weeks - and you can opt out at any time.

image001.jpg
355K

A3. EMBO molecular medicine license

You have full text access to this Open Access content

EMBO Molecular Medicine

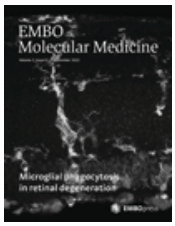

Edited By: Stefanie Dimmeler (Chief Editor), Roberto Buccione and Céline Carret (EMBO Editors)

Online ISSN: 1757-4684

Permissions

All articles accepted from 14 August 2012 are made available under the terms of the Creative Commons Attribution License (http://creativecommons.org/licenses/by/3.0/). Permission is therefore not required for academic or commercial reuse, provided that full attribution is included in the new work.

For articles accepted prior to 14 August 2012, permission is not required for academic re-use, however commercial re-use still requires permission. Please follow the instructions below for obtaining this permission.

*PLEASE NOTE: If the links highlighted here do not take you to those web sites, please copy and paste address in your browser.

Where permission is required, requests are being handled through the Rightslink® online service. This service will also inform you whether or not permission is required.

Simply follow the steps below to obtain permission via the Rightslink® system:

- Locate the article you wish to reproduce on Wiley Online Library (http://onlinelibrary.wiley.com (http://onlinelibrary.wiley.com))

- Click on the 'Request Permissions' link, under the 'ARTICLE TOOLS' menu (also available from Table of Contents or search results)

- Follow the online instructions and select your requirements from the drop down options and click on 'quick price' to get a quote

- Create a RightsLink® account to complete your transaction (and pay, where applicable)

- Read and accept our Terms & Conditions and Download your license

- For any technical queries please contact customercare@copyright.com (mailto:customercare@copyright.com)

- For further information and to view a Rightslink® demo please visit www.wiley.com (http://www.wiley.com) and select Rights& Permissions.

AUTHORS - If you wish to reuse your own article (or an amended version of it) in a new publication of which you are the author, editor or co-editor, prior permission is not required (with the usual acknowledgements). However, a formal grant of license can be downloaded free of charge from RightsLink if required.

If you have any questions about the permitted uses of a specific article, please contact us.

Rights & Licenses
Wiley-VCH Verlag GmbH & Co. KGaA
Boschstrasse 12
69469 Weinheim
Germany
Email: rightsDE@wiley.com (mailto:rightsDE@wiley.com)
Fax: +49 (0) 6201 6063320

To request bulk reprints please contact Bettina Loycke
Email: rightsDE@wiley.com (mailto:rightsDE@wiley.com)

A4. JCI – The Journal of clinical investigation license

Terms of Use

Copyright, American Society for Clinical Investigation.

The American Society for Clinical Investigation holds the rights to and publishes the Journal of Clinical Investigation. The opinions expressed in the JCI are solely those of the authors and are not necessarily endorsed by the ASCI.

Users of the online version of the Journal of Clinical Investigation (JCI) (the publication of the American Society for Clinical Investigation, or ASCI), may view, reproduce, or store copies of the journal providing the information is only for their individual use. Use of the online version of the JCI constitutes an agreement to comply with this and the following terms. Any copies, in whole or in part, must include the copyright notice.

Reproduction of material presented in the journal is governed by the "fair use" limitations of US copyright law (detailed at http://www.loc.gov/copyright/title17/ (http://www.loc.gov/copyright/title17/)). You need to request permission to reproduce material if the use is commercial or if you wish to make multiple copies other than for educational purposes. The Copyright Clearance Center is the authorized agent of the ASCI and JCI for permission requests; a nominal fee is assessed in granting permission to ensure proper handling of requests as well as to protect the interests of the authors, the ASCI, and JCI. Contact the Copyright Clearance Center at:

Copyright Clearance Center Inc.
Re: Journal of Clinical Investigation
222 Rosewood Drive
Danvers, MA 01923, USA
Voice: 978-750-8400
Fax: 978-750-4470
Internet: http://www.copyright.com/ (http://www.copyright.com/)

In no event shall the JCI or the ASCI be liable for any special, incidental, indirect or consequential damages of any kind, or any damages whatsoever resulting from loss of use, data or profits, whether or not advised of the possibility of damage, and on any theory of liability, arising out of or in connection with the use of or reliance on this information. This publication is provided "as is" without warranty of any kind, either expressed or implied, including, but not limited to, the implied warranties of merchantability, fitness for a particular purpose, or non-infringement. Changes in policy or publication may be made at any time. The online version of the JCI is the definitive version and, to the extent any difference exists

---------- Forwarded message ----------
From: **Theresa Kaiser** <staff@the-jci.org>
Date: 2015-09-29 15:01 GMT+01:00
Subject: Re: Authorization for reproduction of material presented in the JCI
To: "Susana P. Pereira" <pereirasusan@gmail.com>

Hi Dr. Pereira,

You may use Figure 1 of the article for your thesis. Please be sure to cite to the JCI as the original source, as follows:

Mitochondrial energy metabolism in heart failure: a question of balance
Janice M. Huss, Daniel P. Kelly
Published March 1, 2005
Citation Information: *J Clin Invest.* 2005;115(3):547-555. doi:10.1172/JCI24405.

Please contact us if you have any questions.
Sincerely,
Theresa Kaiser

On 9/29/15 1:15 AM, Susana P. Pereira wrote:
Who it may concern,

My name is Susana P Pereira, I am a PhD student from Portugal.

I would like to ask for permission to use one image from the paper "Review series Mitochondrial energy metabolism in heart failure : a question of balance" from Huss et al published in the Journal of Clinical Investigation in 2005.

link http://www.ncbi.nlm.nih.gov/pmc/articles/PMC1052011/

I would like to use the "Figure 1" in the introduction of my thesis. The title of my thesis would be "PROGRAMMING OF FETAL CARDIO-RENAL MITOCHONDRIA BY MATERNAL NUTRITION" and will be present to the University of Coimbra, in Portugal.

Best regards,

Susana P. Pereira
CNC - Center for Neuroscience and Cell Biology
MitoXT - Mitochondrial Toxicology and Experimental Therapeutics
UC Biotech Building I Biocant Park Lot 8A I 3060-197 Cantanhede I Portugal
phone: (00351) 231249170 I
fax: (00351) 231249179 I pereirasusan@gmail.com